METAPLASTICITY IN A MOUSE MODEL OF ALZHEIMER'S DISEASE AND POSSIBLE THERAPEUTIC INTERVENTIONS

by
Andrea Lauren Megill

A dissertation submitted to Johns Hopkins University in conformity with the requirements for the degree of Doctor of Philosophy

Baltimore, Maryland
August 2014

ABSTRACT

Alzheimer's disease (AD) is a progressive neurodegenerative disorder, causing loss of synaptic contacts and cognitive decline. It is widely believed that AD is initiated by synaptic dysfunction caused by production of Aβ peptides. Therefore, understanding how the progression of amyloidogenesis alters synaptic function is imperative in developing effective therapeutics for disease intervention.

While many studies have focused on how Aβ peptides and the progression of AD affect frequency-dependent long-term potentiation and long-term depression (LTP/LTD), it is unclear whether synaptic dysfunction is at the level of induction or expression of synaptic plasticity mechanisms. Here we report that there is an age-dependent alteration in synaptic plasticity at the Schaffer collateral inputs to CA1 of APPswe;PS1deltaE9 AD transgenic (Tg) mice. Young pre-amyloidogenic Tgs showed enhanced LTP at the expense of LTD, while adult post-amyloidogenic Tgs showed enhanced LTD at the expense of LTP. The apparent shift in plasticity was mediated by altered LTP/LTD expression mechanisms, and in particular due to an absence of a normal age-dependent shift in pull-push metaplasticity. These results suggest that the main synaptic deficit in AD Tg mice is due to their inability to developmentally regulate LTP/LTD expression in accord with the pull-push metaplasticity model.

Current AD therapeutics provide only temporary symptomatic relief, but need to strive to mitigate the long term progression of the disease by targeting the specific cellular mechanisms that become disrupted. Recognizing that cognitive decline during AD is correlated with loss of dendritic spine density, we examined two novel therapies that increase dendritic spine density through a Ras/ERK dependent mechanism. We found that the increase in dendritic spine density was better correlated with cognitive performance than the absolute magnitude of LTP. While

these therapies were investigated in wild type mice, they both exhibit potential as drug candidates for AD treatment and warrant further studies to determine their effects in mouse models of AD.

In summary, this project provides a novel mechanistic viewpoint in understanding the synaptic dysfunction seen in AD that can lead to the development of more effective therapeutics by specifically targeting the fundamental cellular mechanisms that are disrupted, such as pull-push metaplasticity.

Dissertation Committee:
Hey-Kyoung Lee (Advisor)
Philip C. Wong (Chair)
Alfredo Kirkwood
Michela Gallagher

Dedication

To my beloved grandmother, Ella Hollenbach, who had more strength than one woman should ever need to possess.

Acknowledgements

I would first like to thank my advisor, Hey-Kyoung. You have afforded me opportunities that I could never have attained myself. Thank you for having the patience to explain concepts over and over, until I was comfortable with their understanding, and always having an open door (to your office and your home). You have been an excellent mentor, giving me advice on all aspects of my graduate education and also my future career. You have allowed me to further explore my passion for research and develop my scientific research career in the areas of interest that I want to pursue. I wish to one day be able to speak as eloquently and easily about synaptic plasticity as you do. Thank you for never doubting me, but always being my advocate and encouraging me to accomplish beyond what I thought I could achieve.

I would also like to thank my co-advisor, Alfredo Kirkwood. Your love of science is tangible. The passion and excitement you bring to your scientific investigation strengthens my own pursuit. The way with which you develop scientific explanation seems effortless, and you are always there to lend sound advice. Thank you for sharing your charisma.

To my colleagues in the Lee and Kirkwood labs, thank you for making the lab an enjoyable environment to work in everyday. Each of you has enriched my life with your unique personalities, and I have enjoyed getting to know you individually. I want to specifically thank Emily, Hui, and Jess. Emily, I am so grateful that there was someone sharing every step of this crazy PhD experience with me. I am also thankful that you were always a little bit ahead of me so I didn't have to be the first to do something new- thanks for being the guinea pig! Hui, you're such a sweet soul. I have learned so much from you. Thank you for not only teaching me numerous lab skills, but also how to handle the pressures of a PhD program, and difficulties of research with such humility and poise. Jess, I am so thankful you joined the lab when you did. You reinvigorated my passion for pursuing science. Thank you for so many insightful scientific and non-scientific discussions.

I would also like to thank my committee members. Our meetings are always so encouraging. Thank you for all your valuable suggestions and advice. In addition, I am grateful for the impact that the faculty at both University of Maryland, College Park, and Johns Hopkins University have had on my study and education during my PhD program. I would specifically like to thank the students, faculty, and staff of the Neuroscience department at JHU for your warm welcome, allowing my transfer to be easy and stress free.

Lastly and most importantly, I want to thank my Dad, my Mom, my brother, and my fiancé (future husband!). I would never have been able to pursue or finish this degree without your constant support, love, and encouragement. I know we have all put a lot of miles on our cars, but I think we can all agree it has been well worth it, and I am finally coming home!!!!

Table of Contents

List of Tables

List of Figures

Chapter 1: Introduction

Published in Neural Plasticity:

H. Wang*; **A. Megill***; K. He; A. Kirkwood; H-K. Lee (2012) Neural Plasticity 2012: 272374

*These authors contributed equally to this work

Note: Some parts of this work have been updated to include recent references and discoveries.

Alzheimer's disease (AD) is a progressive neurodegenerative disorder, causing loss of synaptic contacts and cognitive decline. It is widely believed that AD is initiated by synaptic dysfunction, which may be the basis for memory loss in early stages of the disease (Walsh and Selkoe, 2004; Shankar and Walsh, 2009). Current theories implicate the production of amyloid beta (Aβ) as a key molecular event that ultimately leads to neuronal degeneration and the clinical pathology seen in AD (Hardy and Selkoe, 2002). Aβ is produced by sequential proteolytic cleavage of amyloid precursor protein (APP) by two endoproteolytic enzymes, β- and γ-secretase (Fig 1.1). Therefore, inhibiting the activity of these enzymes has surfaced as one of the major disease-modifying approaches for AD (Citron, 2004a). However, in order to develop effective therapeutics, a detailed molecular and cellular understanding of the role of both secretases in synaptic function is necessary. In addition, since accumulating evidence suggests that the initial pathology of AD is a result of synaptic dysfunction (Walsh and Selkoe, 2004; Shankar and Walsh, 2009), understanding how Aβ production alters normal synaptic function and what types of synaptic functions are differentially affected by Aβ becomes important in developing effective therapeutics for disease intervention. This introduction summarizes a number of experimental observations that address how Aβ affects synaptic function, and review data obtained from

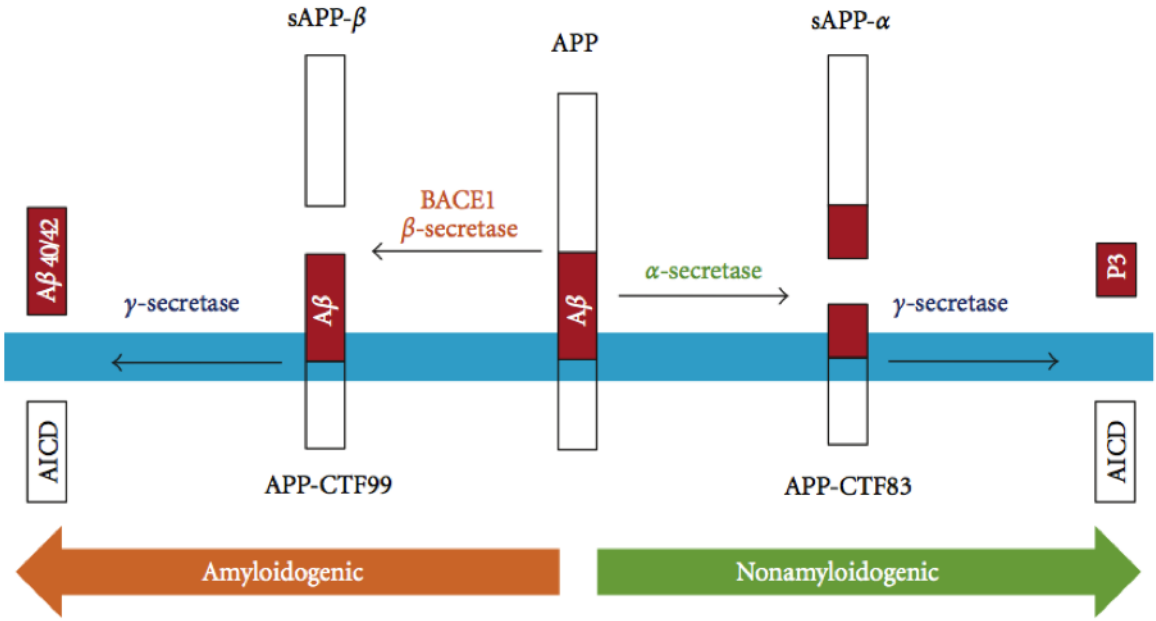

Figure 1.1. A diagram of amyloid precursor protein (APP) processing pathways.

The transmembrane protein APP (membrane indicated in blue) can be processed by two pathways, the nonamyloidogenic α-secretase pathway and the amyloidogenic β-secretase pathway. In the nonamyloidogenic pathway, α-secretase cleaves in the middle of the β-amyloid (Aβ) region (red) to release the soluble APP-fragment sAPP- α. The APP C-terminal fragment 83 (APP-CTF83) is then cleaved by γ-secretase to release the APP intracellular domain (AICD) and P3 fragment. In the amyloidogenic pathway, β-secretase cleaves APP to produce the soluble fragment sAPP-β. APP-CTF99 is then cleaved by γ-secretase to produce Aβ40, Aβ42 and AICD.

genetically altered mice developed to test the feasibility of blocking APP processing enzymes which unveiled functional roles for these enzymes in normal synaptic transmission and plasticity. It also discusses a body of work, which investigates how synaptic function is affected by currently available therapies that target APP processing enzymes. Before this, a brief introduction to the topic and current understanding of synaptic plasticity, which are relevant for the later discussions.

Section 1: Synaptic plasticity and memory formation

It is widely believed that long-term changes in the strength of synaptic transmission underlie the formation of memories. Hebb is often recognized as the first person to crystallize this

idea by proposing that coincident activity of pre- and postsynaptic neurons strengthens synaptic connections (Hebb, 1949). It was subsequently recognized that uncorrelated activity between two neurons should decrease the strength of synaptic transmission between them (Stent, 1973). The strengthening of synaptic connections is termed long-term potentiation (LTP), and is experimentally produced by high frequency stimulation (Bliss and Lomo, 1973), while the weakening of synaptic connections, produced by low frequency stimulation (Dudek and Bear, 1992; Mulkey and Malenka, 1992), is called long-term depression (LTD). Since their initial discovery, both LTP and LTD have been found to occur in a diverse set of synapses across many different brain areas [reviewed in (Malenka and Bear, 2004)]. These long lasting forms of synaptic plasticity share similar mechanisms of induction, expression, and maintenance with those of long-term consolidation of several forms of memory (Lisman, 1989; Bailey et al., 1996; Bear, 1996; Martin et al., 2000; Paulsen and Sejnowski, 2000; Bliss et al., 2003; Lynch, 2004; Barco et al., 2006; Morris, 2006). Moreover, long-term alterations in synaptic transmission, similar to characteristics of LTP and LTD, have been observed *in vivo* during various learning paradigms (Rioult-Pedotti et al., 1998; Rodrigues et al., 2004; Schafe et al., 2005; Stefan et al., 2006; Whitlock et al., 2006; Garner et al., 2012; Liu et al., 2012; Ramirez et al., 2013; Nabavi et al., 2014), which further suggests that LTP and LTD may be cellular substrates for memory formation.

While LTP and LTD are effective models for mediating synapse-specific changes required for memory formation, theoretical considerations indicate that maintaining the stability of the nervous system requires additional homeostatic plasticity mechanisms that operate at a slower time scale (hours to days) (Bienenstock et al., 1982; Bear et al., 1987; Abraham and Bear, 1996; Turrigiano et al., 1998; Turrigiano and Nelson, 2004). For example, without homeostatic regulation, the increase in postsynaptic activity after LTP might result in a vicious cycle of

potentiation that not only degrades the capacity of neural circuits to store specific information, but could also culminate in a run-away excitation of the neural network. There are several mechanisms of homeostasis that can stabilize the nervous system: adjusting excitatory synaptic transmission postsynaptically (Bienenstock et al., 1982; Bear et al., 1987; Turrigiano et al., 1998; Abbott and Nelson, 2000; Turrigiano and Nelson, 2004), modulating the excitability of neurons (Desai et al., n.d.; Aizenman et al., 2003; Maffei et al., 2004), changing inhibitory circuits (Kilman et al., 2002; Morales et al., 2002; Maffei et al., 2004, 2006), and altering presynaptic function (Burrone et al., 2002; Thiagarajan et al., 2002, 2005). While most studies of synaptic plasticity related to memory formation focus on LTP and LTD, it is prudent to understand that alterations in homeostatic plasticity can also affect learning and memory.

Section 2: Molecular mechanisms of synaptic plasticity: a brief overview

While LTP and LTD have been observed in many different brain areas, the majority of knowledge about their molecular mechanisms comes from studies in the hippocampus. This is partly because the hippocampus is an area of the brain that is critically involved in the formation of long-term memories [reviewed in (Lynch, 2004)]. In addition, the hippocampus is one of the areas highly susceptible to amyloid pathology in most AD brains [reviewed in (Walsh and Selkoe, 2004)]. Therefore, a brief review of the mechanisms of synaptic plasticity in the hippocampus is provided.

In the hippocampus, two major forms of LTP and LTD are observed: one that is dependent on NMDA receptor (NMDAR) activation and another that is independent of NMDARs (Nicoll and Malenka, 1995; Lynch, 2004). The most widely studied forms of LTP and LTD are those dependent on NMDARs in the CA1 region; hence, their mechanisms have been fairly well characterized. Therefore, most of this discussion will focus on the NMDAR-dependent forms of

LTP and LTD. NMDARs, due to activity-dependent relief of their Mg^{2+} block (Malenka and Nicoll, 1999), act as coincident detectors for pre- and postsynaptic activity. In addition, activation of NMDARs allows influx of Ca^{2+} (Connor et al., 1999; Yuste et al., 1999; Kovalchuk et al., 2000), which can act as a second messenger to activate various downstream effectors in the postsynaptic neuron. It is thought that both the magnitude and temporal pattern of Ca^{2+} increase determines the expression of either LTP or LTD, by differentially regulating the activity of protein kinases and phosphatases (Lisman, 1989). One of the key downstream events of LTP and LTD is the regulation of synaptic AMPA receptors (AMPARs) [for review see (Malinow and Malenka, 2002; Lee, 2006; Lee and Kirkwood, 2011)]. AMPARs are the major mediators of fast excitatory synaptic transmission in the central nervous system (CNS); therefore, their function directly dictates synaptic strength. Several studies demonstrated that LTP increases the synaptic content of AMPARs, predominantly by an activity-dependent insertion of receptors containing the GluA1 subunit (GluR1) (Shi et al., 1999, 2001; Hayashi et al., 2000). This requires concomitant activation of Ca^{2+}/calmodulin-dependent protein kinase II (CaMKII) and phosphorylation of the AMPAR subunit GluA1 at serine 818 (S818) (Boehm et al., 2006) and serine 845 (S845) (Esteban et al., 2003). GluA1-S818 is a protein kinase C (PKC) phosphorylation site (Boehm et al., 2006) while GluA1-S845 is a protein kinase A (PKA) phosphorylation site (Roche et al., 1996). In addition to these two sites, phosphorylation of GluA1-S831, which can be phosphorylated by both PKC (Roche et al., 1996) and CaMKII (Barria et al., 1997a; Mammen et al., 1997), has been shown to correlate with LTP (Barria et al., 1997b; Lee et al., 2000a). However, this site is not necessary for LTP (Lee et al., 2010a) nor synaptic trafficking of AMPARs (Hayashi et al., 2000). Many studies confirm that CaMKII, PKC, and PKA are involved in NMDAR-dependent LTP [reviewed in (Lee, 2006; Lu and Roche, 2012; Henley and Wilkinson, 2013)]. Consistent with a dominant role for GluA1 in mediating

synaptic potentiation, GluA1 knockout mice (Zamanillo et al., 1999), as well as mice lacking specific phosphorylation sites on GluA1 (Lee et al., 2003), display LTP deficits. On the other hand, NMDAR-dependent LTD is associated with an activity-dependent removal of synaptic AMPARs (Carroll et al., 2001). This process depends on endocytosis of GluA2-containing receptors (Lüthi et al., 1999; Daw et al., 2000; Lin et al., 2000; Man et al., 2000; Osten et al., 2000; Kim et al., 2001a; Lee et al., 2004), but also requires dephosphorylation at GluA1-S845 (Lee et al., 1998, 2000a, 2003).

While regulation of synaptic AMPARs, through synaptic targeting and phosphorylation, is involved in the initial expression of LTP and LTD, maintenance of these forms of plasticity involve additional mechanisms. Collectively, data from many studies report that blocking new protein synthesis inhibits the late phase of long-term synaptic plasticity (Krug et al., 1984; Stanton and Sarvey, 1984; Frey et al., 1988; Huber et al., 2000; Manahan-Vaughan et al., 2000; Kelleher et al., 2004). This parallels the requirement for new protein synthesis in the formation of long-term memory in intact animals (Flexner et al., 1963; Davis and Squire, 1984) [see review (Sutton and Schuman, 2006)]. Transcriptional activation is also necessary for the maintenance of some forms of long-term synaptic plasticity (Nguyen et al., 1994). So far, it is known that multiple transcription factors are activated immediately after induction of LTP. Increased transcription of several immediate early genes (IEG) is especially important (Tischmeyer and Grimm, 1999) since they enhance new protein synthesis (Lynch, 2004; Barco et al., 2006). Interestingly, some, if not all, of these transcriptional regulators are also required for long-term memory formation. Disruption of cAMP Response Element-Binding Protein (CREB) levels, a Ca^{2+}-dependent transcription factor, in either the hippocampus or the amygdala has been found to impair specific long-term memory but not initial acquisition or short-term memory formation (Guzowski and McGaugh, 1997; Lamprecht et al., 1997; Silva et al., 1998). Inhibiting the

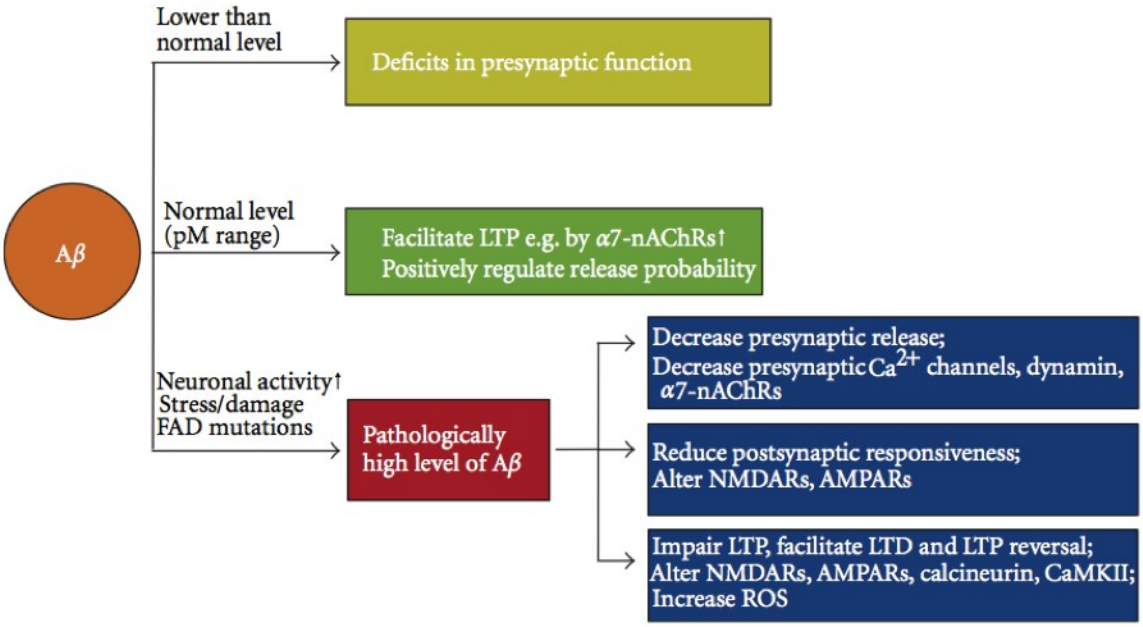

Figure 1.2. Concentration-dependent effects of Aβ on synaptic function.

At normal physiological levels (picomolar range), Aβ peptides have positive effects on synaptic function: they can positively regulate presynaptic release probability and facilitate learning and LTP in CA1 by activating α7-nAChRs. However, when the concentration of Aβ peptides is lower than normal, presynaptic function is impaired. On the other hand, under pathological conditions, such as increased neuronal activity, stress, or the presence of familial Alzheimer's disease (FAD) mutations, the increase in Aβ peptide concentration produces pathological effects, including decreased presynaptic neurotransmitter release, reduced postsynaptic responsiveness, LTP impairment, and LTD facilitation. Therefore, maintaining the concentration of Aβ peptides within a normal physiological range is essential and should be the goal for developing effective treatments for Alzheimer's disease.

expression of Arc/Arg 3.1 (activity-regulated cytoskeletal protein/activity regulated gene 3.1), an IEG, in the hippocampus also impairs long-term memory consolidation (Guzowski et al., 2000).

Section 3: Exogenous Aβ application alters synaptic function

Much of the molecular understanding of AD came from studying familial AD (FAD)-linked mutations, which have been found in genes encoding APP and presenilin 1 and 2 (PS1 and 2) in AD patients. These mutations are linked to elevated Aβ production (Scheuner et al., 1996; Lendon et al., 1997). For example, the FAD-linked APP_{swe} mutation makes APP a more favorable substrate for the amyloidogenic cleavage pathway leading to increased Aβ production. Since

FAD patients often harbor multiple mutations, many of the AD mouse models also carry several FAD mutations. However, depending on the combination of the mutations and their variants, distinct phenotypes are observed across age and brain regions studied [for an extensive recent review on electrophysiological studies of various AD transgenic (Tg) mouse models see (Marchetti and Marie, 2011)].

Although different AD mouse models show deficits in synaptic function, it cannot be taken for granted that these deficits are caused directly by the enhanced production of Aβ peptides (especially $A\beta_{42}$, which is the major component of extracellular senile plaques). In order to directly test the role of Aβ in altering synaptic function, many studies have investigated synaptic properties and synaptic plasticity following exogenous application of various Aβ peptides.

In vitro studies done in either the medial perforant path to dentate granule cells or the Schaffer collateral inputs to CA1 neurons, reported that application of subneurotoxic concentrations of Aβ peptides (i.e. $A\beta_{42}$, $A\beta_{40}$, or $A\beta_{25\text{-}35}$) inhibits LTP induction without affecting basal synaptic transmission (Chen et al., 2000, 2002; Zhao et al., 2004). A similar result was found in an *in vivo* study, where naturally secreted Aβ collected from cells expressing mutated APP (V717F mutation in APP_{751}) was injected into the CA1 region of hippocampus which prevented stable LTP maintenance (Walsh et al., 2002). This study further showed that soluble Aβ oligomers, not monomeric Aβ, or Aβ fibrils, are responsible for blocking LTP (Walsh et al., 2002). In addition, *in vivo* injection of Aβ peptides (i.e. $A\beta_{42}$ or the C-terminal of APP which contains the Aβ fragment) is reported to facilitate LTD and LTP reversal (called depotentiation) in the CA1 region (Kim et al., 2001b). A majority of studies suggest that while fibrillar Aβ accumulation is found in senile plaques that are a hallmark of AD, it is the soluble Aβ

oligomers that disturb synaptic function and lead to neurodegeneration in AD (Walsh et al., 2002; Tanzi, 2005).

Subsection 1: Postsynaptic alterations by Aβ

Soluble Aβ oligomers in AD brains have been found to bind to neuronal surfaces (Gong et al., 2003), specifically to a subset of synapses where they colocalize with a postsynaptic density marker PSD95 (Lacor et al., 2004), suggesting that Aβ may regulate postsynaptic function directly. One candidate target of Aβ is NMDARs. It was found that synthetic $A\beta_{40}$ peptides can selectively augment NMDAR currents, without affecting AMPAR currents, in the dentate gyrus of acute hippocampal slices (Wu et al., 1995). Consistent with this, APP_{Ind} (V717F mutation) Tg mice show an enhancement in the ratio of NMDAR-to-AMPAR-mediated synaptic transmission in the CA1 region (Hsia et al., 1999). However, contradictory results are reported from later studies. A recent study showed that both application of synthetic $A\beta_{42}$ peptides and naturally secreted Aβ, from APP_{Swe} (K670N/M671L mutation) Tg mice, promote endocytosis of surface NMDARs and hence depress NMDAR currents in wild type cultured cortical neurons (Snyder et al., 2005). Moreover, they also found reduced surface expression of NMDARs in cultured cortical neurons from APP_{Swe} Tg mice (Snyder et al., 2005). Other studies found down-regulation of surface AMPARs in neurons overexpressing either wild type or $APP_{Swe,}$ or when wild type neurons were treated with exogenous $A\beta_{42}$ peptides (Almeida et al., 2005; Hsieh et al., 2006). This is mediated not only by endocytosis of synaptic AMPARs via mechanisms shared by LTD (Hsieh et al., 2006), but also through a reduction in basal levels of GluA1-S845 phosphorylation by activating the calcium-dependent phosphatase, calcineurin, as well as interrupting extrasynaptic delivery of AMPARs (Miñano-Molina et al., 2011). Contradictory results on the effects of Aβ on AMPAR and NMDAR regulation may be due to several variables. First, there is evidence that $A\beta_{40}$ and $A\beta_{42}$ peptides may have distinct functions in AD pathology.

For example, a majority of FAD-linked PS1 mutations cause a reduction in $A\beta_{1-40}$ peptides and therefore an increase in the $A\beta_{42}/A\beta_{40}$ ratio (Borchelt et al., 1996; Thinakaran and Sisodia, 2006). Second, there are differences in experimental preparations. Both Wu et al. (Wu et al., 1995) and Hsia et al. (Hsia et al., 1999) were working with acute adult hippocampal slices, while Snyder et al. (Snyder et al., 2005), Almeida et al. (Almeida et al., 2005), Hsieh et al. (Hsieh et al., 2006) and Minano-Molina et al. (Miñano-Molina et al., 2011) were using either cultured neurons from embryonic mice or organotypic hippocampal slice cultures prepared from early postnatal mice. Third, the presence or absence of APP itself may have also affected the results. Indeed, there is evidence that uncleaved full-length APP may promote synapse formation and enhance excitatory synaptic function [see (Hoe et al., 2012) for a recent review].

In any case, Aβ mediated alterations in NMDAR function suggests that Aβ will affect downstream Ca^{2+}-dependent signaling pathways. Calcineurin, a Ca^{2+}-activated protein phosphatase, may be one of the downstream signaling molecules affected by Aβ, since it is required for the inhibition of perforant pathway LTP (Chen et al., 2002), endocytosis of surface AMPARs (Hsieh et al., 2006), as well as dephosphorylation of GluA1-S845 (Miñano-Molina et al., 2011). In addition to activating calcineurin, Aβ prevents the activation of CaMKII, a Ca^{2+}-dependent protein kinase necessary for LTP, and decreases the synaptic clustering of CaMKII, which correlates with a reduction in the phosphorylation of GluA1-S831, surface expression of GluA1, and AMPAR mediated EPSCs (Zhao et al., 2004; Gu et al., 2009). Together, these data are consistent with the idea that Aβ oligomers impair LTP and facilitate LTD (Lee et al., 2000a; Knobloch et al., 2007; Li et al., 2009).

Aβ has also been found to modify regulation of gene expression. Aβ peptides have been found to alter CREB signaling, causing synaptic dysfunction and memory deficits [reviewed in (Saura and Valero, 2011)]. In addition, treating cultured hippocampal neurons with soluble Aβ

oligomers induces rapid expression of the IEG Arc/Arg 3.1 (Lacor et al., 2004), which is implicated in synaptic plasticity (Guzowski et al., 2000; Steward and Worley, 2001; Shepherd et al., 2006). Because overexpression of Arc/Arg 3.1 causes learning deficits (Guzowski, 2002), possibly via reducing surface expression of GluA1-containing AMPARs (Shepherd et al., 2006), this would suggest that Aβ oligomer-induced Arc/Arg3.1 expression may in fact interfere with normal synaptic plasticity. However, this study is seemingly at odds with the results of Echeverria and colleagues, which reported a strong inhibition of BDNF-induced increase in Arc expression in cultured cortical neurons treated with Aβ oligomers (Echeverria et al., 2007). Similarly, there is also a report that synaptic plasticity related genes, including Arc/Arg3.1, are reduced in transgenic mice expressing FAD-linked mutations in APP and PS1 (Dickey et al., 2003). The apparent differences in Arc expression caused by Aβ could be due to different experimental systems, or to the differential effects of different concentrations of Aβ oligomers.

Subsection 2: Presynaptic alterations by Aβ

Besides influencing postsynaptic function, Aβ is also implicated in presynaptic modifications. A recent study reported that 8 nM $A\beta_{42}$ globulomer (a highly stable globular oligomeric Aβ) could directly inhibit presynaptic P/Q type Ca^{2+} channels and decrease vesicle release (Nimmrich et al., 2008). Moreover, application of synthetic Aβ to cultured hippocampal neurons causes a down-regulation of dynamin, a protein critical for synaptic vesicle endocytosis, and interrupts synaptic vesicle recycling (Kelly et al., 2005; Kelly and Ferreira, 2007). This result is consistent with the observed reduction in dynamin levels in human AD brains (Yao et al., 2003). These findings may explain the observation that $A\beta_{42}$ globulomer causes a decrease in basal synaptic transmission at the Schaffer collateral to CA1 synapses in hippocampal slice culture (Nimmrich et al., 2010). Recently, Kelly et al. reported that the reduction in dynamin is dependent on Ca^{2+} influx through activated NMDARs as well as activation of a calcium-activated

intracellular cysteine protease, calpain (Kelly et al., 2005; Kelly and Ferreira, 2006). These results not only suggest that there may be retrograde signaling from postsynaptic to presynaptic terminals, but also establish an interesting relationship between Aβ, NMDARs and calpain. It has been found that $A\beta_{42}$ peptides can activate calpain-mediated cleavage of p35 to p25 (Lee et al., 2000b), which then upregulates mRNA and protein expression of β-secretase (BACE1) (Wen et al., 2008; Liang et al., 2010), a critical enzyme for Aβ formation (discussed in the following sections). This indicates that there is a positive feedback between Aβ production and calpain activation. Calpain inhibitors can fully prevent deficits in basal synaptic transmission caused by Aβ globulomer application in hippocampal slice culture to a comparable level as using an NMDAR antagonist memantine (Nimmrich et al., 2010). This suggests that Aβ acts through NMDARs and calpain: a potential signaling cascade being NMDAR-medicated Ca^{2+} influx activating intracellular calpain, which then promotes p25/cdk5 dependent transcription of downstream genes, including BACE1 (Wen et al., 2008).

Subsection 3: Other targets of Aβ that affect synaptic plasticity

Recent studies suggest that the α7-nicotinic acetylcholine receptor (α7-nAChR), a Ca^{2+}-permeable homopentameric ion channel highly expressed in the hippocampus and cerebral cortex (Séguéla et al., 1993), is another potential target of Aβ. High affinity binding between $A\beta_{42}$ peptides and α7-nAChRs (Wang et al., 2000a, 2000b) either inhibit (Guan et al., 2001; Liu et al., 2001a; Pettit et al., 2001; Chen et al., 2006) or activate α7-nAChR signaling (Dineley et al., 2001). It is possible that $A\beta_{42}$ peptides may facilitate α7-nAChRs at low concentrations, but may inhibit α7-nAChRs when the burden of Aβ increases (Dineley et al., 2001; Dougherty et al., 2003). This concentration-dependent role of Aβ peptides is suggested from studies showing that at normal concentrations (picomolar range), Aβ peptides positively regulate presynaptic release at hippocampal synapses and facilitate CA1 LTP and learning by activating α7-nAChRs; whereas

when the level of Aβ is low or high (nanomolar range), Aβ peptides cause either deficits in presynaptic function or abolish hippocampal LTP and learning via its interaction with α7-nAChRs (Puzzo et al., 2008; Abramov et al., 2009; Palop and Mucke, 2010a).

Moreover, the concentration-dependent effect of Aβ is also reflected by its ability to regulate reactive oxygen species (ROS). ROS have been found to have physiological roles in maintaining normal synaptic plasticity. However, high levels of ROS have been found in both AD animal models and human patients, leading to oxidative damage related to AD pathology [reviewed in (Massaad and Klann, 2011)]. Recently, Ma and colleagues found that exogenous treatment of $A\beta_{42}$ (500 nM) increased mitochondria superoxide, which they reported is a cause of synaptic dysfunction induced by Aβ. In particular, decreasing mitochondrial superoxide levels reversed Aβ-induced CA1 LTP impairments (Ma et al., 2011). Given the normal physiological role of Aβ and ROS at intermediate levels, this finding suggests that ROS imbalance, caused by Aβ toxicity, may lead to synaptic dysfunction in AD. It also implies that Aβ levels exceeding the normal range may initiate the abnormalities in synaptic function (Fig 1.2).

In summary, pathologically high levels of Aβ can disturb the ROS balance and interfere with both pre- and postsynaptic function, presumably by affecting NMDARs, presynaptic P/Q Ca^{2+} channels, and/or α7-nAChRs, thereby interrupting subsequent Ca^{2+} signaling leading to altered synaptic function.

Section 4: Neuronal activity can regulate APP processing and Aβ levels

Data from both transgenic mice and exogenous Aβ application studies suggest that alterations in Aβ levels change neuronal activity and synaptic function. *In vivo* two-photon Ca^{2+} imaging of APP23xPS45 mice showed that cortical neurons near amyloid plaques are hyperactive, while the percentage of hypoactive cortical neurons is enhanced at locations further

away from a plaque (Busche et al., 2008, 2012). The disparate change in neuronal activity caused by the location of a neuron relative to amyloid plaques may reflect differences in local Aβ concentration. It is now evident that neuronal activity itself can also regulate APP processing leading to alterations in Aβ production. In 1993, a study reported that electrical stimulation not only increases neurotransmitter release in rat hippocampal slices, but also enhances the release of APP cleavage products (Nitsch et al., 1993). In agreement with this finding, ten years later, Kamenetz and colleagues (Kamenetz et al., 2003) found that neuronal activity can bidirectionally control Aβ levels in organotypic hippocampal slice cultures from APP_{Swe} Tg mice. Blocking neuronal activity in this preparation by tetrodoxin (TTX) treatment reduced Aβ levels, while increasing neuronal activity with picrotoxin (PTX) enhanced Aβ secretion (Kamenetz et al., 2003). The experimental paradigm used by Kamenetz et al. to manipulate neuronal activity is reported to produce homeostatic synaptic plasticity termed "synaptic scaling" (Turrigiano et al., 1998), which globally up- or down-regulates all excitatory synapses following prolonged decrease or increase, respectively, in neuronal activity (Turrigiano and Nelson, 2004). Indeed, a recent paper from our lab showed that the absence of Aβ in mice lacking BACE1 (β-secretase) result in an inability to appropriately scale synapses in response to experience-dependent changes in activity (Petrus and Lee, 2014). This suggests that Aβ may play a role in regulating homeostasis of excitatory synapses in normal brains. In addition, the cellular mechanism responsible for regulating APP processing and Aβ production in response to neuronal activity, is possibly through enhancing the accessibility of APP to γ-secretase cleavage (Kamenetz et al., 2003) and/or depressing γ-secretase function (Lesné et al., 2005). It has recently been shown that PS1, the catalytic subunit of the γ-secretase complex, is necessary to scale up excitatory synapses following reduced network activity and that PS1 knockout mice show deficits in synaptic scaling (Pratt et al., 2011b). Moreover, Wu and colleagues have reported that the immediate early gene

Arc is required for the activity-dependent increase in Aβ production (Wu et al., 2011). They found that Arc directly binds the N terminus of PS1 and plays an important role in trafficking the γ-secretase complex to early endosomes where APP is processed through the amyloidogenic pathway to produce Aβ peptides. In addition, Arc contributes to Aβ levels and plaque load in APPswe;PS1deltaE9 mice, and Arc expression is elevated in the medial frontal cortex of AD patients (Wu et al., 2011). These results provide a cellular mechanism coupling Aβ generation to neuronal activity, and may explain why people who suffer from hypoxia, which usually causes an abnormal enhancement in neuronal activity (Talos et al., 2006), have a higher risk for developing AD (Desmond et al., 2002).

Consistent with the idea that Aβ induces homeostatic adaptation to increases in activity, *in vivo* studies have also shown that either electrical stimulation or endogenous whisker activity proportionally regulate interstitial fluid (ISF) Aβ levels in Tg2576 mice, which overexpress human APP carrying the Swedish (K670N/M671L) mutation (Cirrito et al., 2005, 2008; Bero et al., 2011). However, there are also contradictory results. Tampellini et al. have shown that synaptic activity decreases intracellular Aβ in primary neuronal culture, as well as in the barrel cortex of 4-month old Tg19959 mice, which overexpress human APP carrying the Swedish (K670N/M671L) and Indiana (V717F) mutations (Li et al., 2004), likely by enhancing Aβ degradation (Tampellini et al., 2009). Zhang et al. have reported that prolonged olfactory deprivation facilitates amyloid plaque deposition in the olfactory bulb and piriform cortex of 7-24-month old Tg2576 mice (Zhang et al., 2010c). These contradictions may be due to age, region, and paradigm differences. Another possibility is that normal neuronal activity regulates Aβ levels by balancing Aβ release and degradation, and that either hyperactivity or hypoactivity may break this balance leading to Aβ accumulation.

Section 5: Physiological roles of APP and Aβ

Proteolytic processing of APP not only produces Aβ peptides, but also other products. Some functions of these products have been identified [reviewed in (Pearson and Peers, 2006; Chow et al., 2010; Zhang et al., 2011)]. For example, the cytoplasmic tail of APP, APP intracellular domain (AICD), is shown to participate in transcriptional regulation (Cao and Südhof, 2001). To evaluate other normal physiological roles of APP, mice lacking APP were generated. APP knockouts show enhanced excitatory synaptic activity and neurite growth (Priller et al., 2006), which is consistent with the finding that APP-deficient mice are more susceptible to glutamate-induced toxicity (Steinbach et al., 1998). Similar to APP, Aβ peptides also have normal physiological functions. Normal levels (picomolar range) of Aβ peptides regulate synaptic function by positively increasing presynaptic release at hippocampal synapses and facilitating learning and LTP in CA1 (Puzzo et al., 2008; Abramov et al., 2009; Palop and Mucke, 2010a). Moreover, normal levels of Aβ may be essential for neurons, because preventing Aβ production by adding β- or γ-secretase inhibitors in cultured neurons causes cell death, which can be rescued by applying synthetic Aβ peptides to culture medium (Plant et al., 2003). In addition, activity-dependent changes in Aβ may in fact play a role in maintaining homeostasis by acting as a negative feedback regulator of excitatory synaptic transmission (Kamenetz et al., 2003).

Collectively, these data suggest that proteolytic processing of APP and the presence of a normal physiological dose of Aβ may be required for maintaining proper neuronal activity and brain function. While the therapeutic benefits of targeting APP processing and Aβ production are still attractive, it should be noted that AD pathology is most likely triggered only when Aβ levels exceed the normal range, and that the physiological processing of APP and Aβ production may be important in maintaining normal brain functions. Therefore, partial inhibition, but not complete blockade, of Aβ production might be a useful approach for AD therapeutics. A recent study

supports this view. Immunizing APP_{Ind} Tg mice against Aβ, which lowered Aβ levels, decreased senile plaque formation, and rescued loss of neuronal integrity seen previously in aged mice (Buttini et al., 2005). However, Aβ-immunotherapy in clinical trials reported severe complications, which must be overcome [for review articles on this topic please see (Schenk et al., 2001; Lemere, 2009; Town, 2009; Spencer and Masliah, 2014)].

Section 6: Role of BACE1 in synaptic function

As mentioned above, Aβ peptides are generated by sequential cleavage of APP by β- and γ-secretase (Fig 1.1). In the brain, BACE1, a transmembrane aspartic protease, has been found to be the major neuronal β-secretase (Vassar et al., 1999; Cai et al., 2001; Luo et al., 2001; Roberds et al., 2001). Mice lacking the BACE1 gene show no β-secretase activity and essentially no Aβ ($Aβ_{40}$ and $Aβ_{42}$) production in the brain compared to wild type littermates. Initial characterization of BACE1 knockouts (BACE1 -/-) showed that they are viable and fertile, with no gross differences in behavior or development (Cai et al., 2001; Luo et al., 2001; Roberds et al., 2001; Ohno et al., 2004). Furthermore, knocking out the BACE1 gene in mouse models of AD was able to rescue hippocampus-dependent memory deficits (Ohno et al., 2004, 2006; Laird et al., 2005) and ameliorate impaired hippocampal cholinergic regulation of neuronal excitability (Ohno et al., 2004). These findings were quite encouraging and suggested that BACE1 may be a good therapeutic target for treating AD (Citron, 2002, 2004a, 2010; Vassar, 2002).

However, recent studies have found that BACE1 has normal physiological functions in synaptic transmission and plasticity in both CA1 and CA3 regions of the hippocampus (Table 1.1). Laird et al. found that BACE1 -/- mice display deficits in both synaptic transmission and plasticity at the hippocampal Schaffer collateral to CA1 synapses (Laird et al., 2005). While BACE1 -/- mice display normal AMPAR- and NMDAR-mediated synaptic transmission, these

synapses show a larger paired-pulse facilitation (PPF) ratio compared to wild type littermates when tested with paired-pulse stimuli at a 50 ms interstimulus interval (Laird et al., 2005). Changes in PPF ratio are linked to alterations in presynaptic function (Manabe et al., 1993). Therefore, the increase in PPF ratio observed in BACE1 -/- mice indicates a reduction in presynaptic function, which is consistent with the high expression of BACE1 in presynaptic terminals (Laird et al., 2005). In addition to reflecting presynaptic changes, recent data suggest that alterations in PPF ratio can also be caused by postsynaptic modifications, such as by varying the subunit composition of AMPARs (Rozov et al., 1998). Therefore, it is possible that knockout of BACE1 may also affect postsynaptic AMPAR function. Besides alterations in PPF ratio, BACE1 -/- mice also showed a larger de-depression (reversal of LTD) induced by high frequency theta burst stimulation (TBS) at the Schaffer collateral inputs to CA1 (Laird et al., 2005). In contrast, the same TBS protocol induced-LTP remained unchanged (Laird et al., 2005). As LTP and de-depression have separate underlying mechanisms (Lee et al., 2000a), these data suggest BACE1 may play a regulatory role in the de-depression pathway, while not affecting the mechanisms that lead to LTP. Laird and colleagues also found evidence that the enhanced de-depression is due to larger summation of responses during TBS, specifically following LTD induction. Enhanced summation of synaptic responses during the induction of de-depression despite normal basal synaptic transmission suggests that BACE1 may play a specific role in activity-dependent high frequency information transfer across synapses. Also, the abnormal increase in the magnitude of de-depression reflects that LTD expression may be easily disrupted when knocking out BACE1, which could interfere with memory formation and storage. Consistent with this interpretation, detailed behavioral studies of BACE1 -/- mice reported problems in both cognitive and emotional memory tests (Harrison et al., 2003; Laird et al., 2005; Ma et al., 2007).

Although the majority of studies characterizing synaptic function of BACE1 -/- mice have been performed in the CA1 region of the hippocampus (Ohno et al., 2004; Laird et al., 2005; Ma et al., 2007), the expression of BACE1 is most prominent in the mossy fiber terminals that synapse onto CA3 pyramidal neurons (Laird et al., 2005; Zhao et al., 2007). Recently, our lab reported that BACE1 -/- mice display severe deficits in presynaptic function at these synapses, including a reduction in presynaptic release and an absence of mossy fiber LTP, which is normally expressed by a long-term increase in presynaptic release (Wang et al., 2008; Nicoll and Schmitz, 2005).

Moreover, BACE1 -/- mice exhibited a slightly larger mossy fiber LTD, which could not be reversed (Wang et al., 2008). These results suggest that BACE1 function is crucial for normal synaptic transmission and activity-dependent presynaptic potentiation at these synapses. We further found evidence that the presynaptic dysfunction in BACE1 -/- mice is likely at the level of presynaptic Ca^{2+} signaling, because the mossy fiber LTP deficit in BACE1 -/- mice could be recovered by increasing the extracellular Ca^{2+} concentration. This suggests that the signaling downstream of Ca^{2+} is more or less intact in BACE1 -/- mice, which was confirmed by the fact that the magnitude of presynaptic potentiation resulting from direct activation of the cAMP signaling pathway is normal in BACE1 -/- mice (Wang et al., 2008). Therefore, it is possible that manipulations that enhance presynaptic Ca^{2+} may overcome the synaptic deficits caused by inhibiting BACE1 activity. In line with this, our lab recently showed that activation of Ca^{2+}-permeable α7-nAChRs, by nicotine or α7-nAChRs agonist, can restore PPF ratio and mossy fiber LTP in BACE1 -/- mice (Wang et al., 2010). The cellular mechanism of nicotine-induced rescue is dependent on the recruitment of Ca^{2+}-induced Ca^{2+}-release (CICR) from intracellular Ca^{2+} stores through ryanodine receptors (Wang et al., 2010). These results suggest that nicotine and

α7-nAChR agonists may be a potential pharmacological means to circumvent the synaptic dysfunctions caused by BACE1 inhibition.

Since synaptic deficits are seen in both the CA1 and CA3 regions of BACE1 -/- mice, it indicates that BACE1 may play a general role in regulating presynaptic function. Reduced Aβ levels have been shown to produce deficits in presynaptic function (Abramov et al., 2009), which may explain the synaptic phenotype seen in BACE1 -/- mice. However, whether presynaptic deficits in BACE1 -/- mice are solely due to a lack of APP processing is unclear. An alternative possibility is that the synaptic dysfunction seen in BACE1 -/- mice may arise from abnormal processing of substrates other than APP (Fig 1.3).

It has been shown that the auxiliary β2 subunit of the voltage-gated sodium channel (Na_v1), is a substrate of BACE1 (Wong et al., 2005; Kim et al., 2007). The β2 subunit of the Na_v1 channel is important for plasma membrane expression of functional Na^+ channels, which are critical for generating action potentials. Among the ten different types of Na_v1 channels, $Na_v1.1$, $Na_v1.2$, $Na_v1.3$ and $Na_v1.6$ are expressed mainly in the CNS (Lai and Jan, 2006). BACE1 regulates the surface expression of these types of Na_v1 channels by cleaving the β2 subunit. In transgenic mice overexpressing BACE1, there is an increase in the $Na_v1.1$ α-subunit mRNA and protein levels, but a decrease in the surface expression of functional $Na_v1.1$ channels due to cleavage of the β2 subunits (Kim et al., 2007; Kim and Kovacs, 2011). The interpretation is that the full-length β2 subunit promotes surface expression of $Na_v1.1$ channels, but the β2-intracellular domain (ICD), which is produced by a sequential cleavage by BACE1 and γ-secretase, increases transcription of the $Na_v1.1$ α-subunit gene. Consistent with this, BACE1 -/- mice display a decrease in $Na_v1.1$ α-subunit mRNA and protein (Kim et al., 2011). However, there is a compensatory increase in the surface expression of $Na_v1.2$ in BACE1 -/- mice, which correlates with the hyperexcitability and seizure phenotypes seen in these mice (Hu et al., 2010). These

results suggest that the ability of BACE1 to regulate the Na_v1 family of Na^+ channels is rather complex, but suggests a role for BACE1 in regulating neuronal excitability.

Another candidate substrate for BACE1 is neuregulin-1 (NRG1), which is an axonal signaling molecule critical for regulating myelination (Lemke, 2006). Willem and colleagues found that BACE1 -/- mice show hypomyelination in the peripheral nerves (Willem et al., 2006), while another study detected loss of myelination in the central nerves (Hu et al., 2006b). Both of these studies showed an accumulation of unprocessed NRG1 and a reduction in its cleavage products, suggesting that NRG1 is a potential substrate for BACE1 cleavage and that this process is important for myelination of axons (Hu et al., 2006b; Willem et al., 2006). Recently, it has been shown that the absence of NRG1 processing in BACE1 -/- mice decreased postsynaptic function of ErbB4, a receptor for NRG1 (Savonenko et al., 2008). NRG1/ErbB4 signaling has been suggested to regulate synaptic function and plasticity, mainly via regulation of postsynaptic glutamate receptors (Huang et al., 2000; Gu et al., 2005; Li et al., 2007). Additionally, abnormal processing of NRG1 may also affect presynaptic release by regulating the expression of α7-nAchRs (Liu et al., 2001b; Zhong et al., 2008) which allows Ca^{2+} influx. Indeed, presynaptic nAchRs can increase glutamate release (McGehee et al., 1995; Gray et al., 1996; Maggi et al., 2003), likely via the α7 containing nAchRs (Le Magueresse et al., 2006). These results suggest that a lack of NRG1 cleavage resulting from BACE1 inhibition can alter synaptic function both pre- and postsynaptically.

Accumulating data on the biological roles of BACE1, particularly evidence that complete inhibition of BACE1 activity has a deleterious effect on normal neuronal function, suggests caution for using BACE1 inhibitors as a treatment for AD. In order to improve the development of effective therapeutics that target this enzyme, we need to identify ways to avoid the synaptic dysfunction associated with complete knockdown of BACE1, which may include partial

Table 1.1: Summary of known synaptic effects of altering BACE1.

	Age	Aβ	Basal synaptic transmission	Presynaptic function	LTP	LTD	Reference
BACE1 KO	3 – 6mo	No $A\beta_{40}$ or $A\beta_{42}$	Normal (CA1 and CA3)	Increased PPF ratio (CA1 and CA3)	Normal LTP (4x TBS) but larger dedepression in CA1; no mossy fiber LTP (3x 100 Hz) and no dedepression in CA3	Normal LTD (paired- pulse 1Hz) in CA1, but slightly larger LTD (paired-pulse 1 Hz) in CA3	(Laird et al., 2005; Wang et al., 2008)
BACE1 KO + activation of α7-nAChRs	3 – 6mo	No $A\beta_{40}$ or $A\beta_{42}$	Normal (CA3)	Restored PPF ratio (CA3)	Rescued mossy fiber LTP (CA3) (3x 100 Hz)		(Wang et al., 2010)
$BACE1^{+/-}$; 5XFAD (Tg6799)	6 mo	66% decrease in $A\beta_{40}$ and 57% in $A\beta_{42}$ in brain; reduced amyloid burden in hippocampus by 78% and anterior cingulate cortex by 44%	Remained reduced (CA1)		Restored LTP to WT control levels (CA1) (3x TBS)		(Kimura et al., 2010)
Adenoviral-Fbx2* in Tg2576	12 - 14 mo	30% decrease in $A\beta_{42}$	No change		Improved the impaired LTP (CA1) (3x TBS) 4 weeks after adenoviral injection		(Gong et al., 2010)

inhibition strategies.

Subsection 1: Partial inhibition or conditional knockdown of BACE1

It has been shown that Aβ burden is dose-dependent on BACE1 activity; therefore, partial inhibition or conditional knockdown of BACE1 may be beneficial for AD treatment. To test this, Kimura and colleagues crossed BACE1 heterozygous mice with a line of transgenic mice carrying a combination of 5 FAD-linked mutations in human APP and PS1 (5XFAD). They found that partial reduction of BACE1 improved remote and recent memory and restored CA1 LTP (Kimura et al., 2010). Researchers have also successfully suppressed BACE1 activity by using RNA interference (RNAi) *in vitro* (Kao et al., 2004; Hu et al., 2006a) and *in vivo* (Laird et al., 2005; Singer et al., 2005). Lentiviral BACE1 siRNA delivered into the hippocampus has been found to effectively reduce Aβ production, neurodegeneration, and behavioral deficits in APP transgenic mice (Laird et al., 2005; Singer et al., 2005). Characterizing synaptic function in the BACE1 siRNA knockdown models may provide information about acute effects of inhibiting BACE1 function. In addition, siRNA knockdown of BACE1 in APP transgenic lines will better approximate clinical situations, hence allowing us to better estimate the feasibility of developing an effective treatment for AD using BACE1 inhibition.

Subsection 2: BACE1 inhibitors

Since the identification of BACE1, the development of BACE1 inhibitors has been initiated. However, the progress was slow, likely due to the difficulty of identifying small molecules that could bind and inhibit the large catalytic pocket of BACE1, penetrate the blood brain barrier, maintain high stability, and possess good pharmacokinetics (Citron, 2004b; Ghosh et al., 2008a). To date, numerous BACE1 inhibitors have been discovered, but not many have been able to advance in human clinical trials due to toxicity concerns [see review (Ghosh et al., 2008a; Luo and Yan, 2010; Yan and Vassar, 2014)]. MK-8931 has advanced the farthest to Phase

2/3 clinical trials, which are expected to conclude in 2017 and 2018 (Yan and Vassar, 2014). Many BACE1 inhibitors have been shown to decrease soluble Aβ production, amyloid plaque deposition, as well as improve cognitive function in AD animal models (Hussain et al., 2007; Ghosh et al., 2008c; Fukumoto et al., 2010; Takahashi et al., 2010; Zhu et al., 2010; Chang et al., 2011). Surprisingly, none of them have been tested to determine their ability to improve synaptic dysfunction, the cellular mechanism that correlates with cognitive decline. A critical question is whether these inhibitors can recover synaptic deficits seen in AD models, or whether they may produce additional defects as seen in BACE1 -/- mice.

Subsection 3: Transcriptional and miRNA regulation of BACE1

There are several reports of transcriptional regulation of BACE1. Nie et al. have shown that activation of α4β2 nAChR can decrease BACE1 transcription through the ERK1-NFκB pathway *in vitro* (Nie et al., 2011); Wen and colleagues reported that overexpression of p25, an

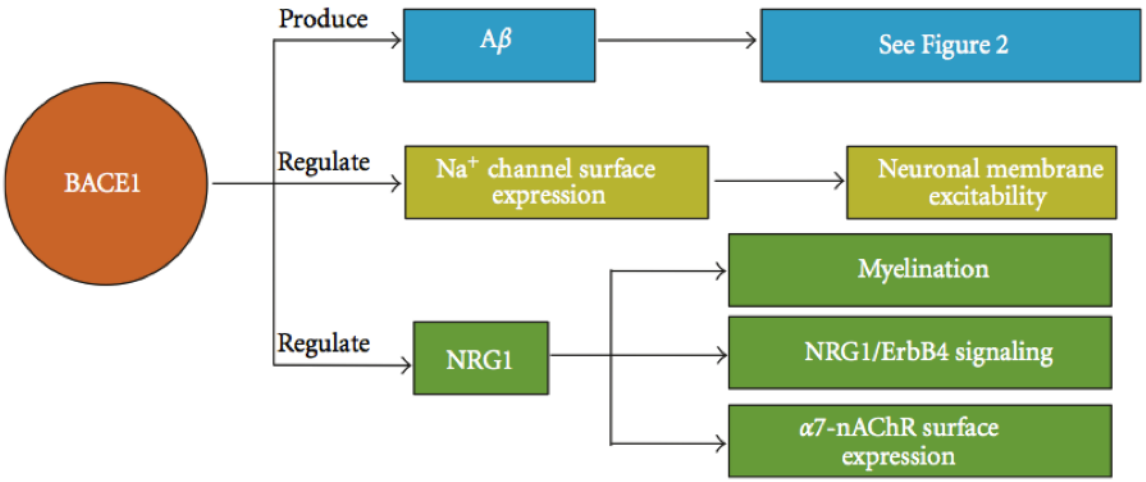

Figure 1.3. The roles of BACE1 in synaptic function.

Besides cleaving APP to produce Aβ peptides, BACE1 has been found to have other substrates. It can process the β2 subunit of the voltage-gated sodium (Na+) channels, which can regulate Na+ channel surface expression and in turn modulate neuronal excitability. In addition, BACE1 can cleave NRG1, which plays a crucial role in myelination and NRG1/ErbB4 signaling. Recently, it has been showed that NRG1 can regulate cell surface expression of α7-nAChRs, which can also affect synaptic transmission.

activator of cdk5, can increase BACE1 mRNA and protein levels likely through interactions of signal transducer and activator of transcription (STAT3) with the BACE1 promoter (Wen et al., 2008). In addition, in the brains of sporadic AD patients, an increase in BACE1 levels is correlated with a decrease in a subset of microRNAs (miRNA), especially the miR-29a/b-1 miRNA cluster (Hébert et al., 2008). miRNAs regulate mRNA translation. Therefore, it is possible that an increase in specific miRNA levels can decrease BACE1 protein expression and decrease Aβ burden. These findings provide various ways to regulate BACE1 expression.

Subsection 4: Endogenous BACE1 activity modulators

Recently, studies have shown that during sporadic AD or in AD animal models, the activities of certain endogenous molecules are modified, causing an increase in BACE1 activity. For example, sphingosine-1-phosphate (S1P) phosphorylation of the translation initiation factor eIF2α and calpain activity are increased in AD, which can lead to an increase in BACE1 activity (O'Connor et al., 2008; Liang et al., 2010; Nimmrich et al., 2010; Ill-Raga et al., 2011; Takasugi et al., 2011). On the other hand, decreased activity in conjugated linoleic acid (CLA), acetylcholinesterase inhibitor galantamine (Gal), copper chaperone for superoxide dismutase (CCS), PPARγ co-activator-1α (PGC-1α), the trafficking molecule GGA3, as well as Fbx2-E3 ligase during AD can lead to increased BACE1 protein levels (Tesco et al., 2007; Sarajärvi et al., 2009; Gong et al., 2010; Gray et al., 2010; Kang et al., 2010; Li et al., 2010, 2011; Katsouri et al., 2011). So far, only the effect of Fbx2 on synaptic plasticity has been tested. Adenoviral-Fbx2 transfection significantly improves CA1 LTP in Tg2576 mice without affecting basal synaptic transmission (Gong et al., 2010). While these molecules may be potential targets for controlling BACE1 activity, further studies need to verify whether synaptic function can be improved by manipulating the activity of these BACE1 modulators.

Section 7: Presenilin: its physiological roles and relationship with Alzheimer's disease

Presenilin 1 (PS1) is the catalytic component of the γ-secretase complex. Following BACE1 cleavage, γ-secretase cleaves the transmembrane domain of APP, releasing Aβ peptides (Fig 1.1). The active γ-secretase complex is composed of four different proteins, all of which are required for the protease to function [for a good review on the composition of γ-secretase, see (De Strooper, 2003)]; however, PS1 receives the most attention stemming from its identification as the major locus for early onset FAD (Sherrington et al., 1995). Since the accumulation and deposition of extracellular Aβ has been emphasized in the progression of AD (Tanzi, 2005), the identification of several FAD-linked mutations in PS1 led to many studies investigating how dysfunction of this protein contributes to AD. FAD-linked mutations in PS1 facilitate the production of the more pathogenic $A\beta_{42}$ peptide (Borchelt et al., 1996; Scheuner et al., 1996), which is the major constituent of senile plaques found in the brains of AD patients. This section will briefly summarize the functions of presenilins and focus on how they play a role in normal synaptic regulation and also during AD. Key points are summarized in Table 1.2.

To investigate the normal physiological functions of PS1, many genetic knockout experiments have been conducted. Knockout of PS1 causes abnormal development and perinatal death (Shen et al., 1997; Wong et al., 1997; De Strooper et al., 1998; Donoviel et al., 1999; Marjaux et al., 2004). FAD-linked mutations have also been discovered in Presenilin 2 (PS2), which is highly similar to PS1 in both sequence and structure (Levy-Lahad et al., 1995); however, PS2 knockout mice are viable and fertile with only mild age-dependent pulmonary fibrosis and hemorrhage (Herreman et al., 1999). This suggests PS1 is sufficient to maintain the majority of regular physiological activities and that these two homologs share little overlapping function. Another study using PS1+/-;PS2-/- mice found that they could live normally until 6- months of age, after which most developed an autoimmune disease and benign skin hyperplasia

Table 1.2: Summary of alterations in synaptic function by altering presenilin or γ-secretase activity.

	Age	Aβ	Basal synaptic transmission	Presynaptic function	LTP	LTD	Other	Reference
PS1 cKO	3 – 6 mo	Cortical $A\beta_{40}$ and $A\beta_{42}$ are decreased	Normal (CA1)	Normal PPF ratio (CA1)	Normal (CA1) (5xTBS) Normal (CA1) (3x100 Hz)	Normal (CA1)		(Yu et al., 2001)
PS cDKO	2 mo		Normal (CA1)	Decreased PPF ratio (CA1)	Decreased (CA1) (5xTBS)	Normal (CA1)	Reduced NMDAR function (CA1); decreased cortical synaptic levels of NR1, NR2A, αCaMKII, and CRE-dependent genes	(Saura et al., 2004)
	6 mo		Increased (CA1)	Decreased PPF ratio (CA1)	Decreased (CA1) (5xTBS)	Normal (CA1)		
	2 mo						Increased expression of the NR2A subunit of NMDARs, specifically at postsynaptic density and presynaptic terminals of axo/dendritic synapses, trapped at synapses (CA1)	(Aoki et al., 2009)
	5 wk			Decreased CA^{2+}-dependent frequency facilitation and release probability (CA1)	Normal (CA1) (5xTBS)		Normal NMDAR-mediated synaptic response (CA1)	(Zhang et al., 2010a)
	6 wk				Decreased (CA1) (5xTBS)		Reduced NMDAR-mediated synaptic response (CA1)	

Table 1.2: Continued.

	Age	Aβ	Basal synaptic transmission	Presynaptic function	LTP	LTD	Other	Reference
CA1-PS cDKO	2 mo			Normal (CA1)	Normal (CA1) (5xTBS)		Normal NMDAR/AMPAR ratio	(Zhang et al., 2009)
CA3-PS cDKO	2 mo			Decreased CA^{2+}-dependent frequency facilitation and release probability (CA1)	Decreased (CA1) (5xTBS)		Normal NMDAR/AMPAR ratio	(Zhang et al., 2009)
AppTg (Swe/Ind)	3 mo	Age dependent increase in Aβ levels and plaque deposition	Normal (CA1)	Normal (CA1)	Increased (CA1) (5xTBS)			(Saura et al., 2005)
	6 mo		Decreased (CA1)	Normal (CA1)	Decreased (CA1) (5xTBS)			
AppTg; $PS1^{-/-}$	3 mo	Decreased cortical Aβ peptides and plaque formation	Normal (CA1)	Normal (CA1)	Increased (CA1)			(Saura et al., 2005)
	6 mo		Decreased (CA1)	Normal (CA1)	Decreased (CA1) (5xTBS)			

Table 1.2: Continued.

	Age	Aβ	Basal synaptic transmission	Presynaptic function	LTP	LTD	Other	Reference
Tg2576	3 – 4 mo		Normal (CA1)		Normal (CA1)			(Townsend et al., 2010)
	6 – 7 mo	50% increase in soluble Aβ	Decreased (CA1) – stronger stimulus required to elicit similar sized postsynaptic responses		Decreased (CA1)			
	14 – 15 mo	1000% increase in soluble Aβ	Decreased (CA1) but similar to 6 -7 months		Normal (CA1			
Tg2576 w/ MRK-560 (γ-secretase inhibitor)	6 – 7 mo	1, 3, or 7 days of treatment reduced soluble Aβ levels	Partial recovery but not significant		Recovered (CA1)			(Townsend et al., 2010)
	15 mo	3 month of treatment reduced soluble Aβ levels	No improvement		Recovered (CA1)			
Tg2576 w/ CHF5074 (γ-secretase modulator)	6 mo	4 – week, subchronic oral treatment reduced Aβ levels			Recovered (CA1)			(Balducci et al., 2011)

(Tournoy et al., 2004). The lethal effect of knocking out PS1 is not surprising considering that γ-secretase is involved in the processing of many other substrates beside APP (Uemura et al., 2003; Kopan and Ilagan, 2004; Lleó, 2008), one of the most important being the Notch receptor, a protein that is critical in cell differentiation during embryonic development (Shen et al., 1997; Handler et al., 2000; Uemura et al., 2003; Kopan and Ilagan, 2004).

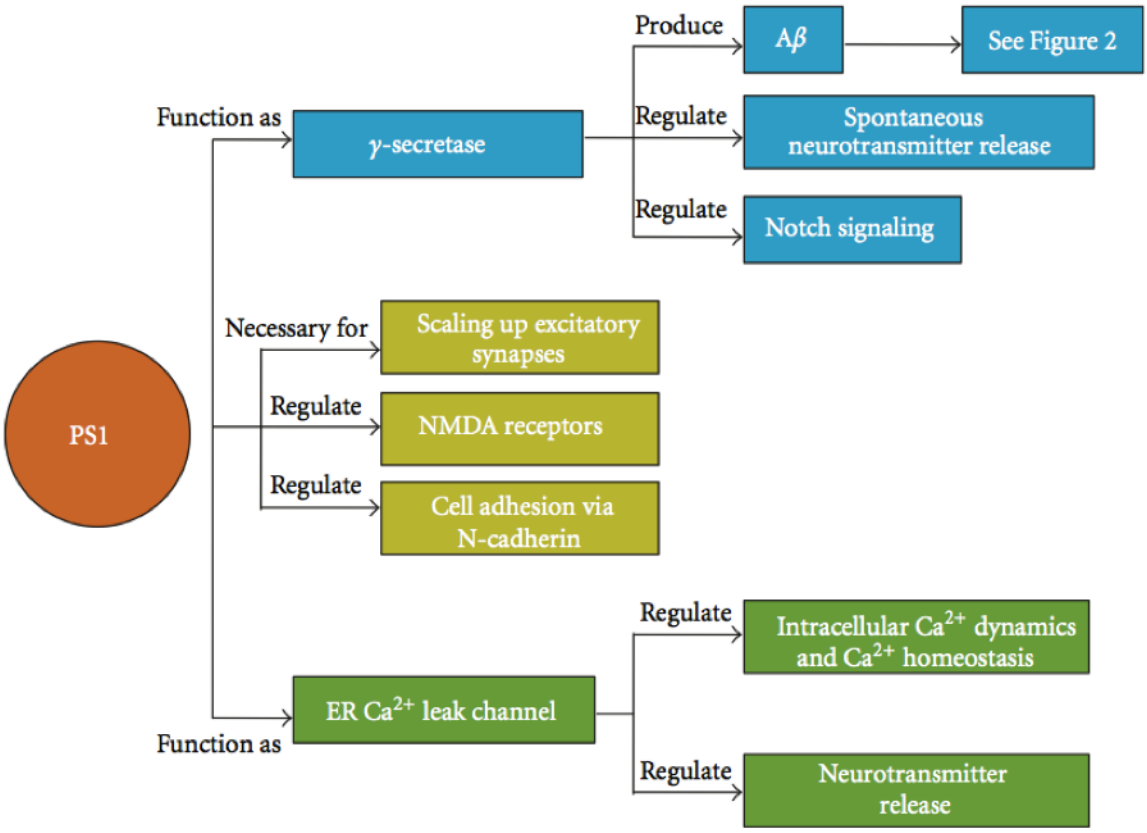

Figure 1.4. The roles of presenilin 1 in synaptic function.

Two main functions of presenilin 1 (PS1) focused on in this section are its ability to function as part of the γ-secretase cleavage complex and also to function as an ER Ca2+ leak channel. The γ-secretase complex is responsible for the final cleavage of APP in the production of Aβ peptides. The γ-secretase complex has also been shown to regulate spontaneous neurotransmitter release and is crucial for the regulation of the notch signaling pathway especially during early development. The PS1 holoprotein has been proposed to function as an ER Ca2+ leak channel. It is responsible for regulating intracellular calcium dynamics and calcium homeostasis required for proper signaling and neurotransmitter release. In addition to these two main functions, knockout studies have shown that the PS1 protein is important for synaptic scaling, proper NMDAR-mediated responses, as well as cell adhesion mediated by N-cadherin. Through these studies it is clear that PS1 plays an important role in synaptic transmission and plasticity.

γ-Secretase still remains to be a promising candidate for AD drug targets because it is thought that the function of PS1 might not be as critical in the adult brain, unlike during embryonic development, and/or partial inhibition of the enzymatic activity may still be feasible. Encouragingly, mice with conditional knockout (cKO) of PS1, in which PS1 expression was eliminated in most neurons of the cerebral cortex in the postnatal brain, were viable and had nearly normal phenotypes, including normal basal synaptic transmission and plasticity, with only mild deficits in long-term spatial memory (Yu et al., 2001; Saura et al., 2004). $A\beta_{40}$ and $A\beta_{42}$ levels were also reduced in the cortex of PS1 cKO mice, providing evidence in support of targeting PS1 as a potential anti-amyloid therapy in AD. Another promising finding was that regulation of Notch activity in the adult brain was unaffected and independent of PS1, contrasting the dependency of Notch signaling during embryonic brain development. This suggests PS2 may be able to compensate for the loss of PS1 in the adult brain, and leads one to question whether knockout of both PS1 and PS2 will lead to more extreme deficits. To test this hypothesis, Saura and colleagues (Saura et al., 2004) generated forebrain specific PS1/PS2 conditional double knockout (PS cDKO) mice. These mice exhibit cognitive impairments as well as deficits in hippocampal synaptic plasticity, which appear earlier than in the PS1 cKO mice. PS cDKO mice also developed age-dependent and progressive neurodegeneration, including loss of dendritic spines and presynaptic terminals (Saura et al., 2004). Together, this suggests that in the adult brain the role of PS1 in regulating Notch signaling may not be as important, but that presenilins are required for normal hippocampal synaptic plasticity, memory formation, and age dependent neuronal survival.

It is encouraging that conditional inactivation of PS1 is able to decrease Aβ levels in the adult brain, without effecting Notch signaling (Yu et al., 2001). In order to examine the possibility of using inactivation of PS1 as a therapy for AD, PS1 cKO mice have been crossed

with transgenic mice expressing different FAD-linked mutations in APP. The first study developed postnatal neuron-specific inactivation of PS1 (PS1-/-) in transgenic mice overexpressing human APP with the London mutation (V717I), APPxPS1(-/-) (Dewachter et al., 2002). This group had previously shown that APP(V717I) mice had increased levels of $A\beta_{42}$ peptides as early as 2 months, leading to plaque development at 13-months old, as well as cognitive impairment and reduced hippocampal LTP (Moechars et al., 1999). APPxPS1(-/-) mice showed reduced Aβ and amyloid plaque formation, even at 18 months. While hippocampal CA1 LTP was rescued in APPxPS1(-/-) mice, they still showed impaired cognition. A second study used the forebrain-specific PS1 cKO mice, mentioned previously (Yu et al., 2001; Saura et al., 2004), to inactivate PS1 in an APP transgenic that overexpressed human APP containing the Swedish (K670N/M671L) and Indiana (V717F) mutations to generate PS1 cKO;APP Tg (Saura et al., 2005). Similar to the previous study, these mice also had reduced amyloid-phenotypes compared to APP Tg mice, but there was still no long-term improvement in cognitive function. Conditional inactivation of PS1 was only able to rescue learning and memory deficits seen in young but not old mice (Saura et al., 2005). Together, these data indicate a causative role for Aβ peptides in LTP deficits and demonstrate that inactivation of PS1 in Tg mice can decrease the amyloid pathology of AD and restore LTP impairments in young mice. One question elicited from the above studies is that, if conditional knockout of PS1 is able to reduce amyloid pathologies and rescue certain LTP impairments, why is it not able to rescue cognitive deficits seen in these AD mice, and why is it not able to sustain LTP improvements in older mice? One possible explanation is the age-dependent accumulation of the APP C-terminal fragments (CTFs) caused by a lack of γ-secretase activity after conditional inactivation of PS1, leading to the buildup of γ-secretase substrates (Saura et al., 2005). Another explanation is the non γ-secretase

functions of PS1 may be involved in aspects of memory formation, storage, or consolidation, by regulating intracellular calcium dynamics.

In addition to its proteolytic activity, PS1 is implicated in regulating neurotransmitter release (Zhang et al., 2009; Pratt et al., 2011a) and intracellular calcium dynamics (Bezprozvanny and Mattson, 2008; Supnet and Bezprozvanny, 2010; Zhang et al., 2010b) (Fig 1.4). It has been proposed that the full length PS1 can act as a passive endoplasmic reticulum (ER) Ca^{2+} leak channel (Tu et al., 2006), and that some FAD-linked PS1 mutations lack this property. However, it remains controversial (Thinakaran and Sisodia, 2006; Gandy et al., 2006; Shilling et al., 2012) whether Ca^{2+} dysregulation that occurs during AD can be directly linked to alterations in ER Ca^{2+} leak channels formed by PS1. While the exact mechanism may be unknown, there is ample evidence that FAD-linked mutations in PS1 contribute to augmented cytosolic Ca^{2+} concentrations resulting from changes in intracellular ER Ca^{2+} dynamics (Smith et al., 2005; Stutzmann et al., 2006; Bezprozvanny and Mattson, 2008; Cheung et al., 2010; Supnet and Bezprozvanny, 2010; Zhang et al., 2010a, 2010b). FAD-linked mutations in PS1 appear to influence Ca^{2+} homeostasis by causing enhanced Ca^{2+} responses of ryanodine receptors (RyRs) (Smith et al., 2005; Stutzmann et al., 2006, 2007; Supnet et al., 2006; Chakroborty et al., 2009; Goussakov et al., 2010) and inositol-1,4,5-triphosphate receptors (IP_3Rs) (Stutzmann et al., 2004; Cheung et al., 2008, 2010) found in the ER (Berridge, 1998), enhanced filling of ER Ca^{2+} stores (Leissring et al., 1999; Green et al., 2008), and attenuation of capacitive Ca^{2+} entry (CCE) stores (Leissring et al., 2000; Yoo et al., 2000; Smith et al., 2002; Herms et al., 2003). Presenilins have also been found to play a normal physiological role in regulating sarco ER Ca^{2+}-ATPase (SERCA) pumps that help maintain low cytosolic Ca^{2+} concentrations by pumping Ca^{2+} into ER stores (Green et al., 2008). SERCA activity also influences Aβ production, such that increased SERCA activity increases Aβ production (Green et al., 2008).

Synaptic transmission and plasticity are important cellular mechanisms underlying cognitive functions, and there is evidence that presenilins play a role in these mechanisms. Mice with PS1 cKO in the cortex, showed normal basal synaptic transmission, LTP, and LTD in the hippocampal Schaffer collateral pathway (Yu et al., 2001), suggesting that in the adult brain, activity of PS2 is sufficient to maintain normal synaptic properties when PS1 is absent. In contrast to PS1 cKO mice, PS1/PS2 conditional double knockout (PS cDKO) show reduced LTP and a decreased PPF ratio at these synapses as early as 2 months of age. By 6 months, PS cDKO mice showed even greater synaptic deficits, including loss of presynaptic inputs and enhanced basal synaptic transmission, in addition to reduced LTP and PPF ratio (Saura et al., 2004). These synaptic impairments may explain the age-dependent deterioration in the cognition of the PS cDKO mice (Saura et al., 2004). Collectively, these studies suggest that presenilins are essential for synaptic plasticity as well as learning and memory in the adult brain.

What is the cellular mechanism that mediates the effects of PS1 on synaptic plasticity? Saura et al. (Saura et al., 2004) found a reduction in the postsynaptic NMDAR-mediated response in PS cDKO mice, which correlated with a decrease in the cortical levels of synaptic NMDAR expression. Saura et al. also found that synaptic localization and delivery of NMDARs may depend on certain interactions with presenilins. Therefore, the downregulation of postsynaptic NMDARs is a reasonable explanation for why LTP and memory are impaired in PS cDKO mice. Loss of presenilin function also decreased the expression of both dendritic and synaptic αCaMKII levels as well as multiple CRE-dependent genes (Saura et al., 2004), which are all involved in the downstream signaling of NMDAR activation associated with LTP and memory formation [for a review on LTP and memory and the involved molecules, see (Lynch, 2004)]. This indicates that presenilins not only exert regulatory effects on NMDARs, but also the signaling cascades that lead to LTP and memory formation. Surprisingly, later studies that looked specifically at CA1

neurons in the hippocampus, revealed that, at 2 months, PS cDKO mice show an unexpected increase in the number of pre- and postsynaptic sites labeled for the NR2A subunits of NMDARs (Aoki et al., 2009). This increase is not accompanied by synapse loss or alterations in spine size, in agreement with previously documented morphology of PS cDKO mice at this age (Saura et al., 2004). The authors (Aoki et al., 2009) suggested that NMDARs become trapped at the synaptic membrane leading to excitotoxicity and eventual neurodegeneration that is present in PS cDKO mice at 6 months (Saura et al., 2004). In addition, they suggested that LTP impairments are not due to a reduction in NMDAR number, but may be more tightly linked to the reduced levels of αCaMKII present in the dendritic spines (Aoki et al., 2009).

As previously mentioned, presynaptic function was also altered in PS cDKO mice: a reduced PPF ratio, which was attributed to abnormal presynaptic Ca^{2+} signaling, and a reduction in presynaptic release probability was observed (Zhang et al., 2009, 2010a). In addition, there was a loss of presynaptic inputs in older PS cDKO mice suggesting that certain signals necessary for maintaining axon terminals may be missing. PS1 has been found to localize at the synapse and regulate adhesive contact of pre- and postsynaptic compartments, mediated by N-cadherin (Uemura et al., 2003), the major molecule that mediates Ca^{2+}-dependent cell-cell interaction (Tepass et al., 2000). The diminution of N-cadherin-mediated cell-cell adhesion when presenilins are inhibited might cause the presynaptic defects in PS cDKO mice. One study sought to address the temporal progression of pre- and postsynaptic impairments in the Schaffer collateral pathway of PS cDKO mice (Zhang et al., 2010a). They found that the decrease in presynaptic calcium-dependent facilitation and neurotransmitter release preceded postsynaptic impairments in NMDAR-mediated responses and LTP. Previous experiments in which presenilins were conditionally knocked out in either presynaptic, CA3, or postsynaptic, CA1 neurons (Zhang et al., 2009), demonstrated that loss of presynaptic presenilin is sufficient to cause impaired glutamate

neurotransmitter release and LTP, due to altered intracellular calcium signaling. However, loss of pre- or postsynaptic presenilin alone was not sufficient to cause impairments in NMDAR-mediated responses (Zhang et al., 2009). The authors propose a "trans-synaptic mechanism" to explain the alterations in postsynaptic NMDAR function (Zhang et al., 2010a). In any case, presenilins are likely essential for regulating the intracellular calcium signals required for proper neurotransmitter release to insure normal short- and long-term plasticity. Indeed, several recent studies have found that PS1 function is important in regulating homeostatic plasticity (Pratt et al., 2011b) and neuronal ER Ca^{2+} homeostasis (Zhang et al., 2010b), as well as a novel function of the γ-secretase complex in regulating spontaneous neurotransmitters release (Pratt et al., 2011a). Therefore, presynaptic dysfunction and altered calcium dynamics may be an early event leading to neuronal degeneration and pathogenesis in AD.

Subsection 1: Gamma-secretase inhibitors and modulators

The γ-secretase complex is critical in the formation of Aβ peptides, hence it is one of the key therapeutic targets for stopping the progression of AD. Although many classes of compounds exist that target the γ-secretase complex, not many have investigated their effects on synaptic transmission and plasticity. Numerous studies have documented the ability of different classes of γ-secretase inhibitors (GSI) and modulators (GSM) to reduce Aβ levels in the brain (Dovey et al., 2001; Eriksen et al., 2003; Yan et al., 2003; Imbimbo et al., 2007, 2011; Wolfe, 2008; Martone et al., 2009; Basi et al., 2010; Kounnas et al., 2010; Pettersson et al., 2011), as well as their effects on cognitive function in hippocampal dependent memory task such as the Morris water maze or contextual fear conditioning (Comery et al., 2005; Dash et al., 2005; Kukar et al., 2007; Imbimbo et al., 2009). There are two studies (Townsend et al., 2010; Balducci et al., 2011) that looked at the effects of drug treatment on synaptic plasticity in a mouse model of AD. Both studies used Tg2576 mice to investigate the ability of the GSI, MRK-560 (Townsend et al., 2010), or the

GSM, CHF5074 (Balducci et al., 2011), to restore hippocampal memory and synaptic plasticity. Each study used different initial starting times and durations of treatment. To understand the interaction between the age dependent increase in Aβ and its effect on basal synaptic transmission and plasticity in the CA1 region of the hippocampus, Townsend et al. (Townsend et al., 2010) compared synaptic activity across three different ages, young (3-4 months), middle (6-7 months), and old (14-15 months) mice. Basal synaptic transmission was assessed by measuring the input/output activity in CA1. Even though Aβ levels continue to increase with age, the greatest synaptic deficits in Tg2576 mice were seen at 6-7 months, and in particular LTP was impaired at this middle age, but was normal in both young and old mice (Townsend et al., 2010). This suggests that soluble Aβ is inversely correlated with LTP, until plaque deposition occurs, when soluble Aβ can no longer predict LTP impairments (Townsend et al., 2010). Since 6-7 month old mice showed the greatest deficits, they were given oral doses for 1, 3, or 7 days with the GSI, MRK-560. After 1 day, Aβ levels were significantly reduced and LTP began to improve. LTP improvements reached significance after 3 days of dosing. After 7 days of treatment, basal synaptic transmission began to recover but did not reach significance. This supports the theory that lowering Aβ levels can recover synaptic plasticity in 6-7 month old Tg2576 mice, before plaque deposition. Balducci et al. (Balducci et al., 2011) also focused on how the GSM, CHF5074 may be able to rescue synaptic deficits seen in plaque-free Tg2576 mice. After acute subcutaneous treatment with the GSM, CHF5074, 5-month old Tg2576 mice showed significantly reduced contextual memory impairments (Balducci et al., 2011). At 6-months old, after receiving a 4-week subchronic oral treatment, which reduced intraneuronal Aβ level, the impairments in recognition memory and hippocampal LTP were reversed.

To determine if aged mice would also show improvements after treatment, daily doses of the GSI, MRK-560 were given to Tg2576 mice from 12-15 months of age (Townsend et al.,

2010). Since LTP was similar to wild type mice at this age, the focus was on basal synaptic transmission. Similar to middle aged animals, treatment with MRK-560 significantly reduced Aβ levels; however, there was no improvement in basal synaptic transmission. The lack of functional recovery in the older age group was also seen in APP Tg mice crossed with PS1 cKOs (Saura et al., 2005). These results reveal that even though conditional inactivation of PS1 can successfully reduce Aβ production and the amyloid associated neuropathological alterations, it does not prevent the impairments in both synaptic and cognitive functions (Saura et al., 2005). Collectively, these studies suggest that the effects of Aβ on basal synaptic transmission and plasticity differ with age, and that successful reduction of Aβ levels by targeting APP processing enzymes may not recover synaptic dysfunction.

Section 8: Conclusion

It is clear that successful AD treatments will need to do more than just lower Aβ production, they will need to rescue cognitive as well as synaptic dysfunctions. Increasing evidence suggests the cognitive syndromes found in AD patients are preceded by changes in synaptic efficacy [reviewed in (Selkoe, 2002; Shankar and Walsh, 2009)]. Therefore, examining whether different strategies that target APP processing enzymes rescue synaptic dysfunctions associated with AD is important. Several current reviews state why certain APP processing drug therapies have failed in recent clinical trials and why current trials have not been able to generate more beneficial or significant results (Imbimbo et al., 2010; Sastre and Gentleman, 2010; Galimberti and Scarpini, 2011). Testing the effects of potential AD therapeutics on synaptic function, in addition to behavioral analyses, will provide a better mechanistic understanding of the potential problems. It is also important to remember how different animal models may affect the outcome of results. For example, in mouse studies, genetic background has been shown to

influence the effectiveness of certain γ-secretase targeting drugs (Czirr et al., 2007; Page et al., 2008; Hahn et al., 2011). In addition, many AD mouse models have been generated from FAD-linked mutations, and may not fully recapitulate sporadic AD cases. In sum, a mechanistic understanding of the normal synaptic functions of APP processing enzymes will benefit the development of more effective treatments for AD.

Section 9: Overview

It is clear from the above summary of current literature that a further basic understanding of AD pathology at a cellular level is needed to design effective therapeutics. The phenotype of synaptic deficits seen in various AD mouse models has yielded controversial results on how FAD-linked mutations alter LTP and LTD (Marchetti and Marie, 2011). The ability to regulate these forms of plasticity is termed metaplasticity and states that synaptic modification is governed by the recent synaptic history of a cell (Abraham and Bear, 1996), such that previously low levels of synaptic activity will facilitate later LTP induction, while previously high levels of synaptic activity will inhibit its induction. Therefore, metaplasticity is triggered by integrated prior neuronal activity and acts to provide stability in neuronal function within a dynamic range (Bear et al., 1987; Bear, 1995). When synapses lose their ability to modify subsequent neuronal responses, based on previous synaptic activity, synaptic weights may become stuck at extremes within the LTP/LTD dynamic range. An inability to regulate metaplasticity would limit the responsiveness of synapses to further subsequent modification following a plasticity-inducing activity pattern. The resulting synaptic phenotypes may be just as detrimental as a complete lack of plasticity and may explain synaptic dysfunction seen in many FAD-linked mutants. In this work, we investigate two different models for regulating metaplasticity in APPswe;PS1deltaE9 AD Tg mouse model: the sliding threshold and pull-push models. Regardless of which model is

mediating the metaplasticity, getting stuck at different set points for inducing plasticity within this dynamic range will result in LTP/LTD deficits.

The main goal of this study is to test the hypothesis that amyloidogenic progression leads to defective metaplasticity of NMDAR-dependent LTP and LTD. Typically, this has been studied in various AD Tg mouse models using frequency-dependent LTP/LTD induction protocols (i.e. high and low frequency stimulations). However, these studies have only focused on changes in the absolute magnitude of LTP/LTD, rather than changes in metaplasticity. To our knowledge, no one has tried to explain AD in terms of defects in metaplasticity or to target metaplasticity for normalizing synaptic function. In addition, in most studies it is unclear whether the synaptic deficits found in various AD models are related to changes in LTP/LTD induction and/or expression mechanisms. The rationale for choosing the APPswe;PS1deltaE9 AD Tg mouse model is because they exhibit an accelerated amyloidogenic phenotype [e.g. accumulation of Aβ and amyloid plaques by 6 months of age (Jankowsky et al., 2004; Garcia-Alloza et al., 2006)]. They not only express high levels of Aβ and amyloid plaques, but also other pathological phenotypes of AD, including synaptic dysfunction, increased inflammation, cognitive deficits, hyperphosphorylated tau in dystrophic neurites, and cholinergic axon breakdown (Tomidokoro et al., 2001; Kurt et al., 2003; Jankowsky et al., 2005; Samura et al., 2006; Reiserer et al., 2007; Ding et al., 2008; Crouch et al., 2009; Phillips et al., 2011; Cramer et al., 2012; Wu et al., 2014). Since LTP/LTD are cellular substrates for learning and memory and important for encoding new information, deficits in metaplasticity may be relevant to other phenotypes, such as cognitive deficits, seen in this AD model.

This study also seeks to investigate how novel therapeutics for AD may affect synaptic function and plasticity in both wild type and AD mice, and compare their effects to compounds that inhibit APP processing enzymes, discussed previously. Drugs that target APP processing

enzymes have not been as successful as originally anticipated. This is largely due to mechanism-based toxicity caused by adverse side effects related to other proteins processes by these enzymes, besides APP. Hence, an alternative approach may be needed. The above discussion also emphasizes a lack of sufficient investigation into the effect of novel therapeutics on basic synaptic function and plasticity. To gain a complete understanding of new drug therapies, initial testing should include investigation of not only their ability to decrease Aβ peptide and plaques levels, but also their effects on cognitive and synaptic function. Current therapies provide only temporary symptomatic relief and do not alter the progression of AD pathogenesis. A comprehensive understanding like this, that includes functional data, will enable a better mechanistic approach to overcome synaptic deficits that occur early in AD, when treatment may be most effective. Understanding how bidirectional synaptic plasticity becomes altered throughout the progression of AD will help to determine the specific synaptic events that underlie the synaptic dysfunction associated with cognitive decline in AD patients. In addition, an understanding of these basic mechanisms will not only lead to the development of more effective therapeutics, but also enable progress by overcoming the unforeseen side effects produced by many current therapies that have failed.

Chapter 2: Defective age-dependent regulation of metaplasticity in a mouse model of Alzheimer's disease

This manuscript is in preparation.

Putative authors: **Andrea Megill**, Kiara Eldred, Nathanael J. Lee, Philip C. Wong, Hang-Sook Hoe, and Hey-Kyoung Lee

My contribution: All of the experiments performed in this study except Golgi staining analysis and some Western blot analysis.

Section 1: Introduction

Alzheimer's disease (AD) is a progressive neurodegenerative disorder causing a loss of synaptic contacts and cognitive decline. Current theories implicate the production of Aβ peptides as the key molecular event that ultimately leads to neurodegeneration and clinical pathologies (Hardy and Selkoe, 2002; Walsh and Selkoe, 2004; Shankar and Walsh, 2009). It is widely believed that cognitive deficits in AD patients are preceded by synaptic dysfunction, which may be the basis for memory loss in early stages of the disease (Walsh and Selkoe, 2004; Shankar and Walsh, 2009).

Much of the molecular understanding of AD comes from studying FAD-linked mutations, which have been found in genes encoding APP and PS1 and PS2 in AD patients. Numerous Tg mouse models have been generated to study AD; however, depending on the combination of the FAD-linked mutations and their variants, distinct phenotypes are observed across age and brain regions studied. In addition, in many of these studies, it is unclear whether synaptic dysfunction is at the level of induction or expression of synaptic plasticity mechanisms.

Hippocampal LTP and LTD are effective models for mediating synapse-specific changes required for memory formation (Dudek and Bear, 1992; Mulkey and Malenka, 1992; Paulsen and Sejnowski, 2000; Lynch, 2004; Malenka and Bear, 2004; Whitlock et al., 2006). Bidirectional modifications in synaptic strength allow synapses to adjust the strength of their synaptic connections based on incoming activity. However, the induction threshold of LTP and LTD is not static but is itself adjusted by past neuronal activity by a metaplasticity process termed the "sliding threshold" (Bear, 2003; Yashiro and Philpot, 2008). NMDAR activation is important for determining the magnitude and polarity of plasticity. In addition, activity-dependent alterations in the NMDAR subunit composition have been shown to be responsible for sliding the threshold for inducing frequency-dependent LTP and LTD, due to their different electrophysiological properties (Philpot et al., 2001b; Bear, 2003a; Yashiro and Philpot, 2008; Gray et al., 2011). Therefore, a shift in NMDAR subunit composition can mediate a shift in the synaptic modification threshold (crossover point for LTD/LTP).

An alternative process to the sliding threshold, which can result in similar metaplasticity, is called the "pull-push" hypothesis (Huang et al., 2012), which demonstrates that distinct neuromodulatory systems promote LTP and LTD by acting on their expression mechanisms. One mechanism of pull-push metaplasticity has been shown to be due to the ability of specific G-protein coupled receptors (GPCRs) to promote the expression of LTP/LTD by changing phosphorylation states of AMPARs. For example, adenylyl cyclase (AC) coupled signaling cascades, leading to PKA activity promote LTP, while phospholipase C (PLC) signaling cascades, leading to PKC activity promote LTD. A key difference between the sliding threshold model and pull-push model of metaplasticity is that the former is traditionally supported by changes in NMDAR gain that are responsible for changing plasticity induction mechanisms. However, the pull-push model states that metaplasticity results from regulating LTP/LTD

expression mechanisms by effecting signaling that is downstream of NMDAR activation and therefore, downstream of plasticity induction mechanisms (Seol et al., 2007; Huang et al., 2012).

Alterations in memory networks have been seen early in AD patients, prior to clinical pathologies, and manifest as increases in activity within these systems (Sperling et al., 2010). In addition, Aβ-induced increases in activity have also been seen in mouse models of AD, suggesting that aberrant excitatory neuronal activity may be an early symptom leading to cognitive decline seen in AD patients (Palop et al., 2007; Palop and Mucke, 2009). Metaplasticity is triggered by integrated prior neuronal activity, and acts to provide stability in neuronal function (Bear et al., 1987; Bear, 1995). Numerous studies have focused on how Aβ peptides and the progression of AD effects frequency-dependent LTP/LTD; however, changes in LTP/D are not always the best correlate of behavioral deficits (Marchetti and Marie, 2011). Perhaps it is not just the change in LTP/LTD magnitude that is driving cognitive deficits, but the inability of the system to adequately adapt to changes in neural activity to produce metaplasticity. Therefore, we determined whether changes in frequency-dependent synaptic plasticity seen in APPswe;PS1deltaE9 Tg mice are due to altered metaplasticity. Our results indicate that there is a differential contribution of FAD-linked mutations on LTP/LTD magnitude in young versus adult Tg mice, but the major defect is in the developmental regulation of metaplasticity leading to altered expression mechanisms of LTP/LTD across age.

Section 2: Materials and Methods

Subsection 1: Animals

Young 1-month and adult 6-month old APPswe;PS1deltaE9 Tg and wild type (WT) mice (129/C57BL6 mixed background) were used. Genotypes were distinguished by polymerase chain reaction (PCR) of isolated genomic DNA obtained from each pup after weaning. Young

pre-adolescent mice were of either sex, while adult older mice were only male. APPswe;PS1deltaE9 Tg mice have accelerated amyloid pathologies and have a substantial number of plaque deposits by 6 months of age (Jankowsky et al., 2004; Savonenko et al., 2005). Therefore, these mice were used at both pre- and post-amyloidogenic ages. The Institutional Animal Care and Use Committees of Johns Hopkins University approved all procedures involving animals.

Subsection 2: Preparation of acute hippocampal slices

Acute hippocampal slices were prepared from 1-month and 6-months old WT and APPswe;PS1deltaE9 Tg mice as described previously (Lee et al., 2003). Briefly, each mouse was euthanized by decapitation following overdose of isoflurane. Hippocampi were rapidly removed and sectioned into either 300-μm (for whole-cell recording) or 400-μm (for field potential recording) slices on a vibratome (Vibratome 3000 series, Ted Pella Inc.) Hippocampi were dissected using oxygenated ice-cold dissection buffer (composition in mM: 212.7 sucrose; 2.6 KCl; 1.23 NaH_2PO_4; 26 $NaHCO_3$; 10 dextrose; 3 $MgCl_2$; and 1 $CaCl_2$) and recovered at room temperature in artificial cerebrospinal fluid (ACSF, composition in mM: 124 NaCl; 5 KCl; 1.25 NaH_2PO_4; 26 $NaHCO_3$; 10 dextrose; 1.5 $MgCl_2$; and 2.5 $CaCl_2$).

Subsection 3: Field potential recordings from Schaffer collateral inputs to CA1

All recordings were done in a submersion recording chamber perfused with ACSF (29–30°C, 2 ml/min) bubbled with 95% O_2-5% CO_2. For field potential (FP) recordings, synaptic responses were delivered through a bipolar glass stimulating electrode placed to activate the Schaffer collaterals with a 0.2 ms duration pulse (baseline stimulation at 0.0333 Hz), and recorded from the dendritic field of CA1. Synaptic responses were digitized and stored on-line using IGOR Pro software (WaveMetrics). Input-output curves were generated by measuring extracellular field potential responses with varying stimulus intensities. For measurement of

paired-pulse facilitation (PPF), 25, 50, 100, 200, 400, 1000, and 2000 ms interstimulus intervals (ISIs) were used. LTP was induced using a theta burst stimulation [TBS: four trains, each consisting of ten 100-Hz bursts (four pulses) given at 5 Hz, repeated at 10-s intervals] (Larson et al., 1986). LTD in young mice was induced using 1Hz, 900 pulses stimulation protocol. LTD in adult mice was induced using a paired-pulse 1 Hz (50 ms ISI), 900 pluses stimulation. An intermediate stimulation frequency of 10 Hz, 900 pulses, was chosen because it was close to the modification threshold.

For certain experiments 10 μM TBOA was used to induce spillover of glutamate. In these experiments CA3 was cut away during dissection and high divalents were added to the ACSF (4 mM $MgCl_2$ and 4 mM $CaCl_2$) in addition to 100 μM D,L-APV, 2.5 μM Gabazine. Field potential slopes were measured, and data are expressed as mean ± SE of mean.

Subsection 4: Whole-cell recording of evoked NMDAR-mediated excitatory postsynaptic currents (EPSC) and their sensitivity to a GluN2B antagonist

Slices were visualized using an upright microscope (E600 FN, Nikon) with infrared (IR) oblique illumination. NMDAR-mediated EPSCs were pharmacologically isolated by adding 20 μM Bicuculline and 10 μM NBQX to the ACSF [(ACSF, composition in mM: 124 NaCl; 2.5 KCl; 1.25 NaH_2PO_4; 26 $NaHCO_3$; 5 dextrose; 4 $MgCl_2$; and 4 $CaCl_2$), (30 ±1°C, saturated with 95% O_2 and 5% CO_2)], which was continually perfused at a rate of 2 ml/min. Target cells in CA1 were identified by the pyramid-shaped soma. These neurons were patched using a whole-cell patch pipette (tip resistance 3–5 MΩ), which was filled with internal solution (in mM: 120 Cs-methanesulfonate, 5 $MgCl_2$, 8 NaCl, 1 EGTA, 10 HEPES, 2 Mg-ATP, 0.5 Na_3GTP, and 1 QX-314; pH 7.3, 280–290 mOsm). NMDAR-mediated currents were measured at +40 mV. A double-barrel glass stimulating electrode filled with ACSF was placed in the stratum radiatum of CA1 to activate Schaffer collateral inputs. To test the portion of these currents mediated by GluN2B

containing NMDARs, 3 μM of the GluN2B antagonist, ifenprodil, was added to the ACSF. To evaluate the amplitude and decay kinetics of the NMDAR-EPSCs in a given condition, 20-40 traces were averaged and normalized. The decay was then fitted with two exponentials; one fast and one slow, using Igor. To measure the decay, a weighted time constant (τ_w) was calculated according to the following equation as described (Rumbaugh and Vicini, 1999; Philpot et al., 2001a): $\tau_w = \tau_f (I_f /(I_f+I_s)) + \tau_s (I_s /(I_f+I_s))$, where τ_f and τ_s are the time constant for the fast and slow components, while I_f and I_s are their respective amplitudes. Only the cells and recording conditions that met the following criteria were studied: no obvious multiple EPSCs or polysynaptic waveforms, $R_{input} \geq 125$ MΩ and $R_{series} \leq 30$ MΩ, and R_{input} or R_{series} changed less than 25% during the course of the experiment. Data are the means ± SE. Comparison between the two conditions was done using paired Student's t test.

Subsection 5: Whole-cell recording of miniature $GABA_A$R-mediated IPSCs (mIPSCs)

For mIPSC from CA1 pyramidal cells, the recording pipette was filled with intracellular solution (in mM: 140 CsCl, 8 KCl, 10 EGTA, 10 HEPES, and 0.01 QX-314 (pH 7.3, 275-285 mOsm) in the presence of 1 μM TTX, 100 μM D,L-APV, and 10 μM NBQX in the ACSF to isolate GABAR-mediated currents. The Axon patch-clamp amplifier 700B (Molecular Devices) was used for voltage-clamp recordings. Cells were held at -70 mV, and the recorded mIPSC data were digitized at 10 kHz with a data acquisition board (National Instruments) and acquired through custom-made programs using the Igor Pro software (WaveMetrics). The MiniAnalysis program (Synaptosoft) was used to analyze the acquired mIPSCs. The threshold for detecting mIPSCs was set at three times the root mean square (RMS) noise. Recordings were excluded from analysis if the series resistance was >25 MΩ or input resistance was <100 MΩ. To minimize the impact of dendritic filtering, we adopted the standard approach of excluding mIPSCs with a

rise time of > 5 ms. 300-400 hundred consecutive mIPSCs that met the rise-time criteria were analyzed from each cell.

Subsection 6: Golgi staining and morphological analysis of dendritic spines

To analyze dendritic spine density *in vivo,* Golgi staining was performed using FD Rapid GolgiStain Kit (FD NeuroTechnologies) according to the manufactures protocol, as previously described (Megill et al., 2013). Brains from 1-month old WT and APPswe;PS1deltaE9 Tg mice (n = 3 per group) or from 6-month old WT and APPswe;PS1deltaE9 Tg mice (n = 3 per group) were immersed in Solution A and B for 2 weeks and then transferred into Solution C for 24 hr. After 24 hr of incubation, it was replaced with fresh Solution C and kept at 4°C for 3 days. After the 3-day incubation, the brains were sliced using a Vibratome at 150-µm thickness. Images were acquired using an Axioplan 2 microscope (Zeiss) under bright-field illumination. Dendritic spines (0.2 to 2 µm in length) from apical oblique (AO) and basal shaft (BS) dendrites were counted manually in a blinded manner.

Subsection 7: Western blot analysis of major AMPAR and NMDAR subunits

The hippocampus from 1-month and 6-month old WT and APPswe;PS1deltaE9 Tg mice was homogenized in ice-cold 0.2% SDS/1% Triton X-100 immunoprecipitation buffer (TX-IPB; 20 mM Na_3PO_4, 150 mM NaCl, 10 mM EDTA, 10 mM EGTA, 10 mM $Na_4P_2O_7$, 50 mM NaF, and 1 mM Na_3VO_4, pH 7.4; with 1 µM okadaic acid and 10 kIU/ml aprotinin), sonicated and centrifuged for 10 min at 13,200 × g, at 4°C. Protein concentration of the supernatant was normalized to 0.6 – 3.0 mg/ml. The total homogenate from WT and Tg mice of the same age was run on one gel and processed for immunoblot analysis using GluA1 (sc-55509, Santa Cruz Biotechnology), GluN2A (07–632, Millipore), and GluN2B (71–8600, Invitrogen) antibodies.

GluA1-phosphorylation site-specific antibodies were previously generated as described (Mammen et al., 1997). AMPAR blots were probed simultaneously with GluA1 and either of the phospho-antibodies. GluA1-phosphorylation sites and NMDAR subunit blots were developed using enhanced chemifluorescence substrate (ECF substrate, GE Healthcare), while GluA1 was developed with a second antibody linked to Cy5. All blots were scanned using Typhoon 9400 (GE Healthcare), and quantified using Image Quant TL software (GE Healthcare). For each gel, a

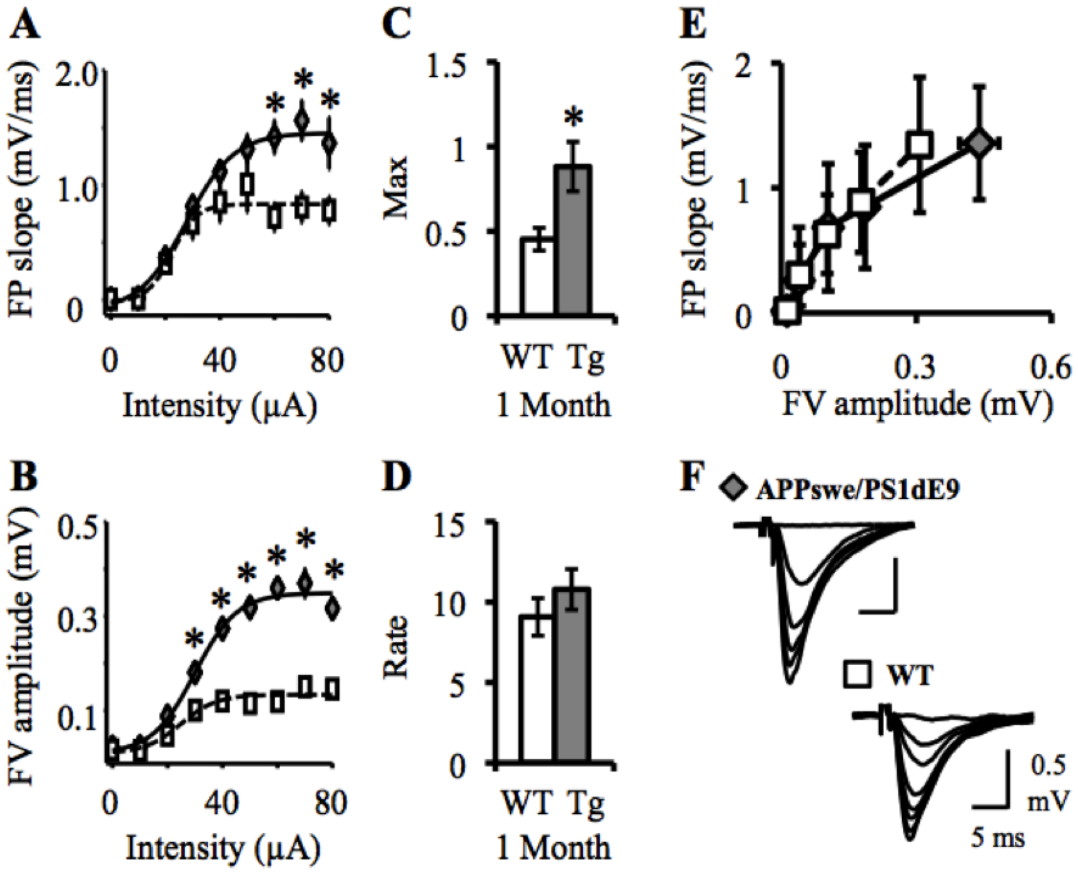

Figure 2.1. Basal synaptic function in young WT and APPswe;PS1deltaE9 Tg mice.

(A-B) Increase in input-output function with stimulation intensity in 1-month Tg mice. **A.** Field Potential (FP) slope plotted against stimulus intensity (ANOVA, *p < .001). **B.** Fiber Volley (FV) amplitude plotted against stimulus intensity (ANOVA, *p < .001). (**C-D)** Average data when data points in Graph B were fit with sigmoidal curves. **C.** Increase in the maximal FV/axonal response (WT: 0.45 ± 0.07; Tg: 0.88 ± 0.15; t test, *p < 0.02). **D.** No change in the rate at which axons are recruited (WT: 9.07 ± 1.16; Tg: 10.78 ± 1.26; t test, p = 0.328). **E.** FP slope normalized to FV amplitude (WT: n = 16 slices 6 mice; Tg: n = 22 slices, 6 mice). **F.** Representative FP traces.

control WT and Tg sample was loaded at three different concentrations to determine the linear range of signal for quantification. Only the samples that produced a signal within the linear range were used for analysis. The signal of each sample on a blot was normalized to the average signal from the WT group to obtain the percentage of average WT values, which were compared across groups using unpaired Student's t test.

Section 3: Results

Subsection 1: Basal synaptic function and dendritic spine density in young APPswe;PS1deltaE9 Tg mice

We examined synaptic function in hippocampal CA1 using field potential recording in acute hippocampal slices from WT and APPswe;PS1deltaE9 Tg mice at two ages. Given the inconclusiveness in the field (Marchetti and Marie, 2011) we first wanted to see what basic phenotypes these mice displayed in our hands, given our experimental conditions and paradigms. At the Schaffer collateral inputs to CA1 young, 1-month old Tg mice show an increase in input-output function with stimulus intensity (Fig 2.1 A&B). Fiber volley (FV) amplitude data (Fig 2.1 B) were fit with sigmoidal curves to determine if this increase was due to an increase in maximal FV response, or a difference in the rate at which axons were recruited. There was an increase in the maximum FV amplitude (Fig 2.1 C) without a change in the rate at which axons are recruited (Fig 2.1 D). This suggests that there was an increase in the total number of axons or increased axon density in the stratum radiatum of CA1. There was no change in the input-output function when synaptic transmission was normalized to the FV amplitude (Fig 2.1 E), which suggests that the strength of synaptic transmission per activated axon fiber is normal in the young Tg mice.

To determine if the increase in axonal density was associated with an increase in dendritic spine density, we measured spine density in CA1 and cortical layers II/III using Golgi

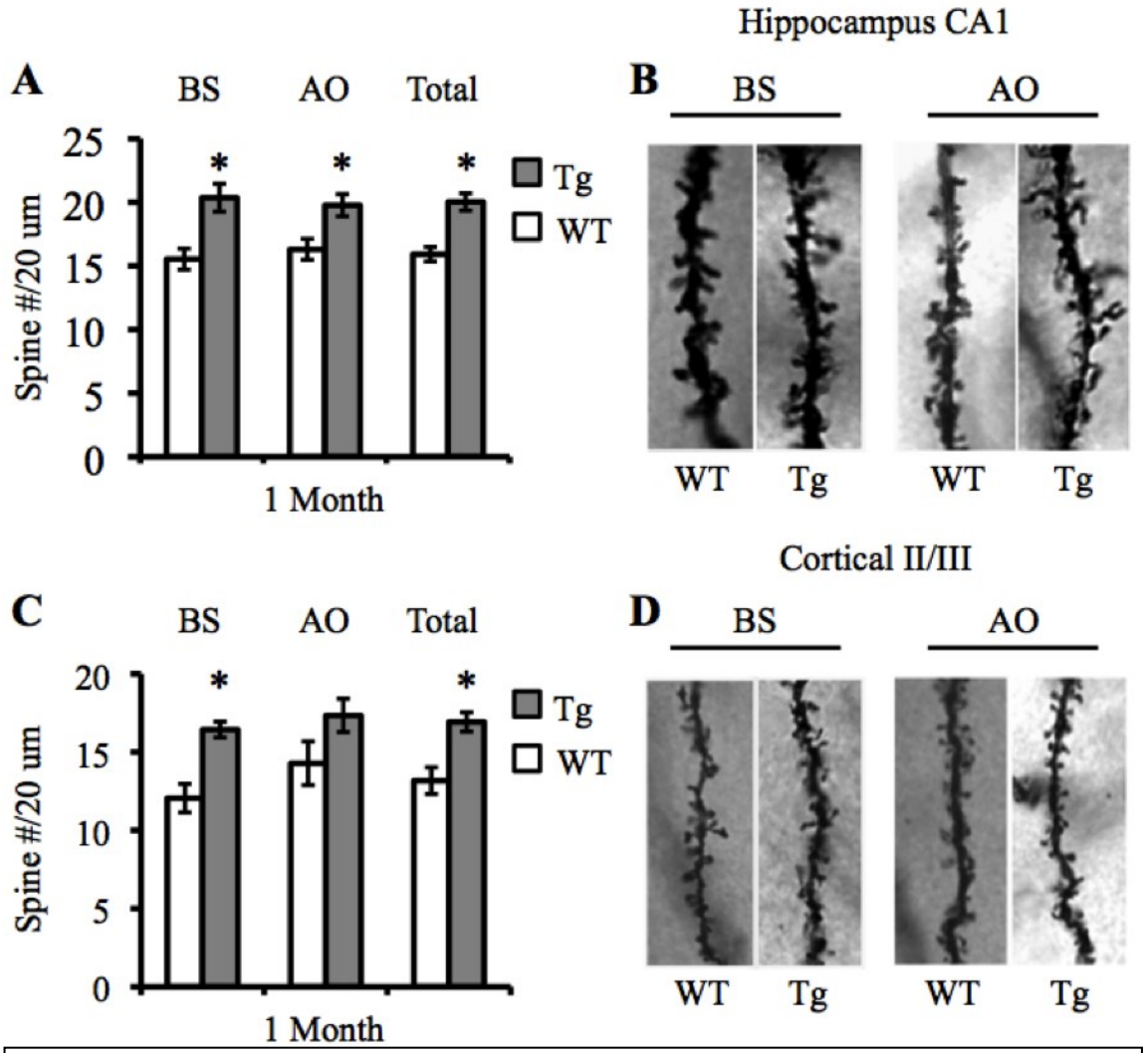

Figure 2.2. Dendritic spine density in CA1 and cortical II/III of young WT and APPswe;PS1deltaE9 Tg mice.

(A-B) Increase in dendritic spine density in CA1 of 1-month Tg mice. **A.** Left, Spine density in hippocampal basal shaft (BS) dendrites (n = 3 mice; t test, *p < 0.01). Middle, Spine density in hippocampal apical oblique (AO) dendrites (n = 3 mice; t test, *p < 0.01). Right, Total spine density (BS + AO) in hippocampal dendrites (n = 3 mice; t test, *p <0.01). **B.** Representative BS and AO dendrites from hippocampal CA1 neurons from WT and Tg mice, as indicated. (**C-D**). Increase in dendritic spine density in cortical layers II/III. **C.** Left, Spine density in cortical II/III basal shaft (BS) dendrites (n = 3 mice; t test, *p < 0.01). Middle, Spine density in hippocampal apical oblique (AO) dendrites (n = 3 mice; t test, p = 0.095). Right, Total spine density in hippocampal dendrites (n = 3 mice; t test, *p <0.01). **D.** Representative BS and AO dendrites from cortically layers II/III neurons from WT and Tg mice, as indicated.

staining (Fig 2.2). We found that total spine density in young Tg mice was increased compared to young WT mice in CA1 and cortical layers II/III. In CA1, the increase in dendritic spine

density was not restricted to the apical oblique (AO) dendrites, but was also see in the basal shaft (BS) dendrites (Fig 2.2 A&B). This suggests that there is a global increase in excitatory synapse number in the 1-month old Tg mice across different brain areas.

Subsection 2: Basal synaptic function and dendritic spine density in adult APPswe;PS1deltaE9 Tg mice

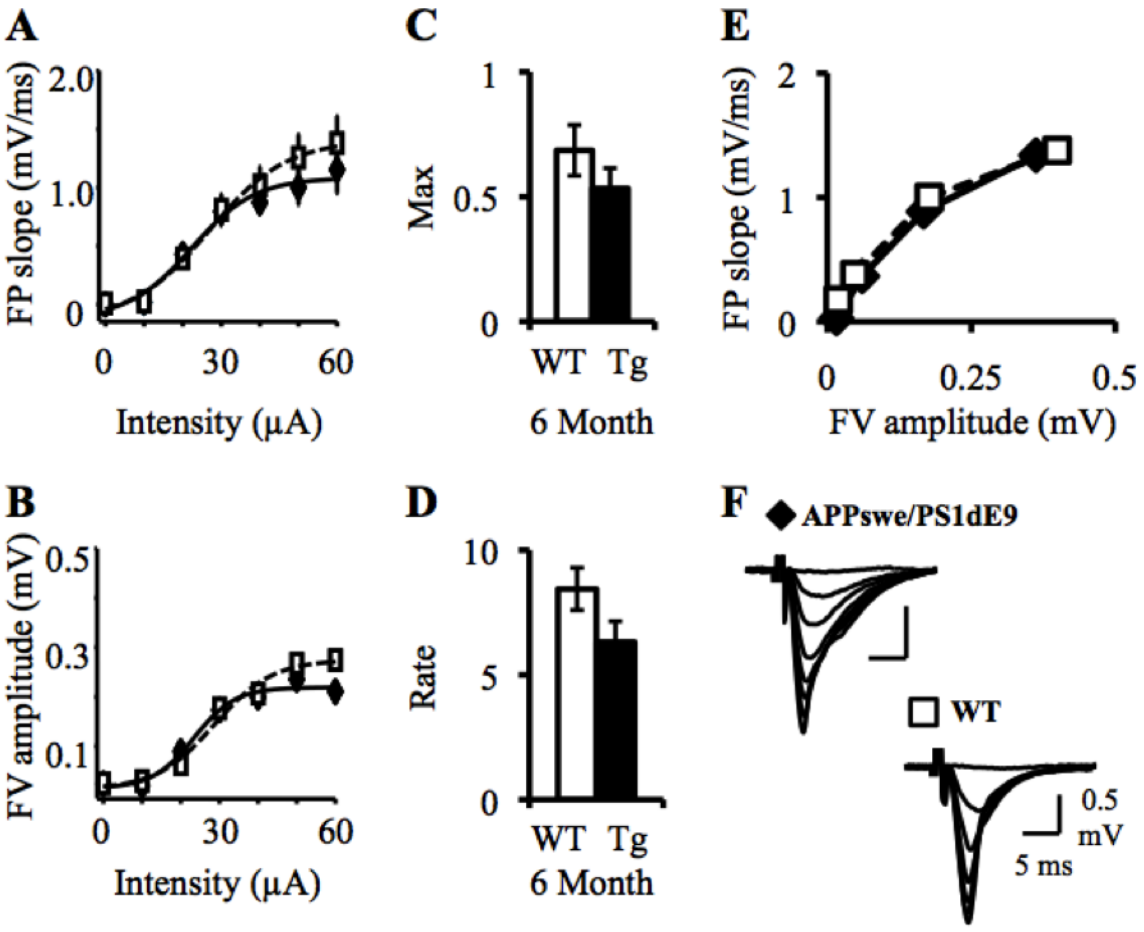

Figure 2.3. Basal synaptic function in adult WT and APPswe;PS1deltaE9 Tg mice.

(A-B) No change in input-output function with stimulation intensity in 6-month Tg mice. **A.** FP slope plotted against stimulus intensity. **B.** FV amplitude plotted against stimulus intensity. (**C-D)** Average data when data points in Graph B were fit with sigmoidal curves. **C.** No change in the maximal FV/axonal response (WT: 0.69 ± 0.10; Tg: 0.53 ± 0.08; t test, p = 0.253). **D.** No change in the rate at which axons are recruited (WT: 8.43 ± 0.84; Tg: 6.31 ± 0.82; t test, p = 0.086). **E.** FP slope normalized to FV amplitude (WT: n = 16 slices, 7 mice; Tg: n = 22 slices, 7 mice). **F.** Representative FP traces.

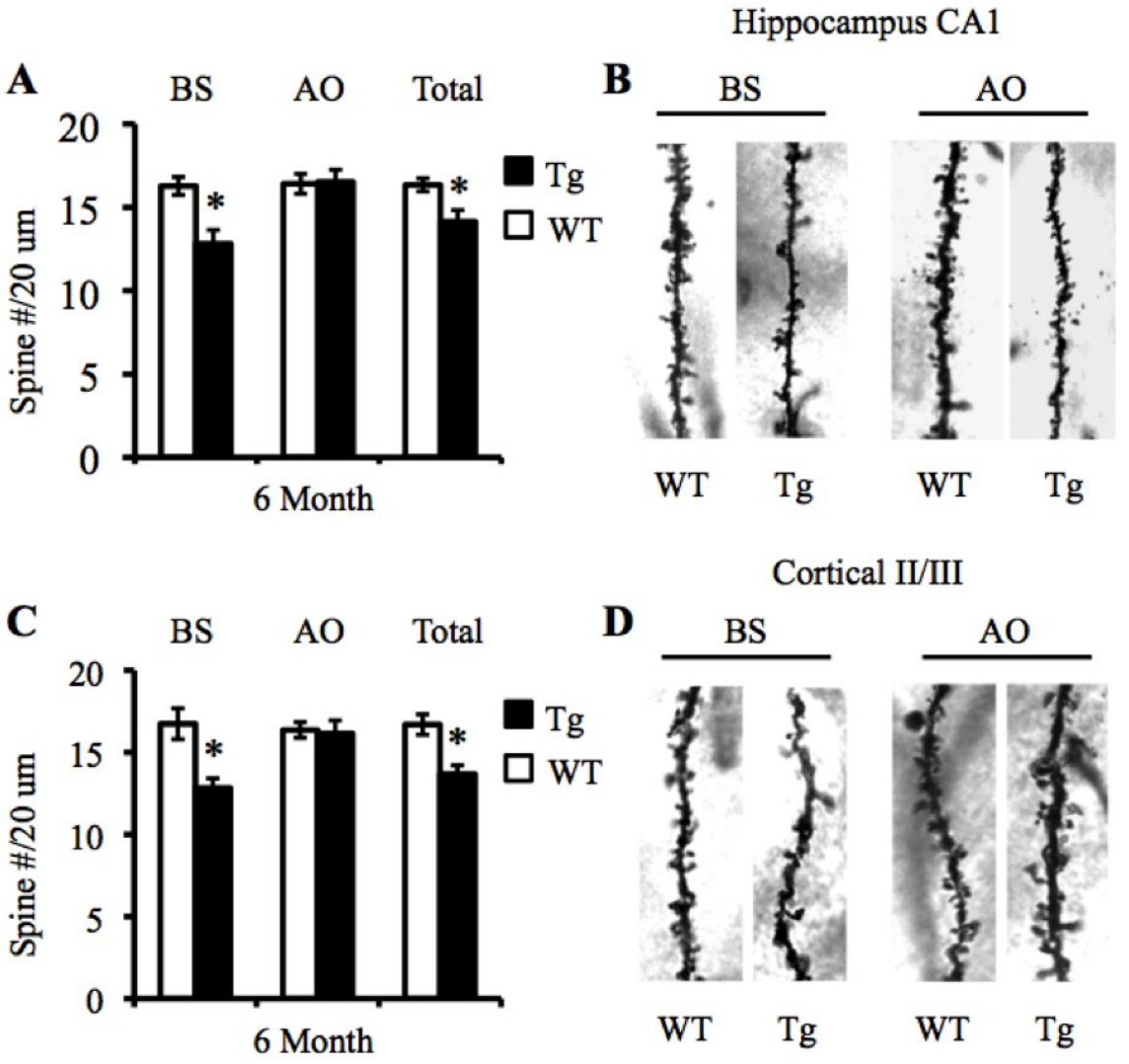

Figure 2.4. Dendritic spine density in CA1 and cortical II/III of adult WT and APPswe;PS1deltaE9 Tg mice.

(A-B) Selective decrease in dendritic spine density of basal dendrites in CA1 of 6-month Tg mice. **A.** Left, Spine density in hippocampal basal shaft (BS) dendrites (n = 3 mice; t test, *p < 0.01). Middle, Spine density in hippocampal apical oblique (AO) dendrites (n = 3 mice; t test, p = 0.595). Right, Total spine density (BS + AO) in hippocampal dendrites (n = 3 mice; t test, *p < 0.05). **B.** Representative BS and AO dendrites from hippocampal CA1 neurons from WT and Tg mice, as indicated. **(C-D)** Selective decrease in dendritic spine density of basal dendrites in cortically layers II/III of 6-month Tg mice. **C.** Left, Spine density in cortically II/III basal shaft (BS) dendrites (n = 3 mice; t test, *p < 0.01). Middle, Spine density in cortical II/III apical oblique (AO) dendrites (n = 3 mice; t test, p = 0.817). Right, Total spine density in cortical II/III dendrites (n = 3 mice; t test, *p < 0.001). **D.** Representative BS and AO dendrites from cortically layers II/III neurons from WT and Tg mice, as indicated.

To examine how the progression of amyloidogenesis and other FAD-linked factors affect basal synaptic transmission adult, 6-month old Tg mice were studied. In contrast to the young, 1-month old Tg mice, there was no change in input-output function with stimulus intensity (Fig 2.3 A&B), the maximal FV response (Fig 2.3 C), or the rate at which axons were recruited (Fig 2.3 D). Also, there was no change in synaptic transmission when normalized to the presynaptic FV amplitude (Fig 2.3 E). Consistent with the rather normal basal synaptic transmission at the Schaffer collateral to CA1, we found that the dendritic spine density of apical oblique dendrites of CA1 neurons, which receive Schaffer collateral inputs, is also normal in adult Tg mice (Fig 2.4 A&B). Interestingly, we found a selective decrease in dendritic spine density at BS dendrites in CA1 and cortical layers II/III in adult Tg mice (Fig 2.4), which suggests that the inputs to BS dendrites may be more vulnerable at this age across different brain areas.

Subsection 3: Paired pulse facilitation in young and adult APPswe;PS1deltaE9 Tg mice

To determine whether there is any alteration in presynaptic function, we measured the paired pulse facilitation (PPF) ratio. This form of short-term plasticity occurs when two stimulation pulses are given very close to one another allowing for summation of calcium in the presynaptic terminal causing the second response to be larger than the first. The PPF ratio is the ratio of the slope of the second field potential (FP) response over the slope of the first FP, and it is commonly used as a correlate of the release probability of the presynaptic cell. Young Tg mice showed no change in PPF ratio over all interstimulus intervals (ISIs) (Fig 2.5 A). In contrast, PPF ratio was decreased at early ISIs in adult Tg mice (Fig 2.5 B), which could suggest enhancement in presynaptic function. An alternative explanation is that altered calcium dynamics lead to an inability to summate the responses, resulting in decreased facilitation.

Subsection 4: Frequency-dependent plasticity in young and adult APPswe;PS1deltaE9

Tg mice

To determine whether changes in frequency-dependent synaptic plasticity seen in APPswe;PS1deltaE9 Tg mice are due to altered metaplasticity, we measured synaptic plasticity

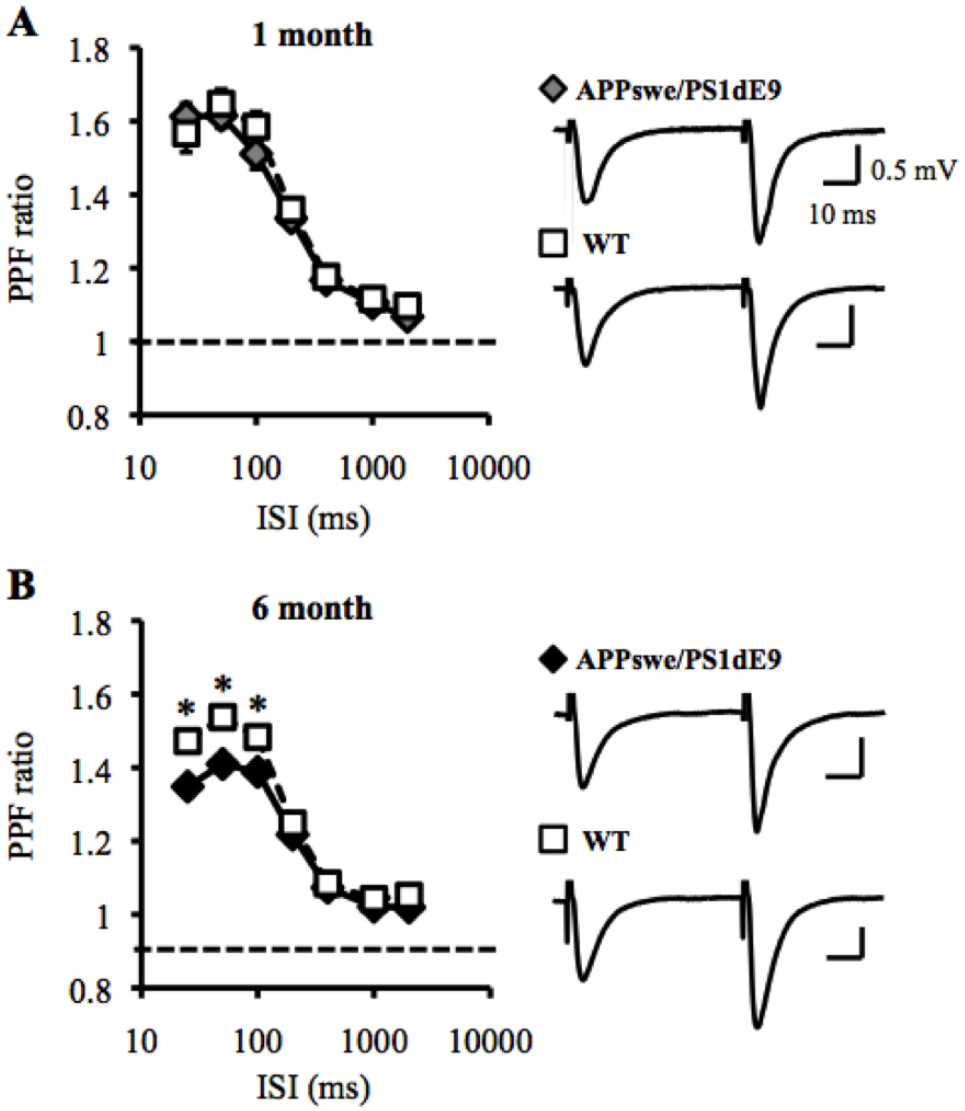

Figure 2.5. PPF ratio in young and adult WT and APPswe;PS1deltaE9 Tg mice.

A. No change in paired pulse facilitation (PPF) ratio in 1-month Tg mice. Left, PPF ratio at different interstimulus intervals (ISI). Right, Representative traces at 50 ms ISI (WT: n = 20 slices, 6 mice; Tg: n = 30 slices, 6 mice.) **B.** Decreased PPF ratio at shorter ISIs (25, 50, and 100 ms) in 6-month Tg mice. Left, PPF ratio at different ISIs. Right, Representative traces at 50 ms ISI (WT: n = 22 slices, 7 mice; Tg: n = 23 slices, 5 mice; t test at 25, 50, 100 ms ISIs, *p < 0.01).

using standard LTP/LTD protocols, as well as an intermediate simulation frequency close to the modification threshold. In young Tg mice, high frequency theta burst induced LTP is increased (Fig 2.6 C), while low frequency stimulation induced LTD is decreased (Fig 2.6 A). An intermediate frequency (10 Hz, 900 pulses) produced reliable LTD in young WT mice but no long-term change in young Tg mice (Fig 2.6 B). This is consistent with the modification threshold for inducing plasticity being shifted to the left in favor of LTP (Fig 2.6 D). In adult Tg mice, high frequency theta burst induced LTP is decreased (Fig 2.6 G), while low frequency stimulation induced LTD is increased (Fig 2.6 E). Despite the fact that synaptic changes at an intermediate stimulation frequency did not reach statistical significance (Fig 2.6 F), our data are consistent with the modification threshold for inducing plasticity being shifted to the right to promote LTD (Fig 2.6 H). Taken together, these data suggest that metaplasticity is altered in both young and adult Tg mice, but in opposite directions.

Figure 2.6. Frequency-dependent plasticity in young and adult WT and APPswe;PS1deltaE9 Tg mice.

A. A decrease in the magnitude of LTD following 1 Hz, 900 pulses protocol in 1-month Tg mice (WT: 71.11 ± 3.67% of baseline at 1-hour after onset of 1 Hz, n = 9 slices, 3 mice; Tg: 80.19 ±1.91%, n = 15 slices, 5 mice; t test, *$p < 0.05$). Top, Representative traces (baseline: thin line, post-LTD: thick line). **B.** Significant difference in plasticity following an intermediate 10 Hz, 900 pluses protocol in 1-month Tg mice (WT: 87.98 ± 2.98% of baseline at 1-hour after onset of 10 Hz, n = 15 slices, 5 mice; Tg: 98.88 ± 2.91%, n = 16 slices, 5 mice; t test, *$p < 0.05$). Top, Representative traces (baseline: thin line, post-LTD: thick line). **C.** An increase in the magnitude of LTP following 4xTBS protocol in 1-month Tg mice (WT: 124.26 ± 3.75% of baseline at 1-hour after 4xTBS, n = 11 slices, 5 mice; Tg: 141.38 ± 5.95%, n = 10 slices, 6 mice; t test, *$p < 0.05$). Top, Representative traces (baseline: thin line, post-LTD: thick line). **D.** The modification threshold for LTP/D is shifted to the left in young, 1-month Tg mice, which shows enhanced LTP at the expense of LTD compared to WT mice. **E.** An increase in the magnitude of LTD following pp-1 Hz, 900 pulses protocol in 6-month Tg mice (WT: 92.20 ± 2.18% of baseline 1-hour after onset of pp-1 Hz, n = 11 slices, 4 mice; Tg: 81.97 ± 2.41%, n = 12 slices, 4 mice; t test, *$p < 0.01$). Top, Representative traces (baseline: thin line, post-LTD: thick line). **F.** No significant difference in plasticity following an intermediate 10 Hz, 900 pluses protocol in 6-month Tg mice (WT: 111.73 ± 3.82% of baseline 1-hour after onset of 10 Hz, n = 14 slices, 5 mice; Tg: 102.22 ± 3.26%, n = 15 slices, 5 mice; t test, $p= 0.069$). Top, Representative traces (baseline: thin line, post-LTD: thick line). **G.** A decrease in the magnitude of LTP following 4xTBS protocol in 6-month Tg mice (WT: 172.31 ± 11.68% of baseline at 1-hour after 4xTBS, n = 10 slices, 6 mice; Tg: 139.34 ± 7.24%, n = 12 slices, 5 mice; t test, *$p < 0.05$). Top, Representative traces (baseline: thin line, post-LTD: thick line). **H.** The modification threshold for LTP/D is shifted to the right in adult 6-month Tg mice, which shows impaired LTP and enhanced LTD compared to WT mice.

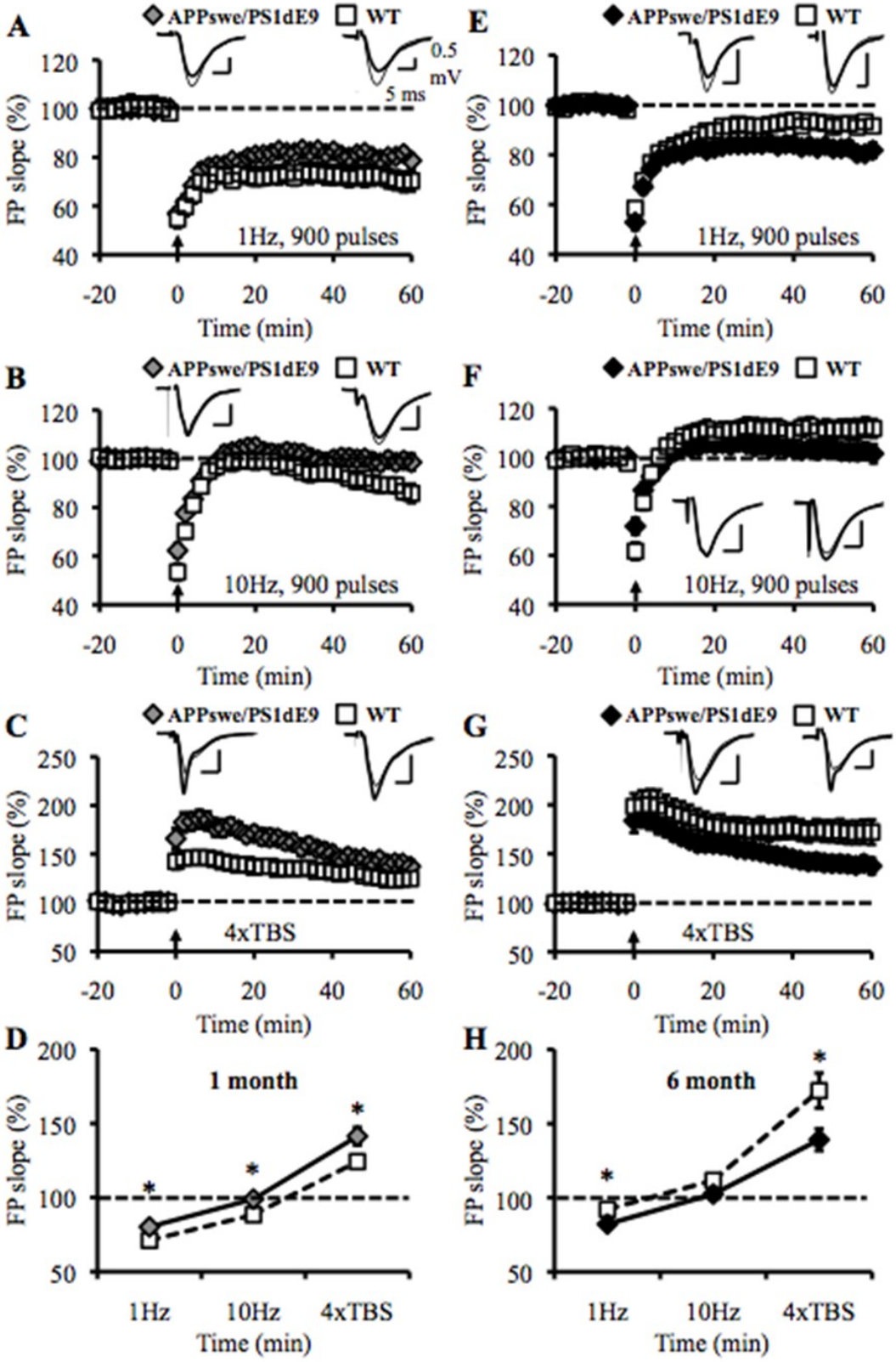
A
APPswe/PS1dE9
WT
0.5 mV
5 ms
FP slope (%)
1Hz, 900 pulses
Time (min)
B
10Hz, 900 pulses
C
4xTBS
D
1 month
1Hz
10Hz
4xTBS
E
F
G
H
6 month

We also observed an unexpected phenomenon when looking at plasticity across development in WT and Tg mice. While WT mice show a developmental increase in frequency-dependent LTP, Tg mice lacked this developmental change (Fig 2.7). Therefore, Tg mice produce similar magnitudes of LTP/LTD in both young and adult ages, despite having larger LTP than

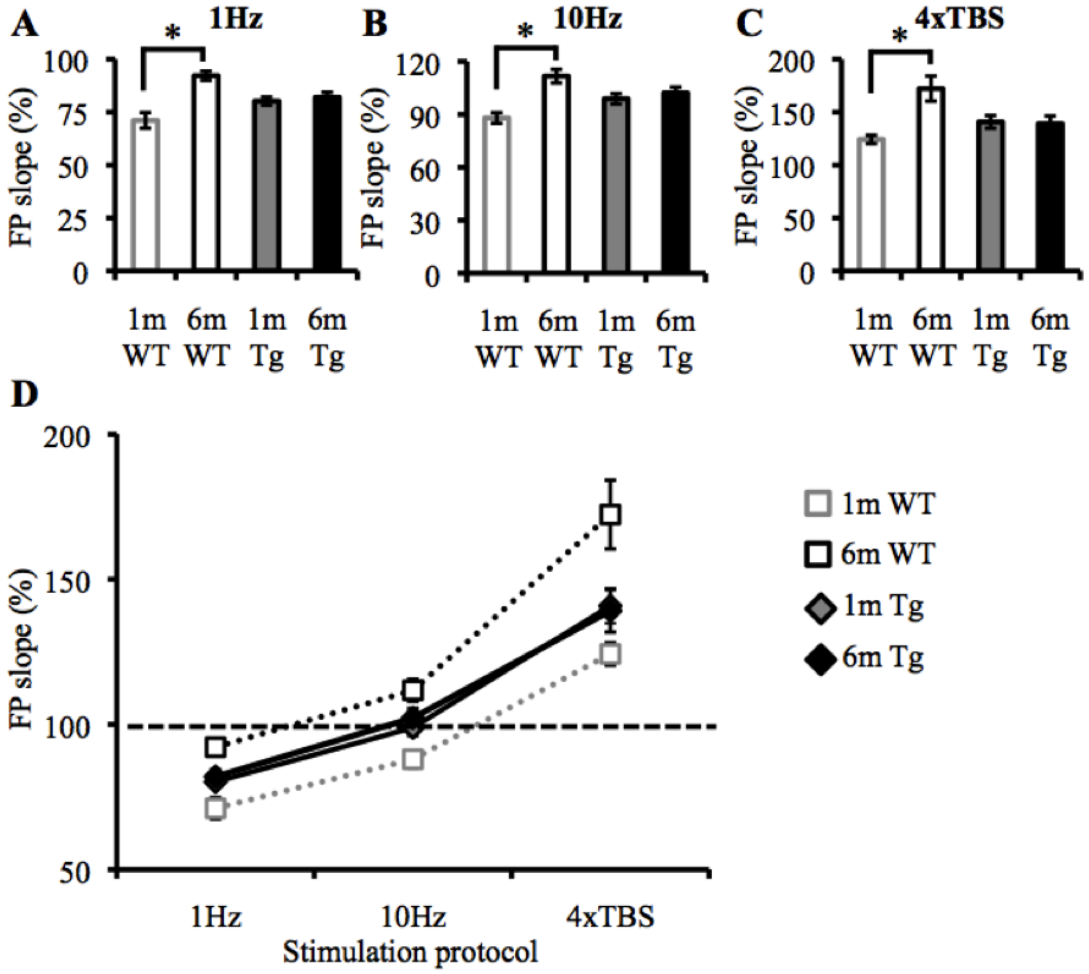

Figure 2.7. Deficit in developmental regulation of metaplasticity in APPswe;PS1deltaE9 Tg mice.

A. WT mice show a reduction in the magnitude of LTD with age. Magnitude of LTD following 1 Hz protocol does not change over development from 1-month to 6-month Tg mice (n = same as Fig 2.6, t test, *p <0.001). **B.** WT mice show a developmental change in the polarity of 10 Hz-induced plasticity. In contrast, the magnitude of plasticity following an intermediate 10 Hz protocol does not change over development from 1-month to 6-month Tg mice (n = same as Fig 2.6, t test, *p <0.001). **C.** The magnitude of LTP induced with 4xTBS increased with age in WT mice, which is absent in Tg mice (n = same as Fig 2.6, t test, *p <0.01). **D.** WT mice show a shift in their modification threshold during development. Tg mice appear to be unable to regulate metaplasticity during development and do not shift their modification threshold.

WT at 1-month of age and smaller LTP than WT at 6-months of age. Therefore, in WT mice the modification threshold is shifted to the left during development; however, Tg mice do not undergo this developmental shift (Fig 2.7 D). This suggests that the developmental regulation of metaplasticity is altered in Tg mice.

Subsection 5: NMDAR gain and other factors that control induction threshold in young and adult APPswe;PS1deltaE9 Tg mice

Due to our sparse sampling of frequency-dependent plasticity, the alterations in metaplasticity observed in Tg mice at either age, can be explained by either the sliding threshold or pull-push models. To differentiate which mode of metaplasticity is altered, we looked at NMDAR gain in young and adult mice. In young Tg mice, the summation of synaptic responses during high frequency LTP induction was increased (Fig 2.8 A). This suggests an altered induction mechanism for LTP in young Tg mice. Enhanced NMDAR function during induction of LTP could be attributed to a decrease in the GluN2A/GluN2B ratio as suggested by the sliding threshold model. To directly test whether alterations in the ratio of NMDAR subunit composition may be mediating the changes associated with sliding the threshold for inducing plasticity in young Tg mice, we biochemically measured if there were changes in the expression of the NR2A/NR2B ratio. There was no difference in the NR2A/NR2B ratio between young WT and Tg mice (Fig 2.8 B). To verify that there was no change in synaptic NMDAR function, we pharmacologically isolated NMDAR current and tested their sensitivity to a GluN2B subunit antagonist, ifenprodil. There was no change in the decay constant (Fig 2.8 C, middle) or the percent of the response blocked by ifenprodil (Fig 2.8 C, left). This suggests that NMDAR subunit composition is similar between WT and Tg mice at this age. Therefore, changes in the ratio of NMDAR subunits cannot account for changing the threshold for inducing frequency dependent plasticity.

Other factors such as inhibitory synaptic transmission, also have a large influence on plasticity induction (Steele and Mauk, 1999). However, we saw no change in mIPSC amplitude (Fig 2.8 D), frequency (Fig 2.8 F), or charge transfer (Fig 2.8 E), suggesting that there is no significant change in inhibitory synaptic transmission in young Tg mice. Together, this suggests that the resulting changes in plasticity induction mechanisms in young Tg mice are likely via mechanisms other than regulation of NMDARs or inhibitory function.

In adult Tg mice, there was no change in the summation of synaptic responses during high frequency LTP induction (Fig 2.8 G). There was also no change in NR2A/NR2B ratio expression (Fig 2.8 H). This would indicate that induction mechanisms are not altered in adult Tg mice, and hence it rules out the sliding threshold model of metaplasticity.

Figure 2.8. NMDAR gain and inhibitory synaptic transmission in young and adult WT and APPswe;PS1deltaE9 Tg mice.

A. Increase in the summation of synaptic responses during 4xTBS induction protocol in 1-month Tg mice (ANOVA, *$p < 0.01$). Top, Representative traces (WT: black line, Tg: grey line). **B.** No difference in total NR2A/NR2B ratio in 1-month mice (WT: 100.82 ± 3.22% of average WT, n = 10 mice; Tg: 78.05 ± 11.16% of average WT, n = 10 mice; t test, p = 0.077). **(C)** No difference in the NMDAR-mediated response blocked by GluN2B antagonist ifenprodil (3 μM) in 1-month Tg mice. **C.** Left, Percent of the response amplitude blocked by ifenprodil (WT: 48.03 ± 8.64%, n = 7 cells, 5 mice; Tg: 47.66 ± 5.95%, n = 10 cells, 5 mice; t test, p = 0.973). Middle, Average changes in the decay constant (WT: control = 183.23 ±38.77 ms, ifenprodil = 97.02 ± 13.87 ms, n = 7 cells, 5 mice; Tg: control = 163.41 ± 18.02 ms, ifenprodil = 92.48 ± 13.99 ms, n = 10 cells, 5 mice; t test before, p = 0.654; t test after, p = 0.821). Right, Pharmacologically isolated NMDAR-mediated EPSCs recorded before (black line) and after bath application of ifenprodil (dark grey line). The normalized responses after ifenprodil are also included (light grey line). The traces are normalized to the peak amplitude in control ACSF and represent averages across all cells recorded in each condition (20-40 responses per cell). **(D-F).** No difference in whole-cell recording of miniature $GABA_A$R-mediated IPSCs (mIPSCs). **D.** No change in average mIPSC amplitude of CA1 pyramidal cells from 1-month Tg mice (WT: 42.28 ± 5.19 pA, n = 15 cells, 10 mice; Tg: 48.07 ± 4.19 pA, n = 15 cells, 9 mice; t test, p = 0.393). Right, Average mIPSC trace from each group. **E.** No change in charge transfer as measured by area under the curve in 1-month Tg mice (WT: 222.10 ± 33.57 fC, n = 12 slices, 10 mice; Tg: 276.74 ± 52.71 fC, n = 15 slices, 9 mice; t test, p = 0.391). **F.** No change in average mIPSC frequency of CA1 pyramidal cells from 1-month Tg mice. Left, Comparison of average mIPSC frequency (WT: 15.19 ± 1.18 Hz, n = 15 cells, 10 mice; Tg: 14.32 ± 1.24 Hz, n = 15 cells, 9 mice; t test, p = 0.615). Right, representative mIPSC traces taken from cells of each group. **G.** No change in the summation of synaptic responses during 4xTBS induction protocol in 6-month Tg mice. Top, Representative traces (WT: grey line, Tg: black line). **H.** No difference in total NR2A/NR2B ratio in 6-month mice (WT: 91.16 ± 12.06%, n = 8 mice; Tg: 102.11 ± 15.18%, n = 8 mice; t test, p = 0.581).

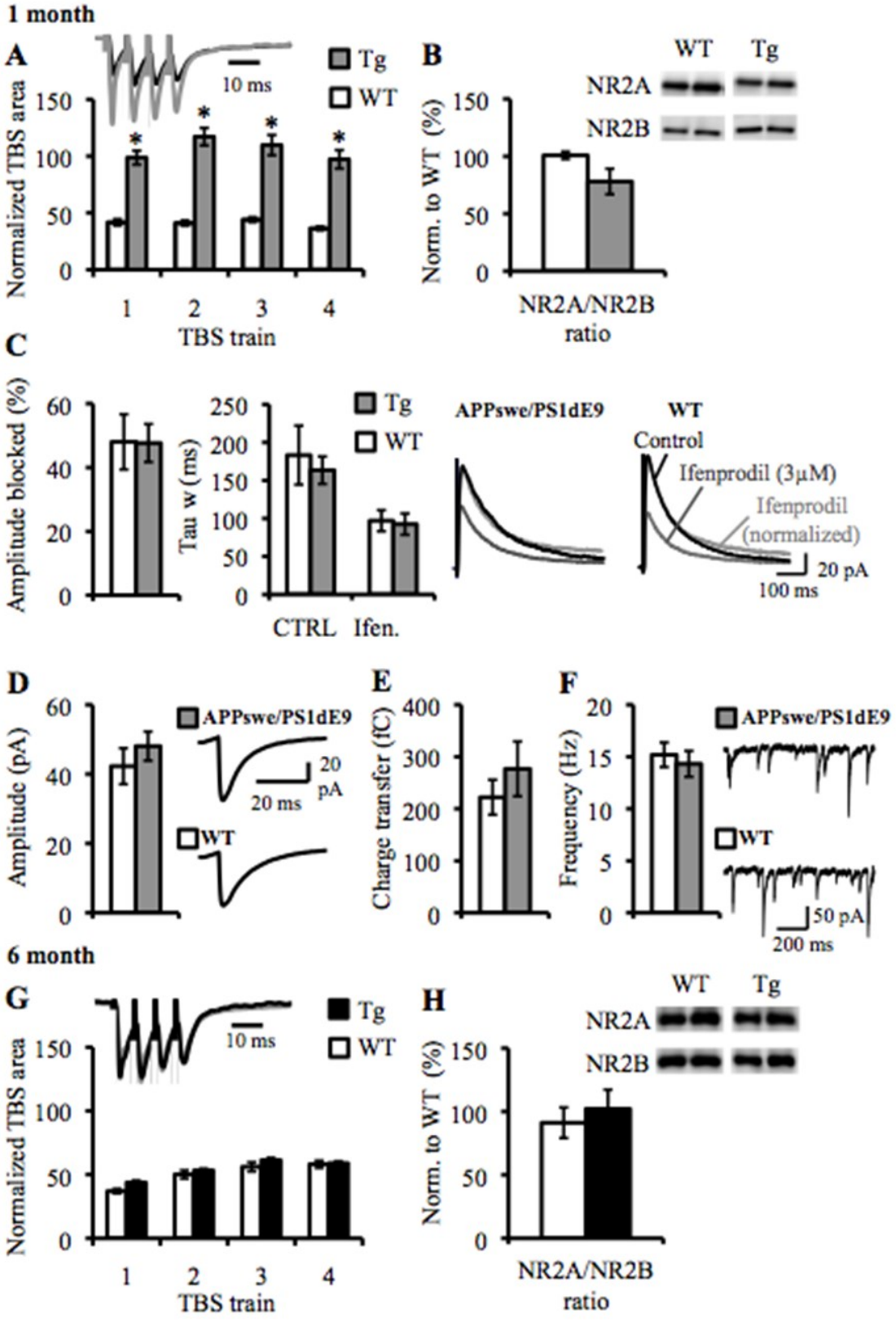
1 month
A
Normalized TBS area
150
100
50
0
10 ms
Tg
WT
1
2
3
4
TBS train
B
WT
Tg
NR2A
NR2B
Norm. to WT (%)
150
100
50
0
NR2A/NR2B
ratio
C
Amplitude blocked (%)
60
40
20
0
Tau w (ms)
250
200
150
100
50
0
Tg
WT
CTRL
Ifen.
APPswe/PS1dE9
WT
Control
Ifenprodil (3μM)
Ifenprodil
(normalized)
20 pA
100 ms
D
Amplitude (pA)
60
40
20
0
APPswe/PS1dE9
20 pA
20 ms
WT
E
Charge transfer (fC)
400
300
200
100
0
F
Frequency (Hz)
20
15
10
5
0
APPswe/PS1dE9
WT
50 pA
200 ms
6 month
G
Normalized TBS area
150
100
50
0
10 ms
Tg
WT
1
2
3
4
TBS train
H
WT
Tg
NR2A
NR2B
Norm. to WT (%)
150
100
50
0
NR2A/NR2B
ratio

Subsection 6: Regulation of AMPA receptors in young and adult APPswe;PS1deltaE9 Tg mice

Changes in frequency-dependent plasticity especially in adult Tg mice appear to be mediated by dysregulation of pull-push metaplasticity, leading to altered expression mechanisms for controlling LTP/LTD. The pull-push model states that neuromodulators acting on specific G-protein coupled receptors (GPCRs) promote the expression of LTP/LTD by changing phosphorylation states of AMPARs, thereby priming the synapse for LTP or LTD. Therefore, a key feature of the pull-push model is the size of the perisynaptic AMPAR population and the regulation of AMPAR phosphorylation. To measure the former, we used TBOA, a glutamate transporter inhibitor, to induce spill over of glutamate that will activate perisynaptic AMPARs (Fig 2.9 A&B). While the amplitude of FP recordings increased after TBOA application in WT and Tg mice at both ages, there was no significant difference between genotypes at either age (Fig 2.9 A&B). This suggests that the size of the perisynaptic pool is similar between WT and Tg mice. We noted that there might be a developmental increase in the size of the perisynaptic pool

Figure 2.9. Quantification of perisynaptic AMPAR population and major AMPAR phosphorylation sites in young and adult WT and APPswe;PS1deltaE9 Tg mice.

A. Amplitude of FP recordings from CA1 of 1-month WT and Tg mice is similar following 10 μM TBOA (WT: 105.83 ± 3.99% of baseline at 40-min post-TBOA, n = 12 slices, 4 mice; Tg: 106.30 ± 2.76%, n = 10 slices, 4 mice; t test, p = 0.922). Top, Representative traces (before TBOA: thin line, after TBOA: thick line). **B.** Amplitude of FP recordings from CA1 of 6-month WT and Tg mice is similar following 10 μM TBOA (WT: 112.63 ± 2.74% of baseline at 40-min post-TBOA, n = 13 slices, 4 mice; Tg: 117.46 ± 4.63%, n = 13 slices, 4 mice; t test, p = 0.380). Top, Representative traces (before TBOA: thin line, after TBOA: thick line). **(C-D).** Top, representative immunoblots. Bottom, average data of glutamate receptor signal normalized to average WT control. **C.** No difference in total GluA1 (WT: 97.15 ± 2.88%, n = 7 mice; Tg: 77.83 ± 10.16%, n = 11 mice; t test, p = 0.093), decrease in total S845/GluA1 ratio (WT: 103.34 ± 5.31% of average WT, n = 7 mice; Tg: 80.73 ± 6.60% of average WT, n = 10 mice; t test, *p < 0.05), and increase in total S831/GluA1 ratio (WT: 102.88 ± 6.30%, n = 8 mice; Tg: 208.39 ± 29.09%, n = 9; t test, *p < 0.01) in hippocampal samples from 1-month Tg mice. **D.** No difference in total GluA1 (WT: 101.10 ± 7.86%, n = 10 mice; Tg: 81.93 ± 7.85%, n = 10 mice; t test, p = 0.102), S845/GluA1 ratio (WT: 99.41 ± 4.82%, n = 9 mice; Tg: 133.93 ± 18.54%, n = 10 mice; t test, p = 0.101), and S831/GluA1 ratio (WT: 101.28 ± 6.25%, n = 8 mice; Tg: 109.11 ± 5.44%, n = 8 mice; t test, p = 0.362) in hippocampal samples from 6-month WT and Tg mice.

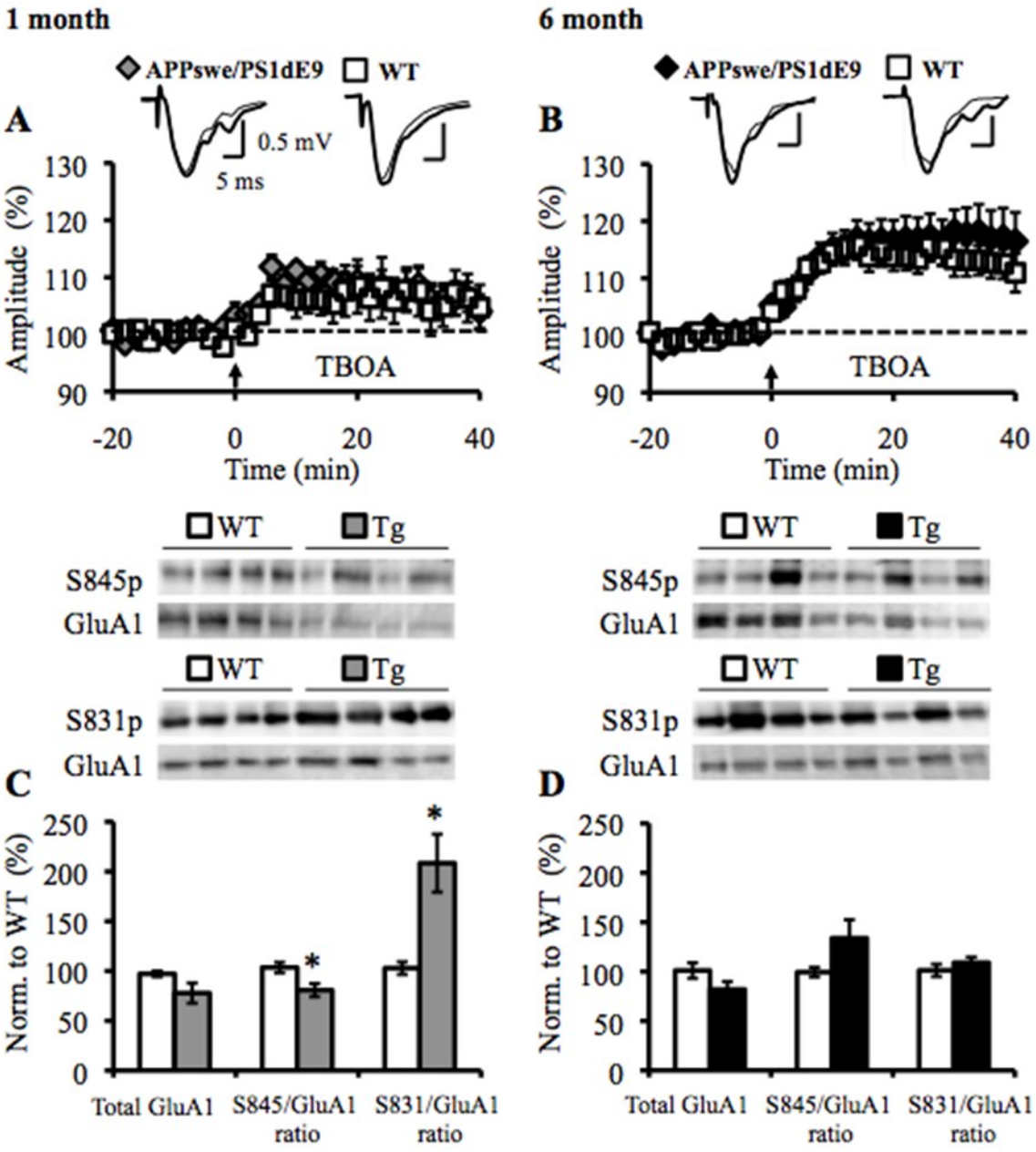

as measured as changes in FP after TBOA, however only the Tg mice showed a significant difference between young and adult mice (ANOVA, *$p < 0.05$; Fig 2.9 A&B).

Specific phosphorylation sites on AMPAR subunit GluA1, such as GluA1-S845 and GluA1-S831, have been correlated with LTP and LTD (Lee et al., 2000a, 2003). It has also been proposed that soluble Aβ peptides can alter AMPAR endocytosis by modulating downstream

kinases and phosphatases, leading to decreased GluA1-S845 phosphorylation and cell surface AMPARs (Miñano-Molina et al., 2011). Furthermore, changes in GluA1-S845 and S831 phosphorylation sites have been correlated with pull-push model of metaplasticity (Seol et al., 2007; Huang et al., 2012). Young Tg mice show a decrease in the S845/GluA1 ratio (Fig 2.9 C) but an increase in the S831/GluA1 ratio (Fig 2.9 C) compared to WT mice, with no difference in total GluA1 (Fig 2.9 C). This suggests a possible correlation between GluA1-S831 phosphorylation and increased LTP magnitude. In adult Tg mice, there was no change in total GluA1, S845/GluA1 ratio, and S831/GluA1 ratio (Fig 2.9 D). Together these data support a change in the expression mechanisms of LTP/LTD in the Tg mice, which supports a defect in the pull-push model as a way to explain the observed altered metaplasticity in young and adult Tg mice.

Section 4: Discussion

We investigated age-dependent alterations in basal synaptic function and plasticity in APPswe;PS1deltaE9 Tg mice. We observed altered metaplasticity in young and adult Tg mice (Fig 2.6). In young Tg mice, a shift in the modification threshold to the left favors LTP, but in adult Tg mice, a shift in the modification threshold to the right promotes LTD. Despite enhanced summation of synaptic responses in young Tg mice (Fig 2.8 A), conventional induction mechanisms for controlling the sliding threshold of metaplasticity were normal in both young and adult Tg mice (Fig 2.8). Most interesting was that Tg mice appear to be developmentally stuck and unable to regulate metaplasticity with age (Fig 2.7). Therefore, we suggest dysregulation of pull-push metaplasticity, leads to altered expression mechanisms for controlling LTP/LTD in Tg mice across ages (Fig 2.9).

Subsection 1: Differential contribution of FAD-linked mutations across age

Mouse models have been generated expressing FAD-linked mutations in APP, PS1, or PS2 in order to study synaptic transmission and plasticity changes associated with AD. While many of these studies have focused on hippocampal plasticity, specifically frequency-dependent LTP, there is still no clear picture of how synaptic dysfunction progresses in these AD Tg mouse models (Marchetti and Marie, 2011). The resulting inconclusiveness is likely due to differences in FAD-linked contributing factors seen across synaptic parameters studied. It is important to consider how, and if, different FAD-linked mutations will result in different synaptic phenotypes, which may become important when generating effective therapies and may lead to the need for personalized medicine. For example, the APP and PS1 FAD mutations in our mouse model may contribute differently to synaptic dysfunction due to a difference in their relative contribution to synaptic phenotypes with age. In young, 1-month old animals, the contribution of Aβ peptides to synaptic phenotypes is small and therefore any phenotypes seen in young mice may be due exclusively to the FAD-linked mutation in PS1. In addition to enhanced LTP (Fig 2.6 C), we observed an increase in basal synaptic function (Fig 2.1) and dendritic spine density (Fig 2.2). These phenotypes have been shown by others to occur in single PS1 Tg mice at this age (Zaman et al., 2000; Dewachter et al., 2008; Inoue et al., 2009; Jung et al., 2011; Marchetti and Marie, 2011), so we conclude that these phenotypes may be attributed to the FAD-linked mutation in PS1.

In adult, 6-month old animals, the impact of Aβ peptides would now be evident in addition to effects of altered PS1. Reduced LTP (Fig 2.6 G) and decreased dendritic spine density (Fig 2.4) have been seen in other mouse models expressing mutated APP protein (Chapman et al., 1999; Fitzjohn et al., 2001; Trinchese et al., 2004; Spires et al., 2005; Jacobsen et al., 2006; Palop et al., 2007). We believe this phenotype can be attributed to Aβ accumulation since these phenotypes are not observed in adult PS1 Tg mice. The observed differences in presynaptic

function in adult Tg mice (Fig 2.5 B) is likely due to altered calcium dynamic caused by the FAD-linked mutation in PS1, which is known to enhance the ER Ca^{2+} leak channel function of PS1 (Tu et al., 2006). In addition, mice expressing a single APPswe mutation at this age do not show changes in PPF ratio (Chapman et al., 1999; Palop et al., 2007; Harris et al., 2010).

The opposite LTP/LTD phenotype seen in young versus adult Tg mice could be attributed to difference in amyloid load. This is in line with a recent study which showed that mild cognitive impairment (MCI) and AD patients display opposite gene expression profiles compared to normal aged controls (Berchtold et al., 2014). Perhaps pre- and post-amyloidogenic mice are also not on a continuum from WT mice, but display opposing phenotypes compared to WT mice, similar to MCI and AD patients.

Subsection 2: Altered induction mechanisms for LTP/LTD in young APPswe;PS1deltaE9 Tg mice

It remains unclear at what level cellular mechanisms for regulating plasticity are becoming disrupted, leading to the conserved deficits in synaptic plasticity. Enhanced LTP in young Tg mice is likely due to altered induction mechanisms since we observed an increase in response summation during TBS used for LTP induction (Fig 2.8 A). However, we saw no functional change in NMDAR subunit composition (Fig 2.8 C), no change in the NMDAR ratio (Fig 2.8 B), and no change in inhibitory synaptic transmission (Fig 2.8 D-F). Changes in NMDAR ratio and inhibition have been implicated as major mechanisms for mediating the sliding threshold of metaplasticity (Steele and Mauk, 1999; Bear, 2003). Here we find that an alternative mechanism is at play to regulate the induction mechanisms of LTP/LTD in young Tg mice. We surmise that this may be due to the observed changes in AMPAR function. GluA1-S831 phosphorylation is known to selectively increase conductance of GluA1 homomers (Oh and Derkach, 2005), which are inward rectifying and Ca^{2+}-permeable (Cull-Candy et al., 2006).

Inward rectifying AMPARs can summate responses better, because they do not produce outward current when the membrane is depolarized (Bowie and Mayer, 1995). Therefore, if the increase in GluA1-S831 phosphorylation (Fig 2.9 C), observed in young Tg mice, was found on inward rectifying GluA1 homomers, this could increase the summation of synaptic responses during LTP induction. In support of this idea, GluA1 phosphorylation at S845 and S831 has been shown to decrease the threshold for producing LTP (Makino et al., 2011; Hu et al., 2007), similar to what we observed in young Tg mice (Fig 2.6 D). In addition, the enhanced LTP in young Tg mice could be due to dysregulated intracellular calcium dynamics due to the FAD-linked mutation in PS1 (Cheung et al., 2010). Indeed, it has been shown that a rise in intracellular calcium alone is sufficient to alter the signaling cascades downstream of NMDARs (Horne and Dell'Acqua, 2007; Thore et al., 2004), like AC and PLC, involved in pull-push regulation of metaplasticity responsible for altering plasticity expression mechanisms.

In addition to the altered induction mechanism, the reduction of LTD in young Tg mice could be due to the decrease in GluA1-S845 phosphorylation (Fig 2.6 A). S845 dephosphorylation correlates with LTD expression (Lee et al., 1998, 2000a), and S845 phosphorylation site is necessary for LTD (Lee et al. 2003; Lee et al. 2010). Therefore, reduced basal phosphorylation of S845 is predicted to occlude further LTD.

Subsection 3: Altered expression mechanisms of LTP/LTD in adult APPswe;PS1deltaE9 Tg mice

In adult Tg mice, we did not observe changes in the summation of synaptic responses during LTP induction (Fig 2.8 G) nor in NMDAR subunit composition (Fig 2.8 H). Therefore, it is clear that the synaptic deficits at this age are most likely due to altered expression mechanisms as suggested by the pull-push model. However, dysregulation of expression mechanisms is not at the level of changes in basal phosphorylation of AMPARs, as both the S831 and S845

phosphorylation on the GluA1 subunit were similar between adult WT and Tg mice. Instead, the defect may reflect an ineffective upstream neuromodulatory signal or lie downstream of AMPAR phosphorylation. A proposed key mechanism of LTP expression is synaptic recruitment and stabilization of AMPARs from a perisynaptic pool, but we did not observe a change in the size of the perisynaptic AMPAR pool in adult Tg (Fig 2.9 B). This suggests that the deficit in LTP is not due to insufficient AMPARs available for synaptic insertion. Rather, it suggests a failure to stabilize AMPARs at synapses following LTP induction. This is supported by our observation that the initial phase of LTP is normal in adult Tg mice, but it decays. Synaptic stabilization of AMPARs is thought to occur via interaction of AMPAR with a hypothetical "slot" protein at the PSD (Kessels and Malinow, 2009). We surmise that the ability to generate new "slots" during LTP is compromised in adult Tg mice, hence the newly inserted synaptic AMPARs are not stabilized.

Subsection 4: Defective developmental change of LTP/LTD in APPswe;PS1deltaE9 Tg mice

Finally, we observed an unexpected and interesting developmental deficit in the Tg mice (Fig 2.7). We found that the magnitude of frequency-dependent LTP/LTD in young Tg mice is similar to adult Tg mice and does not undergo enhancement as was seen during normal development in WT mice. Based on our electrophysiological and biochemical data, we provide a model in Figure 2.10. In WT mice, we observed a developmental increase in LTP magnitude (Fig 2.7 C), which we surmise is due to enhanced synaptic recruitment and stabilization of AMPARs (Fig 2.10 A).

In young Tg mice the perisynaptic pool of AMPARs is similar to that of WT (Fig 2.9 A); however, they show larger LTP. This suggests that the rate at which AMPARs are inserted into the membrane and/or the number of "slots" for stabilizing AMPARs is increased compared to

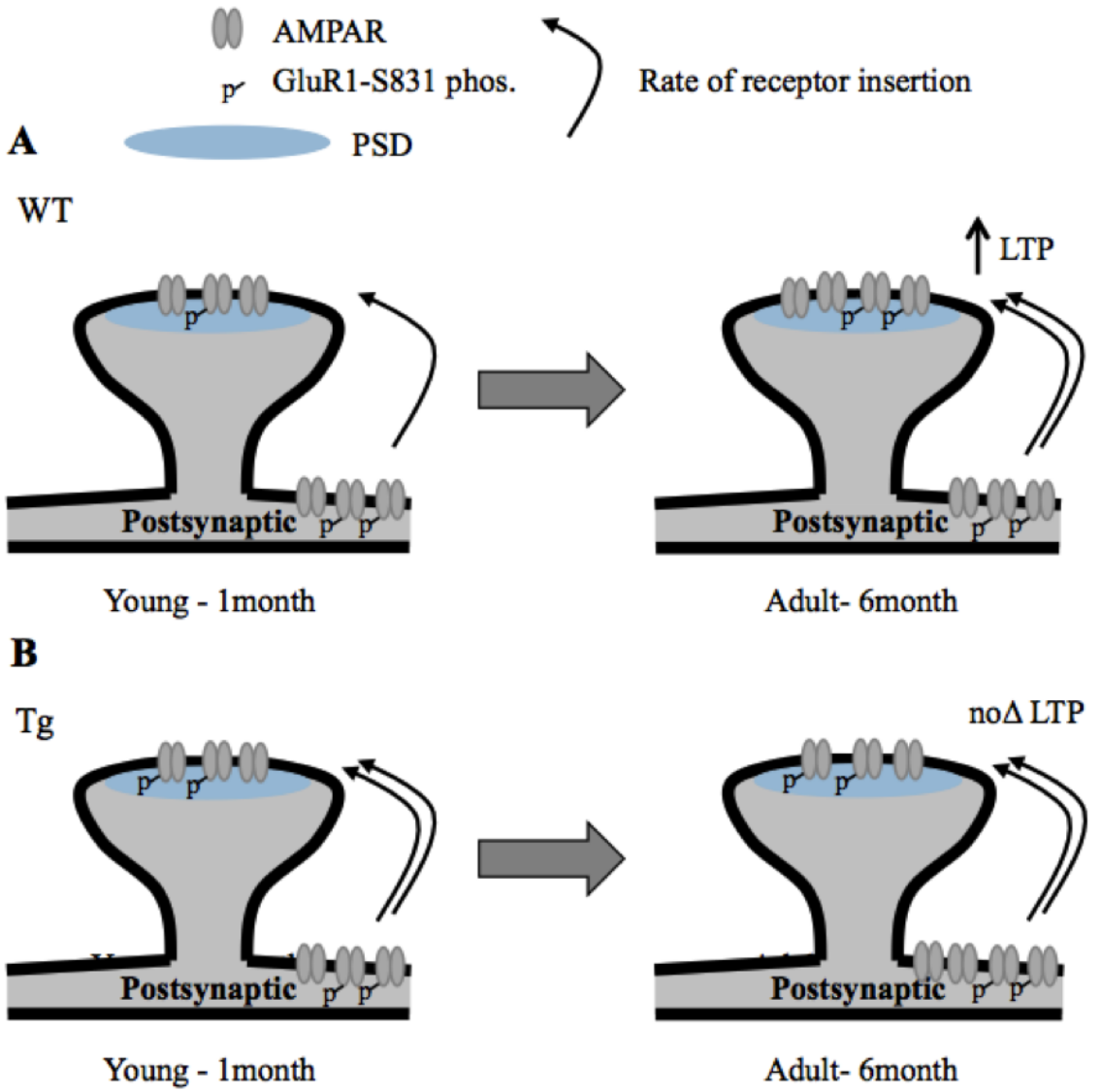

Figure 2.10. Working model of AMPAR regulation throughout development in WT and APPswe;PS1deltaE9 Tg mice.

A. Development in WT mice. As WT mice age, the rate at which AMPARs are inserted at the synapse and the stability of inserted receptors increases with LTP. This increase is likely correlated with an increase in the basal phosphorylation of S831 on the GluA1 subunit (Lee et al., 2010). The result is a larger magnitude of LTP produced in adults, in part due to increased "slot" generation for which AMPAR can be inserted and anchored to the PSD. **B.** Development in Tg mice. Tg mice start with a higher rate of synaptic insertion and a small increase in the ability to generate more "slots" for stabilizing AMPARs at synapses with LTP. This results in a large transient increase in LTP followed by a small, but statistically significant, increase in overall LTP magnitude in young Tg mice. As Tg mice age, the rate at which AMPARs are inserted to synapses or the ability to generate "slots" with LTP does not increase, likely because the S831/GluA1 ratio remains the same. Hence, the magnitude and the shape of LTP in the adults remain the same as in young Tgs. This suggests a defect in developmental changes needed to regulate LTP/D expression mechanisms.

young WT mice, possibly due to an increase in GluA1-S831 phosphorylation (Fig 2.9 C) and presumably larger Ca^{2+} influx based on enhanced synaptic summation during LTP induction (Fig 2.8 A). In adult Tg mice, there is no developmental increase in LTP magnitude even though the level of AMPAR phosphorylation and the perisynaptic AMPAR pool size is similar to those of adult WT mice. This suggests that the developmental deficit is not at the level of synaptic recruitment of AMPARs or the availability of perisynaptic AMPARs, but is likely due to an inability to anchor and stabilize the receptors at the PSD following LTP. Thus, we surmise the lack of developmental changes in LTP is due to an inability to developmentally up-regulate mechanisms for "slot" generation. Considering that the developmental downregulation of LTD magnitude is also defective in Tg (Fig 2.7 A), we propose that the main synaptic dysfunction of Tg mice is its initial "off-set" in LTP/LTD induction threshold and the inability to developmentally regulate LTP/LTD expression mechanisms. In a way, the Tg mice are "stuck" at a defective level of LTP/LTD, and are unable to change as the synapses mature (Fig 2.7 D). The parameters responsible for the sliding threshold model of metaplasticity did not correlate with observed changes in LTP/LTD, rather we observed changes in expression mechanisms. Hence we propose that the defect may lie at the inability to regulate the pull-push model of metaplasticity with age.

Subsection 5: Conclusion

Despite which FAD-linked factors may be mediating the differences in LTP/LTD plasticity in APPswe;PS1deltaE9 Tg mice, the novelty of our data is that the underlying mechanisms for both ages can be explained by noting that these animals are stuck at an altered set point for LTP/LTD induction, and the inability to regulate their metaplasticity mechanisms during development. Therefore, if we can determine a way to normalize this adaptation, we may be able

to recover the synaptic deficits, regardless of which FAD-linked factors contribute to the phenotype.

Chapter 3: A tetra(ethylene glycol) derivative of benzothiazole aniline enhances Ras-mediated spinogenesis

Published in Journal of Neuroscience:

A. Megill*, T. Lee*, A.M. Dibattista, J.M. Song, M.H. Spitzer, M. Rubinshtein, L.K. Habib, C.C. Capule, M. Mayer, R.S. Turner, A. Kirkwood, J. Yang, D.T. Pak, H.K. Lee, H.S. Hoe (2013) J Neurosci 33: 9306–9318

*These authors contributed equally to this work

My contribution: All of the electrophysiology and slice surface biotinylation experiments and analysis.

Section 1: Introduction

Alzheimer's disease (AD) is a neurodegenerative disease characterized by aggregated Aβ plaques in the brain (Finder and Glockshuber, 2007). Extracellular Aβ deposition deteriorates axons, reduces dendritic spine density, and increases oxidative stress (Subbarao et al., 1990), partially by direct interaction between cellular enzymes and Aβ (Lustbader et al., 2004; Habib et al., 2010). Current therapies for AD, such as acetyl cholinesterase inhibitors and NMDA receptor antagonists (memantine), provide only temporary symptomatic relief without altering the long-term progression of the disease. Other leading strategies seek to alter long-term disease progression, but are severely limited by their induction of widespread toxicity. While patients receiving Aβ immunotherapy showed an apparent reduction in Aβ plaque load and slowed cognitive decline, adverse side effects of the treatment have included vasogenic edema (Nicoll et al., 2003; Orgogozo et al., 2003). Likewise, while γ-secretase inhibitors can effectively decrease

Aβ peptide levels and improve memory in a mouse model of AD, widespread inhibition of Notch-mediated signaling following treatment results in developmental defects (Loane et al., 2009). Clearly, novel strategies must be developed in parallel both to treat the underlying pathology of the disease and to prevent the adverse side effects of current therapies.

One novel strategy to overcome AD pathology is the use of small molecules to prevent aggregated Aβ from interacting with cellular components in harmful ways (Selkoe, 2011). Members of the benzothiazole aniline (BTA) family of compounds are characterized as a class of small molecules that have shown great promise in preventing Aβ-protein interactions. Yang et al. previously reported that a tetra-ethylene glycol derivative of BTA (BTA-EG_4) inhibits Aβ-induced cellular damage by surrounding aggregated Aβ with a bioresistive coating, preventing its association with cellular proteins (Inbar et al., 2006; Habib et al., 2010; Capule and Yang, 2012). BTA-EG_4 is able to adhere to aggregated forms of Aβ with high affinity (20 nM), cross the blood-brain barrier, and has adequate solubility in aqueous solutions (Inbar et al., 2006). Thus, BTA-EG_4 is a promising candidate for further *in vivo* study. While the effects of BTA compounds on AD pathogenesis are areas of active investigation, it is also pertinent to understand their effects on normal brain activity and synaptic function.

In the present study, we investigated the biological effects of BTA-EG_4 on synaptic function *in vitro* and *in vivo*. We initially found that BTA-EG_4-injected wild type mice exhibited increased dendritic spine formation, as well as improved memory. The spinogenic activity of BTA-EG_4 is accompanied by an increase in the number of functional synapses, as evidenced by an elevated frequency of AMPA receptor-mediated mEPSCs. Furthermore, BTA-EG_4 acts via APP to increase Ras activity as well as downstream Ras signaling, which is necessary for its ability to increase dendritic spine density. These data suggest that BTA-EG_4 may be beneficial as

a therapeutic treatment for the neuronal and cognitive dysfunction seen in AD by targeting Ras-dependent spinogenesis.

Section 2: Materials and Methods

Subsection 1: Synthesis of 2-(2-(2-(2-hydroxyethoxy)ethoxy)ethoxy)ethyl toluenesulfonate

In a clean, dry 1 L round-bottom flask equipped with a stirbar, tetra-ethylene glycol (10.0 g, 51.5 mmol) was dissolved in 500 ml dry dichloromethane (DCM) and stirred at room temperature. After 5 min, potassium iodide (1.71 g, 10.3 mmol), Ag_2O (17.9 g, 77.2 mmol), and p-toluenesulfonyl chloride (10.8 g, 56.6 mmol) were successively added to the reaction flask. The reaction mixture was stirred vigorously for 2 h, filtered through Celite to remove the solids and concentrated *in vacuo*. The residue was purified via silica column chromatography (100% DCM to 95:5 DCM/CH_3OH) giving 2-(2-(2-(2-hydroxyethoxy)ethoxy)ethoxy)ethyl toluenesulfonate as a colorless oil (13.2 g, 74%): ^{1}H-NMR (400 MHz, $CDCl_3$): δ = 7.74 (d, 8.0 Hz, 2H), 7.30 (d, 8.0 Hz, 2H), 4.11 (t, 4.8 Hz, 2H), 3.66 –3.53 (m, 12H), 2.79 (s, 1H), 2.39 (s, 3H); ^{13}C-NMR (100 MHz, $CDCl_3$); δ = 145.04, 133.17, 130.10 (2C), 128.19 (2C), 70.95, 70.79, 70.70, 69.49, 68.88, 21.87. Electrospray ionization tandem mass spectrometry (ESI-MS) [mass-to-charge ratio (*m/z*)] was calculated for $C_{15}H_{24}O_7S$ $[M]^+$ value of 348.1243; found values were $[M+H]^+$ 348.96, $[M+NH4]^+$ 365.94, and $[M+Na]^+$ 371.08.

Subsection 2: Synthesis of 2-(2-(2-(2-iodoethoxy)ethoxy)ethoxy)ethanol

2-(2-(2-(2- Hydroxyethoxy)ethoxy)ethoxy)ethyl toluenesulfonate (12.01 g, 34.5 mmol), sodium iodide (20.7 g, 137.9 mmol), and 200 ml of dry acetone were combined in a clean, dry, round-bottom flask and heated to reflux with vigorous stirring. After 12 h, the reaction was cooled to room temperature and diluted with 100 ml of ethyl acetate. The organic phase was

washed with 10% $Na_2S_2O_3$ (2x10 ml), deionized H_2O (1x20 ml), and saturated NaCl (1x20 ml); dried over anhydrous Na_2SO_4; filtered; and concentrated *in vacuo* giving 2-(2-(2-(2-iodoethoxy)ethoxy) ethoxy) ethanol as a pale yellow oil (5.61 g, 54%): ^{1}H-NMR (400 MHz, $CDCl_3$), δ = 3.73–3.58 (m, 14H), 3.24 (t, 2H), 2.59 (s, 1H); ^{13}C-NMR (100 MHz, CDCl3), δ = 72.70, 72.19, 70.90, 70.76, 70.58, 70.39, 61.94, 3.07.

Subsection 3: Synthesis of BTA-EG$_4$

A microwave reaction tube was charged with 2-(2-(2-(2-iodoethoxy)ethoxy)ethoxy) ethanol (1.47 g, 4.83 mmol), benzothiazole aniline (3.49 g, 14.5 mmol), potassium carbonate (3.34 g, 24.2 mmol), and 20 ml of dry tetrahydrofuran (THF). The tube was then equipped with a small stirbar, sealed, and placed in a microwave reactor. The reaction was heated at 125°C for 2 h. The reaction was cooled to room temperature and filtered to remove the solids. The solids washed several times with DCM until the filtrate was colorless. The combined organic layers were concentrated *in vacuo* and purified by column chromatography to give the desired BTA-EG$_4$ compound as a yellow solid (1.13 g, 56%): ^{1}H-NMR (400 MHz, $CDCl_3$), δ = 7.87 (d, 8.8 Hz, 2H), 7.83 (d, 8.4 Hz, 1H) 7.63 (s, 1H) 7.23 (d, 8.4 Hz, 1H), 6.68 (d, 8.8 Hz, 2H), 3.76–3.64 (m, 14H), 3.37 (t, 5.2 Hz, 2H), 2.47 (s, 3H); ^{13}C-NMR (100 MHz, CDCl3), δ = 168.03, 152.64, 150.92, 134.87, 134.47, 129.13 (2C), 127.70, 122.88, 122.03, 121.41, 112.82 (2C), 72.86, 70.88, 70.69, 70.43 (2C), 69.64, 61.91, 43.32, 21.70. HR-ESI-MS (*m/z*) calculated for a $C_{22}H_{28}N_2O_4SNa$ [M+Na] value of 439.1662; the found value for $[M+Na]^+$ was 439.1660.

Subsection 4: Cerebrovascular permeability and pharmacokinetic analysis of BTA-EG$_4$ in wild type mice

The partitioning of BTA-EG$_4$ between plasma and brain was studied in male CD-1 mice. The mice were dosed with 10 mg/kg, i.p., BTA-EG$_4$ (in 10% DMSO/90% PBS; n = 2 per time point), and the concentration of BTA-EG$_4$ in the plasma and brain was measured over time.

Blood was collected via cardiac puncture and was pooled in EDTA tubes and centrifuged, and the plasma was isolated. The brain was collected from each mouse, snap frozen, and homogenized in 2 ml of PBS. The concentration of BTA-EG_4 in the plasma and brain at each time point was determined by liquid chromatography/MS/MS, and the concentrations of BTA-EG_4 in the plasma and brain were plotted as a function of time. The following pharmacokinetic parameters for the plasma and brain profile of BTA-EG_4 were also calculated: the half-life ($t_{1/2}$) for BTA-EG_4 in the plasma and brain, the maximum concentration (C_{max}) of BTA-EG_4 in the plasma and brain, the area under the concentration-time curve (AUC), the brain-to-plasma ratio (BB), and the logarithmic brain-to-plasma ratio (Log BB).

Subsection 5: Cell lines

COS7 cells (Lombardi Co-Resources Cancer Center, Georgetown University) were maintained in Opti-MEM (Invitrogen) with 10% fetal bovine serum (FBS; Life Technologies) in a 5% CO_2 incubator. The cells were transiently transfected with 0.5–1 μg of plasmid in FuGENE 6 (Roche) according to the manufacturer's protocol and cultured for 24 h in DMEM containing 10% FBS. For cotransfections, cells were similarly transfected with 0.5–1 μg of each plasmid in FuGENE 6 (Roche) and cultured for 24 h in DMEM with 10% FBS.

Subsection 6: Primary neuron culture and immunostaining

Primary hippocampal neurons from E19 Sprague Dawley rats were cultured at 150 cells/mm^2, as previously described (Pak et al., 2001). Neurons were transfected using Lipofectamine 2000 (Invitrogen) or calcium phosphate precipitation with GFP + poly-$_L$-lysine (PLL), GFP + APP shRNA, or GFP + APP and treated with BTA-EG_4. The following antibodies were used: mouse anti- GFP (9F9.F9, Novus Biologicals), rabbit anti-GFP (A11122, Invitrogen), rabbit anti-GluR1 (PC246, Calbiochem), mouse anti-GluR2 (556341, BD Pharmingen, BD Biosciences), mouse anti-postsynaptic density-95 (PSD-95) (NeuroMabs), mouse anti-

synaptophysin (s5768, Sigma Al- drich), rabbit APP N terminal (A8967, Sigma-Aldrich), anti-Ras (610001, BD Biosciences), anti-RasGRF1 (C-20, Santa Cruz Biotechnol- ogy; 610149, BD Biosciences), anti-ERK1/2 (4695, Cell Signaling Technology), anti-p-ERK1/2 (36880, Invitrogen), anti-CREB (D76D11, Cell Signaling Technology), anti-p-CREB (06–519, Millipore), and mouse anti-c-Myc (9E10, Novus Biologicals). Cultured hippocampal neuron images were acquired by LSM 510 laser scanning confocal microscope (Zeiss). Confocal *z*-series image stacks encompassing entire dendrite segments were analyzed using MetaMorph software (Universal Imaging). We transfected cells with GFP to visualize dendrites and dendritic spines, followed by immunostaining with synaptophysin or PSD-95. Using MetaMorph software, we measured the average puncta number along dendritic segments.

Subsection 7: GST pull-down assay

To measure levels of active Ras, brain lysate homogenized with Ral buffer (25 mM Tris-HCl, pH 7.4, 250 mM NaCl, 0.5% NP40, 1.25 mM $MgCl_2$, and 5% glycerol) from APP transgenic, APP knock-out (KO), or wild type mice was incubated with GST-Raf-RBD purified protein coupled with glutathione Sepharose (GE Healthcare) overnight at 4°C. After 24 h, pellets were washed with Ral buffer and Western blotting was conducted with anti-Ras.

Subsection 8: Cell surface biotinylation

COS7 cells were transiently transfected with APP for 24 h in Opti-MEM containing 10% fetal bovine serum, and then treated with BTA-EG4 or control (CTRL) for 24 h. After 24 h, surface proteins were biotin labeled, immobilized with NeutrAvidin TM Gel and incubated 1 h with SDS-PAGE sample buffer, including 50 mM DTT, as described previously (Minami et al., 2010). Elutes were analyzed for APP by immunoblotting.

Subsection 9: Live cell surface immunostaining

Immunostaining of surface APP in hippocampal neurons was performed as described previously (Hoe et al., 2012). Briefly, live neurons were incubated with APP antibodies (10 μg/ml in conditioned medium) for 10 min, and then briefly fixed in 4% paraformaldehyde (nonpermeabilizing conditions). Surface-labeled APP was detected with Alexa Fluor-555 secondary antibodies. Cells were then permeabilized in methanol (-20°C, 90 s), and incubated with anti-GFP antibody to identify transfected neurons.

Subsection 10: Animals

Wild type C57BL/6J and APP knock-out mice (B6.129S7- APP^{tm1Dbo}/J) were obtained from Jackson Laboratories. CD1 mice were obtained from Vivasource. All animal experiments were approved by the Institutional Animal Care and Use Committees at Georgetown University and Johns Hopkins University. All animals were maintained according to protocols approved by the Animal Welfare and Use Committee at both institutions.

Subsection 11: Golgi staining and morphological analysis of dendritic spines

To analyze dendritic spine density and morphology in the brain, FD Rapid GolgiStain Kit (FD NeuroTechnologies) was used. Dissected mouse brains were immersed in Solution A and B for 2 weeks in dark conditions at room temperature and transferred into Solution C for 24 h at 4°C. Brains were sliced using a VT1000S Vibratome (Leica) at 150 μm thickness. Dendritic images were acquired by Axioplan 2 (Zeiss) under bright-field microscopy. Spine width, length, and linear density of cortical layers II/III and CA1 of hippocampus were measured using Scion image soft- ware (Scion). Images were coded and dendritic spines were counted in a blinded manner. Spines from 0.2 to 2 μm in length were included for analysis. At least 25 apical oblique (AO) and 25 basal shaft (BS) dendrites were measured for spine density from each animal, and these were averaged per animal (n = 5/group). All morphological analysis was performed blind to experimental conditions.

Subsection 12: Aβ ELISA

Mouse brains were homogenized in tissue homogenization buffer containing 250 mM sucrose, 20 mM Tris base, protease, and phosphatase inhibitors. To measure soluble Aβ, diethylamine (DEA) extraction was performed. Crude 10% homogenate was mixed with an equal volume of 0.4% DEA, sonicated, and ultracentrifuged for 1 h at 100,000 x g. The supernatant was collected and neutralized with 10% 0.5 M Tris, pH 6.8. Sensitive and specific ELISAs to rodent Aβ1– 40 was purchased from IBL Transatlantic and conducted per the manufacturer's protocol.

Subsection 13: Morris water maze

To examine the effects of BTA-EG_4 on cognitive performance, we injected wild type (B6) mice with BTA-EG_4 daily for 1 week, and then began behavior testing. We continued daily injections for another week, for a total treatment course of 2 weeks. The Morris water maze task included training mice to locate a submerged, hidden platform using extramaze visuospatial cues. This system consists of a large, white circular pool with a Plexiglas platform painted white and submerged below the surface of the water, made opaque by the addition of white nontoxic paint. During training, the platform was hidden 14 inches from the side wall in one quadrant of the maze. The animals were gently placed at random into one of the four quadrants, separated by 90°, and facing the wall. The time required (latency) to locate the hidden platform was recorded by a blinded observer and tracked using TOPSCAN, and was limited to 90 s. Animals failing to find the platform within 90 s were assisted to the platform. Animals were allowed to remain on the platform for 15 s on the first trial and 10 s on subsequent trials. Twenty-four hours after the final learning trial, a probe trial of 90 s was given. We recorded the percentage of time spent in the quadrant where the platform was previously located. As a control experiment, we tested motor impairment or visual discriminative ability. The animals were required to locate a clearly visible

black platform (placed in a different location), raised above the water surface, at least 12 h after the last trial.

Subsection 14: Fear conditioning

Before initiating fear-conditioning tests, wild type mice were injected daily with BTA-EG_4 or vehicle for 2 weeks (n = 8/group). Mice were subsequently trained by exposure to a conditioning box (context) for 3 min before administering a tone (18 s) and footshock (2 s), which were repeated twice at 1 min intervals. We performed the contextual test 24 h after training by re-exposing the mice to the conditioning context. A measurement of freezing behavior was recorded every minute for 3 min inside of the conditioning box. The cued test was conducted 3 h following the contextual test. Following a 3 min re-exposure to the conditioning box, a tone (18 s) was administered and freezing behavior was measured for 1 min.

Subsection 15: Electrophysiology

Transverse [for Schaffer collateral (SC) input studies] or horizontal [for temporoammonic (TA) input studies] hippocampal slices (400 μm thick) were prepared from adult mice. Slices were made using ice-cold dissection buffer (in mM: 212.7 sucrose, 2.6 KCl, 1.23 NaH_2PO_4, 10 dextrose, 3 $MgCl_2$ and 1 $CaCl_2$; 5% CO_2/95% O_2), and recordings were performed in a submersion-type chamber perfused with artificial CSF (ACSF; in mM: 124 NaCl, 5 KCl, 1.25 NaH_2PO_4, 26 $NaHCO_3$, 10 dextrose, 1.5 $MgCl_2$, and 2.5 $CaCl_2$; 5%CO_2/95% O_2, 29.5– 30.5°C, 2 ml/min). For field potential recordings, synaptic responses were evoked using 0.2 ms duration pulses delivered through a bipolar glass stimulating electrode at 0.0333 Hz. A train of theta burst stimulation (TBS) consisted of a burst of four pulses at 100 Hz repeated 10 times at 5 Hz. For 4xTBS, four trains of TBS were given at 10 s intertrain intervals. For whole-cell recordings, slices were transferred to a submersion-type recording chamber mounted on a fixed stage of an upright microscope (E600 FN, Nikon) with infrared (IR) oblique illumination. AMPA receptor

(AMPAR)-mediated mEPSCs were pharmacologically isolated by adding 1 μM tetrodotoxin (TTX), 20 μM bicuculline, and 100 μM D,L-2-amino-5-phosphonopentanoic acid (APV) to ACSF (30 ±1°C, saturated with 95% O_2 and 5% CO_2), which was continually perfused at a rate of 2 ml/min. Target cells in CA1 were identified by the pyramid- shaped soma. These neurons were patched using a whole-cell patch pipette (tip resistance 3–5 MΩ), which was filled with internal solution (in mM: 120 Cs-methanesulfonate, 5 $MgCl_2$, 8 NaCl, 1 EGTA, 10 HEPES, 2 Mg-ATP, 0.5 Na_3GTP, and 0.001 QX-314; pH 7.3, 280–290 mOsm). Recording was initiated 2–3 min after break-in, and each cell was recorded for 10 –15 min to collect enough mEPSCs for analysis. The Axon patch-clamp amplifier 700B (Molecular Devices) was used for voltage- clamp recordings. Cells were held at -70 mV, and the recorded mEPSC data were digitized at 10 kHz with a data acquisition board (National Instruments) and acquired through custom-made programs using the Igor Pro software (WaveMetrics). The MiniAnalysis program (Synaptosoft) was used to analyze the acquired mEPSCs. The threshold for detecting mEPSCs was set at three times the root mean square (RMS) noise. There was no significant difference in the RMS noise across the groups [BTA-EG4 (30 mg/kg) = 1.6 ±0.09 (n =7), control = 1.6 ±0.05 (n =8); t test, p =0.65]. Recordings were excluded from analysis if the RMS noise was <2, the series resistance was <25 MΩ, and input resistance was >100 MΩ. To minimize the impact of dendritic filtering, we adopted the standard approach of excluding mEPSCs with a rise time of >3 ms, as well as cells showing a negative correlation between mEPSC amplitude and rise time (Rall, 1969). Only ~4% of the total recorded cells (at most, 1 cell per experimental group) were excluded due to negative correlation between mEPSC rise and amplitude. One hundred consecutive mEPSCs that met the rise-time criteria were analyzed from each cell. AMPAR- and NMDAR-mediated currents were measured at -70 and +40 mV, respectively. AMPAR-mediated EPSC amplitudes were measured at the peak of the current at -70 mV. NMDAR-mediated EPSC amplitudes were measured 100 ms after the

stimulation artifact. Data are the means ± SE. Student's t test was used for two-group comparisons. For all statistical tests, p =0.05 was considered statistically significant.

Subsection 16: Slice surface biotinylation

Hippocampal slices (400 μm thick) were prepared as described above. CA3 and DG regions were cut away after the slice preparation to isolate CA1. After 30 min of recovery at room temperature, the slices were transferred to 30°C for an additional 30 min of recovery. The slices were then transferred to ice-cold ACSF for 10 min, and subsequently to ice-cold ACSF containing 1 mg/ml biotin (EZ-Link Sulfo-NHS-SS-Biotin, Pierce) saturated with 5% CO_2/95% O_2 for 15 min. The slices were then washed in TBS (50 mM Tris, 0.9% NaCl, pH 7.4) containing 100 mM glycine 5 times for 1 min each before homogenized in ice-cold 0.2% SDS/1% Triton X-100 immunoprecipitation buffer (TX-IPB; 20 mM Na_3PO_4, 150 mM NaCl, 10 mM EDTA, 10 mM EGTA, 10 mM $Na_4P_2O_7$, 50 mM NaF, and 1 mM Na_3VO_4, pH 7.4; with 1 μM okadaic acid and 10 kIU/ml aprotinin) by 30 gentle strokes using glass- Teflon tissue homogenizers (Pyrex). The homogenates were centrifuged for 10 min at 13,200 x g, at 4°C. Protein concentration of the supernatant was normalized to 0.6 –1.5 mg/ml. Some of the supernatants were saved as inputs, and the remaining supernatant was mixed with NeutrAvidin slurry (1:1 in 1% TX-IPB) and rotated overnight at 4°C. The NeutrAvidin beads were isolated by brief centrifugation at 1000 x g, and washed 3 x 1% TX-IPB, 3 x 1% TX-IPB plus 500 mM NaCl, followed by 2 x 1% TX-IPB. The biotinylated surface proteins were then eluted from the NeutrAvidin beads by rotating at room temperature for 15 min in gel sample buffer with 2 mM DTT. The input (total homogenate) and biotinylated samples (surface fraction) were run on separate gels, and processed for immunoblot analysis using GluA1 (sc-55509, Santa Cruz Biotechnology), GluA2/3 (07–598, Millipore), GluN1 (a gift from Dr. R.L. Huganir, Johns Hopkins University, Baltimore, MD), GluN2A (07– 632, Millipore), and GluN2B (71–8600, Invitrogen) antibodies. NMDAR subunit

blots were developed using enhanced chemifluorescence substrate (ECF substrate, GE Healthcare). AMPAR blots were probed simultaneously with GluR1 and GluR2/3 antibodies followed by second antibodies linked to Cy5 and Cy3. All blots were scanned using Typhoon 9400 (GE Healthcare), and quantified using Image Quant TL software (GE Healthcare). The signal of each sample on a blot was normalized to the average signal from the control group to obtain the percentage of average control values, which were compared across groups using unpaired Student's t test.

Subsection 17: Statistical analyses

All data were analyzed with GraphPad Prism 4 software using either a two-tailed t test or ANOVA with Tukey's post hoc test for multiple comparisons, with significance determined at $p = 0.05$. Cumulative distribution plots were analyzed using the Kolmogorov–Smirnov test. Descriptive statistics were calculated with StatView 4.1 and expressed as the mean ± SEM.

Section 3: Results

Subsection 1: BTA-EG$_4$ decreases Aβ levels in vitro and in vivo

We examined the biological and pharmacokinetic properties of BTA-EG$_4$. BTA-EG$_4$ readily crosses the blood-brain barrier and is rapidly distributed to the brain (Iyer et al., 2002) with an estimated Log BB value of 0.43 (Fig 3.1 A&B). While it is clear from these studies that BTA-EG$_4$ readily distributes to the brain, we make this conclusion from the analysis of brain and plasma samples of only four mice at each time point (two dosed with BTA-EG$_4$ and two dosed with vehicle). The quantitative pharmacokinetic parameter values provided (Fig 3.1 B) should, therefore, be considered only as estimated values. We further found that daily injections of BTA-EG$_4$ (50 mg/kg, i.p.) were well tolerated in wild type mice for 16 d, and necropsy revealed no adverse effects on major organs.

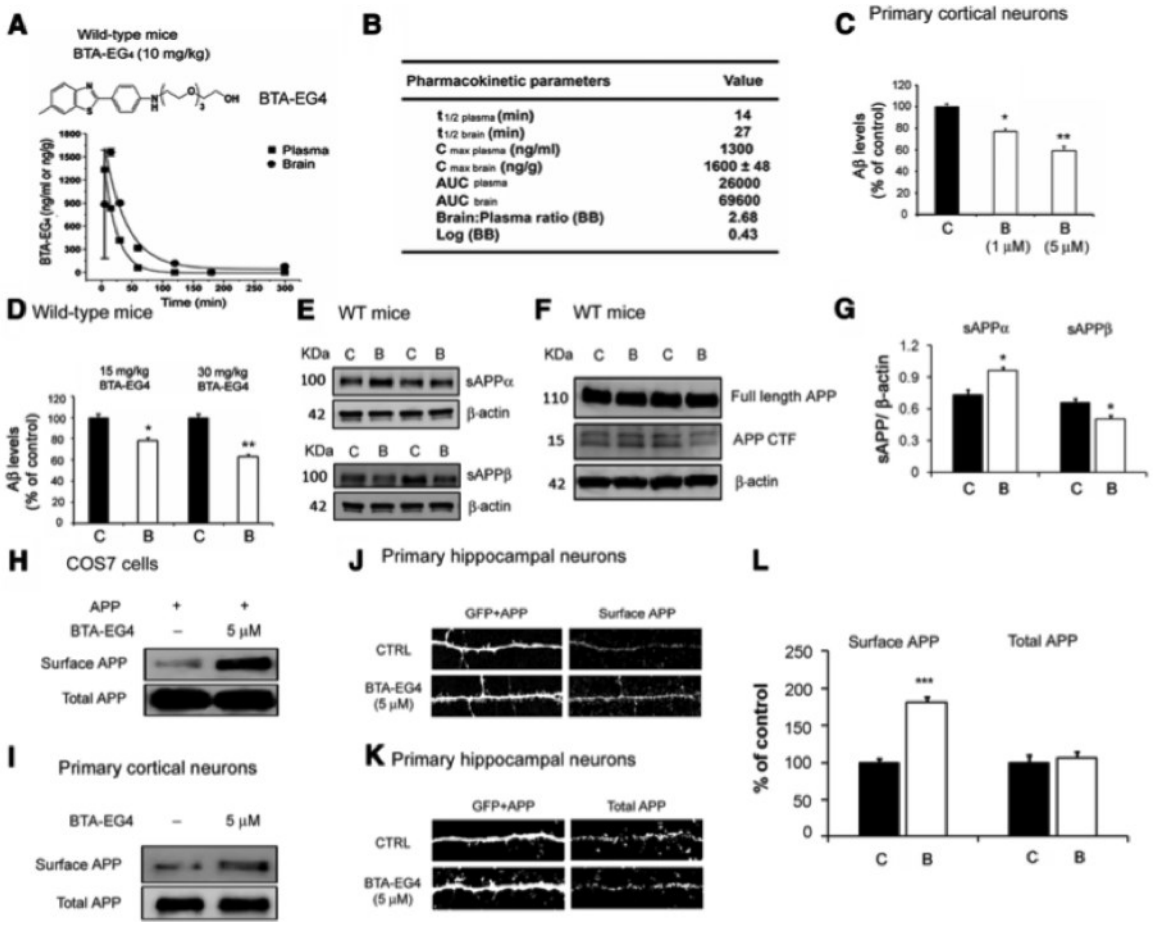

Figure 3.1. BTA-EG$_4$ exhibits low toxicity and crosses the blood-brain barrier *in vivo*.

A. Structure of BTA-EG$_4$ (top) and time-dependent plasma and brain concentrations of BTA-EG$_4$ in wild type mice that were injected (10 mg/kg, i.p.; n = 2 per time point). **B.** Table summarizing the calculated pharmacokinetic parameters for the plasma and brain profile of BTA-EG$_4$. Parameters include the $t_{1/2}$ for BTA-EG$_4$ in the plasma and brain, the C_{max} of BTA-EG$_4$ in the plasma and brain, the AUC, the BB, and the Log BB. **C.** Primary cortical neuronal cells were treated with control, or 1 or 5μM BTA-EG$_4$ for 24 h. Aβ levels in the conditioned media were determined by ELISA (n = 12/group). **D.** Wild type mice were injected with 15 mg/kg, i.p., BTA-EG$_4$ or 30 mg/kg BTA-EG$_4$ daily for 2 weeks, and Aβ levels were measured in the brain (n = 12/group). **(E-F)** Wild type mice were injected with 30 mg/kg BTA-EG$_4$ for 2 weeks and sAPPα, sAPPβ, full-length APP, APP C-terminal fragment (CTF), and β-actin were measured (n = 3). **G.** Quantification of sAPPα and sAPPβ from **E** and **F** (n = 3/group). The sAPPα and sAPPβ signals for each sample were normalized to β-actin. (**H-I)** COS7 cells expressing APP (**H**, n = 3) or primary cortical neurons (**I**, n = 3) were treated with BTA-EG$_4$ (5μM) for 24 h. Cell surface proteins were biotinylated, isolated with avidin-conjugated beads, and immunoblotted with 6E10 or 22C11 antibody. **J.** Cultured hippocampal neurons (DIV18) were transfected with GFP and APP and treated with BTA-EG$_4$ for 24 h, and live cell surface staining was conducted. Left panels, GFP; right panels, surface APP (n = 10/group). **K.** Cultured hippocampal neurons (DIV18) were transfected with GFP and APP, treated with BTA-EG$_4$ for 24 h, and immunostained with anti-APP. Left panels, GFP; right panels, total APP (n = 10/group). **L.** Quantification of surface APP intensity from **(J)** and total APP from (**K)**. *p < 0.05, **p < 0.01, ***p < 0.001. C, Control; B, BTA-EG4.

To test whether BTA-EG_4 alters Aβ production *in vitro*, primary cortical neurons were treated with BTA-EG_4 (1 or 5 μM) or control (10% DMSO), and Aβ levels were measured using ELISA. BTA-EG_4 significantly decreased Aβ protein levels (Fig 3.1 C). We then examined whether BTA-EG_4 can alter Aβ levels *in vivo* by injecting wild type mice daily for 2 weeks with BTA-EG_4 (15 or 30 mg/kg, 10%DMSO in saline, i.p.). We found that wild type mice injected with both doses of BTA-EG_4 had significantly decreased Aβ peptide levels compared with controls (10% DMSO, i.p.) (Fig 3.1 D), suggesting that BTA-EG_4 can also reduce Aβ production *in vivo*. Furthermore, BTA-EG_4 altered APP processing *in vivo*, as monitored by increased sAPPα (α-secretase cleavage product) and decreased sAPPβ (β-secretase cleavage product) levels in BTA- EG_4 injected wild type mice (30 mg/kg, i.p) compared with control-injected mice (Fig 3.1 E–G). These findings suggest that BTA-EG_4 promotes the α-secretase-mediated metabolism of APP at the expense of the β-secretase pathway, which may explain the reduction in Aβ. It is well known that the majority of α-secretase activity occurs on the cell surface, while β- and γ-secretase activity occurs primarily in the early and late endosomes (Huse et al., 2000; Reiss et al., 2006). Thus, if APP is present at the cell's surface, it is preferentially cleaved by α-secretase, resulting in decreased Aβ production. Therefore, we examined whether BTA-EG_4 regulates cell surface expression of APP. To test this initially, COS7 cells were transfected with human APP and treated with BTA-EG_4 (5μM) or control (10% DMSO) for 24 h. After performing cell surface biotinylation, we found that BTA-EG_4 increased cell surface APP (Fig 3.1 H). Furthermore, BTA-EG_4 increased endogenous cell surface APP levels in primary cortical neurons following 24 h of BTA-EG_4 (5μM) treatment compared with control (10% DMSO) treatment (Fig 3.1 I). In an alternative approach to examine the effect of BTA-EG_4 on cell surface APP expression, we conducted live cell-surface immunostaining in primary hippocampal neurons. BTA-EG_4 treatment (5μM) increased cell surface levels of APP relative to vehicle control without affecting

total levels of APP (Fig 3.1 J-L). These results suggest that BTA-EG_4 may reduce Aβ production by increasing the amount of APP present at the cell surface.

Subsection 2: BTA-EG_4 improves cognitive performance in the absence of enhanced long-term potentiation

Several studies have shown that Aβ accumulation contributes to cognitive deficits (Chang et al., 2011; Chételat et al., 2012). Since we observed that BTA-EG_4 decreases Aβ levels both *in vitro* and *in vivo* (Fig 3.1 C&D), we then examined whether BTA-EG_4 affects learning and memory.

The Morris water maze task was used to assess cognitive performance in wild type mice injected with BTA-EG_4 (30 mg/ kg, i.p.) or controls. BTA-EG_4-injected wild type mice exhibited significantly reduced escape latency during training (Fig 3.2 A), which was accompanied by an increase in swim speed (CTRL = 117 ± 3.1 mm/s, BTA = 130 ± 3.6 mm/s; $p < 0.01$), but no difference in path length to the escape platform (Fig 3.2 B). These findings suggest that the apparent reduction in escape latency in the BTA-EG_4 group may simply be a reflection of the effect of the drug on swim speed. The fact that there is no change in the path length to reach the platform, which is a measurement not affected by swim speed, during the training trials suggests that BTA-EG_4 may not improve the learning process. To test whether BTA-EG_4 affects memory, we ran probe trials to measure the percentage of time spent in the correct quadrant and the number of platform crossings. We found that BTA-EG_4-injected wild type mice spent more time in the target quadrant and showed a significantly higher rate of platform crossing during probe trials (Fig 3.2 C&D), suggesting that BTA-EG_4 improves memory in this standard spatial memory task.

Several studies have demonstrated that synaptic plasticity is correlated with learning and memory (Kandel, 2001; VanGuilder et al., 2011). Therefore, we examined whether improved

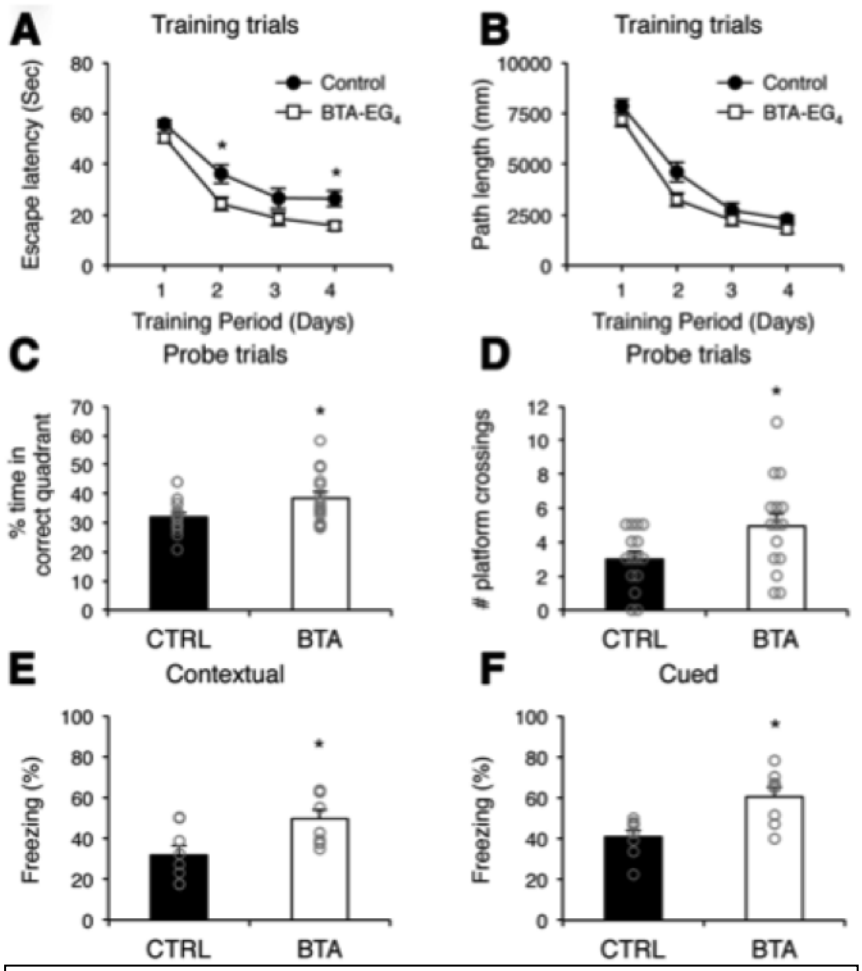

Figure 3.2. BTA-EG$_4$ improves cognitive performance.

(A-D) Spatial learning task for BTA-EG$_4$- injected (intraperitoneally) wild type mice by Morris water maze paradigm. **A.** Escape latencies during the training phase (n = 15; *p < 0.05 for days 2 and 4; p < 0.001 overall). **B.** Path lengths to the platform during training trials (two-way ANOVA, p = 0.6709). **C.** Percentage of time spent in the target quadrant was measured during the probe test on day 5 (*p < 0.05). Individual animal data are shown in gray circles. **D.** Comparison of the number of platform crossings during probe trial on day 5 (*p < 0.05). Individual animal data are shown in gray circles. **(E-F)** Associative learning test for BTA-EG$_4$ injected (intraperitoneally) wild type mice by fear conditioning. **E.** Performance of mice treated with BTA-EG$_4$ (30 mg/kg) daily for 2 weeks before training during the contextual memory test (n = 8/group; *p < 0.05). Individual animal data are shown in gray circles. **F.** Mice were re-exposed to the cue component in a novel context after 24 h, and their behavior was monitored. Mice treated with BTA-EG$_4$ exhibited significantly enhanced freezing in response to the cue component (n = 8/group; *p < 0.05). Individual animal data are shown in gray circles.

cognitive performance following BTA-EG$_4$ treatment is associated with altered synaptic function and plasticity. We conducted electrophysiology experiments in an acute hippocampal slice preparation from wild type mice injected with BTA-EG$_4$ (30 mg/kg, i.p.) or control solution (10% DMSO, i.p) for 2 weeks. At the SC inputs to CA1, BTA-EG$_4$ did not alter basal synaptic transmission or presynaptic function (Fig 3.3 A&B). LTP was either normal or reduced, depending on the induction protocol

(Fig 3.3 C&D). Unexpectedly, the summation of synaptic responses during the LTP induction protocol was reduced (Fig 3.3 E&F), which suggests that the normal LTP expression is likely due to an upregulation of a downstream signaling cascade. Recent evidence suggests that TA inputs to CA1, rather than SC inputs to CA1, support water maze-type learning (Nakashiba et al., 2008). BTA-EG_4 (30 mg/kg, i.p.) treatment reduced the ability to recruit presynaptic axons per stimulation intensity at TA inputs to CA1 (Fig 3.3 H, left), but there was no difference in synaptic transmission when responses were normalized to the presynaptic fiber volley amplitude (Fig 3.3 H, right). There was also not a change in presynaptic function (Fig 3.3 I). Similar to SC inputs to CA1, LTP at TA inputs also showed a similar reduction in the magnitude of LTP (Fig 3.3 J), which occurred in the absence of a change in the response summation during the induction protocol (Fig 3.3 K). Collectively, these results support the idea that the benefit of BTA-EG_4 to improved cognitive performance is not through enhancing LTP.

Subsection 3: BTA-EG_4 increases spinogenesis in vivo

There is precedence that cognitive performance correlates better with dendritic spine

Figure 3.3. BTA-EG_4 does not enhance LTP in CA1.

(A-F) SC inputs to CA1. **A.** No significant difference in input-output function. Left, field potential (FP) slope plotted against stimulation intensity. CTRL: n = 15 slices, 6 mice; BTA: n = 18 slices, 6 mice. Right, FP slope normalized to fiber volley (FV). Top left, Schematic of recording. Top right, Representative FP traces. **B.** No change in presynaptic function. Top, Representative traces at 50 ms interstimulus interval (ISI). Bottom, paired pulse facilitation (PPF) ratio at different ISI. **(C-D)** No difference in the magnitude of LTP induced by 1xTBS (CTRL: n = 9 slices, 6 mice, BTA: n = 10 slices, 5 mice, t test: $p = 0.359$; **C**) and are reduction with 4xTBS (CTRL: n = 8slices, n = 4 mice, BTA: n = 11 slices, 6 mice, t test: $*p < 0.01$; **D**) in the BTA-treated group. Top, Representative traces (baseline: thin line, post-LTP: thick line). **(E-F)** Comparison of response integration during 1xTBS **(E)** and 4xTBS **(F)**, $*p < 0.05$. **(G-K)** TA inputs to CA1. **G.** Isolation of TA inputs by stimulating the stratum lucidum-moleculare (SLM). Left, Schematics of recording. Right, Representative FP traces following stimulation of SC inputs by an electrode placed in stratum radiatum (SR) or SLM when recording from SR or SLM. **H.** A reduction in input-output function with stimulation intensity (left), which is normalized when corrected for presynaptic recruitment of axons (right) (CTRL: n = 24 slices, n = 5 mice, BTA: n = 23 slices, n = 5 mice). Top, Representative traces. **I.** Normal PPF ratio (CTRL: n = 25 slices, n = 5 mice, BTA: n = 22 slices, n = 5 mice). Top, Representative traces taken at 50 ms ISI. **J.** Reduced TA-LTP (CTRL: 120 ± 2.1% at 1 h post-LTP, n = 11 slices, n = 5 mice, BTA: 109 ± 1.2%, n = 10 slices, n = 4 mice; t test, $*p < 0.01$). **K.** Normal summation of responses during TA-LTP induction protocol.

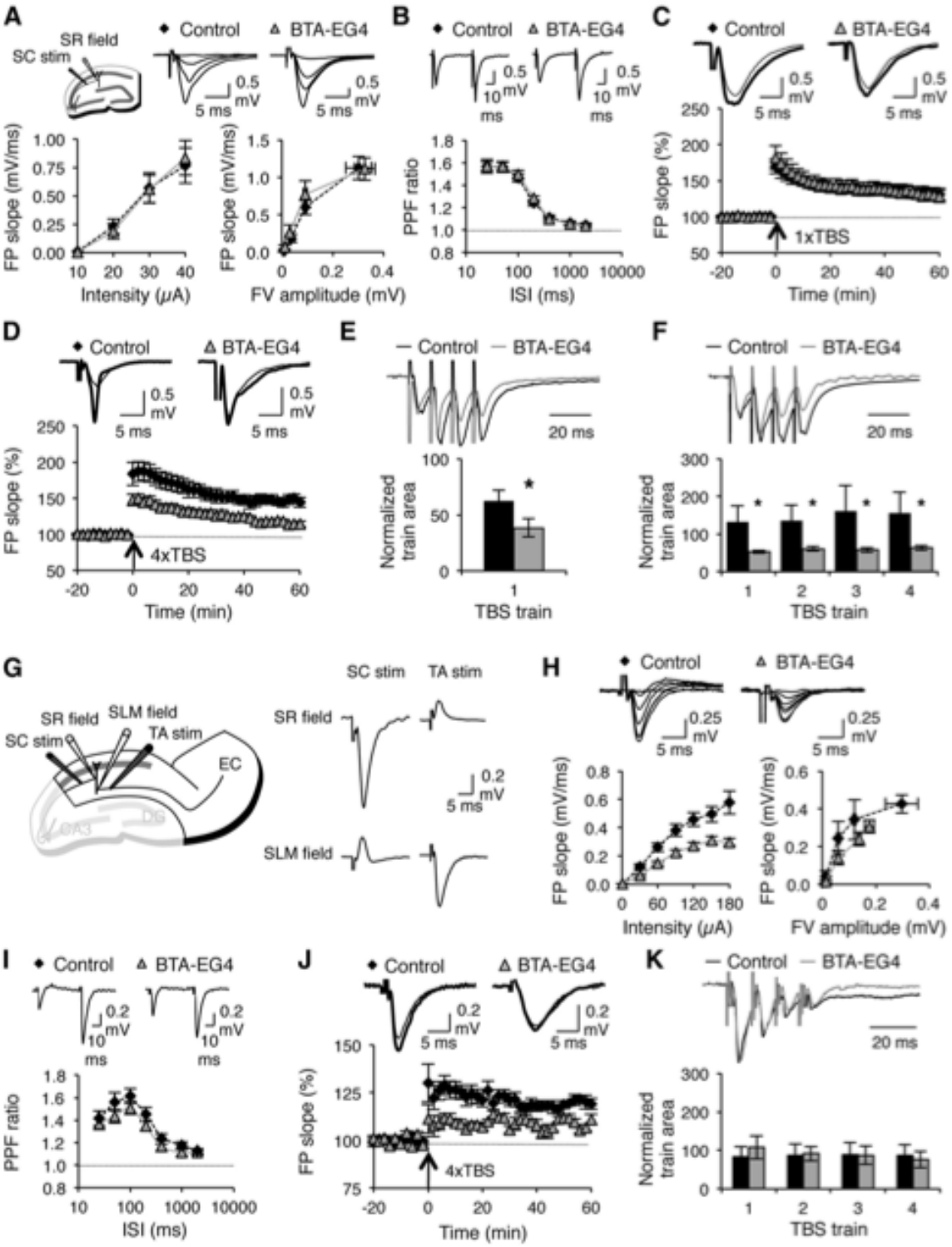

density rather than LTP magnitude (Hayashi et al., 2004; Morgado-Bernal, 2011). Since we observed that BTA-EG$_4$ improves memory without enhancing LTP, we hypothesized that BTA-

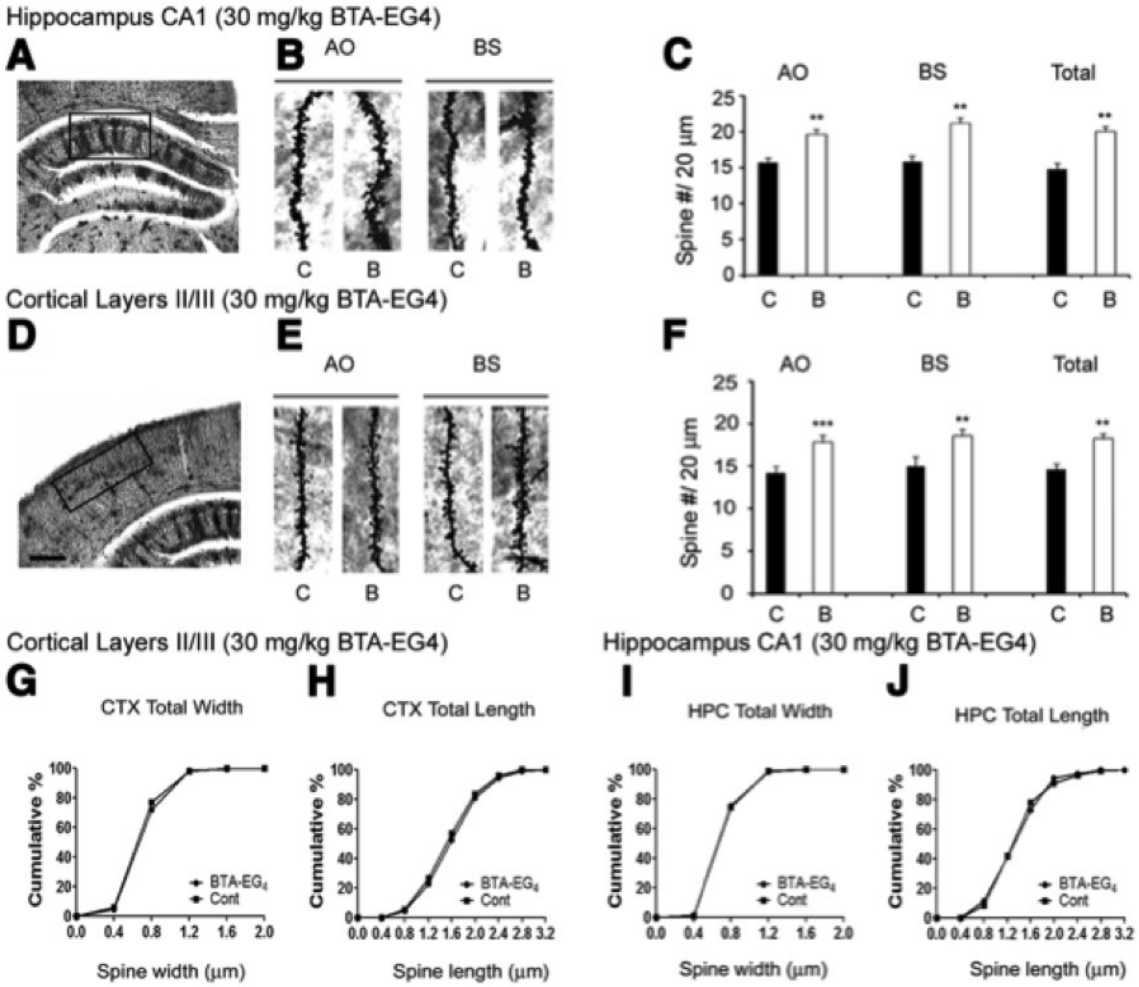

Figure 3.4. BTA-EG$_4$ promotes spinogenesis *in vivo*.

A. Representative Golgi-impregnated wide-field view of the hippocampus (5x magnification). **B.** Representative AO and BS dendrites from hippocampal CA1 neurons from mice treated with control and BTA-EG$_4$ (30 mg/kg), as indicated. **C.** Left, Spine density in hippocampal AO dendrites (n = 5; **p < 0.01). Middle, Spine density in hippocampal BS dendrites (n = 5; **p < 0.01). Right, Total averaged spine density in hippocampal dendrites (n = 5; **p < 0.01). **D.** A representative Golgi-impregnated neuron from cortical layers II/III. **E.** Representative AO and BS dendrites from pyramidal neurons of mice treated with control and BTA-EG$_4$ (30 mg/kg) as indicated. **F.** Left, Average dendritic spine density for cortical AO dendrites (n = 5, ***p < 0.001). Middle, Average dendritic spine density for cortical BS dendrites (n = 5, **p < 0.01). Right, Total average dendritic spine density (n = 5, **p < 0.01). **(G-H)** The cumulative distribution percentage of spine head width and spine length in cortical layers II/III in mice treated with BTA-EG$_4$ (30 mg/kg) (Kolmogorov–Smirnov test). **(I-J)** The cumulative distribution percentage of spine head width and spine length in the hippocampus CA1 in mice treated with BTA-EG$_4$ (30 mg/kg). Scale bar, 0.2 mm. C, Control; B, BTA-EG4, CTX, cortex; HPC, hippocampus.

EG$_4$ promotes cognitive performance by increasing spine density. To test this idea, wild type mice were injected with BTA-EG$_4$ (30 mg/kg) or control for 2 weeks. Subsequently, we

performed Golgi staining and found that BTA-EG_4-treated mice showed significantly increased dendritic spine density in the CA1 region of the hippocampus and cortical layers II/III (Fig 3.4 A-F). However, BTA-EG_4 did not alter spine morphology, including spine head width and spine length, in these areas (Fig 3.4 G-J). These data suggest that BTA-EG_4 promotes dendritic spine formation without affecting spine morphology.

Subsection 4: BTA-EG_4 requires APP to increase dendritic spine density

To examine whether BTA-EG_4 acts via APP to increase dendritic spine density, we acutely knocked down APP using shRNA in primary hippocampal neurons. APP shRNA was cotransfected with GFP to visualize dendritic spines, and control cultures were transfected with GFP and PLL (control vector for shRNA construct). We then treated both cultures with BTA-EG_4 (5μM) or vehicle. We found that knockdown of APP on its own showed a trend of a decrease in dendritic spine density and prevented the increase in dendritic spine density with BTA-EG_4 treatment (Fig 3.5 A&B), which suggests that BTA-EG_4 can only increase dendritic spine density in the presence of APP. To confirm this finding *in vivo*, we examined the effect of BTA-EG_4 on dendritic spine density in APP KO mice. APP KO mice were injected with BTA-EG_4 (30 mg/kg) or vehicle for 2 weeks, and Golgi analysis was conducted on hippocampal CA1 neurons. In APP KOs, we did not find a statistically significant increase in dendritic spine density following BTA-EG_4 treatment (Fig 3.5 C&D). This observation suggests that the ability of BTA-EG_4 to promote spinogenesis is dependent on APP.

Subsection 5: BTA-EG_4 increases the number of functional excitatory synapses

Next, we examined whether the increase in dendritic spine density following BTA-EG_4 treatment reflects an increase in the number of functional excitatory synapses. Primary hippocampal neurons were treated with BTA-EG_4 (5μM) or control, and immunostained with synaptic markers. We found that BTA-EG_4 increased the number of puncta stained for

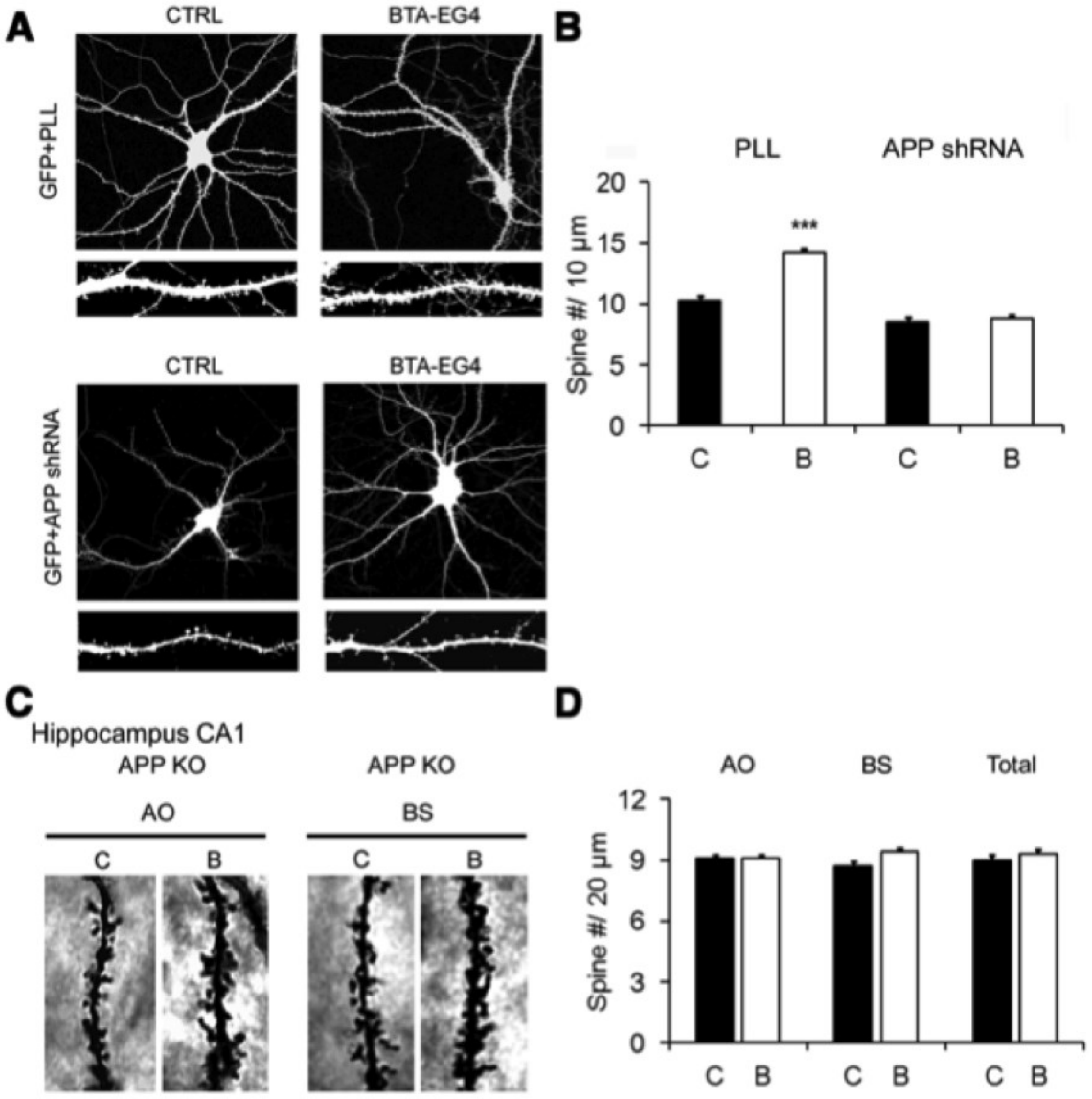

Figure 3.5. BTA-EG$_4$ requires APP to increase spine density.

A. Primary hippocampal neurons were transfected with GFP and PLL (top) or GFP and APP shRNA (bottom), treated with control or BTA-EG$_4$ (5µM), and spine density was measured. **B.** Quantification of data from **A** (n = 15, ***p < 0.001). **C.** Representative images of AO and BS dendrites from APP knock-out mice treated with control or BTA-EG$_4$. APP knock-out mice were injected with control or BTA-EG$_4$ for 2 weeks, and Golgi staining was conducted. **D.** Quantification of data from **C** (n = 5/group). C, Control; B, BTA-EG4.

synaptophysin (presynaptic marker) and PSD-95 (postsynaptic marker) (Fig 3.6 A-C).

To verify that the increase in dendritic spine density and synaptic proteins reflects an increase in functional synapses, we measured mEPSCs from CA1 neurons in hippocampal slices

following *in vivo* administration of BTA-EG_4 (30 mg/kg, i.p.) for 2 weeks. Consistent with an increase in functional synapses, BTA- EG_4 significantly increased the frequency of mEPSCs compared with vehicle-treated controls (Fig 3.6 D). There was no significant difference in the average mEPSC amplitude (Fig 3.6 E), suggesting no postsynaptic alteration in synaptic strength. Furthermore, we did not observe a change in the AMPAR/NMDAR ratio (Fig 3.6 F), which suggests that the new synapses likely contain both NMDAR and AMPAR at normal levels.

To test whether the increase in functional excitatory synapses occurs via cell surface recruitment of glutamate receptors, we performed steady-state surface biotinylation using acute hippocampal slices obtained from mice injected with BTA-EG_4 (30 mg/kg) or control vehicle for 2 weeks. Both the cell surface and total levels of major AMPAR subunits GluA1 and GluA2, as well as NMDAR subunits GluN1, GluN2A, and GluN2B, were quantified. There was no

Figure 3.6. BTA-EG_4 increases the number of functional synapses without altering synaptic strength.

(A-B) Cultured hippocampal neurons (DIV 18) were treated with BTA-EG_4 (5μM) or control for 24 h and stained for synaptophysin (**A**, right) and PSD-95 (**B**, right). Neurons and dendrites were visualized by transfection of GFP (**A** and **B**, left panels). **C.** Quantification of average puncta number of synaptophysin and PSD-95 per 20μm length of dendrite (n = 10, *p < 0.05, **p < 0.01). **D.** BTA-EG_4 (30 mg/kg, i.p.) treated mice showed significantly increased mEPSC frequency in CA1 pyramidal neurons. Left, Comparison of average mEPSC frequency (CTRL: n = 7 cells, 5 mice; BTA: n = 8 cells, 5 mice; t test: *p < 0.05). Values for individual cells are shown in gray circles. Right, Representative three consecutive mEPSC traces (1 s each) taken from cells of CTRL and BTA. **E.** No significant change in average mEPSC amplitude (n, the same as in **D**). Values for individual cells are shown in gray circles. Right, Average mEPSC trace from each group. **F.** No change in the ratio of AMPA/NMDA-mediated synaptic responses. Values for individual cells are shown in gray circles. Right, Overlap of AMPAR-mediated EPSC measured at -70 mV and NMDAR-mediated EPSC measured at +40 mV. Dotted line shows where NMDAR responses were measured. **(G-J)** No change in the total and cell surface levels of AMPAR **(G, H)** and NMDAR **(I, J)** subunits in microdissected CA1 slices obtained from control and BTA (30 mg/kg, i.p.) treated mice. Left, Representative immunoblots. The blots were reprobed for β-actin, which did not show significant difference in signal between control and BTA-EG_4- treated groups (p = 0.269). Right, Average data of glutamate receptor signal normalized to average control (CTRL: n = 8 mice, BTA: n = 8 mice, t test: p > 0.1). There was no significant difference when the signal for each glutamate receptor antibody was normalized to the actin signal for each total homogenate sample (GluA1/β-actin ratio: CTRL = 0.96 ± 0.10, BTA = 1.06 ± 0.12, p = 0.5; GluA2/β-actin ratio: CTRL = 0.98 ± 0.09, BTA = 1.27 ± 0.14, p = 0.1; GluN1/β-actin ratio: CTRL = 0.98 ± 0.12, BTA = 1.27 ± 0.05, p = 0.1; GluN2A/β-actin ratio: CTRL = 1.03 ± 0.08, BTA = 1.04 ± 0.14, p = 1.0; GluN2B/β-actin ratio: CTRL = 1.02 ± 0.11, BTA = 1.33 ± 0.14, p = 0.1). C, Control; B, BTA-EG_4.

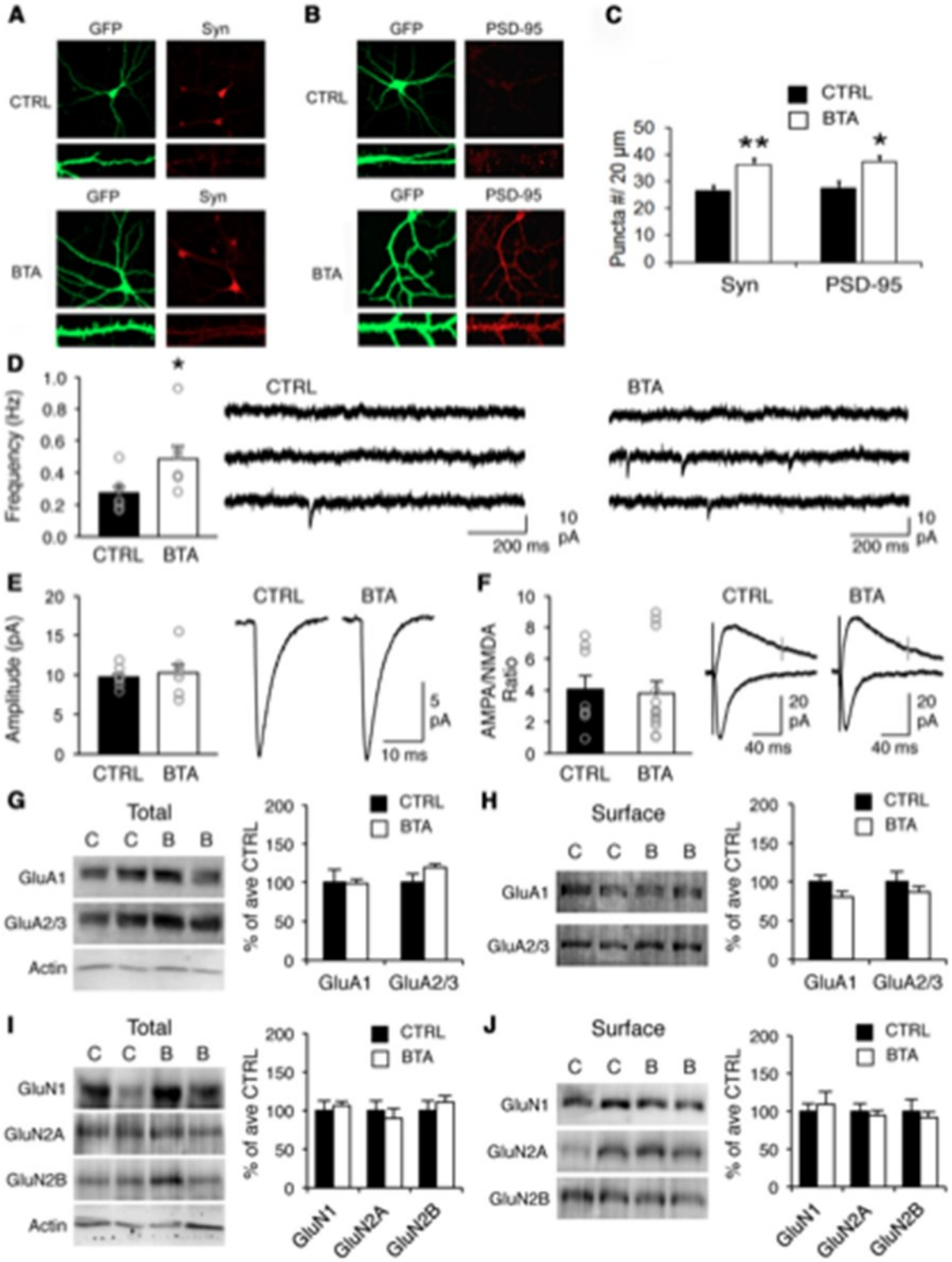

significant change in cell surface or total expression of any of these proteins in hippocampal slices from BTA-EG$_4$-treated mice (Fig 3.6 G-J). These data suggest that BTA-EG$_4$ does not

regulate cell surface or total expression of AMPAR or NMDAR. Hence, the increase in the number of functional synapses is likely due to lateral recruitment of existing cell surface glutamate receptors to new spines.

Subsection 6: BTA-EG$_4$ alters synapse formation through Ras signaling

We next investigated the molecular mechanism by which BTA-EG$_4$ may alter dendritic spine formation. Ras, a small GTPase, is involved in dendritic spine formation and synaptic delivery of AMPA receptors (Zhu et al., 2002; Lee et al., 2011). Moreover, abnormal Ras signaling is associated with neurodegenerative disease, causing cognitive impairments and learning deficits (Stornetta and Zhu, 2011). Thus, we initially investigated the effect of BTA-EG$_4$ on Ras signaling by treating primary hippocampal neurons with BTA-EG$_4$ (5μM) or control for 24 h. Interestingly, we found that BTA-EG$_4$ increased levels of RasGRF1, a guanine nucleotide exchange factor involved in Ras activation (Lee et al., 2010), as measured by immunofluorescence (Fig 3.7 A&H). Further, levels of active Ras were elevated following BTA-EG$_4$ treatment (5μM) in primary cortical neurons (Fig 3.7 B&H) and following BTA-EG$_4$ treatment (30 mg/kg) in wild type mice (Fig 3.7 C&H). We also examined whether BTA-EG$_4$ can alter the activity of downstream Ras signaling proteins, including p-ERK and p-CREB. We found

Figure 3.7. BTA-EG$_4$ increases dendritic spine density through Ras signaling.

A. Cultured hippocampal neurons (DIV18) were treated with BTA-EG$_4$ (5μM) or control for 24 h and stained for RasGRF1. **B.** Pulldown of active Ras in primary cortical neurons using GST-Raf1-RBD (n = 2). **C.** Pulldown of active Ras in brain lysates from wild type mice intraperitoneally injected with BTA-EG$_4$ (30 mg/kg) daily for 2 weeks, using GST-Raf1-RBD (n = 3). **(D-G)** Cultured hippocampal neurons (DIV18) were treated with BTA-EG$_4$ (5μM) or control for 24 h, and stained for p-ERK **(D)**, ERK **(E)**, p-CREB **(F)**, and CREB **(G)**. **(A, D-H)** Quantification and comparison of RasGRF1 (**A**, n = 15), p-ERK (**D**, n = 21), ERK (**E**, n = 30), p-CREB (**F**, n = 15), and CREB (**G**, n = 15) intensities (**p < 0.01; *p < 0.05). **I.** Primary hippocampal neurons were transfected with GFP and PLL (top) or GFP and RasGRF1 shRNA (bottom) and treated with BTA-EG$_4$ (5μM) or control. **J.** Quantification of dendritic spine density from **I** (**p < 0.01; ***p < 0.001). **K.** Primary hippocampal neurons were transfected with GFP and vector, GFP and Ras-WT, and GFP and RasN17, and were treated with BTA-EG$_4$ (5μM) or control. **L.** Quantification of dendritic spine density from **K** (n = 23, *p < 0.05; **p < 0.01; ***p < 0.001). C, Control; B, BTA-EG$_4$.

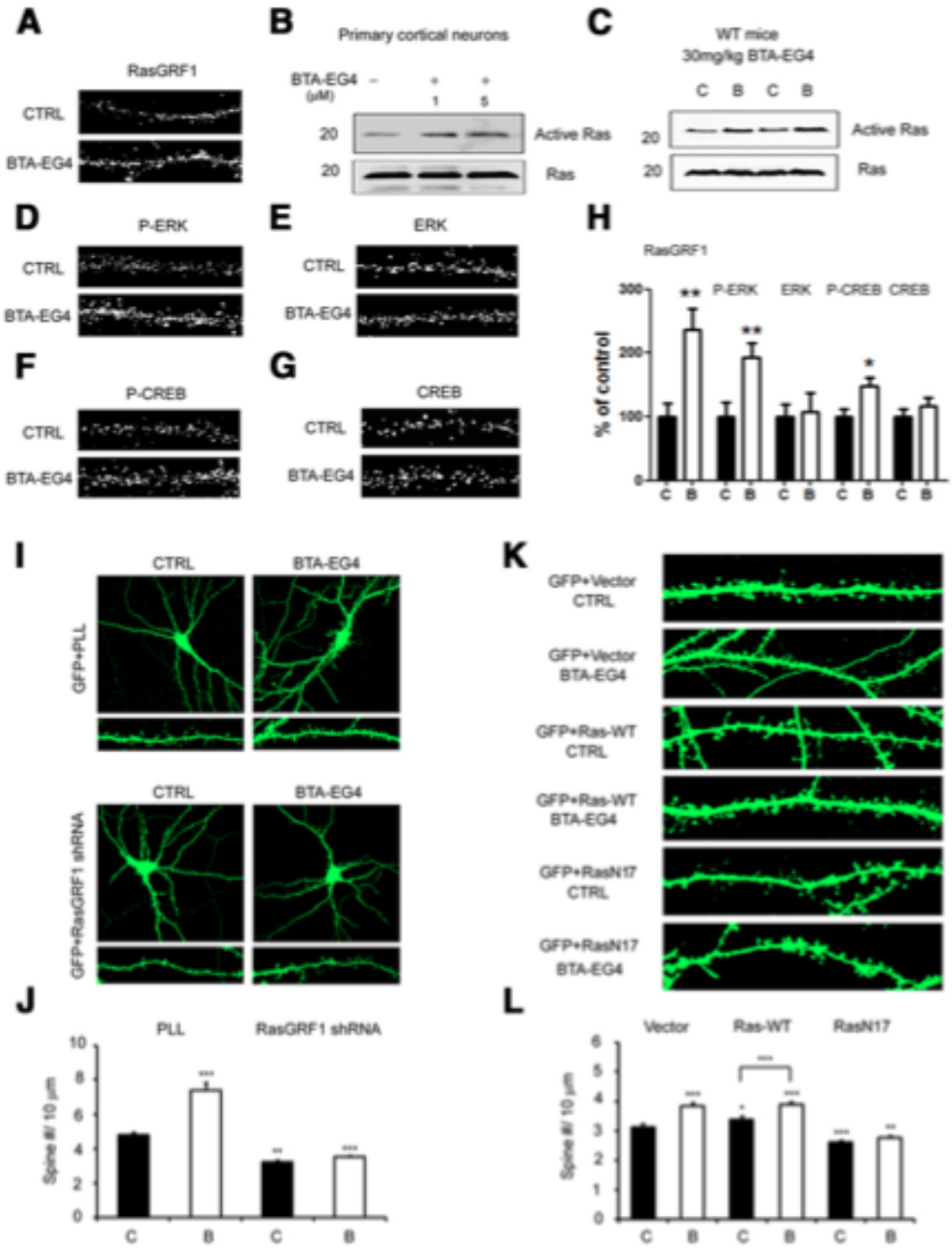

that BTA-EG$_4$ (5μM) increased the phosphorylation of ERK and CREB, the active forms of the signaling molecules downstream of Ras, without altering total ERK or CREB levels (Fig 3.7 D-

H).

To examine whether the effect of BTA-EG_4 on dendritic spine formation is Ras dependent, primary hippocampal neurons were transfected with GFP and RasGRF1 shRNA, or GFP and PLL. After 24 h, we treated with BTA-EG_4 (5μM) or control for another 24 h, and spine density was measured using immunofluorescence. Consistent with our findings above, BTA-EG_4 significantly increased dendritic spine density; however, RasGRF1 knockdown prevented the effect of BTA-EG_4 on dendritic spine formation (Fig 3.7 I&J). In addition, primary hippocampal neurons were transfected with GFP and empty vector, GFP and Ras-WT, or GFP and RasN17 (inactive Ras mutant). After 24 h, we then treated neurons with BTA-EG_4 (5μM) or control for 24 h, and spine density was measured. Ras-WT alone or combined with BTA-EG_4 increased dendritic spine density compared with control (Fig 3.7 K&L). RasN17 decreased dendritic spine density compared with control, and BTA-EG_4 could no longer increase dendritic spine density in the presence of RasN17 (Fig 3.7 K&L). These results suggest that Ras signaling is necessary for mediating the increase in dendritic spine density conferred by BTA-EG_4.

Subsection 7: APP interacts with RasGRF1 and regulates Ras signaling proteins

Since we observed that BTA-EG_4 functions through APP (Fig 3.5) and requires Ras signaling to increase spine density (Fig 3.7), we examined whether APP can increase spine density through Ras signaling. To test this, we examined whether APP can interact with RasGRF1 by immunoprecipitating APP from brain lysates of wild type mice, and probing for RasGRF1 (Fig 3.8 A). Interestingly, we found that APP coimmunoprecipitates with Ras-GRF1 (Fig 3.8 A). Results from immunoprecipitating RasGRF1 and probing for APP also indicated that RasGRF1 coimmunoprecipitates with APP (Fig 3.8 B). Our results indicate that RasGRF1 associates with APP *in vivo*.

Next, to examine whether APP can alter RasGRF1 levels, we examined the effect of APP

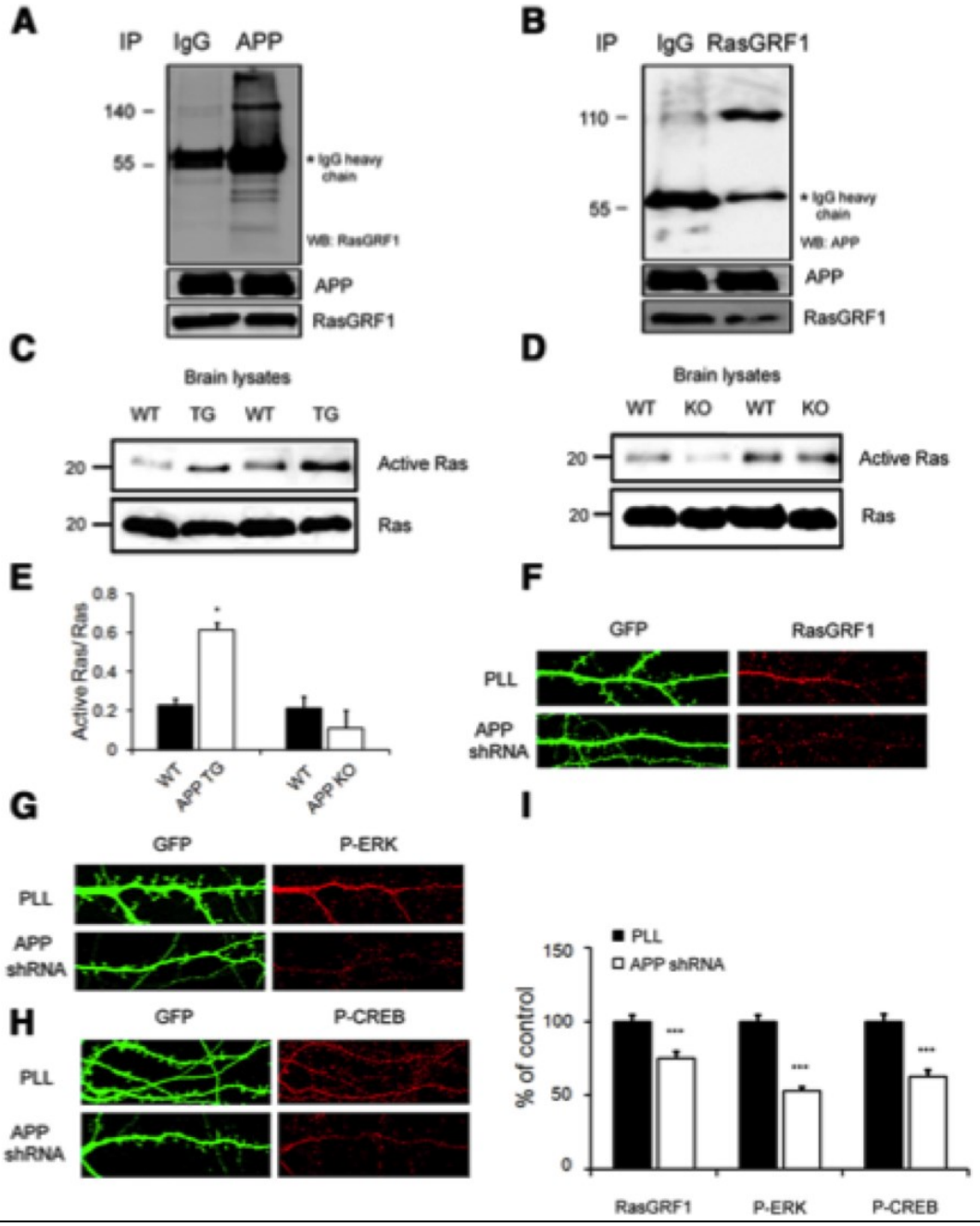

Figure 3.8. APP interacts with RasGRF1 and regulates Ras signaling proteins.

A. Brain lysates from wild type mice were immunoprecipitated (IP) with IgG or APP, and probed with RasGRF1. **B.** Brain lysates from wild type mice were immunoprecipitated with IgG or RasGRF1, and probed with APP. **(C-D)** Pulldown of active Ras from wild type mice (**C**, **D**, n = 5), APP transgenic (TG) mice (1 month old, **C**) or APP knock-out mice **(D)** using GST-Raf1-RBD. **E.** Quantification of data from **C** and **D**. **(F-H)** Primary hippocampal neurons were transfected with GFP and PLL or GFP and APP shRNA, then immunostained with RasGRF1 (**F**, n = 25), p-ERK (**G**, n = 25), and p-CREB (**H**, n = 25). **I.** Quantification of data shown in **F-H**. (***$p < 0.001$).

on Ras activity in APP transgenic mice and APP KO mice using a GST pull-down assay (Fig 3.8 C-E). We found that Ras activity was elevated in 1-month-old APP transgenic mice (overexpressing APP without Aβ pathology at 1 month), but decreased in 10-month-old APP KO mice, compared with wild type mice (Fig 3.8 C-E). Furthermore, we examined whether APP can alter the activity of downstream Ras signaling proteins ERK and CREB. First, to verify the effect of APP on Ras signaling, primary hippocampal neurons were transfected with GFP and PLL or GFP and APP shRNA, and then immunostained against RasGRF1. Knockdown of APP significantly decreased the levels of RasGRF1 compared with control vector (Fig 3.8 F&I). We then immunostained primary hippocampal neurons transfected with GFP and PLL or GFP and APP shRNA against p-ERK and p-CREB. We found that knockdown of APP decreased the phosphorylation of ERK and CREB compared with control vector (Fig 3.8 G-I). These data suggest that APP may regulate dendritic spine formation through increases in Ras activity and downstream Ras signaling pathways.

Subsection 8: BTA-EG$_4$ requires APP to alter Ras signaling

Since we observed that BTA-EG$_4$ and APP could possibly regulate dendritic spine density through Ras-dependent mechanisms, we then examined whether BTA-EG$_4$ requires APP to modulate Ras signaling. To test this hypothesis, primary hippocampal neurons were transfected with GFP and APP shRNA or GFP and APP, treated with control or BTA-EG$_4$ (5μM), then immunostained against RasGRF1 (Fig 3.9 A&B). We found that knockdown of APP did not increase RasGRF1 following BTA-EG$_4$ treatment compared with control, while overexpression of APP significantly increased RasGRF1 following BTA-EG$_4$ treatment compared with control (Fig 3.9 A&B).

Next, we investigated whether BTA-EG$_4$ can alter Ras activity in APP KO mice by injecting control or BTA-EG$_4$ for 2 weeks. We found that BTA-EG$_4$-injected APP KO mice did

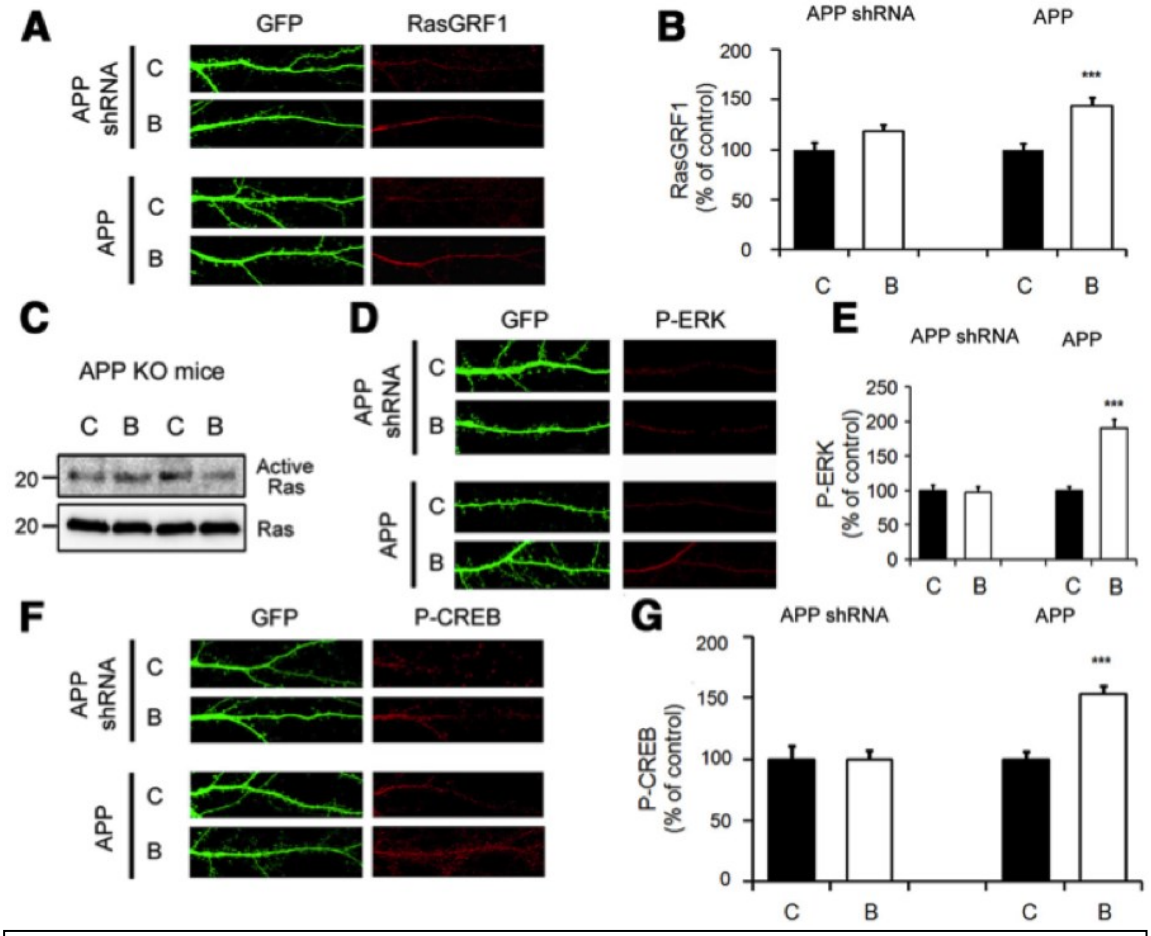

Figure 3.9. BTA-EG$_4$ requires APP to alter Ras signaling.

A. Primary hippocampal neurons were transfected with GFP and APP shRNA (top) or GFP and APP (bottom), treated with control or BTA-EG$_4$ (5μM), then immunostained with RasGRF1. **B.** Quantification of Ras GRF1 levels from **A** (n = 20, ***p < 0.001). **C.** Pulldown of active Ras from APP knock-out mice using GST-Raf1-RBD (Ras binding domain) following injection of control or BTA-EG$_4$ (30 mg/kg, i.p.) for 2 weeks. There was no significant difference in the amount of active Ras between APP KO mice treated with control or BTA-EG$_4$ [CTRL (C) = 100 ± 1.22%, BTA (B) = 103.2 ± 1.26%, n = 5]. **D.** Primary hippocampal neurons were transfected with GFP and APP shRNA (top) or GFP and APP (bottom), treated with control or BTA-EG$_4$ (5μM), then immunostained with p-ERK. **E.** Quantification of p-ERK (n = 20, ***p < 0.001). **F.** Primary hippocampal neurons were transfected with GFP and APP shRNA (top) or GFP and APP (bottom), treated with control or BTA-EG$_4$ (5μM), then immunostained with p-CREB. **G.** Quantification of p-CREB (n = 20, ***p < 0.001).

not have altered Ras activity (Fig 3.9 C). Further, we examined the effect of BTA-EG$_4$ on downstream Ras signaling in the presence or absence of APP. For this experiment, primary hippocampal neurons were transfected with GFP and APP shRNA or APP, treated with BTA-EG$_4$ or control, and then immunostained against p-ERK or p-CREB. We found that BTA-EG$_4$

was ineffective at increasing p-ERK or p-CREB following knockdown of APP, while overexpression of APP significantly increased p-ERK and p-CREB with BTA-EG_4 treatment compared with control (Fig 3.9 D-G). These data strongly support that BTA-EG_4 acts via APP to activate Ras-dependent signaling.

Section 4: Discussion

In the present study, we demonstrate that the Aβ-targeting molecule BTA-EG_4 reduces Aβ levels by facilitating cell surface expression of APP (Fig 3.1). Wild type mice treated with BTA-EG_4 exhibited improved cognitive performance without enhancement of hippocampal LTP (Figs 3.2 & 3.3). Additionally, BTA-EG_4 promotes dendritic spine density, which was accompanied by an increase in the number of functional synapses as determined by elevated mEPSC frequency. Moreover, BTA-EG_4 regulates dendritic spine formation, potentially by increasing the activity of Ras-ERK signaling proteins through APP (Figs.3.7-3.9). Together, these results strongly suggest that BTA-EG_4 works through APP to increase dendritic spine density via a Ras ERK-dependent mechanism. In addition, BTA-EG_4 warrants further investigation to determine its effect in mouse models of AD.

BTA-EG_4 treatment regulates APP metabolism, resulting in reduced Aβ levels and increased cell surface APP. It is known that β-secretase cleavage of APP forms Aβ along the intracellular endosomal pathway. Conversely, α-secretase cleavage of APP occurs at the cell surface and prevents Aβ production (Hyman, 2011). Because BTA-EG_4 did not alter the levels of Aβ degradation enzymes (i.e., insulin-degrading enzyme, neprilysin; data not shown), we believe BTA-EG_4 decreases Aβ levels by specifically increasing cell surface levels of APP, and thus, favoring processing of APP by α-secretase cleavage over processing by β-secretase.

Several recent studies have shown that Aβ aggregation is correlated with deficits in

learning and memory, and therapies that decrease Aβ can rescue these deficits (Loane et al., 2009; Chang et al., 2011). For instance, γ-secretase inhibitor (DAPT)-injected mice had decreased Aβ levels and improved behavioral performance after traumatic brain injury (Loane et al., 2009). Other studies using mouse models of AD showed reduced Aβ levels after treatment with either β-secretase or histone deacetylase (HDAC) inhibitors (Chang et al., 2011; Ricobaraza et al., 2011). These therapies were also able to prevent or improve memory deficits in AD mice. Furthermore, γ-secretase and HDAC inhibitors increase LTP, increase dendritic spine density, and improve cognitive performance (Townsend et al., 2010; Haettig et al., 2011). In contrast to these results, we found that while BTA-EG_4 had positive effects on cognitive performance and dendritic spine density, it did so without a correlated increase in the magnitude of LTP at both SC and TA inputs to CA1 (Fig 3.3). This finding implies that BTA-EG_4 improves cognitive performance through an LTP-independent mechanism, and suggests that targeting spine density alone may be sufficient to improve cognitive function.

We found that BTA-EG_4 specifically acts to increase the number of functional synapses, but individual synapses are not stronger. The lack of an increase in LTP magnitude suggests that the new synapses are available for synaptic plasticity, but there is no enhancement of LTP due to the addition of new synapses. While our LTP findings defy the conventional interpretation of the role of LTP in memory formation, it is not an isolated case. Indeed, in the PAK transgenic model, decreased dendritic spine density was associated with a decrease in cognitive performance, but an enhancement of LTP magnitude (Hayashi et al., 2004). Combined with our results, this suggests that an increase in the number of dendritic spines and functional synapses confer benefits to cognitive function. The reduction in LTP magnitude seen in some cases may be a homeostatic adjustment to the increase in synapse number. For example, higher synaptic density may increase the LTP induction threshold to prevent overexcitation of neuronal activity. This presents an

interesting point by implying that creating new synapses may benefit cognitive function not by enhancing LTP at individual synapses, but by allowing more synaptic contact points to form along the dendrite for potential information storage. It is of interest to note that some of the APP transgenic AD mouse models display larger LTP in younger ages (Marchetti and Marie, 2011; Wang et al., 2012; Chapter 2). It would be of interest to know whether BTA-EG_4 treatment in these young AD mouse models would show beneficial effects. While BTA-EG_4 significantly increased dendritic spine density in cortical layers II/III and the hippocampal CA1 region, this occurred without changes in dendritic spine morphology. Longer and thinner dendritic spines are characterized as immature "plastic" spines, while shorter and wider dendritic spines are characterized as mature "memory" spines (Kasai et al., 2002; Yasumatsu et al., 2008). Thus, BTA-EG_4 increases dendritic spine density without changing the proportion of immature and mature spines.

Here, we investigated the molecular mechanism by which BTA-EG_4 regulates dendritic spine density. One possibility is that BTA-EG_4 may act through a Ras-dependent mechanism because Ras signaling not only plays an important role in dendritic spine formation, but also in neuronal degeneration (Saini et al., 2009; Ye and Carew, 2010; Lee et al., 2011; Stornetta and Zhu, 2011). For instance, AD mice models have increased synaptic depression, which results in decreased activity and levels of RasGRF1, as well as downstream Ras signaling proteins. In contrast, AD patients have increased activity of Rap effectors, including p-JNK, which is accompanied by the removal of synaptic AMPA receptors (Savage et al., 2002; Zhu et al., 2002; Stornetta and Zhu, 2011). Interestingly, we observed that BTA-EG_4 promotes Ras-ERK signaling (Fig 3.7). BTA-EG_4 treatment increased RasGRF1 levels and Ras activity as well as activation of downstream Ras signaling proteins, including p-ERK. We found that Ras activity is necessary for spinogenesis induced by BTA-EG_4, which suggests that one of the main signaling pathways

involved in BTA-EG_4 action is via its ability to activate Ras. Therefore, BTA-EG_4 has the potential to reverse the decrease in Ras signaling seen in AD.

How does BTA-EG_4 activate Ras signaling to increase spine density? One possibility is that BTA-EG_4 binds directly to Aβ to prevent negative functional effects, resulting in protection against synapse loss. We also have data to demonstrate that BTA- EG_4 promotes cell surface expression of APP, which is known to increase dendritic spine formation (Lee et al., 2010b). Here, our novel finding provides evidence that APP promotes spinogenesis through direct or indirect interaction with RasGRF1 to increase Ras activity and downstream signaling to promote spinogenesis (Fig 3.8). Furthermore, the action of BTA-EG_4 on dendritic spine formation and Ras activity both required APP (Fig 3.9). While this does not rule out the possibility that BTA-EG_4 acts via neutralizing Aβ, the more parsimonious explanation is that BTA-EG_4 promotes APP signaling to enhance Ras-dependent spinogenesis. Whether the effect of BTA-EG_4 on APP signaling is strictly through enhancing cell surface APP levels or preventing β-cleavage of APP, perhaps via direct binding to the Aβ domain of APP, remains to be investigated. Nevertheless, there is evidence that Aβ and full-length APP often produce opposite signaling (Hoe et al., 2012); hence, the dual role of BTA-EG_4 in reducing Aβ and promoting APP signaling is likely conferring benefit to synaptic and cognitive function.

Together, our results strongly suggest that BTA-EG_4 treatment decreases Aβ levels and improves cognitive performance. Moreover, BTA-EG_4 increases dendritic spine density through APP- and Ras-dependent mechanisms. Thus, this novel small molecule exhibits potential as a drug candidate for AD treatment and warrants further studies to determine its effect in mouse models of AD.

Chapter 4: F-spondin promotes dendritic spine density through APP and Ras/ERK signaling in mature neurons

Work in this chapter is part of a manuscript in preparation; only the data representing my contribution is shown in this chapter.

Putative authors: **Andrea Megill***, Taehee Lee*, Nari Kim, Yoojin Sohn, Steve Barger, Robert A. Marr, Hey-Kyoung Lee, Hyang-Sook Hoe

*These authors contributed equally to this work

My contribution: All of the electrophysiology experiments and analysis, and organization of hippocampal *in vivo* viral transfections shown in this chapter.

Section 1: Introduction

Alzheimer's disease (AD) is the most common form of dementia, characterized by dendritic spine loss and progressive impairment of memory (Knobloch and Mansuy, 2008). Dendritic spines are small membranous protrusions that provide the sites of excitatory synaptic transmission in the central nervous system. The number of dendritic spines correlates with synaptic and cognitive function (Kasai et al., 2010). The function of dendritic spines is associated with stable LTP regarded as the physiological correlate of memory storage. During LTP induction, AMPARs traffic to the plasma membrane and diffuse to synaptic membrane compartments, such as those containing PSD-95. Therefore, understanding dendritic spine formation and retardation, as well as the synaptic proteins that affect these processes, could be important in understanding how synaptic dysfunction during progressive brain diseases, such as AD, destroy memory processes.

F-spondin is an extracellular matrix protein that has three different domains: N-terminal domain (reelin-N domain), spondin domain, and six C-terminal thrombospondin type 1 repeats (TSRs) (Tan et al., 2008). A recent study has shown that F-spondin regulates neuronal migration during brain development. For instance, F-spondin inhibits the migration of neural crest (NC) cells, suggesting that F-spondin regulates the segmental migration of NC cells (Debby-Brafman et al., 1999). Several studies have shown that F-spondin may play an important role in neuronal outgrowth. Burstyn-Cohen et al., found that the F-spondin TSR domain promotes outgrowth of cultured commissural neurons (Burstyn-Cohen et al., 1999). Another study has shown that the TSR1-4 fragment inhibits neurite outgrowth and TSR 5-6 fragments promote neurite outgrowth (Zisman et al., 2007).

In addition to the role of F-spondin in neuronal migration and neural outgrowth, our collaborators found that F-spondin interacts with APP and ApoE receptor 2 (ApoER2), and affects APP processing and Aβ production (Ho and Südhof, 2004). Additionally, a recent study found that hippocampal F-spondin overexpression can reduce Aβ levels and enhance learning and memory in WT mice (Hafez et al., 2012). Moreover, the same group found that F-spondin injected into a mouse model of AD exhibited decreased Aβ plaque deposition (Hafez et al., 2012). Interestingly, a recent study has shown that a polymorphism in the SPON1 gene locus of F-spondin is involved in brain connectivity in humans and implicates the SPON1 gene variant with rate of cognitive decline during AD (Jahanshad et al., 2013; Sherva et al., 2014). However, it is still unknown whether F-spondin plays a normal role in synaptic function and plasticity and whether it can affect dendritic spine formation associated with learning and memory in the adult brain.

In the present study, we examine whether F-spondin is necessary for normal synaptic function in the adult brain. Interestingly, we found that the levels of F-spondin were increased in

APP Tg mice compared to WT or APP knockout (KO) mice (Megill et al., in preparation). We also found that F-spondin can increase dendritic spine formation *in vitro* and *in vivo*, and increases Ras activity as well as regulating signaling proteins upstream and downstream of Ras, which are involved in dendritic spine formation. However, F-spondin did not alter Rap signaling protein levels, which are associated with dendritic spine retardation. Taken together, these results indicate that F-spondin is important for dendritic spine formation through its interaction with APP and regulation of Ras signaling proteins Here we report that F-spondin is necessary, but is not sufficient, to promote LTP.

Section 2: Methods

Subsection 1: Mice

Wild type mice (C57BL/6J) were obtained from the Jackson Laboratory (Bar Harbor, ME, USA). All procedures were performed in accordance with the protocols approved by the Institutional Animal Care and Use Committees of the Johns Hopkins University.

Subsection 2: In vivo viral transfections

Surgery was done under aseptic conditions. 5-week old male wild type C57BL/6J mice were anesthetized using 1-2% isoflurane mixed with O_2, and were placed into a stereotactic apparatus (with supply of 1-2% isoflurane and O_2). Craniotomy was made using a hand-held drill under a surgical microscope at the location of -2.54 mm from the Bregma, 2.00 mm lateral for CA1. A glass micropipette filled with recombinant lentivirus [the ratio of the virus: F3D(1:2), RL(1:6), F-spond-s-GFP(no dilution), GFP(no dilution)]was lowered into the brain 1.125 mm from the pia, using stereotactic coordinates. A total of 1.5 µl volume of virus was injected (0.15 µl/min) using a digital pump. The wound was wiped with sterile PBS (pH 7.4), and the skin was sutured. After recovery on a warm thermal blanket (~30˚C), mice were returned to the colony

once they were seen to intake water and/or food. The wound was inspected daily, and the mice were kept for 2-3 weeks before use.

Subsection 3: Electrophysiology

Hippocampal slices (400-µm thick) were prepared (Lee et al., 2003). In brief, hippocampi were dissected using oxygenated ice-cold dissection buffer (composition in mM: 212.7 sucrose; 2.6 KCl; 1.23 NaH_2PO_4; 26 $NaHCO_3$; 10 dextrose; 3 $MgCl_2$; and 1 $CaCl_2$) and recovered at room temperature in artificial cerebrospinal fluid (ACSF, composition in mM: 124 NaCl; 5 KCl; 1.25 NaH_2PO_4; 26 $NaHCO_3$; 10 dextrose; 1.5 $MgCl_2$; and 2.5 $CaCl_2$). All recordings were done in a submersion recording chamber perfused with ACSF (29–30°C, 2 ml/min) bubbled with 95% O_2-5% CO_2. Extracellular field potential responses were obtained by stimulating the Schaffer collaterals at about half-maximum intensity and recording from the dendritic field of CA1 using glass pipettes filled with ACSF. Synaptic responses were digitized and stored on-line using IGOR Pro software (WaveMetrics). LTP was induced using a theta burst stimulation [TBS: four trains, each consisting of ten 100-Hz bursts (four pulses) given at 5-Hz, repeated at 10-s intervals]. 10-Hz stimulation protocol was induced using 10-Hz, 900 pulses. For measurement of paired-pulse facilitation (PPF), interstimulus intervals (ISI) of 25, 50, 100, 200, 400, 1000, and 2000 ms were used. Input-output curves were generated by measuring extracellular field potential responses with varying stimulus intensities. Field potential (FP) slopes were measured, and data are expressed as mean ± SE of mean.

Subsection 4: Statistical analyses

All data were analyzed using either a two-Tailed T-test or ANOVA with Graphpad Prism 4 software. Significance determine as $p < 0.05$. All data is expressed as the mean ± SEM.

Section 3: Results

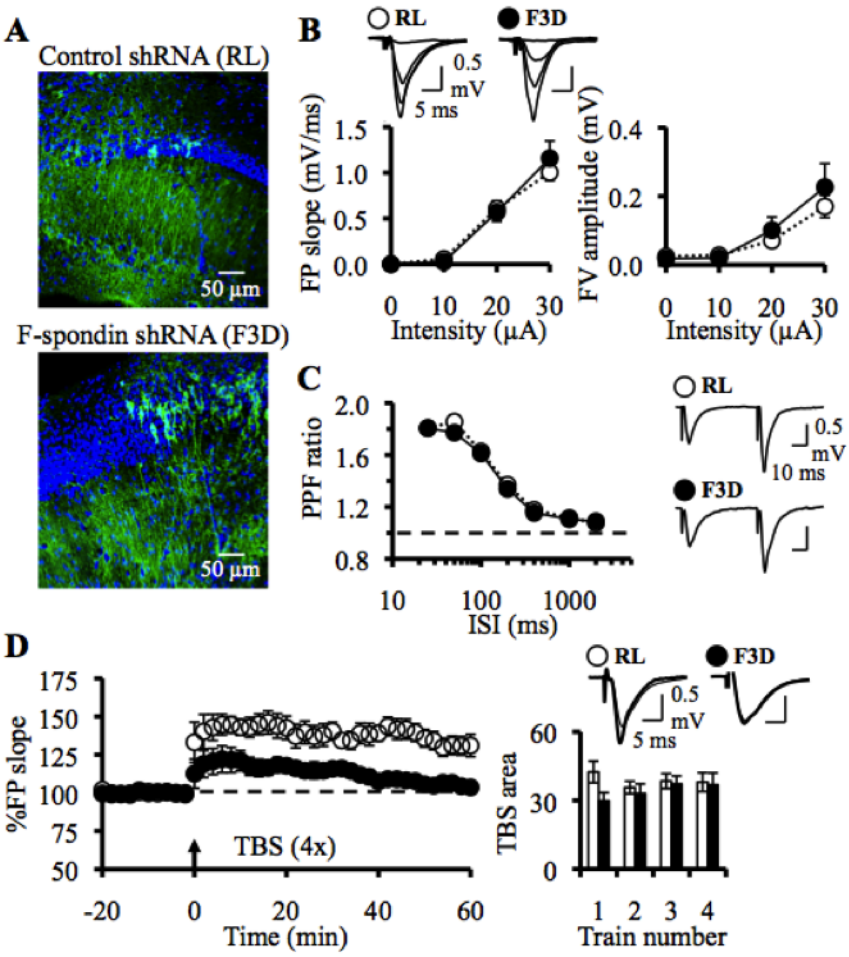

Figure 4.1. F-spondin is necessary for LTP in CA1.

A. Confirmation of *in-vivo* viral injection in CA1 of the hippocampus. CA1 regions of control shRNA (RL, Top panel) and F-spondin shRNA (F3D, Bottom panel) injected mouse. **B.** No significant difference in input-output function. Top: Representative FP traces. Bottom left: FP slope plotted against stimulus intensity (RL: n = 8 slices, 4 mice; F3D: n = 5 slices, 3 mice). Bottom right: FV amplitude plotted against stimulus intensity. There was also no significant difference in the ratio of FP slope to FV amplitude (RL: 7.67 ± 2.00; F3D: 5.06 ± 0.86; t test: p = 0.27). **C.** No change in presynaptic function. Left: PPF ratio at different interstimulus interval (ISI) (RL: n = 15 slices, 4 mice; F3D: n = 18 slices, 5 mice). Right: Representative traces from RL (top) and F3D (bottom) transfected slices at 50 ms ISI. **D.** Reduction in the magnitude of LTP produced by 4xTBS in F3D injected mice (RL: 131.4 ± 5.91% at 1 hour post-LTP, n = 10 slices, 4 mice; F3D: 105.2 ± 3.21% at 1 hour post-LTP, n = 15 slices, 4 mice; t-test: *p < 0.01). Right top: Representative traces (baseline: thin line, post-LTP: thick line). Right bottom: Normal summation of responses during 4xTBS LTP induction protocol (white bars: RL, black bars: F3D).

Subsection 1: F-spondin is necessary for hippocampal LTP

Essentially very little is known about the role of F-spondin in the mature brain, hence we first determined whether F-spondin was necessary for normal synaptic transmission and plasticity. To do this, we stereotactically injected lentiviruses containing either control shRNA (RL) or F-spondin shRNA (F3D) into the CA1 area of 5-week old WT mice. After 2-3 weeks, hippocampal slices were made and the transfection area was

determined by the expression of GFP, which was present in the constructs (Fig 4.1 A). We restricted our recordings to slices that expressed GFP. We found that F-spondin shRNA did not alter basal synaptic transmission when compared to control shRNA as determined by a lack of a change in input-output function (Fig 4.1 B) or PPF ratio at varying interstimulus intervals (Fig 4.1 C). In contrast, we found that F-spondin shRNA significantly impaired LTP without any change in the response summation during the induction protocol (Fig 4.1 D). These results suggest that normal expression of F-spondin is necessary for LTP expression.

Subsection 2: F-spondin is not sufficient to promote LTP

To determine whether F-spondin is sufficient to promote LTP, we overexpressed F-spondin into the CA1 area of 5-week old WT mice. After 2-3 weeks, we verified the transfection by the expression of GFP, which was co-expressed with F-spondin, and restricted the recordings to the slices that showed GFP. We found that similar to F-spondin shRNA, F-spondin overexpression did not alter basal synaptic transmission when compared to controls as determined by a lack of change in input-output function (Fig 4.2 A) or PPF ratio at varying interstimulus intervals (Fig 4.2 B). This suggests that F-spondin levels do not largely affect basal synaptic function in CA1 of adult neurons.

We found that the overexpression of F-spondin did not enhance LTP or alter the summation of responses during the induction protocol (Fig 4.2 C), which suggest that endogenous levels of F-spondin are likely sufficient for optimal LTP expression. To determine whether the lack of an enhancement of LTP with F-spondin overexpression is due to saturation of LTP with the maximal induction protocol used, we used a milder form of stimulation (i.e. 10-Hz) that is known to produce submaximal levels of LTP. Contrary to our expectation, F-spondin overexpression reduced LTP induced at an intermediate stimulation frequency (10-Hz) (Fig 4.2 D), which suggests that there may be an increase in LTP induction threshold.

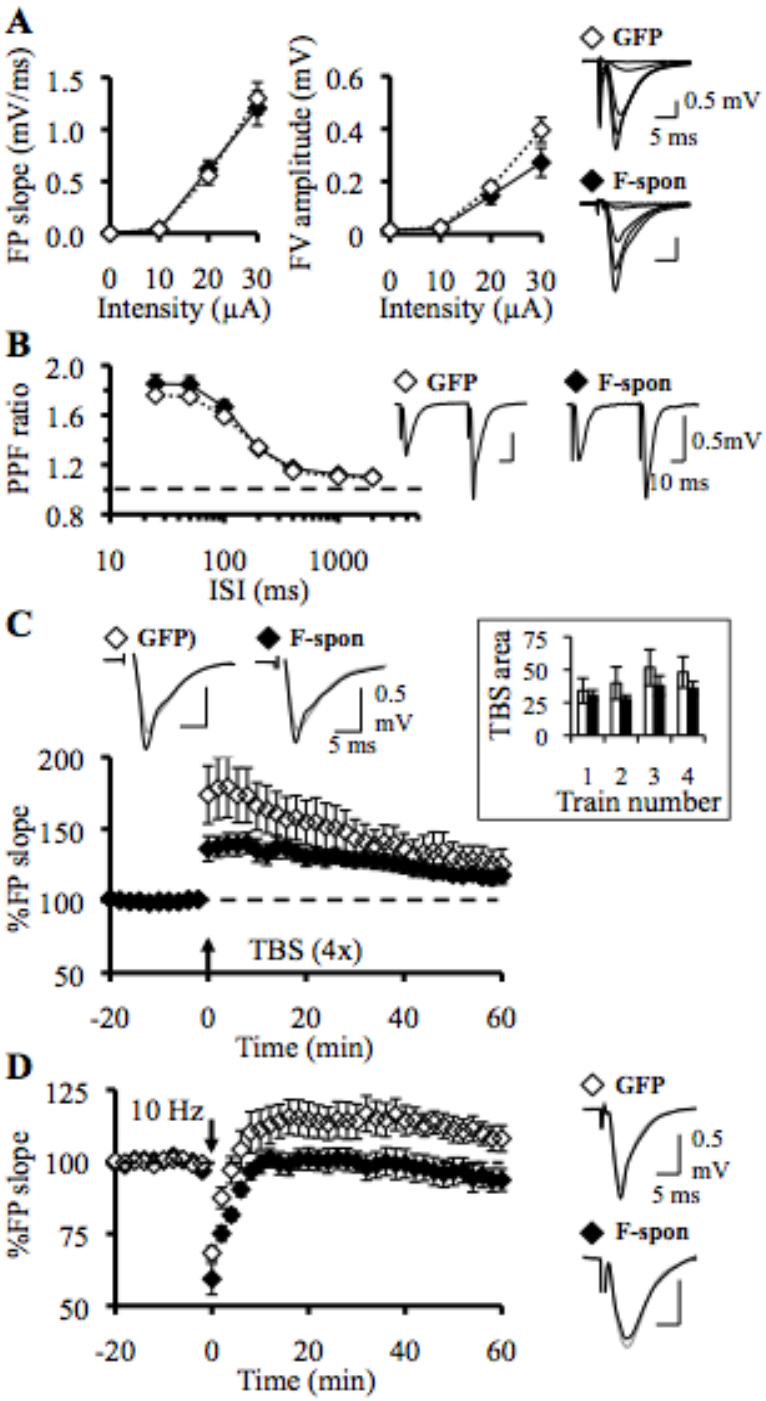

Figure 4.2. F-spondin overexpression does not enhance LTP in CA1 of the hippocampus.

A. No significant difference in input-output function. Left: FP slope plotted against stimulus intensity (GFP: n = 9 slices, 5 mice; F-spondin-s-GFP: n = 10 slices, 5 mice). Middle: FV amplitude plotted against stimulus intensity. Right: Representative FP traces. There was also no significant difference in the ratio of FP slope to FV amplitude (GFP: 3.44 ± 0.70; F-spondin-s-GFP: 3.89 ±0.55; t test: p = 0.62). **B.** No change in presynaptic function. Left: PPF ratio at different ISI (GFP: n = 17 slices, 5 mice, F-spondin-s-GFP: n = 16 slices, 4 mice). Right: Representative traces as 50 ms interstimulus interval (ISI). **C.** No difference in the magnitude of LTP produced by 4xTBS (GFP: 127.2 ± 9.87% at 1 hour post-LTP, n = 10 slices, 5 mice; F-spondin-s-GFP: 117.3 ± 4.21% at 1 hour post-LTP, n = 12 slices, 4 mice; t-test: p = 0.37). Top: Representative traces (baseline: thin line, post-LTP: thick line). Inset: Normal summation of responses during 4xTBS LTP induction protocol. **D.** Reduction in the magnitude of LTP produced by 10 Hz in F-spondin-s-GFP injected mice (GFP: 109.6 ± 4.20% at 1 hour post-LTP, n = 10 slices, 2 mice; F-spondin-s-GFP: 94.7 ± 4.21% at 1 hour post-LTP, n = 10 slices, 3 mice; t-test: *p < 0.05). Right: Representative traces (baseline: thin line, post-LTP: thick line).

Section 4: Discussion

We found a novel functional role of F-spondin in regulating LTP in mature neurons. Endogenous F-spondin is not only necessary for LTP, but its level is optimal for normal LTP. We found that F-spondin knockdown prevents LTP expression, which occurred without significant changes in input-output function or response summation during LTP (Fig 4.1). On the other hand, F-spondin overexpression did not significantly alter the magnitude of LTP, but increased the threshold for LTP induction at an intermediate stimulation frequency (Fig 4.2). These results suggest that endogenous levels of F-spondin are optimal for normal LTP and any deviation would negatively impact LTP. While F-spondin treatment increases dendritic spine density and specific subunits of AMPA and NMDA receptors (data not shown, Megill et al., in preparation), we did not observe significant changes in the input-output function with F-spondin overexpression (Fig 4.2). This may be due to differences in preparation or method of F-spondin overexpression, but suggests that increasing F-spondin levels may only marginally affect basal synaptic function despite having significant effects on dendritic spine plasticity and LTP induction threshold (Fig 4.2). The increase in LTP induction threshold following F-spondin overexpression may reflect a homeostatic adaptation to the increase in dendritic spine density (data not shown; Megill et al., in preparation). A similar reduction in LTP magnitude was also seen in our previous study with an Aβ binding chemical, which increased dendritic spine density via Ras signaling (Megill et al., 2013; Chapter 3). A previous study demonstrated that F-spondin overexpression enhances behavioral performance of WT mice in Morris water maze and novel object recognition tasks (Hafez et al., 2012). Together with our results, this suggests that improvement of dendritic spine density, but not increased magnitude of LTP, better correlates with improved behavioral performance.

Results from our collaborators provide a signaling pathway in which F-spondin acts on APP to activate Ras signaling leading to an increase in dendritic spine density. Furthermore, F-spondin decreased the levels of a key synaptic Ras inhibitor, SynGAP, without affecting Rap signaling molecules. It is of interest to note that SynGAP heterozygotes exhibit similar phenotype as F-spondin overexpression, in that there was an increase in surface AMPA receptor clusters but no change in basal synaptic transmission and reduced LTP induction (Kim et al., 2003). At this point, it is unclear as to whether F-spondin works via direct binding to APP or not, but our study provides a molecular signaling mechanism for F-spondin action in mature neurons. The signaling of F-spondin via APP also has implications for normal physiological functions of APP. Based on our collaborator's results that F-spondin levels are increased in APP Tg mice, we surmise that F-spondin may amplify APP signaling. This amplification may not just result from increased F-spondin activation of APP, but may also result from reduced Aβ production, (Ho and Südhof, 2004; Hoe et al., 2005) [but see (Rice et al., 2013)] considering that Aβ signaling often opposes APP signaling [reviewed in (Hoe et al., 2012)]. F-spondin and APP have been shown to be increased in the CSF of symptomatic AD patients compared to non-symptomatic AD patients and to normal controls (Zhang et al., 2005; Ringman et al., 2012). Variants in the F-spondin gene (SPON1) have also been identified as risk factors for AD and associated with cognitive decline (Jahanshad et al., 2013; Sherva et al., 2014). Collectively, our results place F-spondin as a key regulator of APP-mediated spinogenesis and necessary for LTP in CA1, which may underlie the link between SPON1 and AD.

Chapter 5: Comparing Alzheimer's disease therapies in a mouse model of AD

This manuscript is in preparation.

Putative authors: **Andrea Megill**, Philip C. Wong, Hyang-Sook Hoe, and Hey-Kyoung Lee

My contribution: All of the experiments in this study.

Section 1: Introduction

It is clear that successful AD treatments will need to do more than just lower Aβ production; they will need to rescue cognitive as well as synaptic dysfunction. Increasing evidence suggests the cognitive syndromes found in AD patients are preceded by changes in synaptic efficacy [reviewed in (Selkoe, 2002; Shankar and Walsh, 2009)]. Therefore, examining whether different strategies that target Aβ production and accumulation will rescue synaptic dysfunction associated with AD is also important. We decided to compare two therapies, BTA-EG_4 and GRL-8234, in an established AD mouse model (see Chapter 2).

GRL-8234 is a β-secretase inhibitor. Inhibiting APP processing enzymes, like β- and γ-secretase, emerged among the first possible targets of AD therapeutics [reviewed in (Wang et al., 2012)], in an effort to reduce Aβ production. However, many of these original therapeutics have proven unsuccessful due to either widespread toxicity (Vetrivel et al., 2006; Wolfe, 2008; Svedružić et al., 2013; D'Onofrio et al., 2012) or their poor results after long-term treatment during *in vivo* studies (Ghosh et al., 2008a, 2008b). GRL-8234 and its derivatives have recently been developed and reported to overcome many of these problems, proving to be highly effective and potent at inhibiting β-secretase activity *in vivo* (Ghosh et al., 2008c; Chang et al., 2011). In Tg2576 AD mice, GRL-8234 was able to recue cognitive decline after long-term treatment. This

rescue was also associated with a reduction in soluble Aβ peptides and Aβ plaque number (Chang et al., 2011).

BTA-EG_4 was developed in an effort to find a novel small molecule the was able to bind Aβ peptides and stop their aggregation, as well as prevent their association with other cellular proteins (Inbar et al., 2006; Habib et al., 2010; Capule and Yang, 2012). Recently, with the help of our collaborators, we investigated the effects of BTA-EG_4 on normal brain activity and synaptic function in WT mice. The summary of those results is detailed in Chapter 3. Briefly, we found that BTA-EG_4 decreased soluble Aβ levels by increasing the cell surface expression of APP, thereby altering APP processing. BTA-EG_4 also improved memory through an LTP independent mechanism that correlated with increased spinogenesis. Finally, we found that BTA-EG_4 required APP to regulate dendritic spine density through a Ras-ERK-dependent signaling mechanism (Megill et al., 2013).

Because BTA-EG_4 showed promise as an AD therapeutic, its effects on neural and cognitive dysfunction were next studied in 3xTG AD mouse model (Song et al., 2014). There was an age specific improvement in 3xTg mice treated with BTA-EG_4. Both dendritic spine density and Ras activity were increased in CA1 of 6-10 month old 3xTg mice, but not in 13-16 month old mice. Increased spine density correlated with improved learning and memory in 6-10 month old 3xTg mice, as well as a decrease in Aβ levels (Song et al., 2014).

While both GRL-8234 and BTA-EG_4 have been shown to lower Aβ production and improve cognitive function, previous studies differ in the AD mouse model used, the duration and initiation of treatment, and the mechanism by which treatment proved effective. In addition, and most importantly, neither study investigated the effects of treatment on synaptic function and plasticity in these AD models. Therefore, the goal of this study is to compare and examine

whether short term treatment of BTA-EG_4 or GRL-8234 will effectively rescue synaptic deficits seen in adult APPswe;PS1deltaE9 Tg mice.

Section 2: Materials and Methods

Subsection 1: Animals

Adult 6 to 7-month old WT and APPswe;PS1deltaE9 Tg mice (129/C57BL6 mixed background) were used. Genotypes were distinguished by polymerase chain reaction (PCR) of isolated genomic DNA obtained from each pup after weaning. The Institutional Animal Care and Use Committees of Johns Hopkins University approved all procedures involving animals

Subsection 2: Drug administration

Mice were intraperitoneally (i.p.) injected with either GRL-8234 (33.4ug/g body weight/day) or vehicle solvent (50:50 mixture of PEG300 and D5W, v/v); or BTA-EG_4 (30 mg/kg body weight/day) or vehicle solvent (10% DMSO in 1xPBS) for 10 consecutive days.

Subsection 3: Preparation of acute hippocampal slices

Acute hippocampal slices were prepared as described previously (Lee et al., 2003). Briefly, each mouse was euthanized by decapitation following overdose of isoflurane. Hippocampi were rapidly removed and one was sectioned into 400 μm slices on a vibratome (Vibratome 3000 series, Ted Pella Inc.), the other was saved for Aβ ELISA. The hippocampus was dissected using oxygenated ice-cold dissection buffer (composition in mM: 212.7 sucrose; 2.6 KCl; 1.23 NaH_2PO_4; 26 $NaHCO_3$; 10 dextrose; 3 $MgCl_2$; and 1 $CaCl_2$) and recovered at room temperature in artificial cerebrospinal fluid (ACSF, composition in mM: 124 NaCl; 5 KCl; 1.25 NaH_2PO_4; 26 $NaHCO_3$; 10 dextrose; 1.5 $MgCl_2$; and 2.5 $CaCl_2$).

Subsection 4: Field potential recording from Schaffer collateral inputs to CA1

All recordings were done in a submersion recording chamber perfused with ACSF (29–30°C, 2 ml/min) bubbled with 95% O_2-5% CO_2. For field potential recordings, synaptic responses were delivered through a bipolar glass stimulating electrode placed to activate the Schaffer collaterals with a 0.2 ms duration pulse (baseline stimulation at 0.0333 Hz), and recorded from the dendritic field of CA1. Synaptic responses were digitized and stored on-line using IGOR Pro software (WaveMetrics). Input-output curves were generated by measuring extracellular field potential responses with varying stimulus intensities. For measurement of paired-pulse facilitation (PPF), ISIs of 25, 50, 100, 200, 400, 1000, and 2000 ms were used. LTP was induced using a theta burst stimulation [TBS: four trains, each consisting of ten 100-Hz bursts (four pulses) given at 5 Hz, repeated at 10-s intervals] (Larson et al., 1986). LTD was induced using a paired-pulse 1 Hz (50ms ISI), 900 pluses stimulation. Field potential (FP) slopes were measured, and data are expressed as mean ± SE of mean.

Subsection 5: Aβ ELISA

Each half of the hippocampus was homogenized in tissue homogenization buffer containing 250 mM sucrose, 20 mM Tris base, protease, and phosphatase inhibitors. To measure soluble Aβ, diethylamine (DEA) extraction was performed. Crude 10% homogenate was mixed with an equal volume of 0.4% DEA, sonicated, and ultracentrifuged for 1 h at 47,000 RPM. The supernatant was collected and neutralized with 10% 0.5 m Tris, pH 6.8. Sensitive and specific ELISAs to Human Aβ1–40 and 42 were purchased from Invitrogen and conducted per the manufacturer's protocol.

Subsection 6: Statistical analyses

All data were analyzed with GraphPad Prism 4 software using either a two-tailed t test or ANOVA with Bonferroni *post hoc* test for multiple comparisons. Significance was determined as $p < 0.05$. All data is expressed as the mean ± SEM.

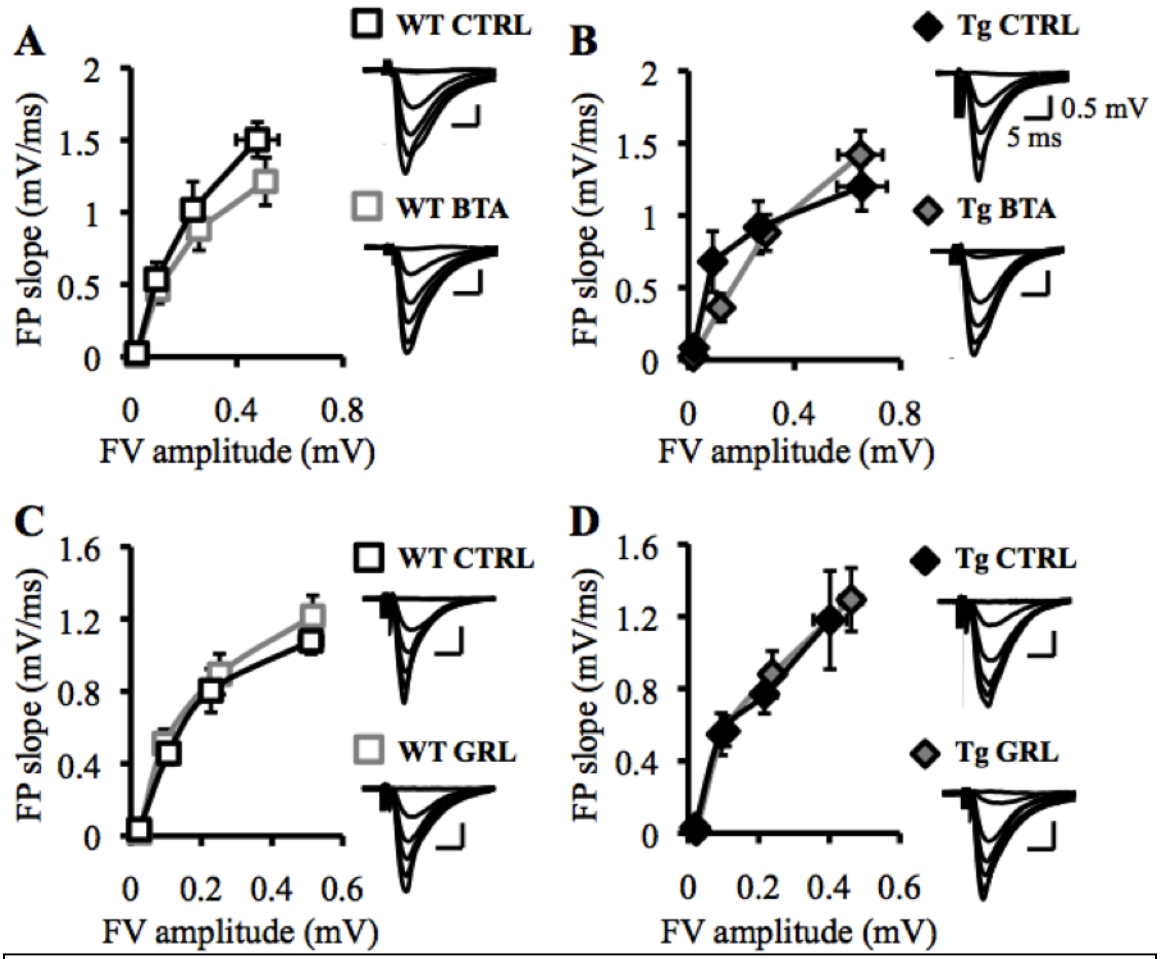

Figure 5.1. Basal synaptic function is unaffected in adult WT and APPswe;PS1deltaE9 Tg mice treated with either BTA-EG$_4$ or GRL-8234.

A. FP slope normalized to FV amplitude in adult (6 to 7-month) WT mice treated with BTA (CTRL: n = 13 slices, 7 mice; BTA: n =11 slices, 6 mice). Right, Representative FP traces. **B.** FP slope normalized to FV amplitude in adult Tg mice treated with BTA (CTRL: n = 14 slices, 5 mice; BTA: n =11 slices, 4 mice). Right, Representative FP traces **C.** FP slope normalized to FV amplitude in adult WT mice treated with GRL (CTRL: n = 20 slices, 7 mice; GRL: n = 20 slices, 6 mice). Right, Representative FP traces. **D.** FP slope normalized to FV amplitude in adult Tg mice treated with GRL (CTRL: n = 13 slices, 4 mice; GRL: n = 19 slices, 5 mice). Right, Representative FP traces.

Section 3: Results

Subsection 1: Basal synaptic function and PPF ratio are unaffected in adult WT and APPswe;PS1deltaE9 Tg mice treated with either BTA-EG$_4$ or GRL-8234

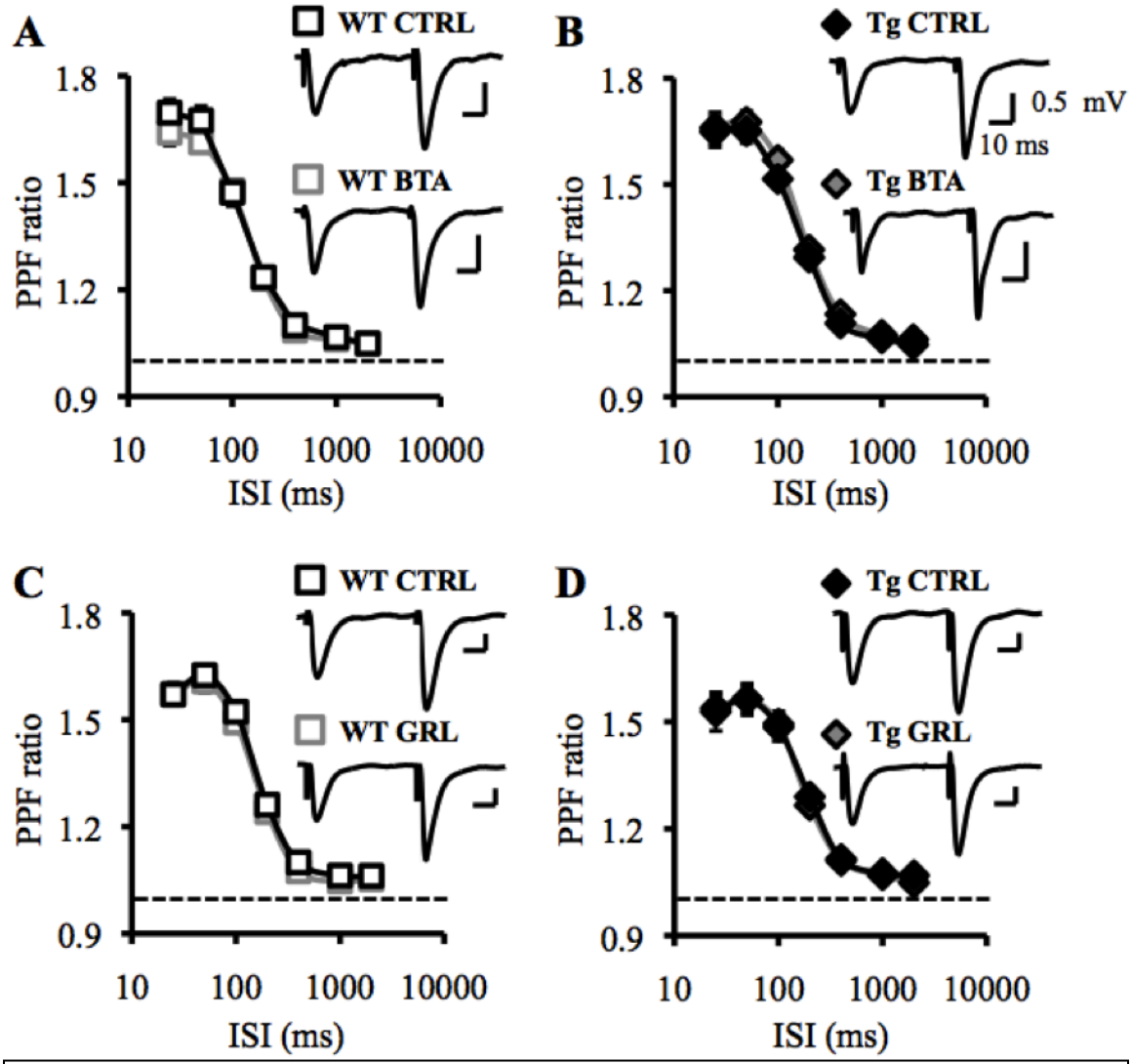

Figure 5.2. PPF ratio is unaffected in adult WT and APPswe;PS1deltaE9 Tg mice treated with either BTA-EG$_4$ or GRL-8234.

A. PPF ratio at different ISIs in adult WT mice treated with BTA (CTRL: n = 25 slices, 7 mice; BTA: n = 22 slices, 6 mice) Right, Representative traces at 50 ms ISI. **B.** PPF ratio at different ISIs in adult WT mice treated with BTA (CTRL: n = 20 slices, 5 mice; BTA: n = 19 slices, 5 mice). Right, Representative traces at 50 ms ISI. **C.** PPF ratio at different ISIs in adult WT mice treated with GRL (CTRL: n = 28 slices, 7 mice; GRL: n = 30 slices, 6 mice). Right, Representative traces at 50 ms ISI. **D.** PPF ratio at different ISIs in adult Tg mice treated with GRL (CTRL: n = 21 slices, 4 mice; GRL: n = 25 slices, 6 mice). Right, Representative traces at 50 ms ISI.

We conducted electrophysiological experiments on adult, 6 to 7-month old WT and APPswe;PS1deltaE9 Tg mice treated with BTA-EG$_4$ (30 mg/kg; i.p.), or GRL-8234 (33.4 mg/kg; i.p.), or the appropriate control (BTA: 10% DMSO, GRL: 50/50 PEG 300, D5W) for 10

consecutive days. Neither BTA-EG$_4$ (Fig 5.1 A&B) nor GRL-8234 (Fig 5.1 C&D) treatment effected basal synaptic function in WT (Fig 5.1 A&C) or Tg (Fig 5.1 B&D) mice. Neither was there a differential effect of either treatment on PPF ratio (Fig 5.2) at individual ISIs in WT (Fig

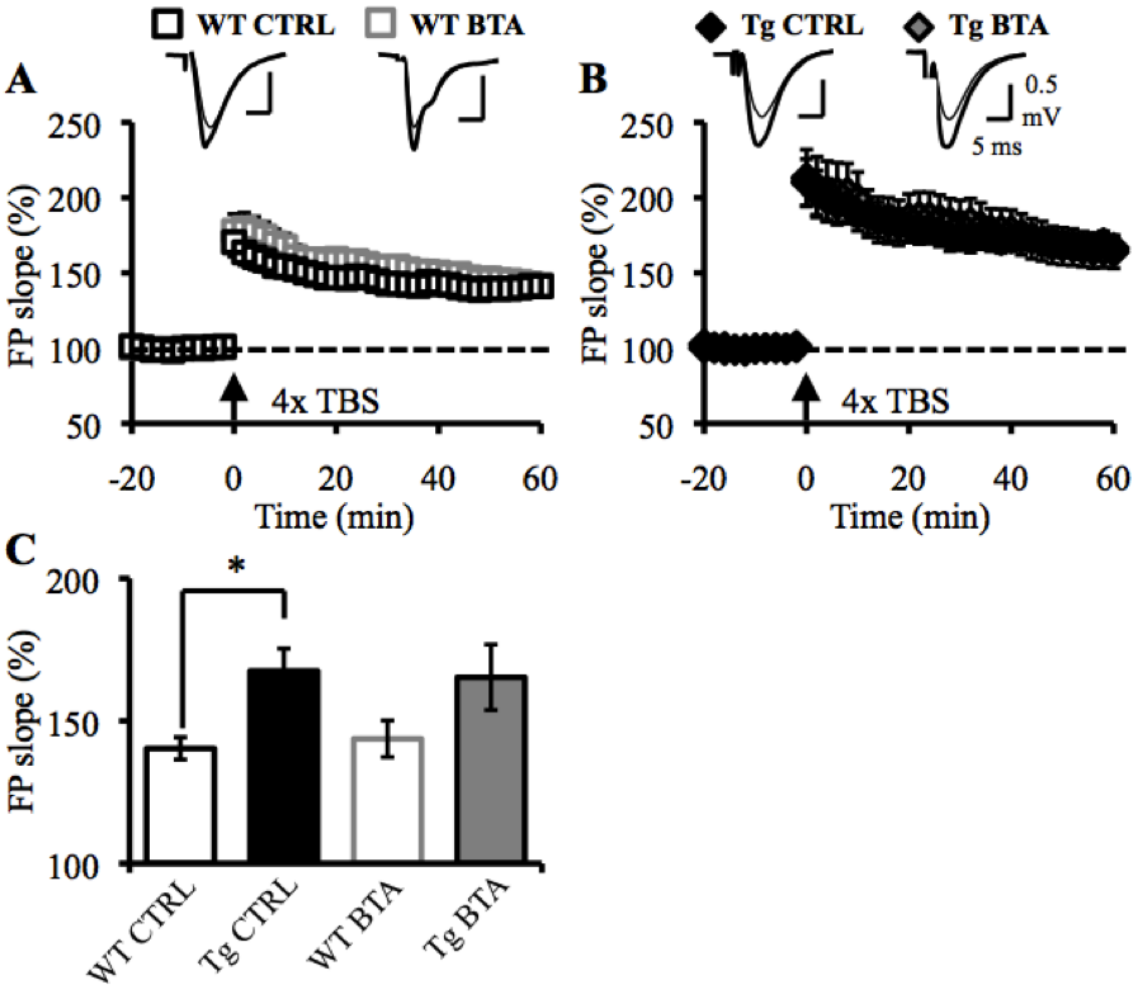

Figure 5.3. LTP in adult WT and APPswe;PS1deltaE9 Tg mice treated with BTA-EG$_4$.

A. BTA treatment has no effect on LTP induced with 4xTBS protocol in adult WT mice (CTRL: 140.34 ± 3.92% at 1 hour post-LTP, n = 12 slices, 5 mice; BTA: 142.74 ± 6.40% at 1 hour post-LTP, n = 11 slices, 4 mice; t test, p = 0.657). Top, Representative FP traces (baseline: thin line, post-LTP: thick line). **B.** BTA treatment has no effect on LTP induced with 4xTBS protocol in adult Tg mice (CTRL: 167.55 ± 7.85% at 1 hour post-LTP, n = 16 slices, 5 mice; BTA: 165.31 ± 11.48% at 1 hour post-LTP, n = 12 slices, 5 mice; t test, p = 0.873). Top, Representative FP traces (baseline: thin line, post-LTP: thick line). **C.** There is a vehicle effect on LTP magnitude seen between WT and Tg mice (values above, Bonferroni post test, *p < 0.05).

5.2 A&C) or Tg (Fig 5.2 B&D) mice.

Subsection 2: Long-term plasticity in adult WT and APPswe;PS1deltaE9 Tg mice treated with BTA-EG$_4$.

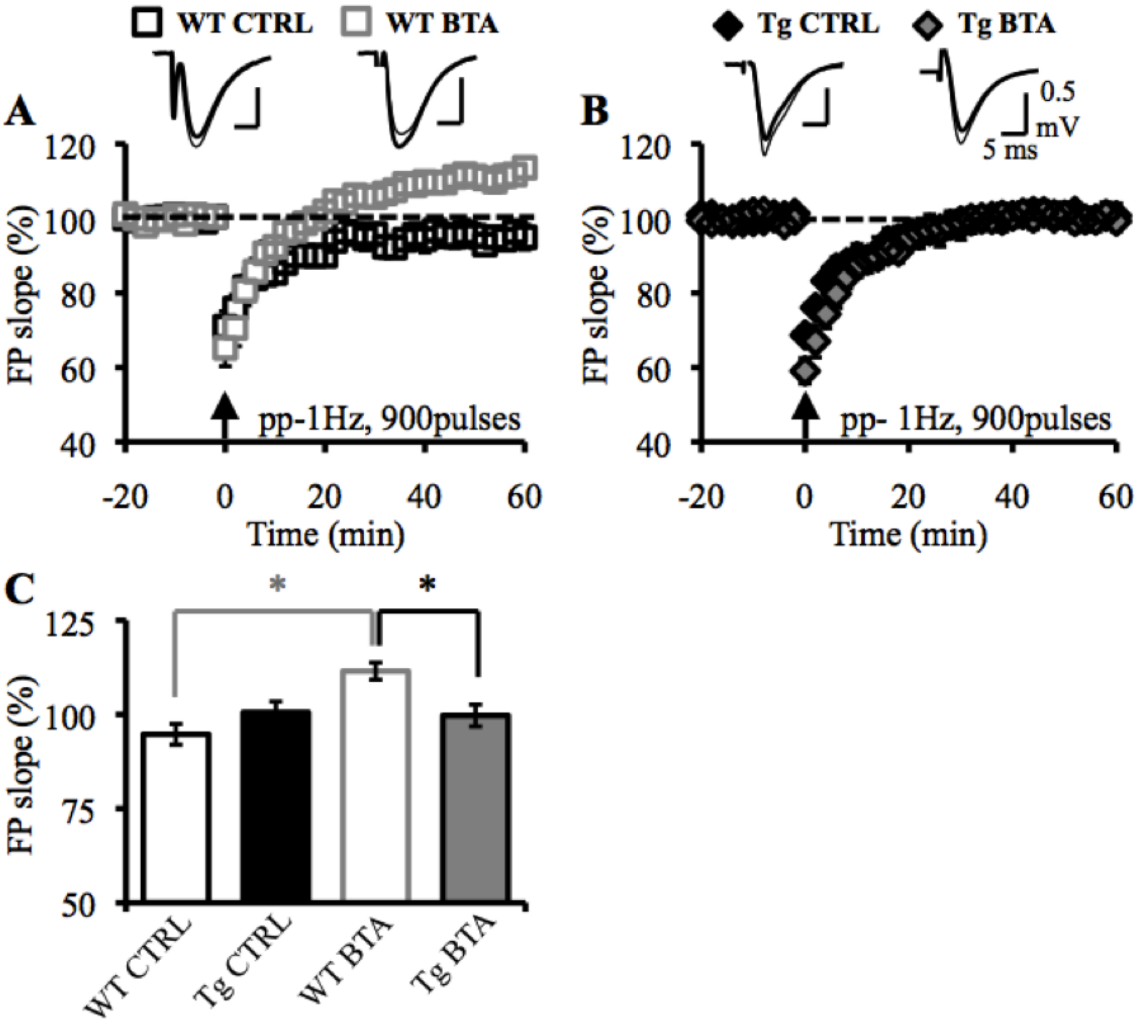

Figure 5.4. LTD in adult WT and APPswe;PS1deltaE9 Tg mice treated with BTA-EG$_4$.

A. BTA treatment causes LTP in adult WT mice following a pp-1Hz, 900 pulses LTD protocol (CTRL: 94.72 ± 2.78% at 1 hour post-LTD, n = 11 slices, 4 mice; BTA: 111.50 ± 2.28% at 1 hour post-LTD, n = 11 slices, 4 mice; t test, *p < 0.001, gray line). Top, Representative FP traces (baseline: thin line, post-LTD: thick line). **B.** BTA treatment has no effect on LTD induced with pp-1Hz, 900 pulses LTD protocol in adult Tg mice (CTRL: 100.54 ± 2.87% at 1 hour post-LTD, n = 13 slices, 5 mice; BTA: 99.72 ± 2.91% at 1 hour post-LTD, n = 11 slices, 4 mice; t test, p = 0.843). Top, Representative FP traces (baseline: thin line, post-LTD: thick line). **C.** LTD is significantly different across WT and Tg mice treated with BTA (values above, Bonferroni post test, *p < 0.01, black line). Vehicle treatment reduced LTD magnitude in adult Tg mice compared to non-treated Tg mice (Chapter 2).

We have previously reported that adult APPswe;PS1deltaE9 Tg mice show deficits in long-term plasticity due to altered expression mechanisms for mediating frequency-dependent LTP/LTD (Chapter 2). This deficit resulted from dysregulated metaplasticity and lead to decreased LTP and increased LTD at this age. LTP and LTD were measured in adult WT and Tg mice treated with BTA-EG_4 to investigate whether either treatment would be effective at rescuing these deficits. BTA-EG_4 treatment did not affect LTP following 4xTBS protocol in WT (Fig 5.3 A) or Tg (Fig 5.3 B) mice. However, there was a vehicle (10% DMSO) effect seen across WT and Tg mice (Fig 5.3 C), as the magnitude of LTP was opposite of what was previously observed in non-treated adult WT and Tg mice (Fig 2.6 G). BTA-EG_4 treatment produced a small potentiation in WT mice (Fig 5.4 A) following pp-1 Hz LTD induction protocol, but did not effect LTD magnitude in Tg mice (Fig 5.4 B). In Tg mice, vehicle treatment nearly abolished LTD compared to what was previously seen in non-treated Tg mice (Fig 2.6 E). These results suggest that vehicle treatment itself reduced LTP in WT mice, enhanced LTP in Tg mice, and prevented LTD in Tg mice, hence complicates the interpretation of results with BTA- EG_4. However, BTA-EG_4 treatment did not differ from vehicle treatment in most cases, except that it changed the polarity of synaptic plasticity induced by a LTD protocol in WT mice.

Subsection 3: Long-term plasticity in adult WT and APPswe;PS1deltaE9 Tg mice treated with GRL-8234.

We next measured LTP and LTD in adult WT and Tg mice treated with GRL-8234, using the same stimulation protocols as above. GRL-8234 reduced the magnitude of LTP in WT mice (Fig 5.5 A) but had no effect on LTP in Tg mice (Fig 5.5 B). The decrease in LTP with GRL-8234 in WT was not due to a decrease in the summation of synaptic response during LTP induction (Fig 5.5 C). There is also a difference in LTP magnitude seen between WT and Tg mice treated with vehicle control (50/50 PEG 300, D5W) (Fig 5.5 D), which is similar in magnitude to

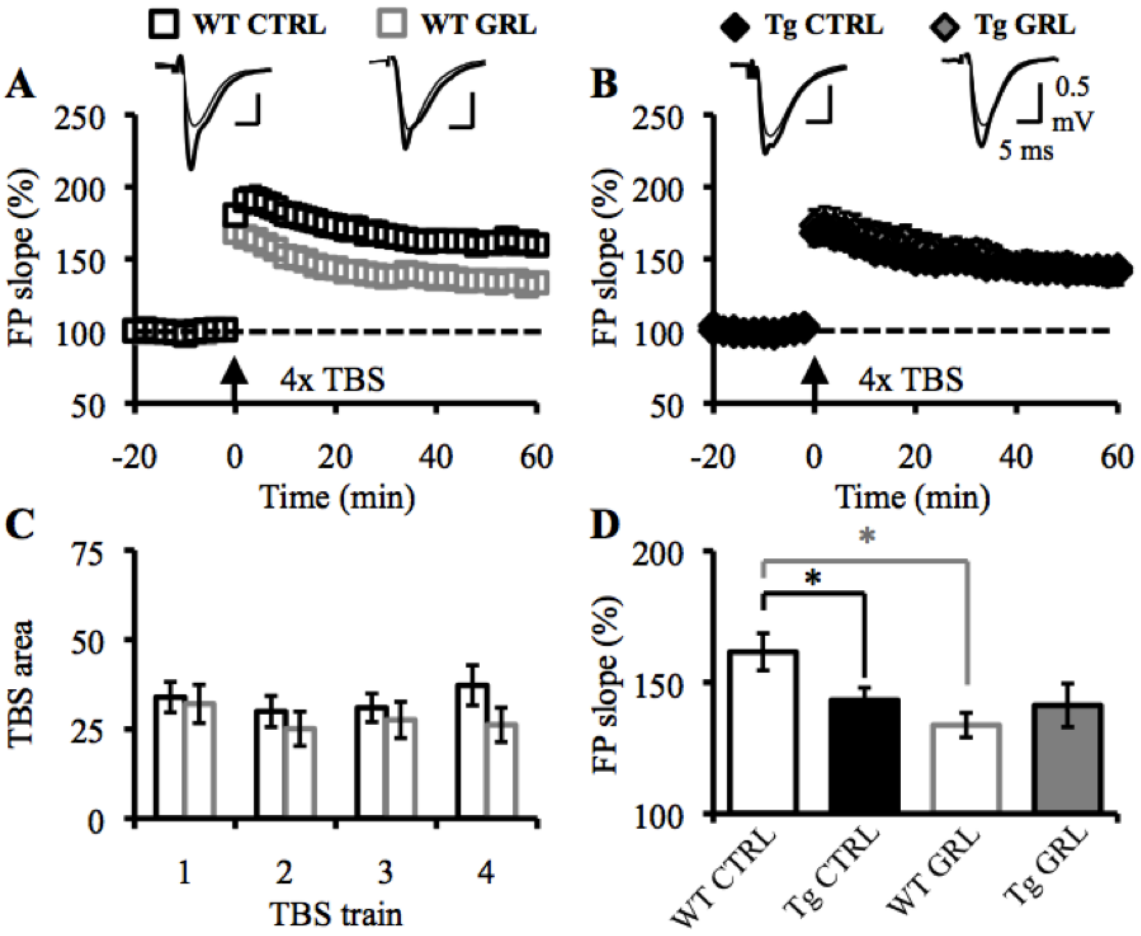

Figure 5.5. LTP in adult WT and APPswe;PS1deltaE9 Tg mice treated with GRL-8234.

A. GRL treatment negatively affects LTP magnitude induced with 4xTBS protocol in adult WT mice (CTRL: 161.60 ± 7.06% at 1 hour post-LTP, n = 14 slices, 4 mice; GRL: 133.71 ± 4.67% at 1 hour post-LTP, n = 14 slices, 4 mice; t test, *p < 0.01, gray line). Top, Representative FP traces (baseline: thin line, post-LTP: thick line). **B.** GRL treatment has no effect of LTP induced with 4xTBS protocol in 6 to 7-month Tg mice (CTRL: 143.22 ± 4.75% at 1 hour post-LTP, n = 10 slices, 3 mice; GRL: 141.28 ± 8.25% at 1 hour post-LTP, n = 10 slices, 4 mice; t test, p = 0.841). Top, Representative FP traces (baseline: thin line, post-LTP: thick line). **C.** Summation of synaptic responses during LTP induction are normal in WT mice treated with GRL. **D.** There is a difference in LTP magnitude in WT and Tg mice treated with vehicle control (values above, Bonferroni, *p < 0.05, black line).

the LTP deficit that is present in Tg mice at this age (Fig 2.6 G). This suggests that the vehicle does not alter LTP in either genotype. GRL-8234 had no effect on LTD in either WT or Tg mice (Fig 5.6). However, there was a vehicle effect seen in Tg mice, as LTD was reduced compared to what was previously seen in non-treated Tg mice (Fig 2.6 E).

Subsection 4: Soluble $A\beta_{40}$ and $A\beta_{42}$ levels in adult APPswe;PS1deltaE9 Tg mice treated with BTA-EG$_4$ or GRL-8234.

Finally, we measured soluble $A\beta_{40}$ and $A\beta_{42}$ levels in adult Tg mice treated with either BTA-EG$_4$ or GRL-8234. Our results are consistent with what has previously been observed in

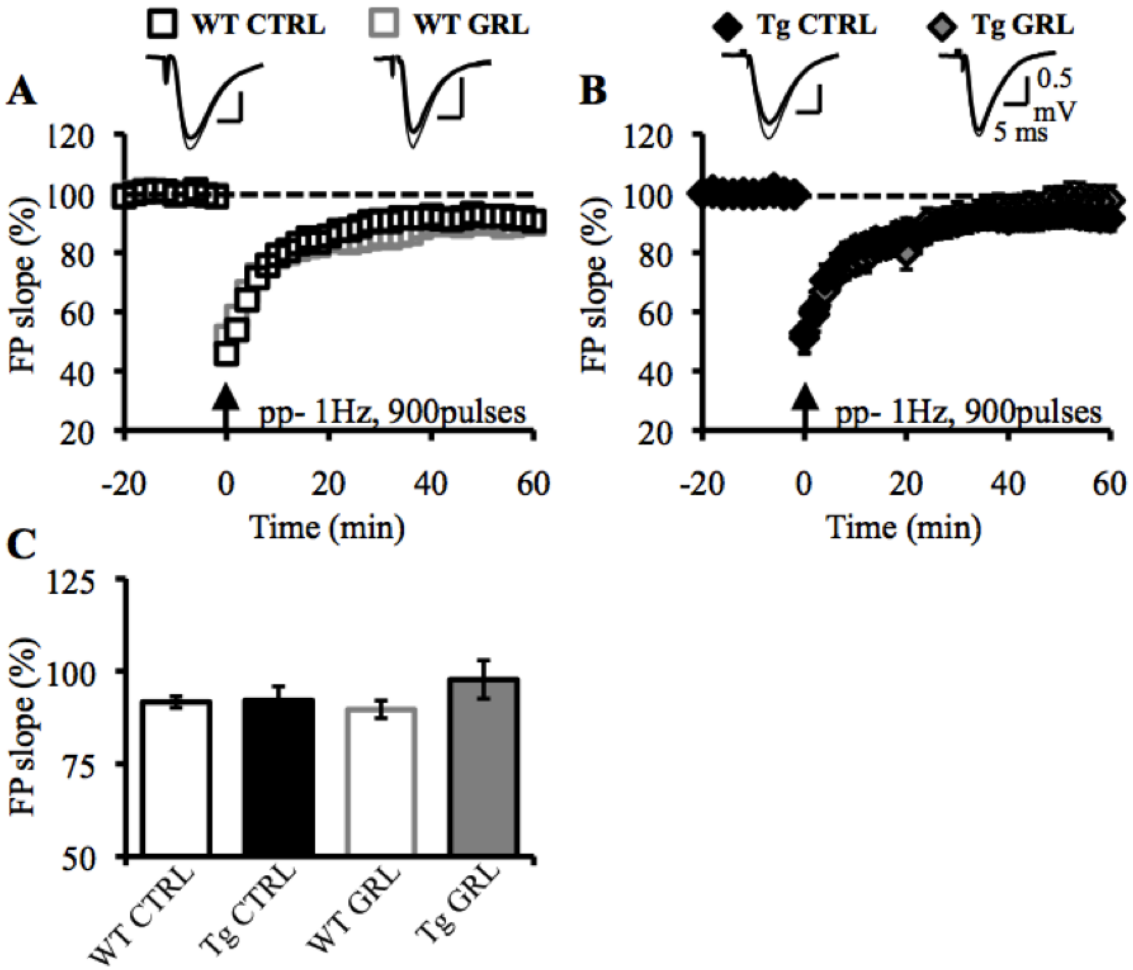

Figure 5.6. LTD in adult WT and APPswe;PS1deltaE9 Tg mice treated with GRL-8234.

A. GRL treatment has no effect on LTD induced with pp-1Hz, 900 pulses protocol in adult WT mice (CTRL: 91.67 ± 1.53% at 1 hour post-LTD, n = 7 slices, 5 mice; GRL: 89.67 ± 2.40% at 1 hour post-LTD, n = 10 slices, 5 mice; t test, p = 0.491). Top, Representative FP traces (baseline: thin line, post-LTD: thick line). **B.** GRL treatment has no effect of LTD induced with pp-1Hz, 900 pulses protocol in adult Tg mice (CTRL: 92.12 ± 3.78% at 1 hour post-LTD, n = 9 slices, 4 mice; GRL: 97.74 ± 5.18% at 1 hour post-LTD, n = 9 slices, 4 mice; t test, p = 0.395) Top, Representative FP traces (baseline: thin line, post-LTD: thick line). **C.** Vehicle treatment reduced LTD magnitude in adult Tg mice compared to non-treated Tg mice (Chapter 2).

studies using Tg mice (Chang et al., 2011; Song et al., 2014). While Aβ levels decreased following both treatments, neither reached statistical significance (Fig 5.7 A-B & D-E). Because

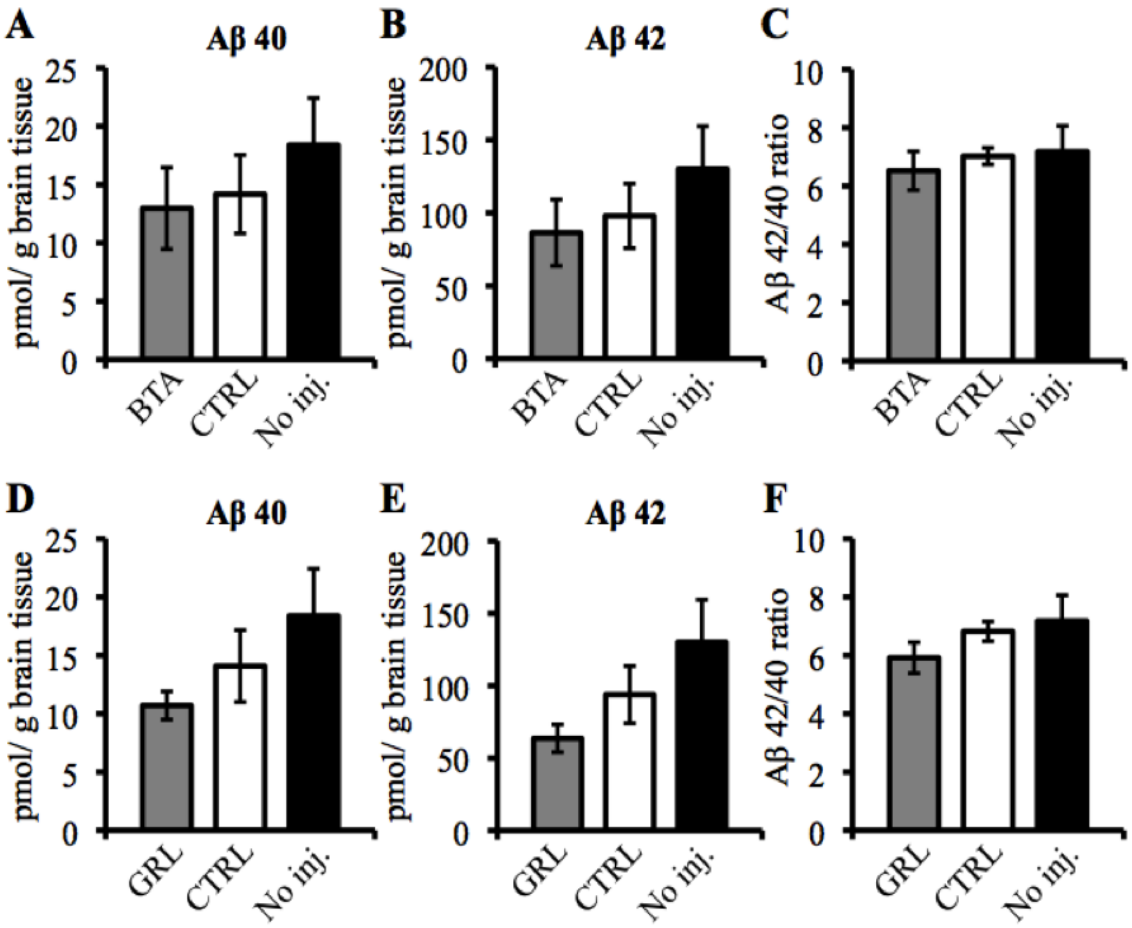

Figure 5.7 Soluble $A\beta_{40}$ and $A\beta_{42}$ levels in adult APPswe;PS1deltaE9 Tg mice treated with BTA-EG_4 or GRL-8234.

(A-C) Aβ ELISAs were conducted to compare Aβ levels in adult Tg mice treated with BTA-EG_4 (BTA), vehicle (CTRL), or non-injected control (No inj.). **A.** BTA does not significantly affect $A\beta_{40}$ levels (BTA: 12.96 ± 3.49, n = 6 mice; CTRL: 14.18 ± 3.36, n = 8 mice; No inj.: 18.38 ± 4.02, n = 6 mice; ANOVA, p = 0.578). **B.** BTA does not significantly affect $A\beta_{42}$ levels (BTA: 86.37 ± 22.76, n = 6 mice; CTRL: 97.91 ± 22.13, n = 8 mice; No inj.: 130.10 ± 29.31, n = 6 mice; ANOVA, p = 0.477). **C.** BTA does not significantly affect the $A\beta_{42}$/ $A\beta_{40}$ ratio (BTA: 6.52 ± 0.66, n = 6 mice; CTRL: 7.02 ± 0.28, n = 8 mice; No inj.: 7.17 ± 0.88, n = 6 mice; ANOVA, p = 0.750). **(D-F)** Aβ ELISAs were conducted to compare Aβ levels in adult Tg mice treated with GRL-8234 (GRL), vehicle (CTRL), or non-injected control (No inj.). **D.** GRL does not significantly affect $A\beta_{40}$ levels (GRL: 10.70 ± 1.20, n = 7 mice; CTRL: 14.07 ± 3.07, n = 5 mice; No inj.: same as in A; ANOVA, p = 0.177). **E.** GRL does not significantly affect $A\beta_{42}$ levels (GRL: 63.66 ± 9.55, n = 7 mice; CTRL: 93.87 ± 19.74, n = 5 mice; No inj.: same as in B; ANOVA, p = 0.088). **F.** GRL does not significantly affect $A\beta_{42}$/ $A\beta_{40}$ ratio (GRL: 5.91 ± 0.53, n = 8 mice; CTRL: 6.82 ± 0.33, n = 5 mice; No inj.: same as in C; ANOVA, p = 0.341).

this Tg AD model exhibits an increased $A\beta_{42}/A\beta_{40}$ ratio due to the FAD-linked PS1 mutation (Jankowsky et al., 2004), a more effective readout of drug efficacy requires measuring this ratio. However, the Aβ ratio was similar between Tg mice of all experimental groups (Fig 5.7 C&F). Unexpectedly, we saw that the vehicle alone affected Aβ levels (Fig 5.7). While this effect did not reach significance, it suggests that the different vehicles used in this study may be inhibiting detection of Aβ proteins by making them inaccessible to the Aβ antibodies or by actually decreasing soluble Aβ.

Section 4: Discussion

In this study we compared BTA-EG_4 treatment to a more conventional BACE1 inhibitory therapy with GRL-8234. To test the effects of these treatments on synaptic function and plasticity in CA1, we used hippocampal slices from adult WT and APPswe;PS1deltaE9 amyloidogenic Tg mice, whose deficits have previously been characterized (See Chapter 2). Unforeseen vehicle effects largely complicated the interpretation of our results. Overall, it appears that neither BTA-EG_4 nor GRL-8234 is able to rescue the metaplasticity deficits seen in adult Tg mice.

Subsection 1: Vehicle treatment effects LTP magnitude in WT and APPswe;PS1deltaE9 Tg mice

Our study emphasizes the importance of proper controls and complete understanding of the properties of vehicle solvents used. WT mice treated with vehicle control (10% DMSO; i.p.) for BTA-EG_4 showed significantly reduced LTP compared to non-treated WT mice (Fig 5.3 & Fig 2.6; $p < 0.05$), while Tg mice treated with vehicle control (10% DMSO; i.p.) showed significantly enhanced LTP compared to non-treated Tg mice (Fig 5.3 & Fig 2.6; $p < 0.05$). DMSO is a commonly used solvent in experimental drug biology; however, in this study it greatly affected synaptic plasticity, which was genotype specific. There are many studies

documenting the toxicity and side effects of DMSO (Gross et al., 1993; Hanslick et al., 2009; Galvao et al., 2014; Morris et al., 2014; Stevens et al., 2014; Zhou et al., 2014). Two more recent studies question the standard 10% DMSO concentration used in many practices and show toxicity even at concentrations below 10% DMSO (Galvao et al., 2014; Morris et al., 2014). Although the vehicle effects of DMSO seen in this study may not be classified as toxic, our results demonstrate that DMSO alters synaptic plasticity mechanisms at the concentration used in many studies.

The fact that summation of synaptic responses during LTP induction is similar in both WT and Tg mice treated with 10% DMSO vehicle (data not shown), suggests that signaling downstream of LTP induction and NMDARs is altered. Indeed, numerous studies have shown that DMSO has the ability to manipulate various enzymatic activities (Zangar and Novak, 1998; McConnell et al., 1999; Rossi and Dianzani, 2000; Grzyska et al., 2002; Ou et al., 2002; Santucci et al., 2002; Yokochi and Robertson, 2004; Yoon et al., 2006; Alsafadi and Paradisi, 2013). Therefore, it could be suggested that DMSO alters LTP magnitude by affecting signaling associated with LTP. For example, DMSO may alter enzymatic activity associated with Ras signaling or kinase activity, leading to changed AMPAR phosphorylation and kinetics.

One unexpected observation is that the effect of DMSO is not uniform between WT and Tg mice. We observed a specific reduction in LTP magnitude in WT mice and enhancement of LTP in Tg mice with 10% DMSO treatment. Certain plasticity related signals follow a bell shaped curve in relation to LTP magnitude. Therefore, an increase in signal strength would increase LTP magnitude; however, at a certain point, a peak is reached and any further increase in signal strength reduces LTP magnitude. Vehicle treatment in WT mice, with an initial LTP magnitude close to the peak, would show a decrease in LTP magnitude in response to increased signal strength. In Tg mice, with an initial low LTP magnitude, LTP magnitude would increase towards the peak in response to increased signal strength following vehicle treatment. While it

would be hard to pinpoint the exact mechanism being manipulated by DMSO, an increase in this type of signaling cascade, downstream of LTP induction, would explain the differential effect of DMSO on LTP magnitude between the genotypes.

An alternative explanation to the difference in LTP magnitude between treated and non-treated mice could simply be that the changes observed are a result of stress caused by the injection. However, this is unlikely, as we did not see alterations in LTP phenotype in mice injected with GRL-8234 or its vehicle control (50/50 PEG300, D5W) (Fig 5.5). The magnitudes of LTP in adult WT or Tg mice treated with vehicle control for GRL-8234 were similar to non-treated controls (Chapter 2), suggesting that PEG300 itself does not modulate LTP signaling and may be a more appropriate biological solvent.

Subsection 2: Increased susceptibility to environmental stressors decreases LTD magnitude in APPswe;PS1deltaE9 Tg mice

Vehicle effects were most strongly noticed when measuring LTD. The resulting phenotype, an almost complete lack of LTD, is seen across drug treatments in treated Tg mice. Therefore, we cannot rule out the possibility that this is a direct consequence of daily injections, suggesting that LTD magnitudes in Tg mice may be more susceptible to environmental stressors. Several recent studies have documented the effect of stress in AD mouse models (Dong et al., 2008; Escribano et al., 2009; Rothman and Mattson, 2010; Rothman et al., 2012). AD Tg mice show increased plasma corticosterone levels compared to WT mice. In addition, stress increases Aβ levels and tau phosphorylation, and decreases CaMKII phosphorylation and BDNF levels [reviewed in (Rothman and Mattson, 2010)]. This suggests that AD Tg mice are more susceptible to the effects of stress, and that stress may worsen cognitive deficits and accelerate the progression of AD. Indeed, deficits in LTD have been linked to cognitive dysfunction associated with memory retrieval, reversal learning, and behavioral flexibility [reviewed in (Collingridge et

al., 2010)]. A decrease in hippocampal LTD following exposure to stress has been observed and is thought to be dependent on activation of voltage-gated calcium channels (VGCC) (Maggio and Segal, 2007, 2009, 2010). Importantly, during AD, VGCCs provide enhanced Ca^{2+} influx as a result of elevated levels of Aβ peptides, disrupting normal calcium homeostasis (Yagami et al., 2012; Cataldi, 2013). Therefore, the altered LTD levels reported in this study could be due to a differential stress response in WT and Tg mice.

Subsection 3: LTP magnitudes differ between WT strains: stress and the influence of genetic background

Just as AD Tg and WT mice respond differently to stress, there are also differences in stress response seen with genetic background (McCutcheon et al., 2008; Cominski et al., 2012). The AD Tg mice used in this study were generated on a 129/C57BL6 (129/B6) mixed background, while WT mice originally treated with BTA-EG_4 (Chapter 3; Megill et al., 2013) were C57BL6 (B6). When comparing plasma corticosterone levels between these strains, the mixed 129/B6 mice showed elevated levels of stress-induced corticosterone compared to B6 mice (McCutcheon et al., 2008). In addition, mice on a 129S6 genetic background showed elevated basal plasma corticosterone levels as well as elevated stress-induced corticosterone (Cominski et al., 2012). These findings demonstrate that genetic background influences stress response and may explain why LTP magnitudes differ between WT strains treated with vehicle control in this study (Chapter 3 vs. Chapter 5). Age, in addition to genetic background, may also cause a difference in response to the effect of the DMSO vehicle or injection. Therefore, although plasticity may be unaffected by injection stress or 10% DMSO in young B6 WT mice (Chapter 3), adult 129/B6 WT mice may have a greater susceptibility to stress related factors, which could result in a decrease in LTP magnitude (Fig 5.3).

Subsection 4: BTA-EG_4 and GRl-8234 treatment alter LTP/D magnitudes in WT mice

Despite the complications of the vehicle effect, overall we did not observe any improvement of LTP or LTD in Tg mice with either BTA-EG_4 or GRL-8234. To appropriately compare between the two treatments, we selected a time course that previously provided beneficial functional and structural synaptic changes in WT mice treated with BTA-EG_4 (Megill et al., 2013). The lack of benefit in this study may be due to the short duration of treatment and suggests the possibility that a longer duration, or earlier initiation, of treatment may be needed to rescue synaptic deficits. Indeed, previous studies using BTA-EG_4 or GRL-8234 treatment in other AD models have also shown similar limited effects on lowering Aβ peptide levels (Chang et al., 2011; Song et al., 2014). Even so, drug efficacy is not determined by Aβ levels alone. Both BTA-EG_4 and GRL-8234 have been previously shown to effectively rescue cognitive function in the absence of significantly decreased Aβ levels (Chang et al., 2011; Song et al., 2014), which suggests that they may be promoting plasticity independent of reducing Aβ levels. Furthermore, the improved cognitive performance observed in 3xTg mice treated with BTA-EG_4 in the previous study may be through an LTP independent mechanism (Song et al., 2014). Indeed, there is existing evidence that cognitive performance does not always correlate with LTP magnitude. Specifically, BTA-EG_4 treatment in WT mice improved cognitive function in the absence of enhanced LTP, and instead better correlated with an increase in dendritic spine density (Chapter 3; Megill et al., 2013). This provides another line of evidence that cognitive performance may better correlate with dendritic spine density rather than LTP magnitude (Chapters 3 and 4).

Subsection 5: Conclusion

Although this study was initiated to investigate the potential of current therapeutics to rescue metaplasticity deficits in an AD mouse model, it instead provided valuable insights into commonly used vehicle controls and the differential effects of stress based on genetic background and genotype. It also demonstrates that cognitive rescue following therapeutic treatment in AD

mouse models, may occur in the absence of reduced amyloid levels, or changes in frequency-dependent plasticity. Understanding how commonly used drug therapies and solvents affect synaptic function and plasticity in normal and diseased states may give insight into their mechanism of action, and reduce unforeseen off target effects in future clinical trials.

Chapter 6: General discussion and future directions

Alzheimer's disease (AD) is the most common form of dementia. It is a devastating neurological disease, which affects approximately 44% of elderly people 75-84 years of age (Hebert et al., 2013). Current theories implicate the production of Aβ as the key molecular event that ultimately leads to neurodegeneration and clinical pathologies of AD (Hardy and Selkoe, 2002). It is clear that successful AD treatments will need to do more than just lower Aβ production; they will need to rescue cognitive deficits, but more importantly, the underlying synaptic dysfunction. Increasing evidence suggests that the cognitive syndromes found in AD patients are preceded by changes in synaptic efficacy (Walsh and Selkoe, 2004; Shankar and Walsh, 2009). The overall goal of this project was to target metaplasticity changes associated with AD to normalize neuronal function. The results from this project provide a novel mechanistic viewpoint in understanding the synaptic dysfunctions seen in AD, which will allow development of more effective therapeutics by targeting the fundamental cellular mechanisms disrupted by AD progression. This section contains discussion about the significance of the results and future directions.

Section 1: Regulation of metaplasticity

Metaplasticity is a change in the ability of a synapse to produce subsequent synaptic plasticity, based on prior synaptic activity (Bear et al., 1987; Bear, 1995). Therefore, metaplasticity acts to provide stability to the neural circuit by regulating LTP and LTD. In this way, the ability of a neural network to store information is preserved by allowing synapses to maintain synaptic weights within a normal range allowing plasticity to be expressed (Abraham, 2008; Mockett and Hulme, 2008).

Alterations in memory networks have been seen early in AD patients, prior to clinical pathologies, and manifest as increases in activity within these systems (Sperling et al., 2010). In addition, Aβ-induced increases in activity have also been seen in mouse models of AD, suggesting that aberrant excitatory neuronal activity may be an early symptom leading to cognitive decline seen in AD patients (Palop et al., 2007; Palop and Mucke, 2009). Under normal conditions Aβ acts to facilitate presynaptic function (Abramov et al., 2009), which is balanced by its ability to act as a negative regulator of postsynaptic function (Kamenetz et al., 2003). During AD, this balance can be overridden resulting in disruption of an activity dependent regulatory mechanisms (Palop and Mucke, 2010a). Therefore, a decrease in excitatory synaptic transmission at the synapse level occurs in concert with aberrant and epileptic form of activity at the circuit and network levels, respectively (Palop and Mucke, 2010b). This suggests that Aβ induced dysfunction is causing destabilization of neural networks and provides evidence that Aβ or other FAD-linked factors may have a role in regulating not only synaptic activity, but also more complex patterns of activity both within and across neural networks (Palop and Mucke, 2010a). Therefore, understanding how Aβ and the progression of AD effects not only the magnitude of LTP/LTD, but the system's ability to adequately adapt to changes in neural activity to produce metaplasticity is worth pursuing.

Here we investigated the sliding threshold and pull-push models for regulating metaplasticity. It is well known that Hebbian synaptic plasticity, such as LTP or LTD can be responsible for the strengthening and weakening of synaptic connections in many brain regions [reviewed in (Malenka and Bear, 2004)]. Both models suggest that the modification threshold, defined as the cross over point from which the postsynaptic activity causes negative synaptic modification (LTD) to positive synaptic modification (LTP), is not static but can slide in a bidirectional manner based on past neuronal activity. Low level of activity will shift the

modification threshold to the left, favoring LTP induction at the expense of LTD. High levels of activity will shift the modification threshold to the right, promoting LTD at the expense of LTP (Bienenstock et al., 1982; Bear et al., 1987). This indicates that the modification threshold is able to slide right or left with changes in activity patterns. A key difference between sliding threshold model and pull-push model of metaplasticity is that the former is traditionally supported by changes in NMDAR gain that are responsible for changing plasticity induction mechanisms (Philpot et al., 2001b; Bear, 2003a; Yashiro and Philpot, 2008; Gray et al., 2011). However, the pull-push model states that metaplasticity results from regulating LTP/LTD expression mechanisms by effecting signaling that is downstream of NMDAR activation and therefore, downstream of plasticity induction mechanisms (Seol et al., 2007; Huang et al., 2012).

Our data suggests that metaplasticity is altered in both young and adult APPswe;PS1deltaE9 Tg mice, but in opposite directions. In young mice the modification threshold was shifted to the left, favoring LTP at the expense of LTD (Fig 2.6 D), but in adult Tg mice the modification threshold was shifted to the right promoting LTD at the expense of LTP (Fig 2.6 H). The parameters responsible for the sliding threshold model of metaplasticity did not correlate with observed changes in LTP/LTD (Fig 2.8). Rather we did observe changes in GluA1-S845 and GluA1-S831 phosphorylation levels (Fig 2.9) which correlate with the pull-push model of metaplasticity (Seol et al., 2007; Huang et al., 2012). Hence we propose that changes in frequency-dependent plasticity at both ages appear to be mediated by dysregulation of pull-push metaplasticity, leading to altered expression mechanisms of LTP/LTD. Additionally, we observed that developmental regulation of metaplasticity is altered in Tg mice. While WT mice show a developmental increase in frequency-dependent LTP, Tg mice lacked this developmental change (Fig 2.7). The observed changes in regulation of AMPAR can account for some, but not all of the synaptic phenotypes observed in the Tg mice. We have proposed a model to account for the

developmental deficits in Tg mice (Fig 2.10). In WT mice, we observed a developmental increase in LTP magnitude (Fig 2.7 C), which we surmise is due to enhanced synaptic recruitment and stabilization of AMPARs (Fig 2.10 A). In young Tg mice, the increase in GluA1-S831 phosphorylation can account for many of the synaptic phenotypes that we observed. GluA1-S831 phosphorylation is known to selectively increase conductance of GluA1 homomers (Oh and Derkach, 2005), which are inward rectifying and Ca^{2+}-permeable (Cull-Candy et al., 2006). Inward rectifying AMPARs can summate responses better, because they do not produce outward current when the membrane is depolarized (Bowie and Mayer, 1995). In young Tg mice we observed enhanced summation of synaptic responses during LTP induction in the absence of functional changes in NMDAR ratio (Fig 2.8). However, we did observe an increased in GluA1-S831 phosphorylation (Fig 2.9 C). If the increase in S831 phosphorylation was found on GluA1 homomers, this suggests an alternative mechanism to regulate induction mechanisms for LTP/LTD leading to the observed increase in LTP magnitude in young Tg mice. Therefore, a logical next step would be to determine whether expression of GluA1 homomers is increased at the synapses of young Tg mice, using philanthotoxin-433 (PhTx) or Naspm, which are selective antagonists of Ca^{2+}-permeable AMPARs.

GluA2 lacking, Ca^{2+}-permeable AMPARs have been called “plasticity inducers” (Man, 2011). This is because they are transiently incorporated into the synapse following plasticity induction but are later replaced with GluA2 containing AMPARs (Plant et al., 2006). In addition, GluA1-S831 phosphorylation has been positively correlated with LTP (Lee et al., 2000a) and together with GluA1-S845 phosphorylation, responsible for decreasing the threshold for producing LTP (Makino et al., 2011; Hu et al., 2007), as observed in young Tg mice. Thus in young Tg mice, the rate at which AMPAR are inserted into the membrane may be increased compared to young WT mice, possibly due to the increase in GluA1-S831 phosphorylation,

resulting in presumable larger calcium influx, enhanced summation (Fig 2.8 A), and larger LTP (Fig 2.6 C).

In adult Tg mice, there is no developmental increase in LTP magnitude even though the levels of AMPAR phosphorylation and the perisynaptic AMPAR pool size are similar to those of adult WT mice (Fig 2.9). This suggests that the developmental deficit is not at the level of synaptic recruitment of AMPARs or the availability of perisynaptic AMPARs, but is likely due to inability to anchor and stabilize the receptors at the PSD following LTP. Previous studies have shown that Aβ peptides have the ability to decrease S845 and S831 phosphorylation sites on GluA1 (Zhao et al., 2004; Miñano-Molina et al., 2011). In normal conditions, these phosphorylation sites correlate with plasticity but their exact role in synaptic plasticity and AMPA trafficking remain unknown especially since mice lacking either the S845 or S831 site still express normal LTP (Lee et al., 2000a, 2003, 2010a). Another important GluA1-phosphorylation site is the PKC phosphorylation site S818 (Boehm et al., 2006). Phosphorylation at this site mediates GluA1 insertion during LTP and helps to stabilize AMPAR at the surface by enhancing the binding of GluA1 to a neuronal actin binding protein 4.1N (Boehm et al., 2006; Lin et al., 2009). In addition, preventing phosphorylation of this site diminishes LTP (Boehm et al., 2006). Therefore, it may be of interest to compare GluA1-S818 phosphorylation in WT and Tg mice, given its role of stabilizing AMPAR to the surface.

We propose that the main synaptic dysfunction of Tg mice is an inability to developmentally regulate LTP/D expression mechanisms due to an initial "off-set" in LTP/LTD induction threshold. In other words, the Tg mice are "stuck" at a defective level for producing LTP/LTD, and are unable to change as the synapses mature. If this is the case, it may also be relevant to compare how AMPAR phosphorylation changes throughout development between WT and Tg mice. Perhaps the reason that AMPAR phosphorylation levels are the same in adult

WT and Tg mice is that WT mice have undergone a developmental increase that correlates with LTP, while Tg levels remain unchanged throughout development.

Section 2: Targeting APP modulation and dendritic spine density in WT mice

This work also investigates two potential AD therapies in WT mice. To gain a more complete understanding of novel therapeutics it is important to investigate their effect on normal synaptic function and plasticity, as well as during diseased states. Even though BTA-EG_4 and F-spondin are very different molecules, they exhibit a similar mechanistic approach in conferring therapeutic benefits. Both BTA-EG_4 and F-spondin increase dendritic spine density through an APP dependent increase in Ras signaling that did not correlate with enhanced LTP (Chapters 3 & 4). Dendritic spine density and Ras signaling are both disrupted during neurodegenerative disease (Knobloch and Mansuy, 2008; Stornetta and Zhu, 2011), therefore finding strategies that overcome these deficits are potential useful for the treatment of AD.

Many leading strategies that seek to alter the long-term progression of AD are limited due to wide spread toxicity. These include therapies that target APP processing enzymes, like β- and γ-secretase (Vetrivel et al., 2006; Wolfe, 2008; Loane et al., 2009; Svedružić et al., 2013; D'Onofrio et al., 2012). An alternative approach to alter Aβ peptide production, rather than inhibiting the activity of these enzymes, may be the modulation of APP expression. Recently, the potential of modulating the steady-state levels of APP was examined in APPswe;PS1deltaE9 Tg mice treated with 2-PMAP (Asuni et al., 2014). This group found that steady-state APP levels were decreased in Tg mice, with a concomitant decrease in Aβ levels following 2-PMAP treatment. They found that 2-PMAP was decreasing the translation of APP to mediate these effects. However, the effects of this drug were not tested in WT mice. Since full-length APP has been shown to increase synaptic function and dendritic spine density [reviewed in (Hoe et al.,

2012)], the use of this drug in WT mice may negatively impact synaptic function. This example emphasizes the need to study the effects of novel therapeutics on normal neuronal function in order to ameliorate unwanted toxicity.

Even though BTA-EG_4 was developed in the hopes of preventing Aβ interactions and aggregation, it is able to modulate APP processing by increasing the cell surface expression of APP (Fig 3.1). APP present on the cell surface is preferentially cleaved by α-secretase, resulting in decreased Aβ production. F-spondin has also been shown to interact with APP and affect its processing (Ho and Südhof, 2004). Furthermore, our collaborators found that F-spondin levels may be regulated by APP (Chapter 4, Megill et al., in preparation). Previous studies have shown that F-spondin interacts with APP signaling by increasing APP on the cell's surface, preventing APP cleavage, and reducing Aβ production (Ho and Südhof, 2004; Hoe et al., 2005; Hafez et al., 2012) [but see (Rice et al., 2013)]. Regulation of APP signaling by F-spondin is quite similar to that of another extracellular matrix protein, Reelin (Hoe et al., 2009). However, regulation of Reelin expression by APP is opposite to that of F-spondin. Our collaborators found that F-spondin levels are increased in APP Tg mice, but Reelin levels are inversely related to APP expression such that Reelin is increased in APP KO mice and decreased in APP Tg mice (Tg2675) (Hoe et al., 2009). This suggests that unlike Reelin, F-spondin may act to amplify APP signaling. While we cannot rule out the possibility that the increase in F-spondin levels in APP Tg mice may reflect an increased retention of F-spondin via its direct binding to APP, (Ho and Südhof, 2004) rather than an increase in its synthesis, it nonetheless suggests that it would enhance APP signaling. This idea is consistent with the observation that the phenotypes seen with F-spondin treatment are quite reminiscent of those mediated by full-length APP. For instance, full-length APP has been shown to increase dendritic spine density [reviewed in (Hoe et al., 2012)], similar to what was observed with F-spondin treatment. Our collaborators observation

that F-spondin mediated effects require APP, further supports the idea that F-spondin acts via APP signaling (Chapter 4, Megill et al., in preparation).

The reduction in LTP magnitude following certain LTP induction protocol in BTA-EG_4 treatment (Fig 3.3), and F-spondin overexpression (Fig 4.2) in WT mice, suggest a homeostatic adjustment to the increase in dendritic spine density. In response to a higher synaptic density an increase in LTP induction threshold may prevent overexcitation of neuronal activity. Indeed, BTA-EG_4 treatment in WT mice provides additional evidence for pull-push regulation of metaplasticity. As previously stated, a key feature of the pull-push model is the size of the perisynaptic AMPAR population and the regulation of AMPAR phosphorylation. Our data would suggest that the perisynaptic pool of AMPARs is decreased in BTA-EG_4 treated WT mice compared to controls, and could explain the decrease in LTP magnitude. Since we saw no difference in cell surface expression of major AMPA- and NMDAR following BTA-EG_4 treatment (Fig 3.6), it suggests that the increase in functional synapses is likely due to lateral recruitment of existing cell surface glutamate receptors, thereby potentially decreasing the overall size of the perisynaptic pool of AMPARs in BTA-EG_4 treated WT mice.

Therefore, this work not only describes the structural and functional benefits of two potential therapeutics, but also an alternative way to provide cognitive benefits, which is to increase the number of functional synapses, providing a larger capacity to store information, in the absence of enhanced LTP. This suggests that targeting the number of functional synapses alone may be sufficient to improve cognitive function and provides an example of how potential therapeutics may alter the regulation of metaplasticity.

Subsection 1: Future directions

Given the therapeutic potential of BTA-EG_4 and F-spondin, their effect on synaptic function and plasticity warrant further study in animal models of AD. This section will focus on

the potential of F-spondin (BTA-EG_4 will be discussed in a later section). However, before F-spondin is further pursued in AD models, further study in WT mice may be useful to add cohesion to the current literature. In this study, the effects of altering F-spondin expression were studied in CA1 of the hippocampus (Chapter 4). We found that F-spondin levels do not largely effect basal synaptic transmission in adult CA1 (Fig 4.1). We also found that endogenous levels of F-spondin were optimal and necessary for producing normal CA1 LTP (Fig 4.1 & 4.2). However, since our collaborators found that F-spondin is highly expressed in the DG of adult APP Tg mice (Chapter 4, Megill et al., in preparation), asking whether F-spondin is necessary for normal LTP in this region would be useful in understanding any alteration that may occur during AD. Here the effects of altering F-spondin expression, as a way to rescue synaptic deficits, may be more prominent and provide greater beneficial results. It is of interest to note that in a previous study, overexpressing F-spondin in the DG, using the same viral construct (Hafez et al., 2012), improved spatial learning and memory in WT mice but was not sufficient to improve memory in AD Tg mice. While Tg mice did show a decrease in Aβ plaque number and increase in synaptophysin staining, the effect of F-spondin overexpression on synaptic function was not studied. Since we know that F-spondin is increased in the DG of APP Tg mice, perhaps this response is a way to compensate for loss of Reelin expression, or in response to other FAD-linked factors. For researchers to have a greater comprehension for why F-spondin was unable to rescue spatial memory deficits in Tg mice, we first need to understand the role F-spondin has in normal synaptic function and plasticity within the DG. Before the beneficial effect of F-spondin are further investigated in AD Tg mice, future studies could include how F-spondin overexpression (and knockdown) in CA1 effects spatial learning and memory, and how its overexpression or knockdown would effect synaptic transmission in the DG of WT mice.

Section 3: The future of AD therapeutics

In order for the potential AD therapies investigated in the study to be beneficial, the current literature and results from this work would suggest that the duration of treatment may need to be longer, and/or the initiation of treatment may need to be earlier. It is worth mentioning that current therapies tested in this work (Chapter 5) and in their previous counterparts (Chang et al., 2011; Song et al., 2014) were unsuccessful at significantly decreasing soluble Aβ levels. This demonstrates that drug efficacy is not solely determined by its ability to lower Aβ, nor should a drug be considered successful by this measurement alone. During the course of this work, our collaborators investigated how BTA-EG_4 treatment affects neuronal function in 3xTg mice (Song et al., 2014). Collectively, our data suggests that BTA-EG_4 treatment may be beneficial during early stages of AD. Our collaborators found an increase in dendritic spine density and improved cognitive performance in 6-10 month, but not 13-16 month old Tg mice, that occurred in the absence of enhanced LTP. This provides evidence that targeting dendritic spine density alone may be sufficient to improve cognitive function early in an AD mouse model. Unfortunately, conclusions from my work regarding the effects of treatment on synaptic function were largely complicated by off-target vehicle effects (Chapter 5) not previously seen in WT treated mice (Chapter 3). This raises awareness of commonly used vehicle solvent and their potential to impact normal neuronal function. The consequences of vehicle treatment may in part be dictated by the current behavioral state of the animal. Therefore, it is possible that these off-target vehicle effects were undetected in previous behavioral and structural measurements. Hence, more refined behavioral analysis may be needed to strengthen the validity of emerging therapeutics.

Since BTA-EG_4 and GRL-8234 were unable to rescue synaptic deficits and displayed either off-target vehicle effects or negative effects on plasticity (Chapter 5), treatments targeting regulation of push-pull metaplasticity warrant future investigation. Although it is not exactly clear

how altered expression mechanism of LTP/LTD would manifest in an inability to generate slots for AMPAR stabilization in the PSD following plasticity induction, treatments that target the initial dysfunction in set point may be beneficial by resetting the "stuck" modification threshold. These treatments may be found by focusing on some of the normal functions of APP, Aβ, and PS1 that are disrupted during AD (Fig 1.2 & 1.4).

Resetting the modification threshold has been proposed as a therapeutic approach to correct amblyopia in adults, and demonstrated to recover function following long-term monocular deprivation in the rodent visual cortex (Cho and Bear, 2010; Montey and Quinlan, 2011). By reducing the NR2A/NR2B ratio the modification threshold is lowered, promoting LTP, thereby promoting synaptic changes that support recovery of function. This demonstrates that sliding the modification threshold through a behavioral manipulation can enhance synaptic activity produced in response to subsequent sensory experiences (Cho and Bear, 2010). In our study, the threshold in adult Tg mice is increased, promoting LTD at the expense of LTP. If the threshold was lowered, by reducing the NR2A/NR2B ratio, this could promote recovery of synaptic function. Even though we did not measure a change in NR2A/NR2B ratio expression in adult Tg mice, it would be interesting to know if changing the subunit composition through genetic or pharmacological means would be an effective way to reset the threshold. Lowering the threshold could be achieved through decreasing the amount of NR2A, or increasing signaling through NR2B. Other questions might be, when would this manipulation be initiated and for how long should it be continued? Since these are questions asked of current therapeutics, this would be an alternative approach to inhibiting APP processing enzymes by targeting the metaplasticity threshold in the hopes of correcting synaptic dysfunction that occurs during AD.

An alternative approach to resetting the threshold may be in the regulation of neuromodulatory systems. The pull-push model provides an example of how important

neuromodulators are in regulating plasticity expression mechanisms. Recent papers have demonstrated that neuromodulatory systems become disrupted in AD Tg mouse models (Coutellier et al., 2014; Nakauchi and Sumikawa, 2014; Wu et al., 2014). These papers focus specifically on the cholinergic and adrenergic neuromodulatory systems. Cholinergic signals modulate neural excitability of neurons within the hippocampus and have been implicated in many physiological function including synaptic plasticity and memory (Yakel, 2013; Molas and Dierssen, 2014). Loss of basal forebrain cholinergic innervation during AD and other neurodegenerative diseases correlates with cognitive decline (Schliebs and Arendt, 2011). Loss of cholinergic innervation, seen as a destruction in cholinergic axons, was seen in APPswe;PS1deltaE9 Tg mice, starting as early as 3 months (Wu et al., 2014). Another recent study discovered a role for nAChRs in the regulation of LTD induction, such that endogenous acetylcholine activating α7-nAChRs during LTD stimulation suppresses LTD induction at the Schaffer collaterals to CA1 synapse (Nakauchi and Sumikawa, 2014). Therefore, loss of this input during AD, or in AD mouse models, would result in loss of suppression, producing more LTD, as seen in adult Tg mice.

The role of β_1- adrenergic receptors in social recognition and memory was also recently characterized in a AD mouse model (Coutellier et al., 2014). This study found that memory deficits were improved when PKA and p-CREB levels were restored to normal levels by pharmacological activation of β_1- adrenergic receptors. While synaptic plasticity was not measured, perhaps activating PKA signaling was able to enhance plasticity expression mechanism by changing AMPAR regulation and phosphorylation states according to the pull-push model. Indeed, isoproterenol, a non-selective β-adrenergic receptor agonist, has been shown to activate receptors coupled to AC/PKA signaling cascades and promote LTP in this way (Huang

et al., 2012). It would be interesting to know whether restoring the metaplasticity threshold lead to the cognitive benefits seen in this study.

These studies provide evidence that loss of neuromodulatory inputs during the progression of AD may lead to deficits in metaplasticity regulation. Therefore, restoring these signals in Tg mice could be beneficial in reinstating the modulation of the LTP/LTD threshold. Indeed, enhancing cholinergic signaling has been studied as a potential therapeutic to rescue cognitive decline, and cholinesterase inhibitors have had some success in mild to moderate AD (O'Brien and Burns, 2011). However, methods to restore neuromodulatory systems may be complicated due to loss of innervation or death of, in this example, cholinergic neurons. In this way, postsynaptic neuron may lose their ability to respond to exogenous neuromodulatory signals. This could provide a potential explanation for why cholinesterase inhibitors work only in early but not late stages of AD.

Finally, understanding how deficits in synaptic activity lead to altered circuit and network activity may be important in determining which aspects of neuronal dysfunction most directly relate to cognitive decline (Palop and Mucke, 2010a). Understanding how metaplasticity becomes altered may provide insights into understanding the relationship between synaptic and network dysfunction seen during AD.

Section 4: General conclusions

It is believed that AD is initiated by synaptic dysfunction, which precedes cognitive deficits and neurodegeneration seen in AD patients. Therefore, it is imperative to know the exact nature of synaptic dysfunction in AD. In many studies that use AD Tg mouse models, it is unclear whether synaptic deficits are at the level of induction or expression of synaptic plasticity mechanisms. Here, I present data that suggest synaptic deficits are at the level of expression

mechanisms due to defects in pull-push regulation of metaplasticity. Our data uncovered a previously undescribed developmental defect in the regulation of metaplasticity causing the AD Tg mice to become "stuck" at different set points for inducing plasticity. Therefore these animals have lost the ability to adjust their synapses to prior synaptic activity and their synaptic weights have been "stuck" within the dynamic range for inducing LTP/LTD. An inability to regulate metaplasticity would limit the responsiveness of synapses to further subsequent modification causing the observed deficits in LTP/LTD magnitude. Our data suggests that it may not only be the change in LTP/LTD magnitude that is driving cognitive deficits, but the inability of the system to adequately adapt to changes in neural activity to produce metaplasticity. If metaplasticity deficits are universal across different models of AD, it may provide an explanation for the similar cognitive deficits in these models despite having varied LTP/LTD phenotypes mediated by different FAD-linked factors. In summary, treatments targeting regulation of pull-push metaplasticity warrant future investigation since currently tested therapies proved unsuccessful at rescuing the observed synaptic deficits in this model of AD.

Bibliography

Abbott LF, Nelson SB (2000) Synaptic plasticity: taming the beast. Nat Neurosci 3 Suppl:1178–1183.

Abraham WC (2008) Metaplasticity: tuning synapses and networks for plasticity. Nat Rev Neurosci 9:387.

Abraham WC, Bear MF (1996) Metaplasticity: the plasticity of synaptic plasticity. Trends Neurosci 19:126–130.

Abramov E, Dolev I, Fogel H, Ciccotosto GD, Ruff E, Slutsky I (2009) Amyloid-beta as a positive endogenous regulator of release probability at hippocampal synapses. Nat Neurosci 12:1567–1576.

Aizenman CD, Akerman CJ, Jensen KR, Cline HT (2003) Visually driven regulation of intrinsic neuronal excitability improves stimulus detection in vivo. Neuron 39:831–842.

Almeida CG, Tampellini D, Takahashi RH, Greengard P, Lin MT, Snyder EM, Gouras GK (2005) Beta-amyloid accumulation in APP mutant neurons reduces PSD-95 and GluR1 in synapses. Neurobiol Dis 20:187–198.

Alsafadi D, Paradisi F (2013) Effect of organic solvents on the activity and stability of halophilic alcohol dehydrogenase (ADH2) from Haloferax volcanii. Extremophiles 17:115–122.

Aoki C, Lee J, Nedelescu H, Ahmed T, Ho A, Shen J (2009) Increased levels of NMDA receptor NR2A subunits at pre- and postsynaptic sites of the hippocampal CA1: an early response to conditional double knockout of presenilin 1 and 2. J Comp Neurol 517:512–523.

Asuni AA, Guridi M, Pankiewicz JE, Sanchez S, Sadowski MJ (2014) Modulation of amyloid precursor protein expression reduces β-amyloid deposition in a mouse model. Ann Neurol 75:684–699.

Bailey CH, Bartsch D, Kandel ER (1996) Toward a molecular definition of long-term memory storage. Proc Natl Acad Sci U S A 93:13445–13452.

Balducci C, Mehdawy B, Mare L, Giuliani A, Lorenzini L, Sivilia S, Giardino L, Calza L, Lanzillotta A, Sarnico I, Pizzi M, Usiello A, Viscomi AR, Ottonello S, Villetti G, Imbimbo BP, Nistico G, Forloni G, Nistico R (2011) The gamma-Secretase Modulator CHF5074 Restores Memory and Hippocampal Synaptic Plasticity in Plaque-Free Tg2576 Mice. J Alzheimers Dis 24:799–816.

Barco A, Bailey CH, Kandel ER (2006) Common molecular mechanisms in explicit and implicit memory. J Neurochem 97:1520–1533.

Barria A, Derkach V, Soderling T (1997a) Identification of the Ca2+/calmodulin-dependent protein kinase II regulatory phosphorylation site in the alpha-amino-3-hydroxyl-5-methyl-4-isoxazole-propionate-type glutamate receptor. J Biol Chem 272:32727–32730.

Barria A, Muller D, Derkach V, Griffith LC, Soderling TR (1997b) Regulatory phosphorylation of AMPA-type glutamate receptors by CaM-KII during long-term potentiation. Science 276:2042–2045.

Basi GS et al. (2010) Amyloid precursor protein selective gamma-secretase inhibitors for treatment of Alzheimer's disease. Alzheimers Res Ther\ 2:36.

Bear MF (1995) Mechanism for a sliding synaptic modification threshold. Neuron 15:1–4.

Bear MF (1996) A synaptic basis for memory storage in the cerebral cortex. Proc Natl Acad Sci U S A 93:13453–13459.

Bear MF (2003) Bidirectional synaptic plasticity: from theory to reality. Philos Trans R Soc Lond B Biol Sci 358:649–655.

Bear MF, Cooper LN, Ebner FF (1987) A physiological basis for a theory of synapse modification. Science (80-) 237:42–48.

Berchtold NC, Sabbagh MN, Beach TG, Kim RC, Cribbs DH, Cotman CW (2014) Brain gene expression patterns differentiate mild cognitive impairment from normal aged and Alzheimer's disease. Neurobiol Aging 35:1961–1972.

Bero AW, Yan P, Roh JH, Cirrito JR, Stewart FR, Raichle ME, Lee J-M, Holtzman DM (2011) Neuronal activity regulates the regional vulnerability to amyloid-β deposition. Nat Neurosci 14:750–756.

Berridge MJ (1998) Neuronal calcium signaling. Neuron 21:13–26.

Bezprozvanny I, Mattson MP (2008) Neuronal calcium mishandling and the pathogenesis of Alzheimer's disease. Trends Neurosci 31:454–463.

Bienenstock EL, Cooper LN, Munro PW (1982) Theory for the development of neuron selectivity: orientation specificity and binocular interaction in visual cortex. J Neurosci 2:32–48.

Bliss TVP, Collingridge GL, Morris RGM (2003) Introduction. Long-term potentiation and structure of the issue. Philos Trans R Soc Lond B Biol Sci 358:607–611.

Bliss T V, Lomo T (1973) Long-lasting potentiation of synaptic transmission in the dentate area of the anaesthetized rabbit following stimulation of the perforant path. J Physiol 232:331–356.

Boehm J, Kang M-G, Johnson RC, Esteban J, Huganir RL, Malinow R (2006) Synaptic incorporation of AMPA receptors during LTP is controlled by a PKC phosphorylation site on GluR1. Neuron 51:213–225.

Borchelt DR et al. (1996) Familial Alzheimer's disease-linked presenilin 1 variants elevate Abeta1-42/1-40 ratio in vitro and in vivo. Neuron 17:1005–1013.

Bowie D, Mayer ML (1995) Inward rectification of both AMPA and kainate subtype glutamate receptors generated by polyamine-mediated ion channel block. Neuron 15:453–462.

Burrone J, O'Byrne M, Murthy VN (2002) Multiple forms of synaptic plasticity triggered by selective suppression of activity in individual neurons. Nature 420:414–418.

Burstyn-Cohen T, Tzarfaty V, Frumkin A, Feinstein Y, Stoeckli E, Klar A (1999) F-Spondin is required for accurate pathfinding of commissural axons at the floor plate. Neuron 23:233–246.

Busche MA, Chen X, Henning H a, Reichwald J, Staufenbiel M, Sakmann B, Konnerth A (2012) Critical role of soluble amyloid-β for early hippocampal hyperactivity in a mouse model of Alzheimer's disease. Proc Natl Acad Sci U S A 109:8740–8745.

Busche MA, Eichhoff G, Adelsberger H, Abramowski D, Wiederhold K-H, Haass C, Staufenbiel M, Konnerth A, Garaschuk O (2008) Clusters of hyperactive neurons near amyloid plaques in a mouse model of Alzheimer's disease. Science 321:1686–1689.

Buttini M, Masliah E, Barbour R, Grajeda H, Motter R, Johnson-Wood K, Khan K, Seubert P, Freedman S, Schenk D, Games D (2005) Beta-amyloid immunotherapy prevents synaptic degeneration in a mouse model of Alzheimer's disease. J Neurosci 25:9096–9101.

Cai H, Wang Y, McCarthy D, Wen H, Borchelt DR, Price DL, Wong PC (2001) BACE1 is the major beta-secretase for generation of Abeta peptides by neurons. Nat Neurosci 4:233–234.

Cao X, Südhof TC (2001) A transcriptionally [correction of transcriptively] active complex of APP with Fe65 and histone acetyltransferase Tip60. Science 293:115–120.

Capule CC, Yang J (2012) Enzyme-linked immunosorbent assay-based method to quantify the association of small molecules with aggregated amyloid peptides. Anal Chem 84:1786–1791.

Carroll RC, Beattie EC, von Zastrow M, Malenka RC (2001) Role of AMPA receptor endocytosis in synaptic plasticity. Nat Rev Neurosci 2:315–324.

Cataldi M (2013) The changing landscape of voltage-gated calcium channels in neurovascular disorders and in neurodegenerative diseases. Curr Neuropharmacol 11:276–297.

Chakroborty S, Goussakov I, Miller MB, Stutzmann GE (2009) Deviant ryanodine receptor-mediated calcium release resets synaptic homeostasis in presymptomatic 3xTg-AD mice. J Neurosci 29:9458–9470.

Chang W-P, Huang X, Downs D, Cirrito JR, Koelsch G, Holtzman DM, Ghosh AK, Tang J (2011) Beta-secretase inhibitor GRL-8234 rescues age-related cognitive decline in APP transgenic mice. FASEB J 25:775–784.

Chapman PF, White GL, Jones MW, Cooper-Blacketer D, Marshall VJ, Irizarry M, Younkin L, Good M a, Bliss T V, Hyman BT, Younkin SG, Hsiao KK (1999) Impaired synaptic plasticity and learning in aged amyloid precursor protein transgenic mice. Nat Neurosci 2:271–276.

Chen L, Yamada K, Nabeshima T, Sokabe M (2006) alpha7 Nicotinic acetylcholine receptor as a target to rescue deficit in hippocampal LTP induction in beta-amyloid infused rats. Neuropharmacology 50:254–268.

Chen Q-S, Wei W-Z, Shimahara T, Xie C-W (2002) Alzheimer amyloid beta-peptide inhibits the late phase of long-term potentiation through calcineurin-dependent mechanisms in the hippocampal dentate gyrus. Neurobiol Learn Mem 77:354–371.

Chen QS, Kagan BL, Hirakura Y, Xie CW (2000) Impairment of hippocampal long-term potentiation by Alzheimer amyloid beta-peptides. J Neurosci Res 60:65–72.

Chételat G, Villemagne VL, Pike KE, Ellis KA, Ames D, Masters CL, Rowe CC (2012) Relationship between memory performance and β-amyloid deposition at different stages of Alzheimer's disease. Neurodegener Dis 10:141–144.

Cheung K-H, Mei L, Mak D-OD, Hayashi I, Iwatsubo T, Kang DE, Foskett JK (2010) Gain-of-function enhancement of IP3 receptor modal gating by familial Alzheimer's disease-linked presenilin mutants in human cells and mouse neurons. Sci Signal 3:ra22.

Cheung K-H, Shineman D, Müller M, Cárdenas C, Mei L, Yang J, Tomita T, Iwatsubo T, Lee VM-Y, Foskett JK (2008) Mechanism of Ca2+ disruption in Alzheimer's disease by presenilin regulation of InsP3 receptor channel gating. Neuron 58:871–883.

Cho K, Bear M (2010) Promoting neurological recovery of function via metaplasticity. Future Neurol 5:21–26.

Chow VW, Mattson MP, Wong PC, Gleichmann M (2010) An overview of APP processing enzymes and products. Neuromolecular Med 12:1–12.

Cirrito JR, Kang J-E, Lee J, Stewart FR, Verges DK, Silverio LM, Bu G, Mennerick S, Holtzman DM (2008) Endocytosis is required for synaptic activity-dependent release of amyloid-beta in vivo. Neuron 58:42–51.

Cirrito JR, Yamada KA, Finn MB, Sloviter RS, Bales KR, May PC, Schoepp DD, Paul SM, Mennerick S, Holtzman DM (2005) Synaptic activity regulates interstitial fluid amyloid-beta levels in vivo. Neuron 48:913–922.

Citron M (2002) Alzheimer's disease: treatments in discovery and development. Nat Neurosci 5 Suppl:1055–1057.

Citron M (2004a) Strategies for disease modification in Alzheimer's disease. Nat Rev Neurosci 5:677–685.

Citron M (2004b) Beta-secretase inhibition for the treatment of Alzheimer's disease--promise and challenge. Trends Pharmacol Sci 25:92–97.

Citron M (2010) Alzheimer's disease: strategies for disease modification. Nat Rev Drug Discov 9:387–398.

Collingridge GL, Peineau S, Howland JG, Wang YT (2010) Long-term depression in the CNS. Nat Rev Neurosci 11:459–473.

Comery TA, Martone RL, Aschmies S, Atchison KP, Diamantidis G, Gong X, Zhou H, Kreft AF, Pangalos MN, Sonnenberg-Reines J, Jacobsen JS, Marquis KL (2005) Acute gamma-secretase inhibition improves contextual fear conditioning in the Tg2576 mouse model of Alzheimer's disease. J Neurosci 25:8898–8902.

Cominski TP, Turchin CE, Hsu MS, Ansonoff MA, Pintar JE (2012) Loss of the mu opioid receptor on different genetic backgrounds leads to increased bromodeoxyuridine labeling in the dentate gyrus only after repeated injection. Neuroscience 206:49–59.

Connor JA, Petrozzino J, Pozzo-Miller LD, Otani S (1999) Calcium signals in long-term potentiation and long-term depression. Can J Physiol Pharmacol 77:722–734.

Coutellier L, Ardestani PM, Shamloo M (2014) β1-adrenergic receptor activation enhances memory in Alzheimer's disease model. Ann Clin Transl Neurol 1:348–360.

Cramer PE, Cirrito JR, Wesson DW, Lee CY, Karlo JC, Zinn AE, Casali BT, Restivo JL, Goebel WD, James MJ, Brunden KR, Wilson DA, Landreth GE (2012) ApoE-directed therapeutics rapidly clear beta-amyloid and reverse deficits in AD mouse models. Science (80-) 335:1503–1506.

Crouch PJ et al. (2009) Increasing Cu bioavailability inhibits Abeta oligomers and tau phosphorylation. Proc Natl Acad Sci U S A 106:381–386.

Cull-Candy S, Kelly L, Farrant M (2006) Regulation of Ca2+-permeable AMPA receptors: synaptic plasticity and beyond. Curr Opin Neurobiol 16:288–297.

Czirr E, Leuchtenberger S, Dorner-Ciossek C, Schneider A, Jucker M, Koo EH, Pietrzik CU, Baumann K, Weggen S (2007) Insensitivity to Abeta42-lowering nonsteroidal anti-inflammatory drugs and gamma-secretase inhibitors is common among aggressive presenilin-1 mutations. J Biol Chem 282:24504–24513.

D'Onofrio G, Panza F, Frisardi V, Solfrizzi V, Imbimbo BP, Paroni G, Cascavilla L, Seripa D, Pilotto A (2012) Advances in the identification of γ-secretase inhibitors for the treatment of Alzheimer's disease. Expert Opin Drug Discov 7:19–37.

Dash PK, Moore AN, Orsi SA (2005) Blockade of gamma-secretase activity within the hippocampus enhances long-term memory. Biochem Biophys Res Commun 338:777–782.

Davis HP, Squire LR (1984) Protein synthesis and memory: a review. Psychol Bull 96:518–559.

Daw MI, Chittajallu R, Bortolotto ZA, Dev KK, Duprat F, Henley JM, Collingridge GL, Isaac JT (2000) PDZ proteins interacting with C-terminal GluR2/3 are involved in a PKC-dependent regulation of AMPA receptors at hippocampal synapses. Neuron 28:873–886.

De Strooper B (2003) Aph-1, Pen-2, and Nicastrin with Presenilin generate an active gamma-Secretase complex. Neuron 38:9–12.

De Strooper B, Saftig P, Craessaerts K, Vanderstichele H, Guhde G, Annaert W, Von Figura K, Van Leuven F (1998) Deficiency of presenilin-1 inhibits the normal cleavage of amyloid precursor protein. Nature 391:387–390.

Debby-Brafman A, Burstyn-Cohen T, Klar A, Kalcheim C (1999) F-Spondin, expressed in somite regions avoided by neural crest cells, mediates inhibition of distinct somite domains to neural crest migration. Neuron 22:475–488.

Desai NS, Rutherford LC, Turrigiano GG (n.d.) BDNF regulates the intrinsic excitability of cortical neurons. Learn Mem 6:284–291.

Desmond DW, Moroney JT, Sano M, Stern Y (2002) Incidence of dementia after ischemic stroke: results of a longitudinal study. Stroke 33:2254–2260.

Dewachter I, Reverse D, Caluwaerts N, Ris L, Kuiperi C, Van den Haute C, Spittaels K, Umans L, Serneels L, Thiry E, Moechars D, Mercken M, Godaux E, Van Leuven F (2002) Neuronal deficiency of presenilin 1 inhibits amyloid plaque formation and corrects hippocampal long-term potentiation but not a cognitive defect of amyloid\precursor protein [V717I] transgenic mice. J Neurosci 22:3445–3453.

Dewachter I, Ris L, Croes S, Borghgraef P, Devijver H, Voets T, Nilius B, Godaux E, Van Leuven F (2008) Modulation of synaptic plasticity and Tau phosphorylation by wild-type and mutant presenilin1. Neurobiol Aging 29:639–652.

Dickey CA, Loring JF, Montgomery J, Gordon MN, Eastman PS, Morgan D (2003) Selectively reduced expression of synaptic plasticity-related genes in amyloid precursor protein + presenilin-1 transgenic mice. J Neurosci 23:5219–5226.

Dineley KT, Westerman M, Bui D, Bell K, Ashe KH, Sweatt JD (2001) Beta-amyloid activates the mitogen-activated protein kinase cascade via hippocampal alpha7 nicotinic acetylcholine receptors: In vitro and in vivo mechanisms related to Alzheimer's disease. J Neurosci 21:4125–4133.

Ding Y, Qiao A, Wang Z, Goodwin JS, Lee ES, Block ML, Allsbrook M, McDonald MP, Fan GH (2008) Retinoic acid attenuates beta-amyloid deposition and rescues memory deficits in an Alzheimer's disease transgenic mouse model. J Neurosci 28:11622–11634.

Dong H, Yuede CM, Yoo H-S, Martin M V, Deal C, Mace AG, Csernansky JG (2008) Corticosterone and related receptor expression are associated with increased beta-amyloid plaques in isolated Tg2576 mice. Neuroscience 155:154–163.

Donoviel DB, Hadjantonakis AK, Ikeda M, Zheng H, Hyslop PS, Bernstein A (1999) Mice lacking both presenilin genes exhibit early embryonic patterning defects. Genes Dev 13:2801–2810.

Dougherty JJ, Wu J, Nichols RA (2003) Beta-amyloid regulation of presynaptic nicotinic receptors in rat hippocampus and neocortex. J Neurosci 23:6740–6747.

Dovey HF et al. (2001) Functional gamma-secretase inhibitors reduce beta-amyloid peptide levels in brain. J Neurochem 76:173–181.

Dudek SM, Bear MF (1992) Homosynaptic long-term depression in area CA1 of hippocampus and effects of N-methyl-D-aspartate receptor blockade. Proc Natl Acad Sci U S A 89:4363–4367.

Echeverria V, Berman DE, Arancio O (2007) Oligomers of beta-amyloid peptide inhibit BDNF-induced arc expression in cultured cortical Neurons. Curr Alzheimer Res 4:518–521.

Eriksen JL, Sagi SA, Smith TE, Weggen S, Das P, McLendon DC, Ozols V V, Jessing KW, Zavitz KH, Koo EH, Golde TE (2003) NSAIDs and enantiomers of flurbiprofen target gamma-secretase and lower Abeta 42 in vivo. J Clin Invest 112:440–449.

Escribano L, Simón A-M, Pérez-Mediavilla A, Salazar-Colocho P, Del Río J, Frechilla D (2009) Rosiglitazone reverses memory decline and hippocampal glucocorticoid receptor down-regulation in an Alzheimer's disease mouse model. Biochem Biophys Res Commun 379:406–410.

Esteban JA, Shi S-H, Wilson C, Nuriya M, Huganir RL, Malinow R (2003) PKA phosphorylation of AMPA receptor subunits controls synaptic trafficking underlying plasticity. Nat Neurosci 6:136–143.

Finder VH, Glockshuber R (2007) Amyloid-beta aggregation. Neurodegener Dis 4:13–27.

Fitzjohn SM, Morton R a, Kuenzi F, Rosahl TW, Shearman M, Lewis H, Smith D, Reynolds DS, Davies CH, Collingridge GL, Seabrook GR (2001) Age-related impairment of synaptic transmission but normal long-term potentiation in transgenic mice that overexpress the human APP695SWE mutant form of amyloid precursor protein. J Neurosci 21:4691–4698.

Flexner JB, Flexner LB, Stellar E (1963) Memory in mice as affected by intracerebral puromycin. Science 141:57–59.

Frey U, Krug M, Reymann KG, Matthies H (1988) Anisomycin, an inhibitor of protein synthesis, blocks late phases of LTP phenomena in the hippocampal CA1 region in vitro. Brain Res 452:57–65.

Fukumoto H, Takahashi H, Tarui N, Matsui J, Tomita T, Hirode M, Sagayama M, Maeda R, Kawamoto M, Hirai K, Terauchi J, Sakura Y, Kakihana M, Kato K, Iwatsubo T, Miyamoto M (2010) A

noncompetitive BACE1 inhibitor TAK-070 ameliorates Abeta pathology and behavioral deficits in a mouse model of Alzheimer's disease. J Neurosci 30:11157–11166.

Galimberti D, Scarpini E (2011) Alzheimer's disease: from pathogenesis to disease-modifying approaches. CNS Neurol Disord Drug Targets 10:163–174.

Galvao J, Davis B, Tilley M, Normando E, Duchen MR, Cordeiro MF (2014) Unexpected low-dose toxicity of the universal solvent DMSO. FASEB J 28:1317–1330.

Gandy S, Doeven MK, Poolman B (2006) Alzheimer disease: presenilin springs a leak. Nat Med 12:1121–1123.

Garcia-Alloza M, Robbins EM, Zhang-Nunes SX, Purcell SM, Betensky R a, Raju S, Prada C, Greenberg SM, Bacskai BJ, Frosch MP (2006) Characterization of amyloid deposition in the APPswe/PS1dE9 mouse model of Alzheimer disease. Neurobiol Dis 24:516–524.

Garner AR, Rowland DC, Hwang SY, Baumgaertel K, Roth BL, Kentros C, Mayford M (2012) Generation of a synthetic memory trace. Science 335:1513–1516.

Ghosh AK, Gemma S, Tang J (2008a) beta-Secretase as a therapeutic target for Alzheimer's disease. Neurotherapeutics 5:399–408.

Ghosh AK, Kumaragurubaran N, Hong L, Koelsh G, Tang J (2008b) Memapsin 2 (beta-secretase) inhibitors: drug development. Curr Alzheimer Res 5:121–131.

Ghosh AK, Kumaragurubaran N, Hong L, Kulkarni S, Xu X, Miller HB, Reddy DS, Weerasena V, Turner R, Chang W, Koelsch G, Tang J (2008c) Potent memapsin 2 (beta-secretase) inhibitors: design, synthesis, protein-ligand X-ray structure, and in vivo evaluation. Bioorg Med Chem Lett 18:1031–1036.

Gong B, Chen F, Pan Y, Arrieta-Cruz I, Yoshida Y, Haroutunian V, Pasinetti GM (2010) SCFFbx2-E3-ligase-mediated degradation of BACE1 attenuates Alzheimer's disease amyloidosis and improves synaptic function. Aging Cell 9:1018–1031.

Gong Y, Chang L, Viola KL, Lacor PN, Lambert MP, Finch CE, Krafft GA, Klein WL (2003) Alzheimer's disease-affected brain: presence of oligomeric A beta ligands (ADDLs) suggests a molecular basis for reversible memory loss. Proc Natl Acad Sci U S A 100:10417–10422.

Goussakov I, Miller MB, Stutzmann GE (2010) NMDA-mediated Ca(2+) influx drives aberrant ryanodine receptor activation in dendrites of young Alzheimer's disease mice. J Neurosci 30:12128–12137.

Gray EH, De Vos KJ, Dingwall C, Perkinton MS, Miller CCJ (2010) Deficiency of the copper chaperone for superoxide dismutase increases amyloid-β production. J Alzheimers Dis 21:1101–1105.

Gray JA, Shi Y, Usui H, During MJ, Sakimura K, Nicoll RA (2011) Distinct modes of AMPA receptor suppression at developing synapses by GluN2A and GluN2B: single-cell NMDA receptor subunit deletion in vivo. Neuron 71:1085–1101.

Gray R, Rajan AS, Radcliffe KA, Yakehiro M, Dani JA (1996) Hippocampal synaptic transmission enhanced by low concentrations of nicotine. Nature 383:713–716.

Green KN, Demuro A, Akbari Y, Hitt BD, Smith IF, Parker I, LaFerla FM (2008) SERCA pump activity is physiologically regulated by presenilin and regulates amyloid beta production. J Cell Biol 181:1107–1116.

Gross SM, Reddy R V, Reddy CS (1993) Alteration in the tissue retention of [14C]-caffeine in pregnant mice by dimethylsulfoxide. Nat Toxins 1:376–380.

Grzyska PK, Czyryca PG, Golightly J, Small K, Larsen P, Hoff RH, Hengge AC (2002) Generality of solvation effects on the hydrolysis rates of phosphate monoesters and their possible relevance to enzymatic catalysis. J Org Chem 67:1214–1220.

Gu Z, Jiang Q, Fu AKY, Ip NY, Yan Z (2005) Regulation of NMDA receptors by neuregulin signaling in prefrontal cortex. J Neurosci 25:4974–4984.

Gu Z, Liu W, Yan Z (2009) {beta}-Amyloid impairs AMPA receptor trafficking and function by reducing Ca2+/calmodulin-dependent protein kinase II synaptic distribution. J Biol Chem 284:10639–10649.

Guan ZZ, Miao H, Tian JY, Unger C, Nordberg A, Zhang X (2001) Suppressed expression of nicotinic acetylcholine receptors by nanomolar beta-amyloid peptides in PC12 cells. J Neural Transm 108:1417–1433.

Guzowski JF (2002) Insights into immediate-early gene function in hippocampal memory consolidation using antisense oligonucleotide and fluorescent imaging approaches. Hippocampus 12:86–104.

Guzowski JF, Lyford GL, Stevenson GD, Houston FP, McGaugh JL, Worley PF, Barnes CA (2000) Inhibition of activity-dependent arc protein expression in the rat hippocampus impairs the maintenance of long-term potentiation and the consolidation of long-term memory. J Neurosci 20:3993–4001.

Guzowski JF, McGaugh JL (1997) Antisense oligodeoxynucleotide-mediated disruption of hippocampal cAMP response element binding protein levels impairs consolidation of memory for water maze training. Proc Natl Acad Sci U S A 94:2693–2698.

Habib LK, Lee MTC, Yang J (2010) Inhibitors of catalase-amyloid interactions protect cells from beta-amyloid-induced oxidative stress and toxicity. J Biol Chem 285:38933–38943.

Haettig J, Stefanko DP, Multani ML, Figueroa DX, McQuown SC, Wood MA (2011) HDAC inhibition modulates hippocampus-dependent long-term memory for object location in a CBP-dependent manner. Learn Mem 18:71–79.

Hafez DM, Huang JY, Richardson JC, Masliah E, Peterson DA, Marr RA (2012) F-spondin gene transfer improves memory performance and reduces amyloid-β levels in mice. Neuroscience 223:465–472.

Hahn S, Bruning T, Ness J, Czirr E, Baches S, Gijsen H, Korth C, Pietrzik CU, Bulic B, Weggen S (2011) Presenilin-1 but not amyloid precursor protein mutations present in mouse models of Alzheimer's disease attenuate the response of cultured cells to gamma-secretase modulators regardless of their potency and structure. J Neurochem 116:385–395.

Handler M, Yang X, Shen J (2000) Presenilin-1 regulates neuronal differentiation during neurogenesis. Development 127:2593–2606.

Hanslick JL, Lau K, Noguchi KK, Olney JW, Zorumski CF, Mennerick S, Farber NB (2009) Dimethyl sulfoxide (DMSO) produces widespread apoptosis in the developing central nervous system. Neurobiol Dis 34:1–10.

Hardy J, Selkoe DJ (2002) The amyloid hypothesis of Alzheimer's disease: progress and problems on the road to therapeutics. Science 297:353–356.

Harris JA, Devidze N, Halabisky B, Lo I, Thwin MT, Yu G-Q, Bredesen DE, Masliah E, Mucke L (2010) Many neuronal and behavioral impairments in transgenic mouse models of Alzheimer's disease are independent of caspase cleavage of the amyloid precursor protein. J Neurosci 30:372–381.

Harrison SM, Harper AJ, Hawkins J, Duddy G, Grau E, Pugh PL, Winter PH, Shilliam CS, Hughes ZA, Dawson LA, Gonzalez MI, Upton N, Pangalos MN, Dingwall C (2003) BACE1 (beta-secretase) transgenic and knockout mice: identification of neurochemical deficits and behavioral changes. Mol Cell Neurosci 24:646–655.

Hayashi ML, Choi S-Y, Rao BSS, Jung H-Y, Lee H-K, Zhang D, Chattarji S, Kirkwood A, Tonegawa S (2004) Altered cortical synaptic morphology and impaired memory consolidation in forebrain-specific dominant-negative PAK transgenic mice. Neuron 42:773–787.

Hayashi Y, Shi SH, Esteban JA, Piccini A, Poncer JC, Malinow R (2000) Driving AMPA receptors into synapses by LTP and CaMKII: requirement for GluR1 and PDZ domain interaction. Science 287:2262–2267.

Hebb DO (1949) The Organization of Behavior. New York, NY, USA: John Wiley & Sons.

Hebert LE, Weuve J, Scherr PA, Evans DA (2013) Alzheimer disease in the United States (2010-2050) estimated using the 2010 census. Neurology 80:1778–1783.

Hébert SS, Horré K, Nicolaï L, Papadopoulou AS, Mandemakers W, Silahtaroglu AN, Kauppinen S, Delacourte A, De Strooper B (2008) Loss of microRNA cluster miR-29a/b-1 in sporadic Alzheimer's disease correlates with increased BACE1/beta-secretase expression. Proc Natl Acad Sci U S A 105:6415–6420.

Henley JM, Wilkinson KA (2013) AMPA receptor trafficking and the mechanisms underlying synaptic plasticity and cognitive aging. Dialogues Clin Neurosci 15:11–27.

Herms J, Schneider I, Dewachter I, Caluwaerts N, Kretzschmar H, Van Leuven F (2003) Capacitive calcium entry is directly attenuated by mutant presenilin-1, independent of the expression of the amyloid precursor protein. J Biol Chem 278:2484–2489.

Herreman A, Hartmann D, Annaert W, Saftig P, Craessaerts K, Serneels L, Umans L, Schrijvers V, Checler F, Vanderstichele H, Baekelandt V, Dressel R, Cupers P, Huylebroeck D, Zwijsen A, Van Leuven F, De Strooper B (1999) Presenilin 2 deficiency causes a mild pulmonary phenotype and no changes in amyloid precursor protein processing but enhances the embryonic lethal phenotype of presenilin 1 deficiency. Proc Natl Acad Sci U S A 96:11872–11877.

Ho A, Südhof TC (2004) Binding of F-spondin to amyloid-beta precursor protein: a candidate amyloid-beta precursor protein ligand that modulates amyloid-beta precursor protein cleavage. Proc Natl Acad Sci U S A 101:2548–2553.

Hoe H-S, Lee H-K, Pak DTS (2012) The upside of APP at synapses. CNS Neurosci Ther 18:47–56.

Hoe H-S, Lee KJ, Carney RSE, Lee J, Markova A, Lee J-Y, Howell BW, Hyman BT, Pak DTS, Bu G, Rebeck GW (2009) Interaction of reelin with amyloid precursor protein promotes neurite outgrowth. J Neurosci 29:7459–7473.

Hoe H-S, Wessner D, Beffert U, Becker AG, Matsuoka Y, Rebeck GW (2005) F-spondin interaction with the apolipoprotein E receptor ApoEr2 affects processing of amyloid precursor protein. Mol Cell Biol 25:9259–9268.

Horne EA, Dell'Acqua ML (2007) Phospholipase C is required for changes in postsynaptic structure and function associated with NMDA receptor-dependent long-term depression. J Neurosci 27:3523–3534.

Hsia AY, Masliah E, McConlogue L, Yu GQ, Tatsuno G, Hu K, Kholodenko D, Malenka RC, Nicoll RA, Mucke L (1999) Plaque-independent disruption of neural circuits in Alzheimer's disease mouse models. Proc Natl Acad Sci U S A 96:3228–3233.

Hsieh H, Boehm J, Sato C, Iwatsubo T, Tomita T, Sisodia S, Malinow R (2006) AMPAR removal underlies Abeta-induced synaptic depression and dendritic spine loss. Neuron 52:831–843.

Hu H, Dong W, Feng G (2006a) Specific suppression of beta-secretase gene expression by short interfering RNA in mammalian cells. J Zhejiang Univ Med Sci 35:622–629.

Hu H, Real E, Takamiya K, Kang M-G, Ledoux J, Huganir RL, Malinow R (2007) Emotion enhances learning via norepinephrine regulation of AMPA-receptor trafficking. Cell 131:160–173.

Hu X, Hicks CW, He W, Wong P, Macklin WB, Trapp BD, Yan R (2006b) Bace1 modulates myelination in the central and peripheral nervous system. Nat Neurosci 9:1520–1525.

Hu X, Zhou X, He W, Yang J, Xiong W, Wong P, Wilson CG, Yan R (2010) BACE1 deficiency causes altered neuronal activity and neurodegeneration. J Neurosci 30:8819–8829.

Huang S, Treviño M, He K, Ardiles A, Pasquale R de, Guo Y, Palacios A, Huganir R, Kirkwood A (2012) Pull-push neuromodulation of LTP and LTD enables bidirectional experience-induced synaptic scaling in visual cortex. Neuron 73:497–510.

Huang YZ, Won S, Ali DW, Wang Q, Tanowitz M, Du QS, Pelkey KA, Yang DJ, Xiong WC, Salter MW, Mei L (2000) Regulation of neuregulin signaling by PSD-95 interacting with ErbB4 at CNS synapses. Neuron 26:443–455.

Huber KM, Kayser MS, Bear MF (2000) Role for rapid dendritic protein synthesis in hippocampal mGluR-dependent long-term depression. Science 288:1254–1257.

Huse JT, Pijak DS, Leslie GJ, Lee VM, Doms RW (2000) Maturation and endosomal targeting of beta-site amyloid precursor protein-cleaving enzyme. The Alzheimer's disease beta-secretase. J Biol Chem 275:33729–33737.

Hussain I, Hawkins J, Harrison D, Hille C, Wayne G, Cutler L, Buck T, Walter D, Demont E, Howes C, Naylor A, Jeffrey P, Gonzalez MI, Dingwall C, Michel A, Redshaw S, Davis JB (2007) Oral administration of a potent and selective non-peptidic BACE-1 inhibitor decreases beta-cleavage of amyloid precursor protein and amyloid-beta production in vivo. J Neurochem 100:802–809.

Hyman BT (2011) Amyloid-dependent and amyloid-independent stages of Alzheimer disease. Arch Neurol 68:1062–1064.

Ill-Raga G, Palomer E, Wozniak MA, Ramos-Fernández E, Bosch-Morató M, Tajes M, Guix FX, Galán JJ, Clarimón J, Antúnez C, Real LM, Boada M, Itzhaki RF, Fandos C, Muñoz FJ (2011) Activation of PKR causes amyloid ß-peptide accumulation via de-repression of BACE1 expression. PLoS One 6:e21456.

Imbimbo BP, Del Giudice E, Colavito D, D'Arrigo A, Dalle Carbonare M, Villetti G, Facchinetti F, Volta R, Pietrini V, Baroc MF, Serneels L, De Strooper B, Leon A (2007) 1-(3',4'-Dichloro-2-fluoro[1,1'-biphenyl]-4-yl)-cyclopropanecarboxylic acid\ (CHF5074), a novel gamma-secretase modulator, reduces brain beta-amyloid pathology in a transgenic mouse model of Alzheimer's disease without causing peripheral toxicity. J Pharmacol Exp Ther 323:822–830.

Imbimbo BP, Hutter-Paier B, Villetti G, Facchinetti F, Cenacchi V, Volta R, Lanzillotta A, Pizzi M, Windisch M (2009) CHF5074, a novel gamma-secretase modulator, attenuates brain beta-amyloid pathology and learning deficit in a mouse model of Alzheimer's disease. Br J Pharmacol 156:982–993.

Imbimbo BP, Panza F, Frisardi V, Solfrizzi V, D'Onofrio G, Logroscino G, Seripa D, Pilotto A (2011) Therapeutic intervention for Alzheimer's disease with gamma-secretase inhibitors: still a viable option? Expert Opin Investig Drugs 20:325–341.

Imbimbo BP, Solfrizzi V, Panza F (2010) Are NSAIDs useful to treat Alzheimer's disease or mild cognitive impairment? Front Aging Neurosci 2.

Inbar P, Li CQ, Takayama SA, Bautista MR, Yang J (2006) Oligo(ethylene glycol) derivatives of thioflavin T as inhibitors of protein-amyloid interactions. Chembiochem 7:1563–1566.

Inoue E, Deguchi-Tawarada M, Togawa A, Matsui C, Arita K, Katahira-Tayama S, Sato T, Yamauchi E, Oda Y, Takai Y (2009) Synaptic activity prompts gamma-secretase-mediated cleavage of EphA4 and dendritic spine formation. J Cell Biol 185:551–564.

Iyer M, Mishra R, Han Y, Hopfinger AJ (2002) Predicting blood-brain barrier partitioning of organic molecules using membrane-interaction QSAR analysis. Pharm Res 19:1611–1621.

Jacobsen JS, Wu CC, Redwine JM, Comery TA, Arias R, Bowlby M, Martone R, Morrison JH, Pangalos MN, Reinhart PH, Bloom FE (2006) Early-onset behavioral and synaptic deficits in a mouse model of Alzheimer's disease. Proc Natl Acad Sci U S A 103:5161–5166.

Jahanshad N, Rajagopalan P, Hua X, Hibar DP, Nir TM, Toga AW, Jack CR, Saykin AJ, Green RC, Weiner MW, Medland SE, Montgomery GW, Hansell NK, McMahon KL, de Zubicaray GI, Martin NG, Wright MJ, Thompson PM (2013) Genome-wide scan of healthy human connectome discovers SPON1 gene variant influencing dementia severity. Proc Natl Acad Sci U S A 110:4768–4773.

Jankowsky JL, Fadale DJ, Anderson J, Xu GM, Gonzales V, Jenkins NA, Copeland NG, Lee MK, Younkin LH, Wagner SL, Younkin SG, Borchelt DR (2004) Mutant presenilins specifically elevate the levels of the 42 residue beta-amyloid peptide in vivo: evidence for augmentation of a 42-specific gamma secretase. Hum Mol Genet 13:159–170.

Jankowsky JL, Melnikova T, Fadale DJ, Xu GM, Slunt HH, Gonzales V, Younkin LH, Younkin SG, Borchelt DR, Savonenko A V (2005) Environmental enrichment mitigates cognitive deficits in a mouse model of Alzheimer's disease. J Neurosci 25:5217–5224.

Jung CKE, Fuhrmann M, Honarnejad K, Van Leuven F, Herms J (2011) Role of presenilin 1 in structural plasticity of cortical dendritic spines in vivo. J Neurochem 119:1064–1073.

Kamenetz F, Tomita T, Hsieh H, Seabrook G, Borchelt D, Iwatsubo T, Sisodia S, Malinow R (2003) APP processing and synaptic function. Neuron 37:925–937.

Kandel ER (2001) The molecular biology of memory storage: a dialogue between genes and synapses. Science 294:1030–1038.

Kang EL, Cameron AN, Piazza F, Walker KR, Tesco G (2010) Ubiquitin regulates GGA3-mediated degradation of BACE1. J Biol Chem 285:24108–24119.

Kao S-C, Krichevsky AM, Kosik KS, Tsai L-H (2004) BACE1 suppression by RNA interference in primary cortical neurons. J Biol Chem 279:1942–1949.

Kasai H, Fukuda M, Watanabe S, Hayashi-Takagi A, Noguchi J (2010) Structural dynamics of dendritic spines in memory and cognition. Trends Neurosci 33:121–129.

Kasai H, Matsuzaki M, Noguchi J, Yasumatsu N (2002) [Dendritic spine structures and functions]. Nihon Shinkei Seishin Yakurigaku Zasshi 22:159–164.

Katsouri L, Parr C, Bogdanovic N, Willem M, Sastre M (2011) PPARγ co-activator-1α (PGC-1α) reduces amyloid-β generation through a PPARγ-dependent mechanism. J Alzheimers Dis 25:151–162.

Kelleher RJ, Govindarajan A, Jung H-Y, Kang H, Tonegawa S (2004) Translational control by MAPK signaling in long-term synaptic plasticity and memory. Cell 116:467–479.

Kelly BL, Ferreira A (2006) beta-Amyloid-induced dynamin 1 degradation is mediated by N-methyl-D-aspartate receptors in hippocampal neurons. J Biol Chem 281:28079–28089.

Kelly BL, Ferreira A (2007) Beta-amyloid disrupted synaptic vesicle endocytosis in cultured hippocampal neurons. Neuroscience 147:60–70.

Kelly BL, Vassar R, Ferreira A (2005) Beta-amyloid-induced dynamin 1 depletion in hippocampal neurons. A potential mechanism for early cognitive decline in Alzheimer disease. J Biol Chem 280:31746–31753.

Kessels HW, Malinow R (2009) Synaptic AMPA receptor plasticity and behavior. Neuron 61:340–350.

Kilman V, van Rossum MCW, Turrigiano GG (2002) Activity deprivation reduces miniature IPSC amplitude by decreasing the number of postsynaptic GABA(A) receptors clustered at neocortical synapses. J Neurosci 22:1328–1337.

Kim CH, Chung HJ, Lee HK, Huganir RL (2001a) Interaction of the AMPA receptor subunit GluR2/3 with PDZ domains regulates hippocampal long-term depression. Proc Natl Acad Sci U S A 98:11725–11730.

Kim DY, Carey BW, Wang H, Ingano LAM, Binshtok AM, Wertz MH, Pettingell WH, He P, Lee VM-Y, Woolf CJ, Kovacs DM (2007) BACE1 regulates voltage-gated sodium channels and neuronal activity. Nat Cell Biol 9:755–764.

Kim DY, Gersbacher MT, Inquimbert P, Kovacs DM (2011) Reduced sodium channel Na(v)1.1 levels in BACE1-null mice. J Biol Chem 286:8106–8116.

Kim DY, Kovacs DM (2011) Surface trafficking of sodium channels in cells and in hippocampal slices. Methods Mol Biol 793:351–361.

Kim JH, Anwyl R, Suh YH, Djamgoz MB, Rowan MJ (2001b) Use-dependent effects of amyloidogenic fragments of (beta)-amyloid precursor protein on synaptic plasticity in rat hippocampus in vivo. J Neurosci 21:1327–1333.

Kim JH, Lee H-K, Takamiya K, Huganir RL (2003) The role of synaptic GTPase-activating protein in neuronal development and synaptic plasticity. J Neurosci 23:1119–1124.

Kimura R, Devi L, Ohno M (2010) Partial reduction of BACE1 improves synaptic plasticity, recent and remote memories in Alzheimer's disease transgenic mice. J Neurochem 113:248–261.

Knobloch M, Farinelli M, Konietzko U, Nitsch RM, Mansuy IM (2007) Abeta oligomer-mediated long-term potentiation impairment involves protein phosphatase 1-dependent mechanisms. J Neurosci 27:7648–7653.

Knobloch M, Mansuy IM (2008) Dendritic spine loss and synaptic alterations in Alzheimer's disease. Mol Neurobiol 37:73–82.

Kopan R, Ilagan MXG (2004) Gamma-secretase: proteasome of the membrane? Nat Rev Mol Cell Biol 5:499–504.

Kounnas MZ et al. (2010) Modulation of gamma-secretase reduces beta-amyloid deposition in a transgenic mouse model of Alzheimer's disease. Neuron 67:769–780.

Kovalchuk Y, Eilers J, Lisman J, Konnerth A (2000) NMDA receptor-mediated subthreshold Ca(2+) signals in spines of hippocampal neurons. J Neurosci 20:1791–1799.

Krug M, Lössner B, Ott T (1984) Anisomycin blocks the late phase of long-term potentiation in the dentate gyrus of freely moving rats. Brain Res Bull 13:39–42.

Kukar T, Prescott S, Eriksen JL, Holloway V, Murphy MP, Koo EH, Golde TE, Nicolle MM (2007) Chronic administration of R-flurbiprofen attenuates learning impairments in transgenic amyloid precursor protein mice. BMC Neurosci 8:54.

Kurt MA, Davies DC, Kidd M, Duff K, Howlett DR (2003) Hyperphosphorylated tau and paired helical filament-like structures in the brains of mice carrying mutant amyloid precursor protein and mutant presenilin-1 transgenes. Neurobiol Dis 14:89–97.

Lacor PN, Buniel MC, Chang L, Fernandez SJ, Gong Y, Viola KL, Lambert MP, Velasco PT, Bigio EH, Finch CE, Krafft GA, Klein WL (2004) Synaptic targeting by Alzheimer's-related amyloid beta oligomers. J Neurosci 24:10191–10200.

Lai HC, Jan LY (2006) The distribution and targeting of neuronal voltage-gated ion channels. Nat Rev Neurosci 7:548–562.

Laird FM, Cai H, Savonenko A V, Farah MH, He K, Melnikova T, Wen H, Chiang H-C, Xu G, Koliatsos VE, Borchelt DR, Price DL, Lee H-K, Wong PC (2005) BACE1, a major determinant of selective vulnerability of the brain to amyloid-beta amyloidogenesis, is essential for cognitive, emotional, and synaptic functions. J Neurosci 25:11693–11709.

Lamprecht R, Hazvi S, Dudai Y (1997) cAMP response element-binding protein in the amygdala is required for long- but not short-term conditioned taste aversion memory. J Neurosci 17:8443–8450.

Larson J, Wong D, Lynch G (1986) Patterned stimulation at the theta frequency is optimal for the induction of hippocampal long-term potentiation. Brain Res 368:347–350.

Le Magueresse C, Safiulina V, Changeux J-P, Cherubini E (2006) Nicotinic modulation of network and synaptic transmission in the immature hippocampus investigated with genetically modified mice. J Physiol 576:533–546.

Lee H-K (2006) Synaptic plasticity and phosphorylation. Pharmacol Ther 112:810–832.

Lee H-K, Kirkwood A (2011) AMPA receptor regulation during synaptic plasticity in hippocampus and neocortex. Semin Cell Dev Biol 22:514–520.

Lee H-K, Takamiya K, Han J-S, Man H, Kim C-H, Rumbaugh G, Yu S, Ding L, He C, Petralia RS, Wenthold RJ, Gallagher M, Huganir RL (2003) Phosphorylation of the AMPA receptor GluR1 subunit is required for synaptic plasticity and retention of spatial memory. Cell 112:631–643.

Lee H-K, Takamiya K, He K, Song L, Huganir RL (2010a) Specific roles of AMPA receptor subunit GluR1 (GluA1) phosphorylation sites in regulating synaptic plasticity in the CA1 region of hippocampus. J Neurophysiol 103:479–489.

Lee HK, Barbarosie M, Kameyama K, Bear MF, Huganir RL (2000a) Regulation of distinct AMPA receptor phosphorylation sites during bidirectional synaptic plasticity. Nature 405:955–959.

Lee HK, Kameyama K, Huganir RL, Bear MF (1998) NMDA induces long-term synaptic depression and dephosphorylation of the GluR1 subunit of AMPA receptors in hippocampus. Neuron 21:1151–1162.

Lee KJ, Hoe H-S, Pak DTS (2011) Plk2 Raps up Ras to subdue synapses. Small GTPases 2:162–166.

Lee KJ, Moussa CEH, Lee Y, Sung Y, Howell BW, Turner RS, Pak DTS, Hoe HS (2010b) Beta amyloid-independent role of amyloid precursor protein in generation and maintenance of dendritic spines. Neuroscience 169:344–356.

Lee MS, Kwon YT, Li M, Peng J, Friedlander RM, Tsai LH (2000b) Neurotoxicity induces cleavage of p35 to p25 by calpain. Nature 405:360–364.

Lee SH, Simonetta A, Sheng M (2004) Subunit rules governing the sorting of internalized AMPA receptors in hippocampal neurons. Neuron 43:221–236.

Leissring MA, Akbari Y, Fanger CM, Cahalan MD, Mattson MP, LaFerla FM (2000) Capacitative calcium entry deficits and elevated luminal calcium content in mutant presenilin-1 knockin mice. J Cell Biol 149:793–798.

Leissring MA, Paul BA, Parker I, Cotman CW, LaFerla FM (1999) Alzheimer's presenilin-1 mutation potentiates inositol 1,4,5-trisphosphate-mediated calcium signaling in Xenopus oocytes. J Neurochem 72:1061–1068.

Lemere CA (2009) Developing novel immunogens for a safe and effective Alzheimer's disease vaccine. Prog Brain Res 175:83–93.

Lemke G (2006) Neuregulin-1 and myelination. Sci STKE 2006:pe11.

Lendon CL, Ashall F, Goate AM (1997) Exploring the etiology of Alzheimer disease using molecular genetics. JAMA 277:825–831.

Lesné S, Ali C, Gabriel C, Croci N, MacKenzie ET, Glabe CG, Plotkine M, Marchand-Verrecchia C, Vivien D, Buisson A (2005) NMDA receptor activation inhibits alpha-secretase and promotes neuronal amyloid-beta production. J Neurosci 25:9367–9377.

Levy-Lahad E, Wasco W, Poorkaj P, Romano DM, Oshima J, Pettingell WH, Yu CE, Jondro PD, Schmidt SD, Wang K (1995) Candidate gene for the chromosome 1 familial Alzheimer's disease locus. Science 269:973–977.

Li B, Woo R-S, Mei L, Malinow R (2007) The neuregulin-1 receptor erbB4 controls glutamatergic synapse maturation and plasticity. Neuron 54:583–597.

Li F, Calingasan NY, Yu F, Mauck WM, Toidze M, Almeida CG, Takahashi RH, Carlson GA, Flint Beal M, Lin MT, Gouras GK (2004) Increased plaque burden in brains of APP mutant MnSOD heterozygous knockout mice. J Neurochem 89:1308–1312.

Li Q, Wu D, Zhang L, Zhang Y (2010) Effects of galantamine on β-amyloid release and beta-site cleaving enzyme 1 expression in differentiated human neuroblastoma SH-SY5Y cells. Exp Gerontol 45:842–847.

Li S, Hong S, Shepardson NE, Walsh DM, Shankar GM, Selkoe D (2009) Soluble oligomers of amyloid Beta protein facilitate hippocampal long-term depression by disrupting neuronal glutamate uptake. Neuron 62:788–801.

Li Y-C, Chen Q, Wan X-Z, Yang X-L, Liu X, Zhong L (2011) Effects of conjugated linoleic acid on cleavage of amyloid precursor protein via PPARγ. Neurol Sci 32:1095–1101.

Liang B, Duan B-Y, Zhou X-P, Gong J-X, Luo Z-G (2010) Calpain activation promotes BACE1 expression, amyloid precursor protein processing, and amyloid plaque formation in a transgenic mouse model of Alzheimer disease. J Biol Chem 285:27737–27744.

Lin D-T, Makino Y, Sharma K, Hayashi T, Neve R, Takamiya K, Huganir RL (2009) Regulation of AMPA receptor extrasynaptic insertion by 4.1N, phosphorylation and palmitoylation. Nat Neurosci 12:879–887.

Lin JW, Ju W, Foster K, Lee SH, Ahmadian G, Wyszynski M, Wang YT, Sheng M (2000) Distinct molecular mechanisms and divergent endocytotic pathways of AMPA receptor internalization. Nat Neurosci 3:1282–1290.

Lisman J (1989) A mechanism for the Hebb and the anti-Hebb processes underlying learning and memory. Proc Natl Acad Sci U S A 86:9574–9578.

Liu Q, Kawai H, Berg DK (2001a) beta -Amyloid peptide blocks the response of alpha 7-containing nicotinic receptors on hippocampal neurons. Proc Natl Acad Sci U S A 98:4734–4739.

Liu X, Ramirez S, Pang PT, Puryear CB, Govindarajan A, Deisseroth K, Tonegawa S (2012) Optogenetic stimulation of a hippocampal engram activates fear memory recall. Nature 484:381–385.

Liu Y, Ford B, Mann MA, Fischbach GD (2001b) Neuregulins increase alpha7 nicotinic acetylcholine receptors and enhance excitatory synaptic transmission in GABAergic interneurons of the hippocampus. J Neurosci 21:5660–5669.

Lleó A (2008) Activity of gamma-secretase on substrates other than APP. Curr Top Med Chem 8:9–16.

Loane DJ, Pocivavsek A, Moussa CE-H, Thompson R, Matsuoka Y, Faden AI, Rebeck GW, Burns MP (2009) Amyloid precursor protein secretases as therapeutic targets for traumatic brain injury. Nat Med 15:377–379.

Lu W, Roche KW (2012) Posttranslational regulation of AMPA receptor trafficking and function. Curr Opin Neurobiol 22:470–479.

Luo X, Yan R (2010) Inhibition of BACE1 for therapeutic use in Alzheimer's disease. Int J Clin Exp Pathol 3:618–628.

Luo Y, Bolon B, Kahn S, Bennett BD, Babu-Khan S, Denis P, Fan W, Kha H, Zhang J, Gong Y, Martin L, Louis JC, Yan Q, Richards WG, Citron M, Vassar R (2001) Mice deficient in BACE1, the Alzheimer's beta-secretase, have normal phenotype and abolished beta-amyloid generation. Nat Neurosci 4:231–232.

Lustbader JW et al. (2004) ABAD directly links Abeta to mitochondrial toxicity in Alzheimer's disease. Science 304:448–452.

Lüthi A, Chittajallu R, Duprat F, Palmer MJ, Benke TA, Kidd FL, Henley JM, Isaac JT, Collingridge GL (1999) Hippocampal LTD expression involves a pool of AMPARs regulated by the NSF-GluR2 interaction. Neuron 24:389–399.

Lynch MA (2004) Long-term potentiation and memory. Physiol Rev 84:87–136.

Ma H, Lesné S, Kotilinek L, Steidl-Nichols J V, Sherman M, Younkin L, Younkin S, Forster C, Sergeant N, Delacourte A, Vassar R, Citron M, Kofuji P, Boland LM, Ashe KH (2007) Involvement of beta-site APP cleaving enzyme 1 (BACE1) in amyloid precursor protein-mediated enhancement of memory and activity-dependent synaptic plasticity. Proc Natl Acad Sci U S A 104:8167–8172.

Ma T, Hoeffer CA, Wong H, Massaad CA, Zhou P, Iadecola C, Murphy MP, Pautler RG, Klann E (2011) Amyloid β-induced impairments in hippocampal synaptic plasticity are rescued by decreasing mitochondrial superoxide. J Neurosci 31:5589–5595.

Maffei A, Nataraj K, Nelson SB, Turrigiano GG (2006) Potentiation of cortical inhibition by visual deprivation. Nature 443:81–84.

Maffei A, Nelson SB, Turrigiano GG (2004) Selective reconfiguration of layer 4 visual cortical circuitry by visual deprivation. Nat Neurosci 7:1353–1359.

Maggi L, Le Magueresse C, Changeux J-P, Cherubini E (2003) Nicotine activates immature "silent" connections in the developing hippocampus. Proc Natl Acad Sci U S A 100:2059–2064.

Maggio N, Segal M (2007) Unique regulation of long term potentiation in the rat ventral hippocampus. Hippocampus 17:10–25.

Maggio N, Segal M (2009) Differential modulation of long-term depression by acute stress in the rat dorsal and ventral hippocampus. J Neurosci 29:8633–8638.

Maggio N, Segal M (2010) Corticosteroid regulation of synaptic plasticity in the hippocampus. ScientificWorldJournal 10:462–469.

Makino Y, Johnson RC, Yu Y, Takamiya K, Huganir RL (2011) Enhanced synaptic plasticity in mice with phosphomimetic mutation of the GluA1 AMPA receptor. Proc Natl Acad Sci U S A 108:8450–8455.

Malenka RC, Bear MF (2004) LTP and LTD: an embarrassment of riches. Neuron 44:5–21.

Malenka RC, Nicoll RA (1999) Long-term potentiation--a decade of progress? Science 285:1870–1874.

Malinow R, Malenka RC (2002) AMPA receptor trafficking and synaptic plasticity. Annu Rev Neurosci 25:103–126.

Mammen AL, Kameyama K, Roche KW, Huganir RL (1997) Phosphorylation of the alpha-amino-3-hydroxy-5-methylisoxazole4-propionic acid receptor GluR1 subunit by calcium/calmodulin-dependent kinase II. J Biol Chem 272:32528–32533.

Man H-Y (2011) GluA2-lacking, calcium-permeable AMPA receptors--inducers of plasticity? Curr Opin Neurobiol 21:291–298.

Man HY, Lin JW, Ju WH, Ahmadian G, Liu L, Becker LE, Sheng M, Wang YT (2000) Regulation of AMPA receptor-mediated synaptic transmission by clathrin-dependent receptor internalization. Neuron 25:649–662.

Manabe T, Wyllie DJ, Perkel DJ, Nicoll RA (1993) Modulation of synaptic transmission and long-term potentiation: effects on paired pulse facilitation and EPSC variance in the CA1 region of the hippocampus. J Neurophysiol 70:1451–1459.

Manahan-Vaughan D, Kulla A, Frey JU (2000) Requirement of translation but not transcription for the maintenance of long-term depression in the CA1 region of freely moving rats. J Neurosci 20:8572–8576.

Marchetti C, Marie H (2011) Hippocampal synaptic plasticity in Alzheimer's disease: what have we learned so far from transgenic models? Rev Neurosci 22:373–402.

Marjaux E, Hartmann D, De Strooper B (2004) Presenilins in memory, Alzheimer's disease, and therapy. Neuron 42:189–192.

Martin SJ, Grimwood PD, Morris RG (2000) Synaptic plasticity and memory: an evaluation of the hypothesis. Annu Rev Neurosci 23:649–711.

Martone RL et al. (2009) Begacestat (GSI-953): a novel, selective thiophene sulfonamide inhibitor of amyloid precursor protein gamma-secretase for the treatment of Alzheimer's disease. J Pharmacol Exp Ther 331:598–608.

Massaad CA, Klann E (2011) Reactive oxygen species in the regulation of synaptic plasticity and memory. Antioxid Redox Signal 14:2013–2054.

McConnell EJ, Wagoner MJ, Keenan CE, Raess BU (1999) Inhibition of calmodulin-stimulated (Ca2+ + Mg2+)-ATPase activity by dimethyl sulfoxide. Biochem Pharmacol 57:39–44.

McCutcheon JE, Fisher AS, Guzdar E, Wood SA, Lightman SL, Hunt SP (2008) Genetic background influences the behavioural and molecular consequences of neurokinin-1 receptor knockout. Eur J Neurosci 27:683–690.

McGehee DS, Heath MJ, Gelber S, Devay P, Role LW (1995) Nicotine enhancement of fast excitatory synaptic transmission in CNS by presynaptic receptors. Science 269:1692–1696.

Megill A, Lee T, Dibattista AM, Song JM, Spitzer MH, Rubinshtein M, Habib LK, Capule CC, Mayer M, Turner RS, Kirkwood A, Yang J, Pak DTS, Lee H-K, Hoe H-S (2013) A Tetra(Ethylene Glycol) Derivative of Benzothiazole Aniline Enhances Ras-Mediated Spinogenesis. J Neurosci 33:9306–9318.

Minami SS, Cordova A, Cirrito JR, Tesoriero JA, Babus LW, Davis GC, Dakshanamurthy S, Turner RS, Pak DT, Rebeck GW, Paige M, Hoe H-S (2010) ApoE mimetic peptide decreases Abeta production in vitro and in vivo. Mol Neurodegener 5:16.

Miñano-Molina AJ, España J, Martín E, Barneda-Zahonero B, Fadó R, Solé M, Trullás R, Saura C a, Rodríguez-Alvarez J (2011) Soluble oligomers of amyloid-β peptide disrupt membrane trafficking of α-amino-3-hydroxy-5-methylisoxazole-4-propionic acid receptor contributing to early synapse dysfunction. J Biol Chem 286:27311–27321.

Mockett BG, Hulme SR (2008) Metaplasticity: new insights through electrophysiological investigations. J Integr Neurosci 7:315–336.

Moechars D, Dewachter I, Lorent K, Reversé D, Baekelandt V, Naidu A, Tesseur I, Spittaels K, Haute C V, Checler F, Godaux E, Cordell B, Van Leuven F (1999) Early phenotypic changes in transgenic mice that overexpress different mutants of amyloid precursor protein in brain. J Biol Chem 274:6483–6492.

Molas S, Dierssen M (2014) The role of nicotinic receptors in shaping and functioning of the glutamatergic system: A window into cognitive pathology. Neurosci Biobehav Rev.

Montey KL, Quinlan EM (2011) Recovery from chronic monocular deprivation following reactivation of thalamocortical plasticity by dark exposure. Nat Commun 2:317.

Morales B, Choi S-Y, Kirkwood A (2002) Dark rearing alters the development of GABAergic transmission in visual cortex. J Neurosci 22:8084–8090.

Morgado-Bernal I (2011) Learning and memory consolidation: linking molecular and behavioral data. Neuroscience 176:12–19.

Morris C et al. (2014) Should the standard dimethyl sulfoxide concentration be reduced? Results of a European Group for Blood and Marrow Transplantation prospective noninterventional study on usage and side effects of dimethyl sulfoxide. Transfusion.

Morris RGM (2006) Elements of a neurobiological theory of hippocampal function: the role of synaptic plasticity, synaptic tagging and schemas. Eur J Neurosci 23:2829–2846.

Mulkey RM, Malenka RC (1992) Mechanisms underlying induction of homosynaptic long-term depression in area CA1 of the hippocampus. Neuron 9:967–975.

Nabavi S, Fox R, Proulx CD, Lin JY, Tsien RY, Malinow R (2014) Engineering a memory with LTD and LTP. Nature.

Nakashiba T, Young JZ, McHugh TJ, Buhl DL, Tonegawa S (2008) Transgenic inhibition of synaptic transmission reveals role of CA3 output in hippocampal learning. Science 319:1260–1264.

Nakauchi S, Sumikawa K (2014) Endogenous ACh suppresses LTD induction and nicotine relieves the suppression via different nicotinic ACh receptor subtypes in the mouse hippocampus. Life Sci.

Nguyen P V, Abel T, Kandel ER (1994) Requirement of a critical period of transcription for induction of a late phase of LTP. Science 265:1104–1107.

Nicoll JAR, Wilkinson D, Holmes C, Steart P, Markham H, Weller RO (2003) Neuropathology of human Alzheimer disease after immunization with amyloid-beta peptide: a case report. Nat Med 9:448–452.

Nicoll RA, Malenka RC (1995) Contrasting properties of two forms of long-term potentiation in the hippocampus. Nature 377:115–118.

Nicoll RA, Schmitz D (2005) Synaptic plasticity at hippocampal mossy fibre synapses. Nat Rev Neurosci 6:863–876.

Nie H-Z, Li Z-Q, Yan Q-X, Wang Z-J, Zhao W-J, Guo L-C, Yin M (2011) Nicotine decreases beta-amyloid through regulating BACE1 transcription in SH-EP1-α4β2 nAChR-APP695 cells. Neurochem Res 36:904–912.

Nimmrich V, Grimm C, Draguhn A, Barghorn S, Lehmann A, Schoemaker H, Hillen H, Gross G, Ebert U, Bruehl C (2008) Amyloid beta oligomers (A beta(1-42) globulomer) suppress spontaneous synaptic activity by inhibition of P/Q-type calcium currents. J Neurosci 28:788–797.

Nimmrich V, Reymann KG, Strassburger M, Schöder UH, Gross G, Hahn A, Schoemaker H, Wicke K, Möller A (2010) Inhibition of calpain prevents NMDA-induced cell death and beta-amyloid-induced synaptic dysfunction in hippocampal slice cultures. Br J Pharmacol 159:1523–1531.

Nitsch RM, Farber SA, Growdon JH, Wurtman RJ (1993) Release of amyloid beta-protein precursor derivatives by electrical depolarization of rat hippocampal slices. Proc Natl Acad Sci U S A 90:5191–5193.

O'Brien JT, Burns A (2011) Clinical practice with anti-dementia drugs: a revised (second) consensus statement from the British Association for Psychopharmacology. J Psychopharmacol 25:997–1019.

O'Connor T, Sadleir KR, Maus E, Velliquette RA, Zhao J, Cole SL, Eimer WA, Hitt B, Bembinster LA, Lammich S, Lichtenthaler SF, Hébert SS, De Strooper B, Haass C, Bennett DA, Vassar R (2008) Phosphorylation of the translation initiation factor eIF2alpha increases BACE1 levels and promotes amyloidogenesis. Neuron 60:988–1009.

Oh MC, Derkach VA (2005) Dominant role of the GluR2 subunit in regulation of AMPA receptors by CaMKII. Nat Neurosci 8:853–854.

Ohno M, Chang L, Tseng W, Oakley H, Citron M, Klein WL, Vassar R, Disterhoft JF (2006) Temporal memory deficits in Alzheimer's mouse models: rescue by genetic deletion of BACE1. Eur J Neurosci 23:251–260.

Ohno M, Sametsky EA, Younkin LH, Oakley H, Younkin SG, Citron M, Vassar R, Disterhoft JF (2004) BACE1 deficiency rescues memory deficits and cholinergic dysfunction in a mouse model of Alzheimer's disease. Neuron 41:27–33.

Orgogozo J-M, Gilman S, Dartigues J-F, Laurent B, Puel M, Kirby LC, Jouanny P, Dubois B, Eisner L, Flitman S, Michel BF, Boada M, Frank A, Hock C (2003) Subacute meningoencephalitis in a subset of patients with AD after Abeta42 immunization. Neurology 61:46–54.

Osten P, Khatri L, Perez JL, Köhr G, Giese G, Daly C, Schulz TW, Wensky A, Lee LM, Ziff EB (2000) Mutagenesis reveals a role for ABP/GRIP binding to GluR2 in synaptic surface accumulation of the AMPA receptor. Neuron 27:313–325.

Ou W-B, Wang R-S, Zhou H-M (2002) Conformational changes and inactivation of rabbit muscle creatine kinase in dimethyl sulfoxide solutions. Biochem Cell Biol 80:427–434.

Page RM, Baumann K, Tomioka M, Perez-Revuelta BI, Fukumori A, Jacobsen H, Flohr A, Luebbers T, Ozmen L, Steiner H, Haass C (2008) Generation of Abeta38 and Abeta42 is independently and differentially affected by familial Alzheimer disease-associated presenilin mutations and gamma-secretase modulation. J Biol Chem 283:677–683.

Pak DT, Yang S, Rudolph-Correia S, Kim E, Sheng M (2001) Regulation of dendritic spine morphology by SPAR, a PSD-95-associated RapGAP. Neuron 31:289–303.

Palop JJ, Chin J, Roberson ED, Wang J, Thwin MT, Bien-Ly N, Yoo J, Ho KO, Yu GQ, Kreitzer A, Finkbeiner S, Noebels JL, Mucke L (2007) Aberrant excitatory neuronal activity and compensatory remodeling of inhibitory hippocampal circuits in mouse models of Alzheimer's disease. Neuron 55:697–711.

Palop JJ, Mucke L (2009) Epilepsy and cognitive impairments in Alzheimer disease. Arch Neurol 66:435–440.

Palop JJ, Mucke L (2010a) Amyloid-beta-induced neuronal dysfunction in Alzheimer's disease: from synapses toward neural networks. Nat Neurosci 13:812–818.

Palop JJ, Mucke L (2010b) Synaptic depression and aberrant excitatory network activity in Alzheimer's disease: two faces of the same coin? Neuromolecular Med 12:48–55.

Paulsen O, Sejnowski TJ (2000) Natural patterns of activity and long-term synaptic plasticity. Curr Opin Neurobiol 10:172–179.

Pearson HA, Peers C (2006) Physiological roles for amyloid beta peptides. J Physiol 575:5–10.

Petrus E, Lee H-K (2014) BACE1 Is Necessary for Experience-Dependent Homeostatic Synaptic Plasticity in Visual Cortex. Neural Plast 2014:128631.

Pettersson M, Kauffman GW, am Ende CW, Patel NC, Stiff C, Tran TP, Johnson DS (2011) Novel gamma-secretase modulators: a review of patents from 2008 to 2010. Expert Opin Ther Pat\ 21:205–226.

Pettit DL, Shao Z, Yakel JL (2001) beta-Amyloid(1-42) peptide directly modulates nicotinic receptors in the rat hippocampal slice. J Neurosci 21:RC120.

Phillips M, Boman E, Osterman H, Willhite D, Laska M (2011) Olfactory and visuospatial learning and memory performance in two strains of Alzheimer's disease model mice--a longitudinal study. PLoS One 6:e19567.

Philpot BD, Sekhar AK, Shouval HZ, Bear MF (2001a) Visual experience and deprivation bidirectionally modify the composition and function of NMDA receptors in visual cortex. Neuron 29:157–169.

Philpot BD, Weisberg MP, Ramos MS, Sawtell NB, Tang YP, Tsien JZ, Bear MF (2001b) Effect of transgenic overexpression of NR2B on NMDA receptor function and synaptic plasticity in visual cortex. Neuropharmacology 41:762–770.

Plant K, Pelkey KA, Bortolotto ZA, Morita D, Terashima A, McBain CJ, Collingridge GL, Isaac JTR (2006) Transient incorporation of native GluR2-lacking AMPA receptors during hippocampal long-term potentiation. Nat Neurosci 9:602–604.

Plant LD, Boyle JP, Smith IF, Peers C, Pearson HA (2003) The production of amyloid beta peptide is a critical requirement for the viability of central neurons. J Neurosci 23:5531–5535.

Pratt KG, Zhu P, Watari H, Cook DG, Sullivan JM (2011a) A novel role for gamma-secretase: selective regulation of spontaneous neurotransmitter release from hippocampal neurons. J Neurosci 31:899–906.

Pratt KG, Zimmerman EC, Cook DG, Sullivan JM (2011b) Presenilin 1 regulates homeostatic synaptic scaling through Akt signaling. Nat Neurosci 14:1112–1114.

Priller C, Bauer T, Mitteregger G, Krebs B, Kretzschmar HA, Herms J (2006) Synapse formation and function is modulated by the amyloid precursor protein. J Neurosci 26:7212–7221.

Puzzo D, Privitera L, Leznik E, Fà M, Staniszewski A, Palmeri A, Arancio O (2008) Picomolar amyloid-beta positively modulates synaptic plasticity and memory in hippocampus. J Neurosci 28:14537–14545.

Rall W (1969) Time constants and electrotonic length of membrane cylinders and neurons. Biophys J 9:1483–1508.

Ramirez S, Liu X, Lin P-A, Suh J, Pignatelli M, Redondo RL, Ryan TJ, Tonegawa S (2013) Creating a false memory in the hippocampus. Science 341:387–391.

Reiserer RS, Harrison FE, Syverud DC, McDonald MP (2007) Impaired spatial learning in the APPSwe + PSEN1DeltaE9 bigenic mouse model of Alzheimer's disease. Genes Brain Behav 6:54–65.

Reiss K, Ludwig A, Saftig P (2006) Breaking up the tie: disintegrin-like metalloproteinases as regulators of cell migration in inflammation and invasion. Pharmacol Ther 111:985–1006.

Rice HC, Young-Pearse TL, Selkoe DJ (2013) Systematic evaluation of candidate ligands regulating ectodomain shedding of amyloid precursor protein. Biochemistry 52:3264–3277.

Ricobaraza A, Cuadrado-Tejedor M, Garcia-Osta A (2011) Long-term phenylbutyrate administration prevents memory deficits in Tg2576 mice by decreasing Abeta. Front Biosci (Elite Ed) 3:1375–1384.

Ringman JM, Schulman H, Becker C, Jones T, Bai Y, Immermann F, Cole G, Sokolow S, Gylys K, Geschwind DH, Cummings JL, Wan HI (2012) Proteomic changes in cerebrospinal fluid of presymptomatic and affected persons carrying familial Alzheimer disease mutations. Arch Neurol 69:96–104.

Rioult-Pedotti MS, Friedman D, Hess G, Donoghue JP (1998) Strengthening of horizontal cortical connections following skill learning. Nat Neurosci 1:230–234.

Roberds SL et al. (2001) BACE knockout mice are healthy despite lacking the primary beta-secretase activity in brain: implications for Alzheimer's disease therapeutics. Hum Mol Genet 10:1317–1324.

Roche KW, O'Brien RJ, Mammen AL, Bernhardt J, Huganir RL (1996) Characterization of multiple phosphorylation sites on the AMPA receptor GluR1 subunit. Neuron 16:1179–1188.

Rodrigues SM, Schafe GE, LeDoux JE (2004) Molecular mechanisms underlying emotional learning and memory in the lateral amygdala. Neuron 44:75–91.

Rossi MA, Dianzani MU (2000) Action of 2-nonenal and 4-hydroxynonenal on phosphoinositide-specific phosopholipase C in undifferentiated and DMSO-differentiated HL-60 cells. Cell Biochem Funct 18:209–214.

Rothman SM, Herdener N, Camandola S, Texel SJ, Mughal MR, Cong W-N, Martin B, Mattson MP (2012) 3xTgAD mice exhibit altered behavior and elevated Aβ after chronic mild social stress. Neurobiol Aging 33:830.e1–12.

Rothman SM, Mattson MP (2010) Adverse stress, hippocampal networks, and Alzheimer's disease. Neuromolecular Med 12:56–70.

Rozov A, Zilberter Y, Wollmuth LP, Burnashev N (1998) Facilitation of currents through rat Ca2+-permeable AMPA receptor channels by activity-dependent relief from polyamine block. J Physiol 511 (Pt 2:361–377.

Rumbaugh G, Vicini S (1999) Distinct synaptic and extrasynaptic NMDA receptors in developing cerebellar granule neurons. J Neurosci 19:10603–10610.

Saini DK, Chisari M, Gautam N (2009) Shuttling and translocation of heterotrimeric G proteins and Ras. Trends Pharmacol Sci 30:278–286.

Samura E, Shoji M, Kawarabayashi T, Sasaki A, Matsubara E, Murakami T, Wuhua X, Tamura S, Ikeda M, Ishiguro K, Saido TC, Westaway D, St George Hyslop P, Harigaya Y, Abe K (2006) Enhanced accumulation of tau in doubly transgenic mice expressing mutant betaAPP and presenilin-1. Brain Res 1094:192–199.

Santucci R, Laurenti E, Sinibaldi F, Ferrari RP (2002) Effect of dimethyl sulfoxide on the structure and the functional properties of horseradish peroxidase as observed by spectroscopy and cyclic voltammetry. Biochim Biophys Acta 1596:225–233.

Sarajärvi T, Haapasalo A, Viswanathan J, Mäkinen P, Laitinen M, Soininen H, Hiltunen M (2009) Down-regulation of seladin-1 increases BACE1 levels and activity through enhanced GGA3 depletion during apoptosis. J Biol Chem 284:34433–34443.

Sastre M, Gentleman SM (2010) NSAIDs: How they Work and their Prospects as Therapeutics in Alzheimer's Disease. Front Aging Neurosci 2:20.

Saura CA, Chen G, Malkani S, Choi SY, Takahashi RH, Zhang D, Gouras GK, Kirkwood A, Morris RG, Shen J (2005) Conditional inactivation of presenilin 1 prevents amyloid accumulation and temporarily rescues contextual and spatial working memory impairments in amyloid precursor protein transgenic mice. J Neurosci 25:6755–6764.

Saura CA, Choi SY, Beglopoulos V, Malkani S, Zhang D, Shankaranarayana Rao BS, Chattarji S, Kelleher 3rd RJ, Kandel ER, Duff K, Kirkwood A, Shen J (2004) Loss of presenilin function causes impairments of memory and synaptic plasticity followed by age-dependent neurodegeneration. Neuron 42:23–36.

Saura CA, Valero J (2011) The role of CREB signaling in Alzheimer's disease and other cognitive disorders. Rev Neurosci 22:153–169.

Savage MJ, Lin Y-G, Ciallella JR, Flood DG, Scott RW (2002) Activation of c-Jun N-terminal kinase and p38 in an Alzheimer's disease model is associated with amyloid deposition. J Neurosci 22:3376–3385.

Savonenko A, Xu GM, Melnikova T, Morton JL, Gonzales V, Wong MPF, Price DL, Tang F, Markowska AL, Borchelt DR (2005) Episodic-like memory deficits in the APPswe/PS1dE9 mouse model of Alzheimer's disease: relationships to beta-amyloid deposition and neurotransmitter abnormalities. Neurobiol Dis 18:602–617.

Savonenko A V, Melnikova T, Laird FM, Stewart K-A, Price DL, Wong PC (2008) Alteration of BACE1-dependent NRG1/ErbB4 signaling and schizophrenia-like phenotypes in BACE1-null mice. Proc Natl Acad Sci U S A 105:5585–5590.

Schafe GE, Doyère V, LeDoux JE (2005) Tracking the fear engram: the lateral amygdala is an essential locus of fear memory storage. J Neurosci 25:10010–10014.

Schenk D, Games D, Seubert P (2001) Potential treatment opportunities for Alzheimer's disease through inhibition of secretases and Abeta immunization. J Mol Neurosci 17:259–267.

Scheuner D et al. (1996) Secreted amyloid beta-protein similar to that in the senile plaques of Alzheimer's disease is increased in vivo by the presenilin 1 and 2 and APP mutations linked to familial Alzheimer's disease. Nat Med 2:864–870.

Schliebs R, Arendt T (2011) The cholinergic system in aging and neuronal degeneration. Behav Brain Res 221:555–563.

Séguéla P, Wadiche J, Dineley-Miller K, Dani JA, Patrick JW (1993) Molecular cloning, functional properties, and distribution of rat brain alpha 7: a nicotinic cation channel highly permeable to calcium. J Neurosci 13:596–604.

Selkoe DJ (2002) Alzheimer's disease is a synaptic failure. Science 298:789–791.

Selkoe DJ (2011) Resolving controversies on the path to Alzheimer's therapeutics. Nat Med 17:1060–1065.

Seol GH, Ziburkus J, Huang S, Song L, Kim IT, Takamiya K, Huganir RL, Lee H-K, Kirkwood A (2007) Neuromodulators control the polarity of spike-timing-dependent synaptic plasticity. Neuron 55:919–929.

Shankar GM, Walsh DM (2009) Alzheimer's disease: synaptic dysfunction and Abeta. Mol Neurodegener 4:48.

Shen J, Bronson RT, Chen DF, Xia W, Selkoe DJ, Tonegawa S (1997) Skeletal and CNS defects in Presenilin-1-deficient mice. Cell 89:629–639.

Shepherd JD, Rumbaugh G, Wu J, Chowdhury S, Plath N, Kuhl D, Huganir RL, Worley PF (2006) Arc/Arg3.1 mediates homeostatic synaptic scaling of AMPA receptors. Neuron 52:475–484.

Sherrington R et al. (1995) Cloning of a gene bearing missense mutations in early-onset familial Alzheimer's disease. Nature 375:754–760.

Sherva R, Tripodis Y, Bennett DA, Chibnik LB, Crane PK, de Jager PL, Farrer LA, Saykin AJ, Shulman JM, Naj A, Green RC (2014) Genome-wide association study of the rate of cognitive decline in Alzheimer's disease. Alzheimers Dement 10:45–52.

Shi S, Hayashi Y, Esteban JA, Malinow R (2001) Subunit-specific rules governing AMPA receptor trafficking to synapses in hippocampal pyramidal neurons. Cell 105:331–343.

Shi SH, Hayashi Y, Petralia RS, Zaman SH, Wenthold RJ, Svoboda K, Malinow R (1999) Rapid spine delivery and redistribution of AMPA receptors after synaptic NMDA receptor activation. Science 284:1811–1816.

Shilling D, Mak DO, Kang DE, Foskett JK (2012) Lack of evidence for presenilins as endoplasmic reticulum Ca2+ leak channels. J Biol Chem.

Silva AJ, Kogan JH, Frankland PW, Kida S (1998) CREB and memory. Annu Rev Neurosci 21:127–148.

Singer O, Marr RA, Rockenstein E, Crews L, Coufal NG, Gage FH, Verma IM, Masliah E (2005) Targeting BACE1 with siRNAs ameliorates Alzheimer disease neuropathology in a transgenic model. Nat Neurosci 8:1343–1349.

Smith IF, Boyle JP, Vaughan PF, Pearson HA, Cowburn RF, Peers CS (2002) Ca(2+) stores and capacitative Ca(2+) entry in human neuroblastoma (SH-SY5Y) cells expressing a familial Alzheimer's disease presenilin-1 mutation. Brain Res 949:105–111.

Smith IF, Hitt B, Green KN, Oddo S, LaFerla FM (2005) Enhanced caffeine-induced Ca2+ release in the 3xTg-AD mouse model of Alzheimer's disease. J Neurochem 94:1711–1718.

Snyder EM, Nong Y, Almeida CG, Paul S, Moran T, Choi EY, Nairn AC, Salter MW, Lombroso PJ, Gouras GK, Greengard P (2005) Regulation of NMDA receptor trafficking by amyloid-β. Nat Neurosci 8:1051–1058.

Song J, DiBattista A, Sung Y, Ahn J, Turner RS, Yang J, Pak DTS, Lee H-K, Hoe H-S (2014) A tetra(ethylene glycol) derivative of benzothiazole aniline ameliorates dendritic spine density and cognitive function in a mouse model of Alzheimer's disease. Exp Neurol 252:105–113.

Spencer B, Masliah E (2014) Immunotherapy for Alzheimer's disease: past, present and future. Front Aging Neurosci 6:114.

Sperling RA, Dickerson BC, Pihlajamaki M, Vannini P, LaViolette PS, Vitolo O V, Hedden T, Becker JA, Rentz DM, Selkoe DJ, Johnson KA (2010) Functional alterations in memory networks in early Alzheimer's disease. Neuromolecular Med 12:27–43.

Spires TL, Meyer-Luehmann M, Stern E a, McLean PJ, Skoch J, Nguyen PT, Bacskai BJ, Hyman BT (2005) Dendritic spine abnormalities in amyloid precursor protein transgenic mice demonstrated by gene transfer and intravital multiphoton microscopy. J Neurosci 25:7278–7287.

Stanton PK, Sarvey JM (1984) Blockade of long-term potentiation in rat hippocampal CA1 region by inhibitors of protein synthesis. J Neurosci 4:3080–3088.

Steele P, Mauk M (1999) Inhibitory Control of LTP and LTD : Stability of Synapse Strength. J Neurophysiol 81:1559–1566.

Stefan K, Wycislo M, Gentner R, Schramm A, Naumann M, Reiners K, Classen J (2006) Temporary occlusion of associative motor cortical plasticity by prior dynamic motor training. Cereb Cortex 16:376–385.

Steinbach JP, Müller U, Leist M, Li ZW, Nicotera P, Aguzzi A (1998) Hypersensitivity to seizures in beta-amyloid precursor protein deficient mice. Cell Death Differ 5:858–866.

Stent GS (1973) A physiological mechanism for Hebb's postulate of learning. Proc Natl Acad Sci U S A 70:997–1001.

Stevens A-S, Pirotte N, Plusquin M, Willems M, Neyens T, Artois T, Smeets K (2014) Toxicity profiles and solvent-toxicant interference in the planarian Schmidtea mediterranea after dimethylsulfoxide (DMSO) exposure. J Appl Toxicol.

Steward O, Worley PF (2001) A cellular mechanism for targeting newly synthesized mRNAs to synaptic sites on dendrites. Proc Natl Acad Sci U S A 98:7062–7068.

Stornetta RL, Zhu JJ (2011) Ras and Rap signaling in synaptic plasticity and mental disorders. Neuroscientist 17:54–78.

Stutzmann GE, Caccamo A, LaFerla FM, Parker I (2004) Dysregulated IP3 signaling in cortical neurons of knock-in mice expressing an Alzheimer's-linked mutation in presenilin1 results in exaggerated Ca2+ signals and altered membrane excitability. J Neurosci 24:508–513.

Stutzmann GE, Smith I, Caccamo A, Oddo S, Laferla FM, Parker I (2006) Enhanced ryanodine receptor recruitment contributes to Ca2+ disruptions in young, adult, and aged Alzheimer's disease mice. J Neurosci 26:5180–5189.

Stutzmann GE, Smith I, Caccamo A, Oddo S, Parker I, Laferla F (2007) Enhanced ryanodine-mediated calcium release in mutant PS1-expressing Alzheimer's mouse models. Ann N Y Acad Sci 1097:265–277.

Subbarao K V, Richardson JS, Ang LC (1990) Autopsy samples of Alzheimer's cortex show increased peroxidation in vitro. J Neurochem 55:342–345.

Supnet C, Bezprozvanny I (2010) The dysregulation of intracellular calcium in Alzheimer disease. Cell Calcium 47:183–189.

Supnet C, Grant J, Kong H, Westaway D, Mayne M (2006) Amyloid-beta-(1-42) increases ryanodine receptor-3 expression and function in neurons of TgCRND8 mice. J Biol Chem 281:38440–38447.

Sutton MA, Schuman EM (2006) Dendritic protein synthesis, synaptic plasticity, and memory. Cell 127:49–58.

Svedružić ŽM, Popović K, Šendula-Jengić V (2013) Modulators of γ-secretase activity can facilitate the toxic side-effects and pathogenesis of Alzheimer's disease. PLoS One 8:e50759.

Takahashi H, Fukumoto H, Maeda R, Terauchi J, Kato K, Miyamoto M (2010) Ameliorative effects of a non-competitive BACE1 inhibitor TAK-070 on Aβ peptide levels and impaired learning behavior in aged rats. Brain Res 1361:146–156.

Takasugi N, Sasaki T, Suzuki K, Osawa S, Isshiki H, Hori Y, Shimada N, Higo T, Yokoshima S, Fukuyama T, Lee VM-Y, Trojanowski JQ, Tomita T, Iwatsubo T (2011) BACE1 activity is modulated by cell-associated sphingosine-1-phosphate. J Neurosci 31:6850–6857.

Talos DM, Follett PL, Folkerth RD, Fishman RE, Trachtenberg FL, Volpe JJ, Jensen FE (2006) Developmental regulation of alpha-amino-3-hydroxy-5-methyl-4-isoxazole-propionic acid receptor subunit expression in forebrain and relationship to regional susceptibility to hypoxic/ischemic injury. II. Human cerebral white matter and cortex. J Comp Neurol 497:61–77.

Tampellini D, Rahman N, Gallo EF, Huang Z, Dumont M, Capetillo-Zarate E, Ma T, Zheng R, Lu B, Nanus DM, Lin MT, Gouras GK (2009) Synaptic activity reduces intraneuronal Abeta, promotes APP transport to synapses, and protects against Abeta-related synaptic alterations. J Neurosci 29:9704–9713.

Tan K, Duquette M, Liu J, Lawler J, Wang J (2008) The crystal structure of the heparin-binding reelin-N domain of f-spondin. J Mol Biol 381:1213–1223.

Tanzi RE (2005) The synaptic Abeta hypothesis of Alzheimer disease. Nat Neurosci 8:977–979.

Tepass U, Truong K, Godt D, Ikura M, Peifer M (2000) Cadherins in embryonic and neural morphogenesis. Nat Rev Mol Cell Biol 1:91–100.

Tesco G, Koh YH, Kang EL, Cameron AN, Das S, Sena-Esteves M, Hiltunen M, Yang S-H, Zhong Z, Shen Y, Simpkins JW, Tanzi RE (2007) Depletion of GGA3 stabilizes BACE and enhances beta-secretase activity. Neuron 54:721–737.

Thiagarajan TC, Lindskog M, Tsien RW (2005) Adaptation to synaptic inactivity in hippocampal neurons. Neuron 47:725–737.

Thiagarajan TC, Piedras-Renteria ES, Tsien RW (2002) alpha- and betaCaMKII. Inverse regulation by neuronal activity and opposing effects on synaptic strength. Neuron 36:1103–1114.

Thinakaran G, Sisodia SS (2006) Presenilins and Alzheimer disease: the calcium conspiracy. Nat Neurosci 9:1354–1355.

Thore S, Dyachok O, Tengholm A (2004) Oscillations of phospholipase C activity triggered by depolarization and Ca2+ influx in insulin-secreting cells. J Biol Chem 279:19396–19400.

Tischmeyer W, Grimm R (1999) Activation of immediate early genes and memory formation. Cell Mol Life Sci 55:564–574.

Tomidokoro Y, Harigaya Y, Matsubara E, Ikeda M, Kawarabayashi T, Shirao T, Ishiguro K, Okamoto K, Younkin SG, Shoji M (2001) Brain Abeta amyloidosis in APPsw mice induces accumulation of presenilin-1 and tau. J Pathol 194:500–506.

Tournoy J, Bossuyt X, Snellinx A, Regent M, Garmyn M, Serneels L, Saftig P, Craessaerts K, De Strooper B, Hartmann D (2004) Partial loss of presenilins causes seborrheic keratosis and autoimmune disease in mice. Hum Mol Genet 13:1321–1331.

Town T (2009) Alternative Abeta immunotherapy approaches for Alzheimer's disease. CNS Neurol Disord Drug Targets 8:114–127.

Townsend M, Qu Y, Gray A, Wu Z, Seto T, Hutton M, Shearman MS, Middleton RE (2010) Oral treatment with a gamma-secretase inhibitor improves long-term potentiation in a mouse model of Alzheimer's disease. J Pharmacol Exp Ther 333:110–119.

Trinchese F, Liu S, Battaglia F, Walter S, Mathews PM, Arancio O (2004) Progressive age-related development of Alzheimer-like pathology in APP/PS1 mice. Ann Neurol 55:801–814.

Tu H, Nelson O, Bezprozvanny A, Wang Z, Lee SF, Hao YH, Serneels L, De Strooper B, Yu G, Bezprozvanny I (2006) Presenilins form ER Ca2+ leak channels, a function disrupted by familial Alzheimer's disease-linked mutations. Cell 126:981–993.

Turrigiano GG, Leslie KR, Desai NS, Rutherford LC, Nelson SB (1998) Activity-dependent scaling of quantal amplitude in neocortical neurons. Nature 391:892–896.

Turrigiano GG, Nelson SB (2004) Homeostatic plasticity in the developing nervous system. Nat Rev Neurosci 5:97–107.

Uemura K, Kitagawa N, Kohno R, Kuzuya A, Kageyama T, Chonabayashi K, Shibasaki H, Shimohama S (2003) Presenilin 1 is involved in maturation and trafficking of N-cadherin to the plasma membrane. J Neurosci Res 74:184–191.

VanGuilder HD, Farley JA, Yan H, Van Kirk CA, Mitschelen M, Sonntag WE, Freeman WM (2011) Hippocampal dysregulation of synaptic plasticity-associated proteins with age-related cognitive decline. Neurobiol Dis 43:201–212.

Vassar R et al. (1999) Beta-secretase cleavage of Alzheimer's amyloid precursor protein by the transmembrane aspartic protease BACE. Science 286:735–741.

Vassar R (2002) Beta-secretase (BACE) as a drug target for Alzheimer's disease. Adv Drug Deliv Rev 54:1589–1602.

Vetrivel KS, Zhang Y, Xu H, Thinakaran G (2006) Pathological and physiological functions of presenilins. Mol Neurodegener 1:4.

Walsh DM, Klyubin I, Fadeeva J V, Cullen WK, Anwyl R, Wolfe MS, Rowan MJ, Selkoe DJ (2002) Naturally secreted oligomers of amyloid beta protein potently inhibit hippocampal long-term potentiation in vivo. Nature 416:535–539.

Walsh DM, Selkoe DJ (2004) Deciphering the molecular basis of memory failure in Alzheimer's disease. Neuron 44:181–193.

Wang H, Megill A, He K, Kirkwood A, Lee H-K (2012) Consequences of inhibiting amyloid precursor protein processing enzymes on synaptic function and plasticity. Neural Plast 2012:272374.

Wang H, Song L, Laird F, Wong PC, Lee H-K (2008) BACE1 knock-outs display deficits in activity-dependent potentiation of synaptic transmission at mossy fiber to CA3 synapses in the hippocampus. J Neurosci 28:8677–8681.

Wang H, Song L, Lee A, Laird F, Wong PC, Lee H-K (2010) Mossy fiber long-term potentiation deficits in BACE1 knock-outs can be rescued by activation of alpha7 nicotinic acetylcholine receptors. J Neurosci 30:13808–13813.

Wang HY, Lee DH, D'Andrea MR, Peterson PA, Shank RP, Reitz AB (2000a) beta-Amyloid(1-42) binds to alpha7 nicotinic acetylcholine receptor with high affinity. Implications for Alzheimer's disease pathology. J Biol Chem 275:5626–5632.

Wang HY, Lee DH, Davis CB, Shank RP (2000b) Amyloid peptide Abeta(1-42) binds selectively and with picomolar affinity to alpha7 nicotinic acetylcholine receptors. J Neurochem 75:1155–1161.

Wen Y, Yu WH, Maloney B, Bailey J, Ma J, Marié I, Maurin T, Wang L, Figueroa H, Herman M, Krishnamurthy P, Liu L, Planel E, Lau L-F, Lahiri DK, Duff K (2008) Transcriptional regulation of beta-secretase by p25/cdk5 leads to enhanced amyloidogenic processing. Neuron 57:680–690.

Whitlock JR, Heynen AJ, Shuler MG, Bear MF (2006) Learning induces long-term potentiation in the hippocampus. Science 313:1093–1097.

Willem M, Garratt AN, Novak B, Citron M, Kaufmann S, Rittger A, DeStrooper B, Saftig P, Birchmeier C, Haass C (2006) Control of peripheral nerve myelination by the beta-secretase BACE1. Science 314:664–666.

Wolfe MS (2008) Inhibition and modulation of gamma-secretase for Alzheimer's disease. Neurotherapeutics 5:391–398.

Wong H-K, Sakurai T, Oyama F, Kaneko K, Wada K, Miyazaki H, Kurosawa M, De Strooper B, Saftig P, Nukina N (2005) beta Subunits of voltage-gated sodium channels are novel substrates of beta-site amyloid precursor protein-cleaving enzyme (BACE1) and gamma-secretase. J Biol Chem 280:23009–23017.

Wong PC, Zheng H, Chen H, Becher MW, Sirinathsinghji DJ, Trumbauer ME, Chen HY, Price DL, Van der Ploeg LH, Sisodia SS (1997) Presenilin 1 is required for Notch1 and DII1 expression in the paraxial mesoderm. Nature 387:288–292.

Wu H, Williams J, Nathans J (2014) Complete morphologies of basal forebrain cholinergic neurons in the mouse. Elife 3:e02444.

Wu J, Anwyl R, Rowan MJ (1995) beta-Amyloid selectively augments NMDA receptor-mediated synaptic transmission in rat hippocampus. Neuroreport 6:2409–2413.

Wu J, Petralia RS, Kurushima H, Patel H, Jung M, Volk L, Chowdhury S, Shepherd JD, Dehoff M, Li Y, Kuhl D, Huganir RL, Price DL, Scannevin R, Troncoso JC, Wong PC, Worley PF (2011) Arc/Arg3.1 regulates an endosomal pathway essential for activity-dependent β-amyloid generation. Cell 147:615–628.

Yagami T, Kohma H, Yamamoto Y (2012) L-type voltage-dependent calcium channels as therapeutic targets for neurodegenerative diseases. Curr Med Chem 19:4816–4827.

Yakel JL (2013) Cholinergic receptors: functional role of nicotinic ACh receptors in brain circuits and disease. Pflugers Arch 465:441–450.

Yan Q, Zhang J, Liu H, Babu-Khan S, Vassar R, Biere AL, Citron M, Landreth G (2003) Anti-inflammatory drug therapy alters beta-amyloid processing and deposition in an animal model of Alzheimer's disease. J Neurosci 23:7504–7509.

Yan R, Vassar R (2014) Targeting the β secretase BACE1 for Alzheimer's disease therapy. Lancet Neurol 13:319–329.

Yao PJ, Zhu M, Pyun EI, Brooks AI, Therianos S, Meyers VE, Coleman PD (2003) Defects in expression of genes related to synaptic vesicle trafficking in frontal cortex of Alzheimer's disease. Neurobiol Dis 12:97–109.

Yashiro K, Philpot BD (2008) Regulation of NMDA receptor subunit expression and its implications for LTD, LTP, and metaplasticity. Neuropharmacology 55:1081–1094.

Yasumatsu N, Matsuzaki M, Miyazaki T, Noguchi J, Kasai H (2008) Principles of long-term dynamics of dendritic spines. J Neurosci 28:13592–13608.

Ye X, Carew TJ (2010) Small G protein signaling in neuronal plasticity and memory formation: the specific role of ras family proteins. Neuron 68:340–361.

Yokochi T, Robertson KD (2004) Dimethyl sulfoxide stimulates the catalytic activity of de novo DNA methyltransferase 3a (Dnmt3a) in vitro. Bioorg Chem 32:234–243.

Yoo AS, Cheng I, Chung S, Grenfell TZ, Lee H, Pack-Chung E, Handler M, Shen J, Xia W, Tesco G, Saunders AJ, Ding K, Frosch MP, Tanzi RE, Kim TW (2000) Presenilin-mediated modulation of capacitative calcium entry. Neuron 27:561–572.

Yoon MY, Kim SJ, Lee B-H, Chung J-H, Kim YC (2006) Effects of dimethylsulfoxide on metabolism and toxicity of acetaminophen in mice. Biol Pharm Bull 29:1618–1624.

Yu H, Saura CA, Choi SY, Sun LD, Yang X, Handler M, Kawarabayashi T, Younkin L, Fedeles B, Wilson MA, Younkin S, Kandel ER, Kirkwood A, Shen J (2001) APP processing and synaptic plasticity in presenilin-1 conditional knockout mice. Neuron 31:713–726.

Yuste R, Majewska A, Cash SS, Denk W (1999) Mechanisms of calcium influx into hippocampal spines: heterogeneity among spines, coincidence detection by NMDA receptors, and optical quantal analysis. J Neurosci 19:1976–1987.

Zaman SH, Parent a, Laskey a, Lee MK, Borchelt DR, Sisodia SS, Malinow R (2000) Enhanced synaptic potentiation in transgenic mice expressing presenilin 1 familial Alzheimer's disease mutation is normalized with a benzodiazepine. Neurobiol Dis 7:54–63.

Zamanillo D, Sprengel R, Hvalby O, Jensen V, Burnashev N, Rozov A, Kaiser KM, Köster HJ, Borchardt T, Worley P, Lübke J, Frotscher M, Kelly PH, Sommer B, Andersen P, Seeburg PH, Sakmann B (1999) Importance of AMPA receptors for hippocampal synaptic plasticity but not for spatial learning. Science 284:1805–1811.

Zangar RC, Novak RF (1998) Posttranslational elevation of cytochrome P450 3A levels and activity by dimethyl sulfoxide. Arch Biochem Biophys 353:1–9.

Zhang C, Wu B, Beglopoulos V, Wines-Samuelson M, Zhang D, Dragatsis I, Sudhof TC, Shen J (2009) Presenilins are essential for regulating neurotransmitter release. Nature 460:632–636.

Zhang D, Zhang C, Ho A, Kirkwood A, Sudhof TC, Shen J (2010a) Inactivation of presenilins causes pre-synaptic impairment prior to post-synaptic dysfunction. J Neurochem 115:1215–1221.

Zhang H, Sun S, Herreman A, De Strooper B, Bezprozvanny I (2010b) Role of presenilins in neuronal calcium homeostasis. J Neurosci 30:8566–8580.

Zhang J, Goodlett DR, Quinn JF, Peskind E, Kaye JA, Zhou Y, Pan C, Yi E, Eng J, Wang Q, Aebersold RH, Montine TJ (2005) Quantitative proteomics of cerebrospinal fluid from patients with Alzheimer disease. J Alzheimers Dis 7:125–33; discussion 173–80.

Zhang X-M, Xiong K, Cai Y, Cai H, Luo X-G, Feng J-C, Clough RW, Patrylo PR, Struble RG, Yan X-X (2010c) Functional deprivation promotes amyloid plaque pathogenesis in Tg2576 mouse olfactory bulb and piriform cortex. Eur J Neurosci 31:710–721.

Zhang Y, Thompson R, Zhang H, Xu H (2011) APP processing in Alzheimer's disease. Mol Brain 4:3.

Zhao D, Watson JB, Xie C-W (2004) Amyloid beta prevents activation of calcium/calmodulin-dependent protein kinase II and AMPA receptor phosphorylation during hippocampal long-term potentiation. J Neurophysiol 92:2853–2858.

Zhao J, Fu Y, Yasvoina M, Shao P, Hitt B, O'Connor T, Logan S, Maus E, Citron M, Berry R, Binder L, Vassar R (2007) Beta-site amyloid precursor protein cleaving enzyme 1 levels become elevated in neurons around amyloid plaques: implications for Alzheimer's disease pathogenesis. J Neurosci 27:3639–3649.

Zhong C, Du C, Hancock M, Mertz M, Talmage DA, Role LW (2008) Presynaptic type III neuregulin 1 is required for sustained enhancement of hippocampal transmission by nicotine and for axonal targeting of alpha7 nicotinic acetylcholine receptors. J Neurosci 28:9111–9116.

Zhou D, Shen X, Gu Y, Zhang N, Li T, Wu X, Lei L (2014) Effects of dimethyl sulfoxide on asymmetric division and cytokinesis in mouse oocytes. BMC Dev Biol 14:28.

Zhu JJ, Qin Y, Zhao M, Van Aelst L, Malinow R (2002) Ras and Rap control AMPA receptor trafficking during synaptic plasticity. Cell 110:443–455.

Zhu Z, Li C, Wang X, Yang Z, Chen J, Hu L, Jiang H, Shen X (2010) 2,2',4'-trihydroxychalcone from Glycyrrhiza glabra as a new specific BACE1 inhibitor efficiently ameliorates memory impairment in mice. J Neurochem 114:374–385.

Zisman S, Marom K, Avraham O, Rinsky-Halivni L, Gai U, Kligun G, Tzarfaty-Majar V, Suzuki T, Klar A (2007) Proteolysis and membrane capture of F-spondin generates combinatorial guidance cues from a single molecule. J Cell Biol 178:1237–1249.

Curriculum Vitae

1. PERSONAL INFORMATION

Name**:**	Andrea Megill
Birth date:	January 15, 1986
Birth location:	Philadelphia, PA
Current Appointment:	PhD Candidate, Dr. Hey-Kyoung Lee's lab
	The Zanvyl Krieger Mind/Brain Institute, Johns Hopkins University
	Department of Neuroscience, Johns Hopkins University School of Medicine
Address:	324 Dunning Hall / 3400 N. Charles St.
	Baltimore, MD 21218
Phone:	484-340-0079 (Cell)
Email:	almegill33@verizon.net

2. EDUCATION

July 2011 - August 2014**: Enrolled in Neuroscience PhD program, *Johns Hopkins University* (JHU, Baltimore, MD)

- Thesis: 'Metaplasticity in a mouse model of Alzheimer's disease and possible therapeutic interventions' which investigates the mechanisms behind age related changes in synaptic transmission and plasticity that occur during the progression of Alzheimer's disease (AD) and the effectiveness of current drug therapies to rescue these deficits.
- Major experimental skills: extracellular field potential recording, whole-cell recordings, protein immunoblot, steady-state surface biotinylation, immunohistochemistry, *in vivo* viral transfection, administering drug therapies through *intraperitoneal* (i.p.) injections
- Relevant course work: Neuroscience and Cognition I & II, Drug Discovery and Design, Neurobiology of Aging

** Expected graduation date

August 2009 - July 2011*: Enrolled in Cell Biology and Molecular Genetics PhD program, *University of Maryland* (UMD, College Park, MD)

- Relevant course work: Synaptic Plasticity, Cellular Neurophysiology, Genetics I & II, Cell Biology I & II, Immunology and Host Defense, Teaching Science, Research Ethics

* My first two years of study were completed at UMD before transferring to JHU

August 2004 - May 2008: B.S. in Cell and Molecular Biology, *West Chester University of Pennsylvania* (WCU, West Chester, PA)

- Independent Research Project: Participated in a molecular cloning project generating a mutation in the catalase gene of *Haemophilus influenzae*, by disruption with a kanamycin cassette, to determine how the catalase gene of *Haemophilus* is regulated *in vitro* and *in vivo*. (Advisor Dr. Xin Fan)
- Major experimental skills: DNA cloning including- isolating plasmid DNA, polymerase chain reaction (PCR), DNA detection, ligation of extracted DNA, TOPO cloning, and maintaining bacteria cultures for the lab
- Relevant course work: General Biology, Zoology, Botany, General Chemistry I & II, Organic Chemistry I & II, Biochemistry, Physics I & II, Genetics, Recombinant DNA, Molecule Genetics, Gene Analysis, Human Genetics, Cell and Molecular Biology, Cell Physiology, Microbiology, Diagnostic Bacteriology, Immunology, Biomedical Ethics, Developmental Psychology in Adults and Aging, Calculus, Statistics

3. RESEARCH EXPERIENCE

January 2010 - present: Graduate Research Assistant, (PI: Dr Hey-Kyoung Lee), *UMD* and *JHU*

- Uncovered deficits in metaplasticity mediated by changes in set point of push-pull regulation underlie deficits in frequency-dependent synaptic phenotypes regardless of age or contribution of AD-linked factors in an AD transgenic (Tg) mouse model.
- Investigated two novel AD therapeutics in wild type (WT) mice, and found that targeting spine density alone via an amyloid precursor protein (APP)/Ras dependent mechanism may be sufficient to improve cognitive function. This work was done in collaboration with Dr. Hyang-Sook Hoe's lab (Georgetown University).
- Compared the effects of two potential AD therapeutics in an AD Tg mouse model. However, this proved unsuccessful at rescuing synaptic deficits and displayed either off target vehicle effects, or negatively effected plasticity.

January 2009 - July 2009: Research Assistant and Lab Manager, (PI: Dr. Hao Shen), *University of Pennsylvania* (U Penn, Philadelphia, PA)

- Solved an ongoing mouse genotyping problem by optimizing PCR conditions and designing new primers
- Aided in infecting mice with both viral and bacterial cultures through i.v. injections, i.p. injections, and nasal inoculation
- Responsible for ordering the lab's supplies and keeping a detailed record of those orders for the monthly budget
- Contributed to grant writing through completion of animal protocols and editing of the PI's grant review papers before submission
- Mice Husbandry: Collected tail and blood samples for PCR and cellular staining, maintained mouse colony of both infected and non-infected cages, collected bronchoalveolar lavage (BAL) and spleen samples
- Major experimental skills: genotyping by PCR, isolated and prepared splenocytes and red blood cells from infected mice for cellular staining with antibodies, analyzed cellular staining through fluorescence-activated cell sorting (FACS) analysis, used FlowJo software to analyze FACS data

June 2007 - August 2007: Research Assistant, (PI: Dr. Hao Shen), *U Penn*

- Research Internship: Participated in a molecular cloning project to clone the cd4 epitope of the influenza virus into *Listeria monocytogenes*. The objective of this project was to develop a vaccine against the influenza virus using *Listeria* as a carrier to bring the influenza antigen to the infected cells.
- Major experimental skills: DNA cloning, electroporation of plasmid DNA into *Listeria*

4. TEACHING EXPERIENCE

January 2013 - December 2013: Adjunct Faculty, *Towson University* (TU, Towson, MD)

- Introduction to Biology (non-majors)
- Taught one section of approximately 45 students per semester
- Worked with Disability Support Services (DSS) to providing services that afford students with disabilities an equal opportunity to participate in all aspects of the educational environment.
- The main goal of this course was to provide students with the knowledge to apply biology facts and concepts to current events and ethical issues.
- Topics include scientific investigation, genetics, evolution, ecology and ethical issues in contemporary biology.

April 2012: Teaching Assistant, *JHU*

- Neuroanatomy lab taken by first year medial students
- Guided 8 medical students in the identification of nearly every brain structure, and helped them determine how different areas of the brain function together.

August 2009 - May 2010: Teaching Assistant, *UMD*

- Introduction to Cell and Molecular Biology lab (majors)
- Instructor for two lab sections of approximately 25 students per semester
- Taught experiment related background and developed weekly quizzes
- Instructed and facilitated experimental procedure
- Graded lab homework, lab quizzes, lab reports, and lecture exams

2009: Private tutor for high school students taking honors and AP chemistry

2005 - 2009: Supplemental Instruction Tutor, *WCU*

- Tutored small groups of students in General Chemistry I and II (majors and non-majors)
- Created worksheets and study guides for the students to encourage their practice of course material
- Completed College Reading and Learning Association (CRLA) Level I, II and III tutor certifications
- Led Level I training course; mentored Level I tutors
- Updated tutor log, attendance log, and student record of session form
- Evaluated tutees' progress in their understanding of course material and study skills throughout the semester

Other:

- Mentored numerous undergraduate and graduate students while working in labs at WCU, U Penn, UMD, and JHU
- Judge at a local middle school science fair- evaluate students' exhibits in a variety of subject areas and award 1st, 2nd, and 3rd place prizes (near UMD)
- Sat on a panel of "experts" at a local middle school career fair (near JHU)- shared with the students why I enjoy science, what kind of background I needed for my chosen career, and what tasks my typical workday involved
- Guide for a group of 5th graders during Community Science Day (hosted by JHU)- toured students through several labs where they were able to get hands on experience in a lab. Topics ranged from genetics to polymers.

5. OTHER WORK EXPERIENCE

2006: Retail Sales, *Charlotte Russe* (Exton, PA)

2005: Maid at local cleaning service (West Chester, PA)

2002 - 2009: Dinning room Server and Hostess, *Freedom Village Brandywine* (Coatesville, PA)

6. AWARDS AND HONORS

August 2012 - December 2013: Towson University Teaching Fellowship, *TU and JHU*

2006: Shirley Umlauf Prize in Botany, *WCU*

2004 - 2008: Dean's List (graduated Summa Cum Laude), *WCU*

7. ACTIVITIES

a. Memberships

2012 - present: Society for Neuroscience (SFN)

2012 - present: Baltimore Chapter of SFN

2006 - 2008: Women in Science Club

2005 - 2008: College Reading and Learning Association (CRLA)

b. Academic activities

November 2013: SFN 40th Annual Meeting (San Diego, CA)

September 2013: JHU Neuroscience Department Retreat and Conference (St. Michaels, MD)

July 2013: Current Trends and Future Directions of Synaptic Plasticity Research Conference (Seattle, WA)

February 2013: JHU Neuroscience Department Recruitment (Baltimore, MD)

October 2012: SFN 39th Annual Meeting (New Orleans, LA)

September 2012: JHU Neuroscience Department Retreat and Conference (St. Michaels, MD)

June 2012: JHU Alzheimer's Disease Day Conference (Baltimore, MD)

February 2012: JHU Neuroscience Department Recruitment (Baltimore, MD)

November 2011: SFN 38th Annual Meeting (Washington D.C.)

September 2011: JHU Neuroscience Department Retreat and Conference (St. Michaels, MD)

May 2011: JHU Alzheimer's Disease Day Conference (Baltimore, MD)

November 2010: UMD Bioscience and Technology Day (College Park, MD)

8. PUBLICATIONS

a. Peer reviewed

Megill, A.*, Lee, T.*, Kim, N., Sohn, Y., Barger, S., Marr, R. A., Lee, H-K., Hoe, H-S. (in preparation) F-spondin promotes dendritic spine density through APP and Ras/ERK signaling in mature neurons.

* Equally contributing authors

Megill, A., Eldred, K., Lee, N. J., Wong, P. C., Hoe, H-S., Lee, H-K. (in preparation) Age-dependent change in metaplasticity threshold in a mouse model of Alzheimer's disease.

Megill, A., Wong, P. C., Hoe, H-S., Lee, H-K. (in preparation) Comparing Alzheimer's disease therapies in a mouse model of AD.

Wang, H., **Megill, A.**, Wong, P. C., Kirkwood, A., Lee, H-K. (2014) Postsynaptic target specific synaptic dysfunction in the CA3 area of BACE1 knockout mice. PLoS ONE 9(3):e92279.

Yang, S., **Megill, A.**, Ardiles, A. O., Ransom, S., Tran, T., Koh, M. T., Lee, H-K., Gallagher, M., Kirkwood, A. (2013) Integrity of mGluR-LTD in the associative/commissural inputs to CA3 correlates with successful aging in rats. Journal of Neuroscience 33(31):12670-8.

Megill, A.*, Lee, T.*, Dibattista, A. M., Song, J. M., Spitzer, M. H., Rubinshtein, M., Habib, L. K., Capule, C. C., Mayer, M., Turner, R. S., Kirkwood, A., Yang, J., Pak, D. T. S., Lee, H-K., Hoe, H-S. (2013) A tetra(ethylene glycol) derivative of benzothiazole aniline enhances ras-mediated spinogenesis. Journal of Neuroscience 33(22):9306-9318.

Wang, H.*, **Megill, A.***, He, K., Kirkwood, A., Lee, H-K. (2012) Consequences of inhibiting amyloid precursor protein processing enzymes on synaptic function and plasticity. Neural Plasticity 2012:272374

Goel, A., Xu, L. W., Snyder, K. P., Song, L., Goenaga-Vazquez, Y., **Megill, A.**, Takamiya, K., Huganir, R. L., Lee, H-K. (2011) Phosphorylation of AMPA receptors is required for sensory deprivation-induced homeostatic synaptic plasticity. PLoS ONE 6(3):e18264.

b. Abstracts

Megill, A., Wong, P.C., Kirkwood, A., Hoe, H-S., Lee, H-K. (2013) Investigating the effects of β-secretase inhibitor, GRL-8234, on age-dependent synaptic deficits in APPswe;PS1deltaE9 mice. *Society for Neuroscience Abstracts/ Current Trends and Future Directions of Synaptic Plasticity Research Conference*

Megill, A., Kirkwood, A., Hoe, H-S., Lee, H-K. (2012) A novel drug candidate for Alzheimer's disease increases the number of functional synapses in the CA1 region of the hippocampus, in the absence of enhanced LTP. *Society for Neuroscience Abstracts/ JHU Neuroscience Department Retreat and Conference*

Megill, A., Wong, P.C., Lee, H-K. (2011) Age-dependent synaptic dysfunctions in APPswe;PS1deltaE9 mice. *Society for Neuroscience Abstracts/ JHU Neuroscience Department Recruitment*

Song, J., Spitzer, M.H., **Megill, A**., Rubinshtein, M., Habib, L.K., Capule. C.C., Xie, Y., Keenoy, K.E., Mayer, M., Turner, R., Yang, J., Pak, D.T., Lee, H-K., Hoe, H-S. (2011) Pharmacological targeting of beta-amyloid enhances dendritic spine density and memory. *Society for Neuroscience Abstracts*

Megill, A., Wang, H., Bezprozvanny, I., Wong, P.C., Lee, H-K. (2011) ER Ca^{2+} leak channel function of PS1 rescues the synaptic deficits at mossy fiber to CA3 synapses in the hippocampus of BACE1 knockouts. *JHU Neuroscience Department Recruitment*

Megill, A., Hoe, H-S., Lee, H-K. (2010) BTA-EG4 increases dendritic spines and synapse number in the CA1 region of the hippocampus without altering synaptic strength. *UMD Bioscience and Technology Day*